

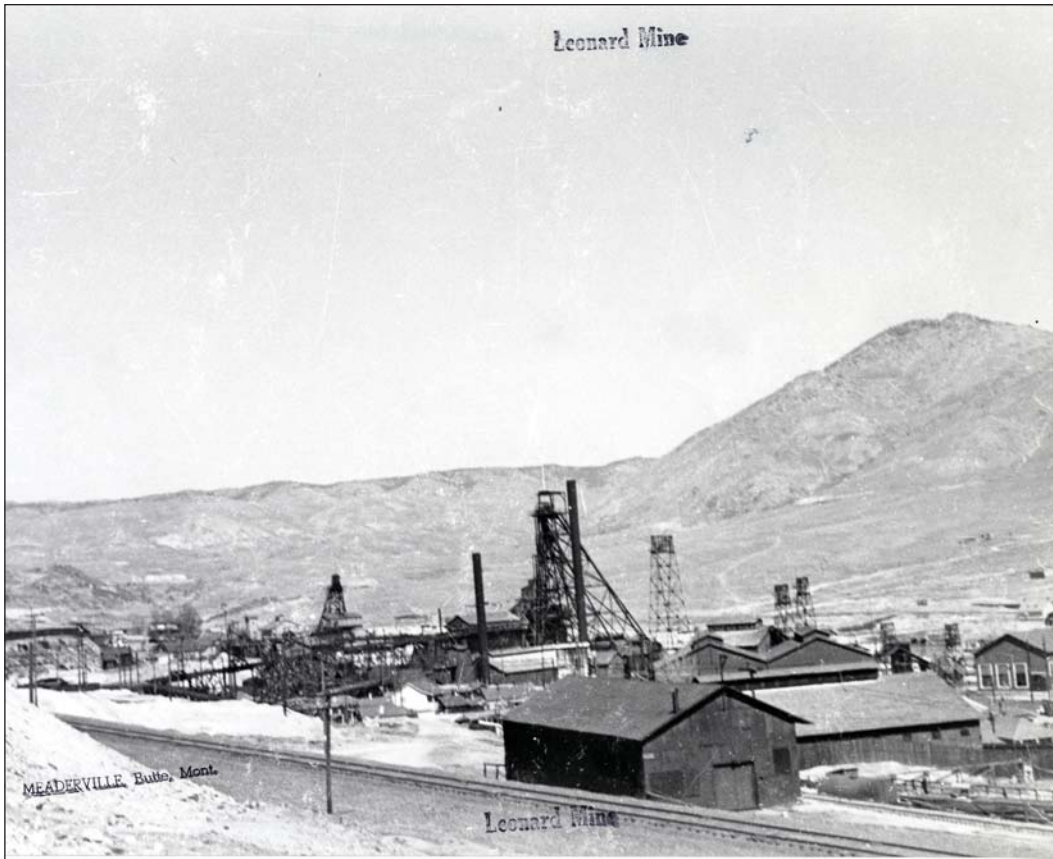


# PROCEEDINGS



*Berkeley and Continental pits. Photo by Mark Thompson, Montana Resources.*

Montana Mining and Mineral Symposium 2019  
October 9–October 11, 2019  
Montana Bureau of Mines and Geology  
Special Publication 121



The Leonard mine shaft #2 head frame circa 1940s. Courtesy of the World Museum of Mining; Butte, MT.



The Butte Hill from the east early 1900s. Courtesy of the World Museum of Mining; Butte, MT.

## TABLE OF CONTENTS

### Extended Abstracts and Technical Papers:

|  |     |
|--|-----|
| Refining Exploration Strategies for Geothermal Systems in Extensional to Transtensional Settings:<br>Lessons Learned from the Great Basin Region, Western US ..... <i>Faulds, Hinz, and Coolbaugh</i>  | 1   |
| A Case Study of Tailings Impoundment Permitting under the New Montana TSF Statute<br>..... <i>Mark Thompson</i>  | 5   |
| Development and Implementation of Unmanned Aerial Vehicles for Use in Mining Remediation<br>..... <i>Fairweather and Jonas</i>   | 9   |
| Best Practices for Waterfowl Management at the Berkeley Pit..... <i>Capoccia and others</i>  | 13  |
| Adventures in Recreational Prospecting in Montana..... <i>Alma Winberry</i>  | 19  |
| Ultraviolet Fluorescence of Montana Sapphires..... <i>Cox and Berg</i>   | 25  |
| Green Pipestone North of Twin Bridges, Madison County, Montana ..... <i>Ted Antonioli</i>  | 31  |
| Mineralogy of Montana Iron Skarn Deposits ..... <i>Michael J. Goble</i>  | 35  |
| Bull Mountain: Four Generations of Gold Seekers ..... <i>Dawson and Gruber</i>   | 49  |
| J.K. Pardee, from Ohio Boyhood to Montana Mining..... <i>Anne Millbrooke</i>   | 57  |
| Two-Event Genesis of Butte Lode Veins: Geologic and Geochronologic Evidence from Ore Veins,<br>Dikes, and Host Plutons..... <i>Lund and others</i>   | 71  |
| Butte Main Stage Veins: Control of Fracturing by the Central Gray Sericitic Zone.... <i>Mark H. Reed</i>   | 75  |
| Mineralogical Investigation of the Sheep Creek Nb-REE Carbonatite Deposits, Southern<br>Ravalli County, Montana ..... <i>Christopher H. Gammons</i>  | 81  |
| Antimony, a Strategic Metal, and USAC..... <i>John C. Lawrence</i>   | 93  |
| New Studies on the Oro Fino Mining District, Deer Lodge County, Montana: Metals, Boron, and<br>Heavy Isotopic Sulfur Sourced in the Revett Formation..... <i>Korzeb and Scarberry</i>  | 99  |
| Black Butte Copper: A High-Grade Underground Movable Copper Deposit in Meagher County,<br>Montana ..... <i>LeLacheur and Zieg</i>  | 111 |
| Supporting the Transition to Deep Porphyry Copper Exploration: SHRIMP U/Pb Radiometric Dating<br>of Titanite (CaTiSiO <sub>5</sub> ) in the Distal and Superjacent Orbicular Alteration Zone of the Clementine<br>Prospect, Southwest Montana..... <i>Brimhall and Fanning</i> | 117 |
| Ore Mineralogy and Stable Isotope Studies of the Hog Heaven Mining District, Montana<br>..... <i>Kallio, Gammons, and Poulson</i>  | 133 |
| The Processing and Recycling of Garnet Tailings for Application in Concrete ..... <i>Das and others</i>  | 143 |
| Merging Historical Data with Google Earth and ArcGIS..... <i>Anthony Roth</i>  | 147 |

### Posters:

|  |     |
|--|-----|
| The Montana–Idaho Alkalic Belt: An Exploration Target for Critical Metals and Industrial Minerals<br>..... <i>Christopher H. Gammons</i>   | 151 |
| Nature and Implications of Breccias at the Lamprophyre-Hosted Sapphire Deposit, Yogo<br>..... <i>Cotterell and Ridley</i>  | 158 |
| Late Cretaceous to Early Eocene Lamprophyric Textural and Pyroxene Mineral Chemistry Variation<br>from Calc-Alkaline Subduction-Related Magmatism and the Central Montana Alkalic Province<br>..... <i>McCane and Ridley</i> | 159 |





The Butte Hill from the south, Never Sweat mine, circa 1910. Courtesy of the World Museum of Mining; Butte, MT.



**PROCEEDINGS,  
MONTANA MINING AND MINERAL SYMPOSIUM 2019  
TECHNICAL PAPERS AND ABSTRACTS**

**Special Publication 121**

Edited by Kaleb C. Scarberry and Susan Barth  
*Montana Bureau of Mines and Geology*

With thanks for editorial contributions from: George Brimhall, Patrick E. Dawson, Stanley L. Korzeb, Alan English, Colleen Elliott, Richard B. Berg, Christopher H. Gammons, and Anne Millbrooke.



Patrick E. Dawson at his grandfather's mining claim in the Bull Mountains north of Whitehall, MT. Courtesy of Patrick E. Dawson.



Sphalerite from Butte, MT. Courtesy of Michael J. Goble.



# **Refining Exploration Strategies for Geothermal Systems in Extensional to Transtensional Settings: Lessons Learned from the Great Basin Region, Western USA**

James E. Faulds, Nicholas H. Hinz, and Mark F. Coolbaugh

*Nevada Bureau of Mines and Geology, University of Nevada, Reno*

Active extensional to transtensional tectonics have induced a high geothermal gradient and abundant geothermal resources in the Great Basin region of Nevada and adjoining states (Blackwell, 1983). Although the region currently hosts ~25 geothermal power plants with a capacity of ~770 MW, it has the potential to produce far greater amounts of energy (Williams and others, 2009). However, discovering new resources and subsequent development have faced various challenges, including locating sufficient permeability at depth. It is generally easier to find adequate temperature than permeability. Furthermore, most geothermal resources in this region are blind, with no surface hot springs or steam vents to guide exploration (Richards and Blackwell, 2002; Coolbaugh and others, 2007). It has long been known that faults are the primary control on geothermal systems in this region (Blackwell and others, 1999), but which types of faults are most conducive to geothermal activity had not been studied in much detail. Over about the past 10 years, we therefore embarked on a systematic program to first characterize the favorable structural settings of known geothermal systems and then synthesize that information with multiple other parameters to discover new blind geothermal systems.

In our characterization of favorable structural settings of ~250 known systems, we found that nearly 90% in the extensional Basin and Range province reside in step-overs (relay ramps) in normal faults, normal fault terminations, fault intersections, or accommodation zones (fig. 1; Faulds and others, 2006, 2011; Faulds and Hinz, 2015). In the transtensional, western part of the Great Basin within and proximal to the Walker Lane, displacement transfer zones (where strike-slip faults end in arrays of normal faults) and pull-parts host many systems. High fault density in these settings facilitates high permeability and fluid flow. Mid segments of major normal faults are generally devoid of geothermal systems, probably due to reduced permeability in clay gouge and periodic stress release in major earthquakes. Step-overs, terminations, intersections, and accommodation zones are critically stressed areas, where fluid pathways more likely remain open due to breccia-dominated faults and more micro-seismicity.

These findings were incorporated into a play fairway analysis (i.e., Doust, 2010), whereby nine geologic, geophysical, and geochemical parameters were synthesized to produce a geothermal potential map of 96,000 km<sup>2</sup> of Nevada (fig. 2). Parameters were grouped in subsets and weighted to delineate rankings for heat and local, intermediate, and regional scale permeability, which collectively defined likely areas for geothermal fluid flow or play fairways (Faulds and others, 2017). Several features were used to assess permeability, including: (1) structural settings, (2) the location, age, slip rates, and slip/dilation tendency of Quaternary faults, (3) geotectonic strain rates, (4) horizontal gravity gradients, and (5) earthquake density. Dozens of prospective areas were identified. Two sites with particularly high potential were selected for temperature-gradient drilling, with results indicating discovery of two blind systems, validating the technique (Craig, 2018; Faulds and others, 2018, 2019). A key lesson learned is that detailed geophysical surveys can play critical roles in identifying favorable structural settings to lower the risks of drilling in the many basins in the region.

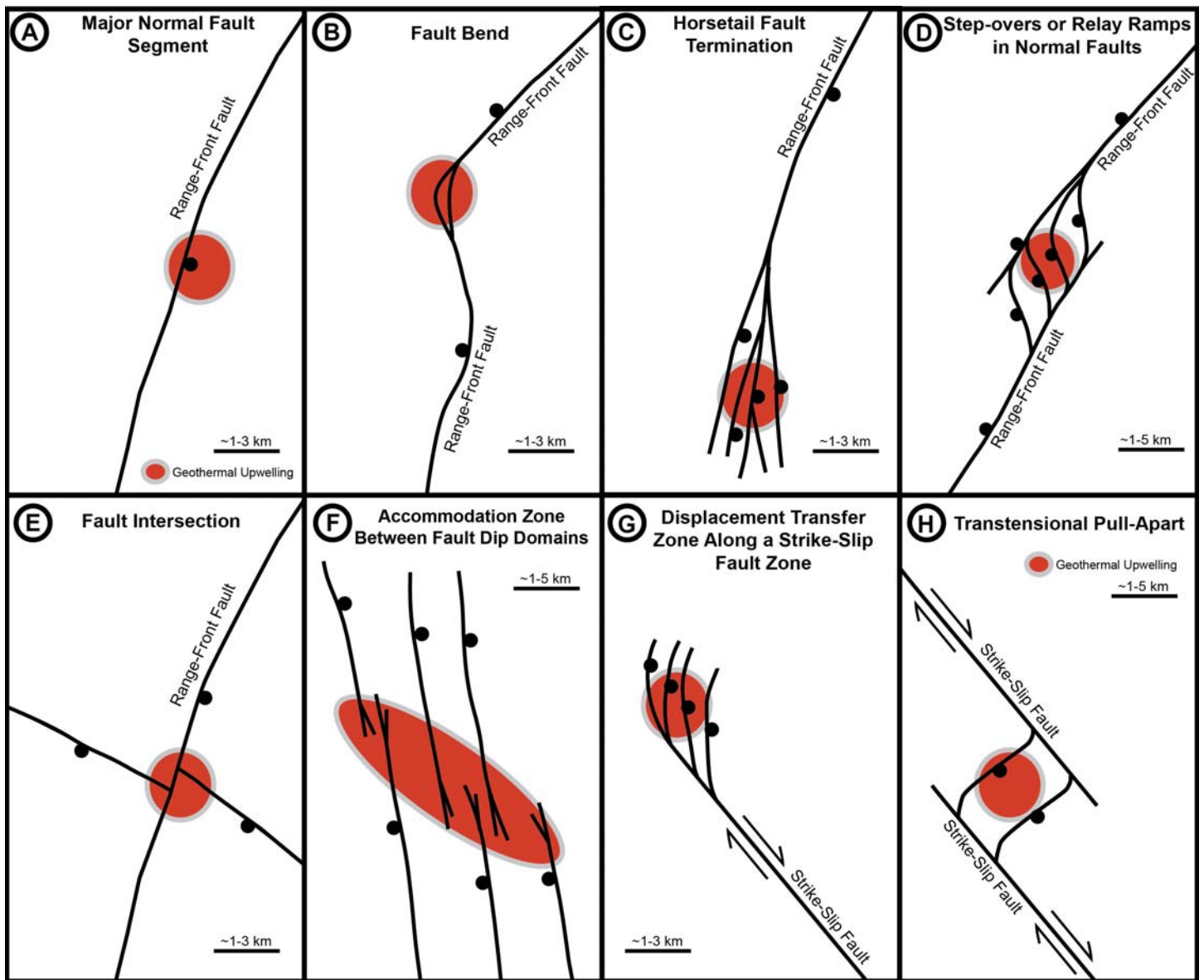


Figure 1. Characteristic structural settings for geothermal systems in the Great Basin region (from Faulds and Hinz, 2015). (A) Major normal fault. (B) Bend in major normal fault. (C) Fault tip or termination with main fault breaking into multiple strands or horsetailing. (D) Fault step-over or relay ramp breached by minor connecting faults. (E) Fault intersection. (F) Accommodation zone, consisting of belt of intermeshing oppositely dipping normal faults. (G) Displacement transfer zone, whereby a major strike fault terminates in an array of normal faults. (H) Transtensional pull-apart in major strike-slip fault zone. Curewitz and Karson (1997) noted similar findings in an earlier global study.



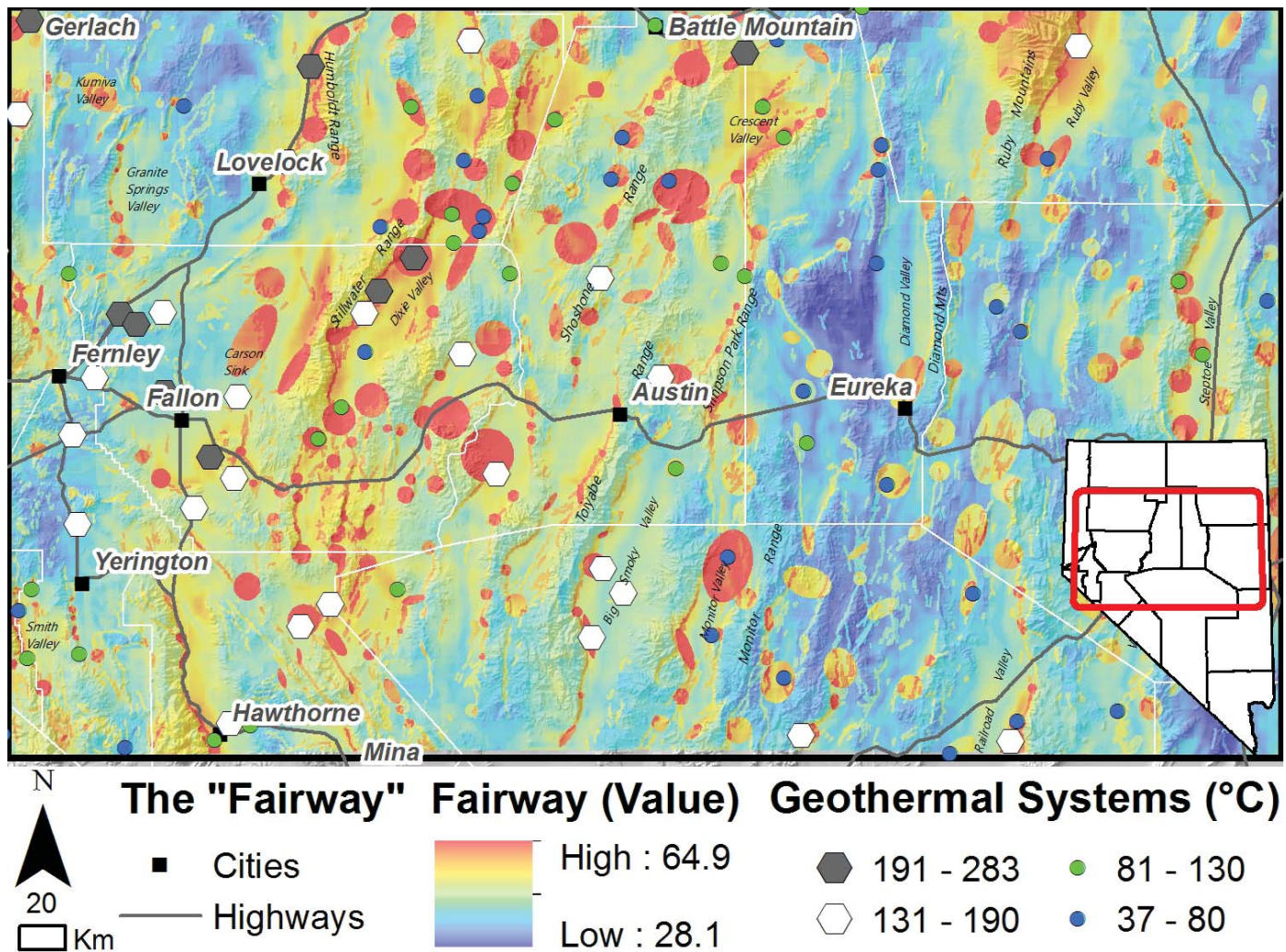


Figure 2. The play fairway model of the study area in west-central to eastern Nevada (modified from Faulds and others, 2018).

### References Cited

Blackwell, D.D., 1983, Heat flow in the northern Basin and Range province, in *The role of heat in the development of energy and mineral resources in the northern Basin and Range province: Geothermal Resources Council Special Report 13*, p. 81–92.

Blackwell, D., Wisian K., Benoit, D., and Gollan, B., 1999, Structure of the Dixie Valley geothermal system, a “typical” Basin and Range geothermal system, in *Thermal and Gravity Data: Geothermal Resources Council Transactions*, v. 23, p. 525–531.

Coolbaugh, M.F., Raines, G.L., and Zehner, R.E., 2007, Assessment of exploration bias in data-driven predictive models and the estimation of undiscovered resources: *Natural Resources Research*, v. 16, no. 2, p. 199–207.

Craig, J.W., 2018, Discovery and analysis of a blind geothermal system in southeastern Gabbs Valley, western Nevada [M.S. Thesis]: University of Nevada, Reno, 111 p.

Curewitz, D., and Karson, J.A., 1997, Structural settings of hydrothermal outflow: Fracture permeability maintained by fault propagation and interaction: *Journal of Volcanology and Geothermal Research*, v. 79, p. 149–168.

Doust, H., 2010, The exploration play: What do we mean by it?: *American Association of Petroleum Geologists Bulletin*, v. 94, p. 1657–1672.

- Faulds, J.E., Coolbaugh, M.F., Vice, G.S., and Edwards, M.L., 2006, Characterizing structural controls of geothermal fields in the northwestern Great Basin: A progress report: Geothermal Resources Council Transactions, v. 30, p. 69–76.
- Faulds, J.E., Coolbaugh, M.F., Hinz, N.H., Cashman, P.H., Kratt, C., Dering, G., Edwards, J., Mayhew, B., and McLachlan, H., 2011, Assessment of favorable structural settings of geothermal systems in the Great Basin, western USA: Geothermal Resources Council Transactions, v. 35, p. 777–784.
- Faulds, N.H., and Hinz, N.H., 2015, Favorable tectonic and structural settings of geothermal settings in the Great Basin Region, western USA: Proxies for discovering blind geothermal systems: Proceedings, World Geothermal Congress 2015, Melbourne, Australia, 6 p.
- Faulds, J.E., Hinz, N.H., Coolbaugh, M.F., Shevenell, L.A., Sadowski, A.J., McConville, E., Craig, J., Sladek, C., and Siler, D.L., 2017, Progress report on the Nevada play fairway project: Integrated geological, geochemical, and geophysical analyses of possible new geothermal systems in the Great Basin region: Proceedings, 42nd workshop on Geothermal Reservoir Engineering, Stanford University, Stanford, California, SGP-TR-212, 11 p.
- Faulds, J.E., Craig, J.W., Coolbaugh, M.F., Hinz, N.H., Glen, J.M., and Deoreo, S., 2018, Searching for blind geothermal systems utilizing play fairway analysis, western Nevada: Geothermal Resources Council Bulletin, v. 47, p. 34–42.
- Faulds, J.E., Hinz, N.H., Coolbaugh, M.F., Ramelli, A., Glen, J.M., Ayling, B.A., Wannamaker, P.E., Deoreo, S.B., Siler, D.L., and Craig, J.W., 2019, Vectoring into potential blind geothermal systems in the Granite Springs Valley area, western Nevada: Application of the play fairway analysis at multiple scales: Proceedings 44th workshop on Geothermal Reservoir Engineering, Stanford University, Stanford, California, SGP-TR-214, p. 74–84.
- Richards, M., and Blackwell, D., 2002, A difficult search: Why Basin and Range systems are hard to find: Geothermal Resources Council Bulletin, v. 31, p. 143–146.
- Williams, C.F., Reed, M.J., DeAngelo, J., and Galanis, S.P. Jr., 2009, Quantifying the undiscovered geothermal resources of the United States: Geothermal Resources Council Transactions, v. 33, p. 995–1002.



# A Case Study of Tailings Impoundment Permitting under the New Montana TSF Statute

Mark Thompson

*Montana Resources, Butte, Montana*

Montana Resources, LLP (MR), the operator of a copper and molybdenum mine in Butte, Montana, received a permit in 2019 to increase storage capacity in the Yankee Doodle Tailings Impoundment (YDTI; fig. 1). This was the first permit issued by the Montana Department of Environmental Quality (MDEQ) where the applicant followed the new Montana Tailing Storage Facility (TSF) statute. The statute is rigorous and involves a third party Engineer of Record and an Independent Review Panel of experts. This article discusses the engineering aspects of the application, the new TSF statute, community involvement, and the lessons learned through the permitting process.



Figure 1. The Yankee Doodle Tailings Impoundment.

## Engineering

MR's current permit allows production of ore and storage of waste rock in excess of 20 years. The YDTI embankment permit is to an elevation of 6,405 ft, with a maximum operating tailing impoundment water level of 6,360 ft. The current water level is 6,358 ft and the tailings rise at about 6 ft per year. Embankment construction above 6,400 ft must start in early 2020. Activities underway include topsoil and overburden stripping and stockpiling, foundation preparation, and toe drain construction. A site investigation is underway that includes test pits and trenches, drill holes to test the foundation strength, deep angle core holes to understand geologic structure at depth, sonic drill holes to verify foundation strengths, and cone penetration holes to verify tailings characteristics.

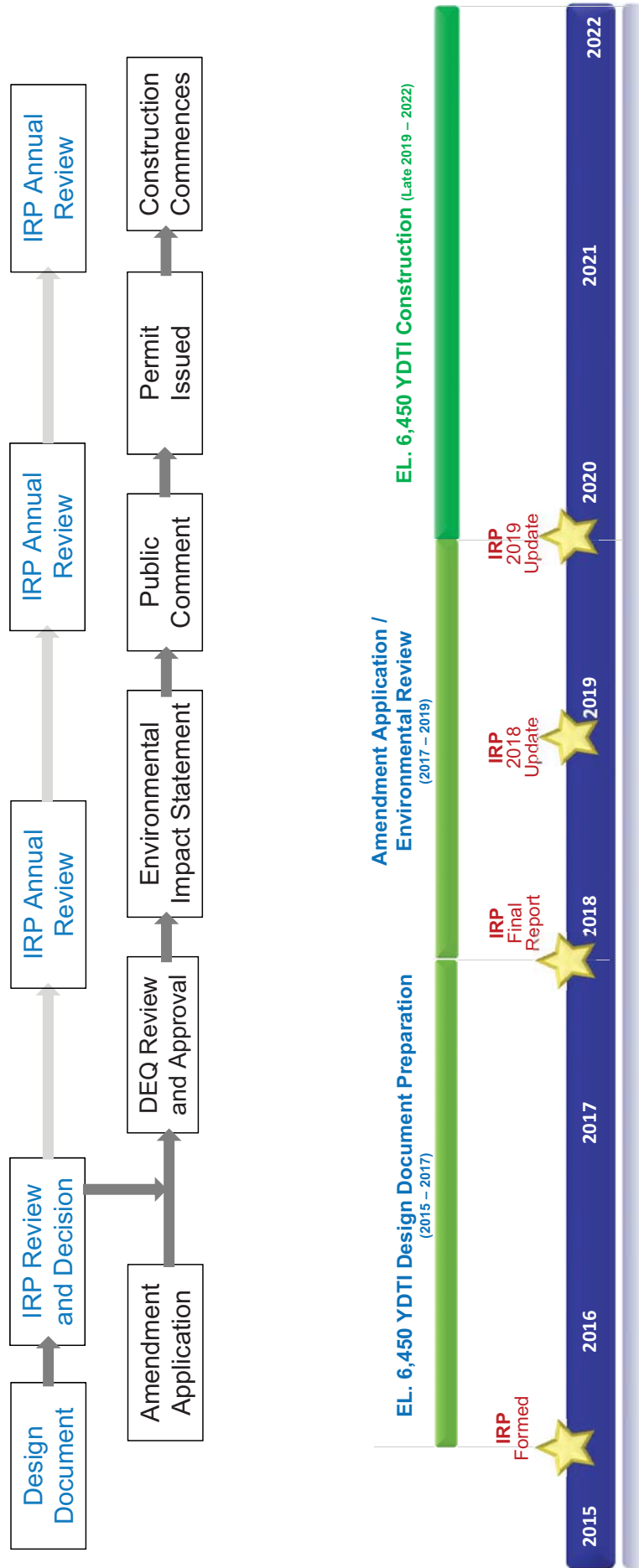


Figure 2. Timeline and tasks performed during the permitting process under the new Montana Tailings Storage Facility statute. IRP, Independent Review Panel; DEQ, Department of Environmental Quality; EL, elevation in feet above sea level.



## Tailings Impoundment Permitting

The permitting process has been ongoing since 2015 (fig. 2). Permit applicants must submit a design document that details how the facility design addresses over 30 specific requirements. Requirements include an analysis that shows that the TSF will withstand a 1 in 10,000-year earthquake event or maximum credible earthquake, whichever is larger, and design criteria to manage the probable maximum flood event. An Independent Review Panel of experts, including Dr. Leslie Smith, James R. Swaisgood, and Dr. Peter Robertson, reviewed and signed the design document before submission to MTEQ.

### Lessons Learned

Engaging the IRP early and often was key to our successful permitting process. Understanding regulatory requirements and processes allowed us to provide MDEQ with what they needed. General takeaways:

- Do not submit a permitting application before it is completely ready, and make sure not to change the application while the permitting process is underway.
- Identify priority stakeholders and interact with them proactively.
- Local support for the permit was important.



Bull Mountains. Courtesy of Patrick E. Dawson.



Silver from the Elkhorn Mine, Jefferson County, MT. Courtesy of Michael J. Goble.



Smithsonite from the Sherman Tunnel, Leadville, CO. Courtesy of Michael J. Goble.



# Development and Implementation of Unmanned Aerial Vehicles for Use in Mining Remediation

Ian S. Fairweather<sup>1</sup> and Jim Jonas<sup>2</sup>

<sup>1</sup>Fairweather IT LLC, Bozeman, Montana

<sup>2</sup>Fairweather IT LLC, Opportunity, Montana

Fairweather IT (FIT) has pioneered the use of unmanned aerial vehicles (UAVs) for various types of mining remediation work. UAVs are now used to safely collect data and environmental samples that were previously collected manually. Monitoring and sampling water-filled mining pits for chemical analysis is a primary concern of liability managers and other stakeholders. Due to acidic pit waters and the geologic instability of pit walls, direct human water sampling is often not recommended or permitted. With the technological advent of UAVs, the FIT team has developed a multi-use unique flying platform capable of collecting water profile data (fig. 1) and physically collecting in situ water samples to depths greater than 446 ft. Our method uses a custom cross-UAV platform we have named WaSP (Water Sampling Platform; fig. 2) that connects to any high-payload (greater than 6 kg) multicopter UAV. FIT also has established methodologies utilizing specialized cameras and sensors for mapping and monitoring surface cover types of mining remediation sites. Thermal infrared, multispectral (fig. 3), and standard optical sensors are being employed to map and characterize the surface and topography of sites with thermal and radiometrically calibrated imagery at centimeter-scale resolution. This is required when comparing multiple remotely sensed data sets collected over time.

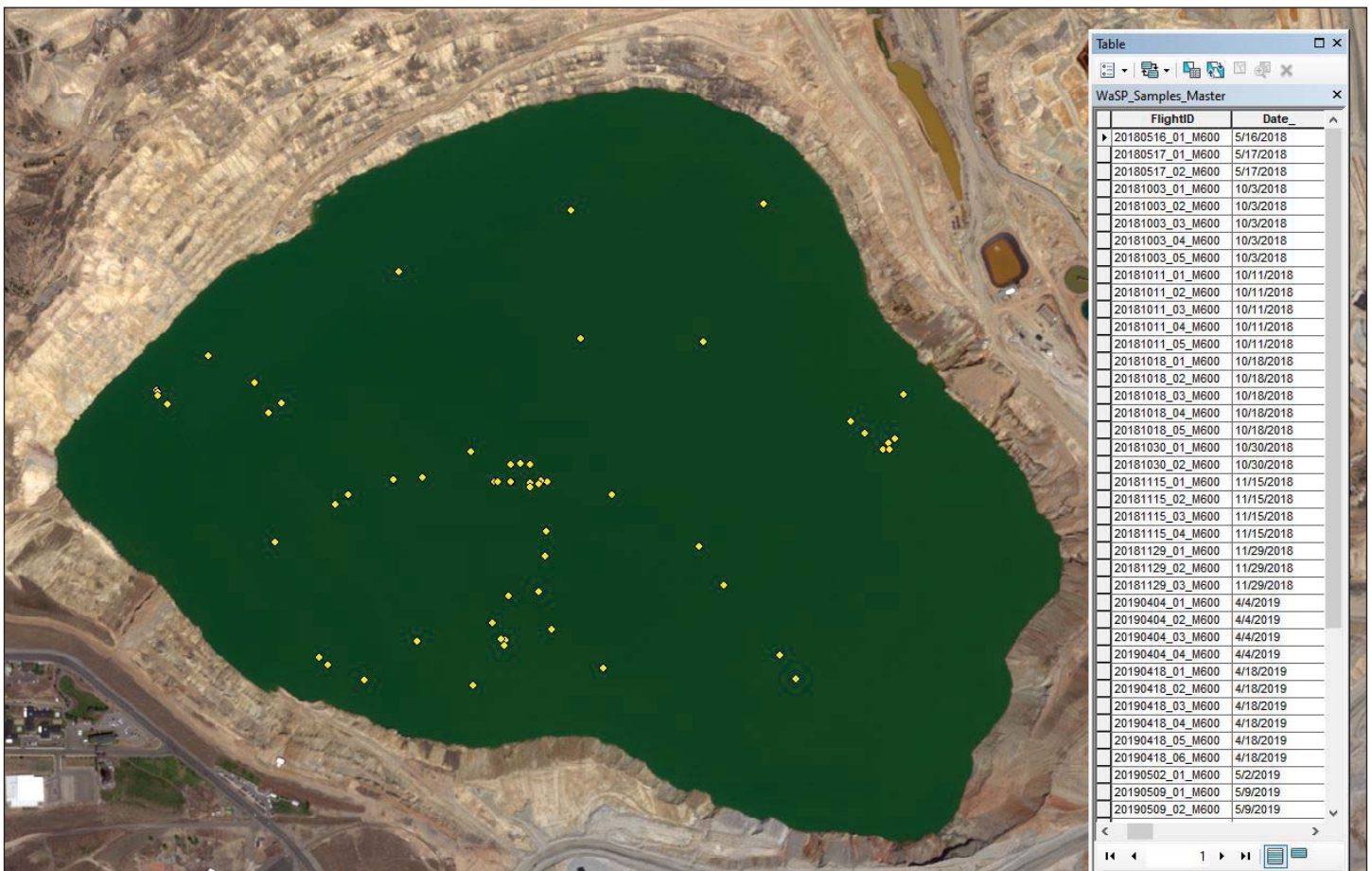


Figure 1. Map of the Berkeley Pit showing locations of water samples collected by unmanned aerial vehicles.





Figure 2. The WaSP holding a sample of Berkeley Pit water.



Figure 3. Multispectral map of the surface topography in a region of past mining activity.





Montana garnet. Courtesy of Alma Winberry.



## Best Practices for Waterfowl Management at the Berkeley Pit

Dr. Stella Capoccia,<sup>1</sup> Gary Swant,<sup>2</sup> Matt Vincent,<sup>3</sup> Mark Mariano,<sup>3</sup> and Jay Selmer<sup>4</sup>

<sup>1</sup>Associate Professor, Biological Sciences, Montana Tech, Butte, Montana

<sup>2</sup>Consultant, Go Bird Montana

<sup>3</sup>Environmental Consultant, Rampart Solutions

<sup>4</sup>Undergraduate, Biological Science, Montana Tech, Butte, Montana

On November 28, 2016, an unprecedented fall migration event resulted in as many as 60,000 Snow Geese (*Anser caerulescens*) and Ross's Geese (*Anser rossii*), often termed light geese as a combined flock, landing in the Berkeley Pit (the Pit). Mine personnel successfully hazed most of these birds off the Pit; however, about 3,000 geese died despite round-the-clock hazing efforts that continued for days. Until that time, the Pit's records on preventing avian mortality showed an overall >99% success rate for moving birds off the water, including light geese. This success draws questions of why the mortality numbers were so high in 2016 and what could be done in the future to improve the deterrent practices (keeping birds off the water) and hazing efforts (moving birds off the water if they do land). This account reports on the progress of an ongoing investigation effort to better understand the way in which birds use the Pit and how that can translate into improved protection efforts. Here, we summarize the history of the Pit, the region as it relates to waterfowl migration, details that historical data can and cannot tell us, and the innovative approaches to adaptive management.

The Berkeley Pit is a former open pit copper mine situated on the western face of the Continental Divide, a part of the region's mining heritage that dates back over 150 years. The Pit mining operations started in 1955 and continued until 1982, when mining was suspended. The open-pit operations tapped into the thousands of miles of underground mine workings in the area as well as the underground aquifer. While mining was active, the Pit was dewatered. When mining ceased, the dewatering pumps were turned off and water percolated in (Gammons and others, 2006). This is a common history for geologists, engineers, miners, and historians alike who are familiar with this region, but this story intersects with the avian activity in ways that would have been difficult for anyone to predict. As the open-pit mine slowly transitioned from a slick to a pond to a growing body of water (fig. 1), it crossed an invisible threshold: at first the water did not appeal to migratory waterfowl and



Figure 1. Sequential images that show how the Berkeley Pit filled with water over time. For many years, conditions in the Berkeley Pit, including low water levels, did not attract birds to land. Image credit: PitWatch.org, corrected by S. Capoccia.

then, one day, it did. This invisible threshold would be difficult for anyone to foresee and, until 1995, there was little known use of the Pit water by migratory waterfowl. This changed in November 1995 when 342 light geese landed on the water and died from exposure to the acidity and mixed metal concentrations (Adams, 1995). The event served as a catalyst for the companies responsible for the Pit to establish a waterfowl mitigation program complete with daily monitoring, deterrents, and hazing efforts aimed at preventing birds from landing and minimizing exposure of birds that did land. This protection plan had been in place for over 20 years, with several modifications, and, as noted above, has been largely successful.

Another factor that amplified the unknown of this invisible threshold of the Pit water level is understanding the region as it relates to waterfowl migration. Butte–Silver Bow County (BSB), in the Summit Valley, is not a primary migratory route for most waterfowl. Avian migratory flyways are broken into major thoroughfares that align with main air currents; Summit Valley sits at the westernmost edge of the Central Flyway (fig. 2) with only diffuse activity. This low-level use may not seem obvious for casual naturalists who marvel at the hundreds of Canada Geese (*Branta canadensis*) and dozens of other species that use this region. In comparison, at the height of migration, the epicenter of the Central Flyway—closer to the Dakotas—boasts numbers that reach into the millions of birds moving through at a furious pace aimed either for winter foraging grounds or summer breeding grounds (Dubovsky, 2019). In order for birds to use Summit Valley, they must deviate from a straight flightpath along the eastern Rocky Mountain Front and crest over the mountain tops to the west,

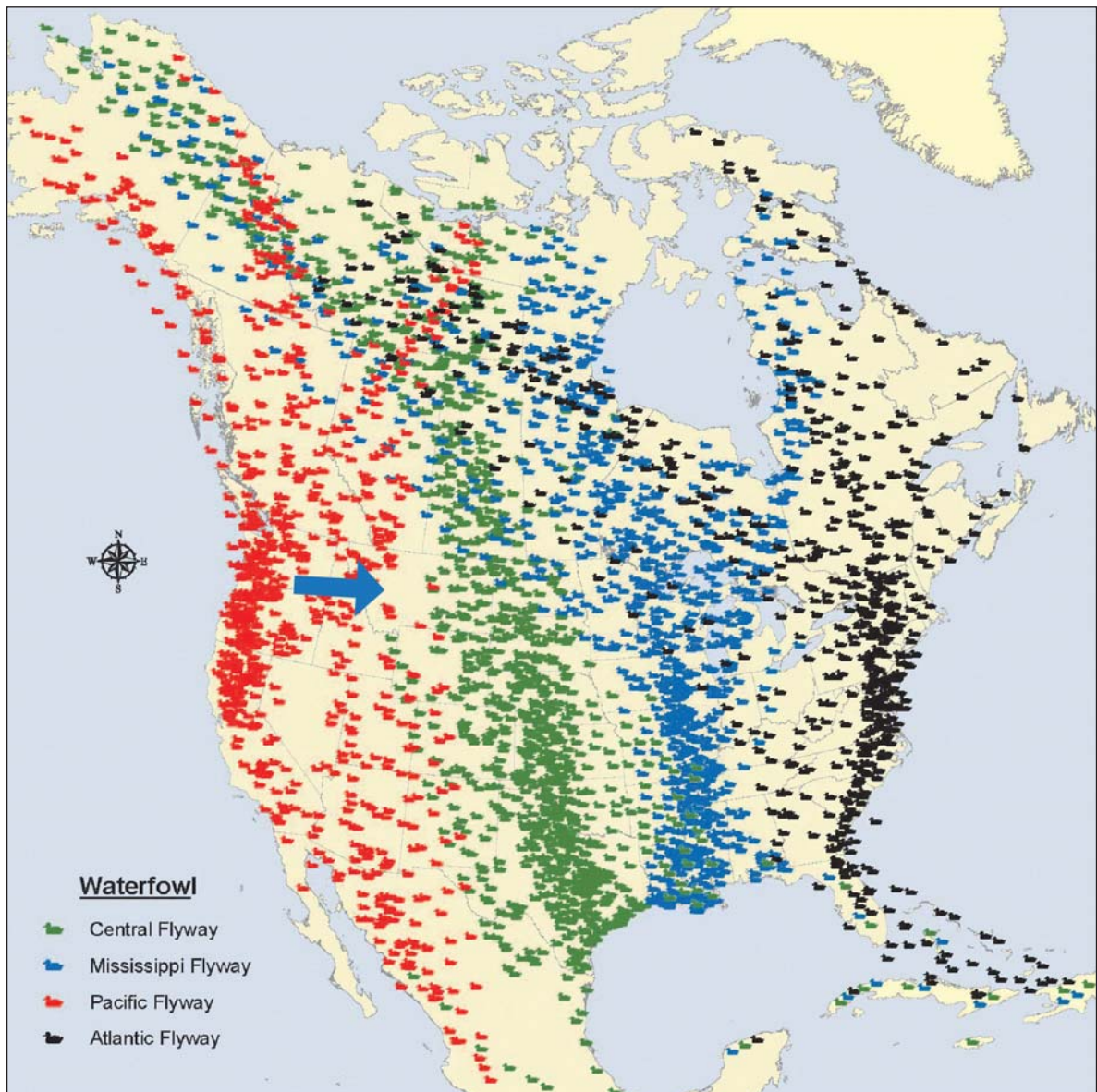


Figure 2. Depiction of the four major avian migratory flyways across the North American continent. Note the reduced activity north of Summit Valley (blue arrow; map from USFWS, 2012).



an effort that takes much more energy than soaring on the fast air currents of the open plains (Bellrose,1968; Bruderer and Salewski, 2008; USFWS, 2012). In short, though utilized by some, BSB is simply not a prime spot for high-density migration, so the incident in 2016 is an outlier to the general trend. In fact, low-level use is supported by a detailed analysis of a 13-year data set (December 2004–December 2017): the average number of birds per sighting (group<sup>1</sup>) is 65.5 individuals. This average is across 67,694 total individual waterfowl observed in 1,057 sightings (a given observation point); only 14 sightings showed groups of more than 500 birds (fig. 3, table 1). It is well accepted that history informs current management (see Niraj and others, 2010), so extrapolating the average of 65.5 birds in a given group to manage for flocks that stretch into the tens of thousands would have been implausible at best. Moreover, the two largest group sightings occurred in September 2017, nearly a full year after the light goose event in 2016, and credit to the protection efforts, n birds in these two groups were hazed successfully.

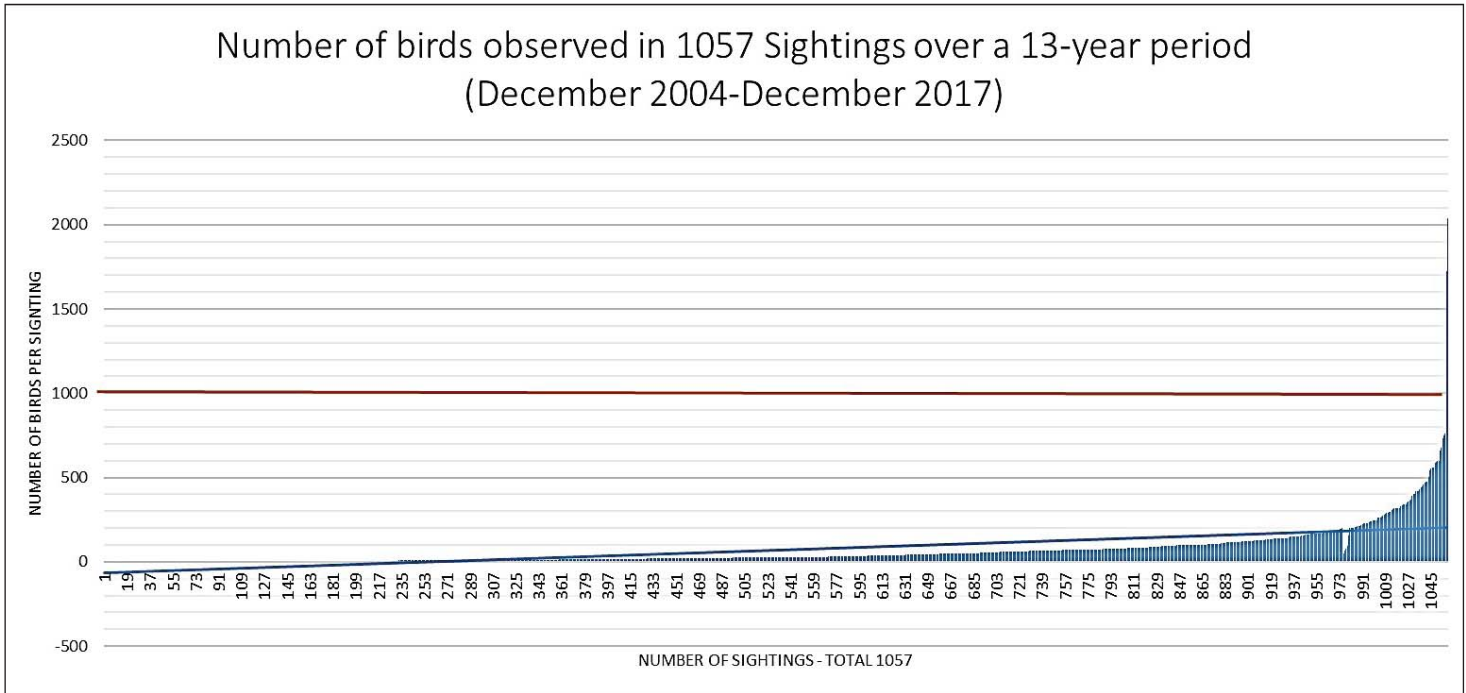


Figure 3. The distribution of group size compared to number of sightings over a 13-year observation period. The total number of birds observed over 1,057 observation periods is estimated at 67,694 individuals in groups that range from 1 to 2,035 birds. The average group size is 65.5 birds. Figure credit: S. Capoccia and E. Vincent.

Table 1. The distribution of group size compared to number of sightings over a 13-year observation period.

| Distribution of Observations by Group Size  |     |             |             |             |             |             |             |             |             |             |                 |                 |                       |
|---|-----|-------------|-------------|-------------|-------------|-------------|-------------|-------------|-------------|-------------|-----------------|-----------------|-----------------------|
| Group size:<br>number of<br>birds<br>counted on<br>the water<br>at one<br>observation | <99 | 100–<br>199 | 200–<br>299 | 300–<br>399 | 400–<br>499 | 500–<br>599 | 600–<br>699 | 700–<br>799 | 800–<br>899 | 900–<br>999 | 1,000–<br>1,999 | 2,000–<br>2,999 | Total<br>observations |
| Frequency<br>of group<br>observation  | 859 | 128         | 31          | 16          | 9           | 4           | 4           | 4           | 0           | 0           | 1               | 1               | 1,057                 |

<sup>1</sup>Group is used over flock, as the number of birds per sighting were not always in a cohesive flock, either mixed or single-species, rather, a collection of birds observed on the water of the Berkeley Pit at a given time.



In addition to average group size, the historical data provide valuable insight into the changing dynamics of the Pit. For example, these data help inform weekly predictions and even test and support the circumstantial trends espoused by the miners who conduct daily observations, such as when activity peaks both daily and seasonally and how regional weather may impact bird survival. These data go even further to validate the miners’ knowledge of the birds’ behavioral differences between fall and spring seasons. For example, fall is considered to be a more intense time at the Pit, and miners feel the birds may be more likely to die. This is not surprising, as many of the fall migrants are juvenile birds making their first transcontinental flight. Juvenile birds are inexperienced fliers, faced with rapidly declining weather, and heavily reliant on the flock cohesion for success. In the spring, however, every bird that migrates has made the trek at least one time prior, their musculature is more developed (Bellrose, 1968), and the wintry weather conditions are subsiding. Despite a pronounced focus on the fall dynamics, data from the past observation records show that the Pit water actually has markedly higher use in the spring season, with a substantial peak in April, whereas fall data show more balanced use, without a defined peak month (fig. 4). A shift in focus from bird numbers to bird mortalities tells us the miners’ observations may be on point. Early analysis shows fall 2018 had 1,372 birds with 4 mortalities, while the following spring 2019 had 5,571 birds with 5 mortalities. This shows a difference in mortality of 70% (0.3% mortality for fall and 0.09% mortality for spring), though both percentages translate over 99% success at moving birds off the Pit water. Being able to characterize the fall as a more vulnerable time for individual birds may help hone in on specific management techniques that align with the birds’ seasonal conditions. A more comprehensive analysis is forthcoming.

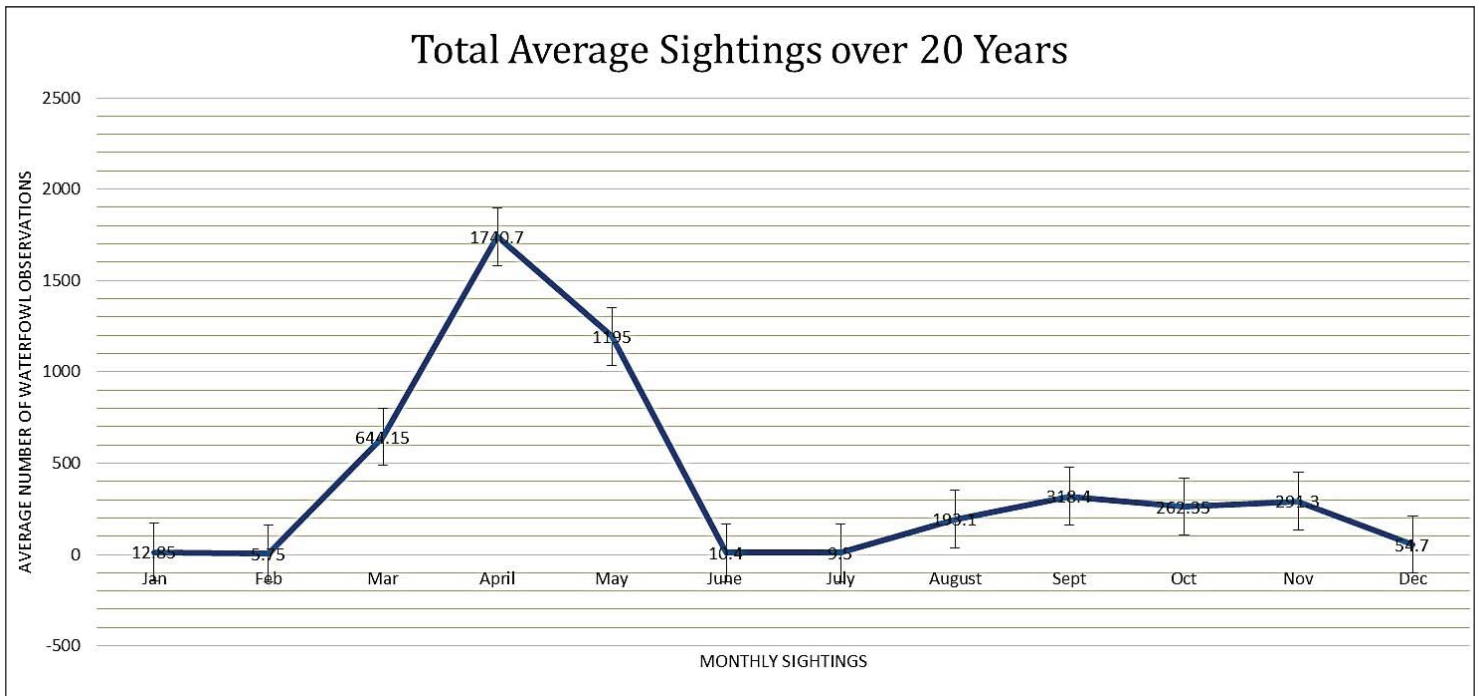






Figure 4. Total average number of bird sightings using 20 years of historical observation data at the Berkeley Pit. Figure credit: S. Capoccia.

What the previous data sets do not tell us is the species diversity. Based on the 1995 mortality event and the data records, it can be deduced that the primary focus has been on light geese and ducks. With few exceptions, most of the species accounts are recorded as simply “ducks” or “geese,” with the occasional colloquialism included as “green head” and “mud duck” and random records of the specific species: “Canada Goose,” “Snow Goose,” or “Northern Shoveler” (*Anas clypeata*). Records from Montana State show that over 50 waterfowl and waterbird species are known to commonly use water bodies in Summit Valley and the neighboring Deer Lodge Valley (MFWP, 2020). We felt that knowledge of the biodiversity would prove useful in the protection efforts, so we turned to the miners and citizen science to help collect the data.

Citizen science, training non-scientists—usually community members or project volunteers—to collect scientific data, dates back over 100 years and is thought to have been first formally utilized by the National Audubon Society for their yearly Christmas bird count. Today, citizen science is considered to be cutting edge for collecting large data sets and increasing observation points and has a growing importance in ecological studies (Cooper and others, 2007; Dickinson and others, 2012). Capitalizing on the daily observations made at the Pit, we established a standardized and rigorous bird-identification training program for the miners and other personnel who were responsible for the surveys. We developed a bird guide specific to the Pit (fig. 5) and generated new data sheets that allow those charged with observations to include their degree of confidence.

## Bird Guide to the Berkeley Pit



---


8


GADW

### Gadwall

*Anas strepera*

IUCN Conservation Status: Least Concern






**Alternate Morphs:**

- No Alternate Morph

**Similar Species: Mallard**



**Size & Shape:** Mid-large sized dabbling duck. Female and juvenile males resemble female Mallards.

**Color Pattern: Breeding Male (Left)**

- Rounded body with speckled white and black breast
- Black lower tail with bright white speculum
- Black bill
- **Thick black butt** sits high out of water

**Season:**  
 Seen breeding **mid May – July**.  
 Transient migration:  
 Arrival: **mid March – mid May**  
 Departure: **early October – mid November**.

**Female (Right)**

- Light brown body with prominent spotting
- Smaller body than male
- Yellow-brown bill

**First Year/Juvenile Mallard male**

- Lacks white speculum
- Body is not as soft as Gadwall
- **Mallard has yellow bill**
- Black eye streak is in front and behind eye on Mallard

Figure 5. Bird guide to the Berkeley Pit, an account of species most likely to use the water at the Pit for staging. The guide includes description, key identifiers, variation in plumage, seasonality, and similar species. Image credits: S. Capoccia.

Currently, we estimate 48 species may use the Berkeley Pit area for seasonal/regional activity, with April and October boasting the highest level of diversity. While light geese certainly dominate the sightings during their peak migration times, other species, such as the Canvasbacks (*Aythya vilsinera*), American Coot (*Fulica Americana*), Western Grebe (*Aechmophorus occidentalis*), and Ruddy Ducks (*Oxyura jamaicensis*) make a strong showing in other parts of the migration seasons. This species-specific knowledge has become an important component in developing strategies in the deterrent and hazing efforts and the ability to reduce mortalities. For example, the protocol for species that migrate at night is different from the day migrators, and diving birds are treated differently than dabblers, which, according to the observations, continue to appear to have a higher response rate to direct hazing with a rifle.

As data collection for the waterfowl protection plan at the Pit improves in both depth (time) and breadth (species/variables), it will be important to compare the success rates of the program before and after the 2016 light goose mortality event. As with any improvement effort, moving the needle a small percentage is often the greatest challenge. It is also important to recognize that 0% mortality should be considered an unrealistic achievement as mortality is a natural occurrence, especially for migration (Bellrose, 1968). Thus far, the efforts made on behalf of protecting the birds have been remarkable and include significant changes in birding optics, deterrent and hazing technology, and closer attention to the biology of the birds. Specifically, the attention to waterfowl trends as they occur between different species and environmental patterns is already showing improvements and strong potential to further enhance deterrent and hazing efforts. Collectively, this work shows how innovative and adaptive waterfowl management can prove vital to minimize the future loss of waterfowl likely to land on the Pit.

## References

- Adams, D. 1995, Did toxic stew cook the goose?: High Country news: Mining, December 11, 1995, <https://www.hcn.org/issues/49/1520> [Accessed February 2020].
- Bellrose, F.C., 1968, Waterfowl migration corridors east of the Rocky Mountains in the United States: Biological Notes No. 61, Illinois Natural History Survey, Urbana, IL, June 1968: Department of Registration and Education, Natural History Survey Division.
- Bruderer, B., and Salewski, V., 2008, Evolution of bird migration in a biogeographical context: *Journal of Biogeography*, v. 35, p. 1951–1959.
- Cooper, C.B., Dickinson, J., Phillips, P., and Bonney, R., 2007, Citizen science as a tool for conservation in residential ecosystems: *Ecology and Society*, v. 12, no. 2, p. 11.
- Dickinson, J.L., Shirk, J., Bonter, D., Bonney, R., Crain, R.L., Martin, J., Phillips, T., and Purcell, K., 2012, The current state of citizen science as a toll for ecological research and public engagement: *Frontiers in Ecology and the Environment* v.10, no. 6, p. 291–297, doi:10.1890/110236.
- Dubovsky, J.A., compiler, 2019, Central Flyway harvest and population survey data book: Lakewood, Colo., USFWS Division of Migratory Bird Management.
- Gammons, C.H., Metesh, K., and Duaine, T.E., 2006, An overview of the mining history and geology of Butte, Montana: *Mine Water and the Environment*, v. 25, p. 70–75.
- Montana Fish, Wildlife & Parks (MFWP), 2020, Fish and wildlife: Species of Montana: Birds, <http://fwp.mt.gov/fishAndWildlife/speciesOfMontana.html> [Accessed February 2020].
- Niraj, S.K., Dayal, V., and Krausman, P.R., 2010, Applying methodological pluralism to wildlife and the economy: *Ecological Economics*, v. 69, p. 1610–1616.
- United States Fish and Wildlife Service (USFWS), 2012, Four flyways—What a concept (Ikenson, Ben): National Wildlife Refuge System, [https://www.fws.gov/refuges/RefugeUpdate/MarApr\\_2012/fourflyways.html](https://www.fws.gov/refuges/RefugeUpdate/MarApr_2012/fourflyways.html) [Accessed February 2020].



# Adventures in Recreational Prospecting in Montana

Alma Winberry

*Owner of centralmontanaprospectorscoalition.com*

## Introduction

The general public views recreational prospecting differently than the educated geologist, mining consultant, or government worker. Recreational prospecting means they can get out in the landscape of Montana with little or no expensive equipment and have access to the minerals of our great State, legally and without much educational background. It is simply their interest in finding some treasure that motivates them and spurs them on to experience the great outdoors. Many politicians, local officials, and State and Federal agencies have their own conflicting opinions and desires concerning recreational prospecting—but there is an avenue where families can flourish and do this fun activity that involves all ages and economic status. It is simply fun. I have chronicled 4 years of this activity from mid-May until late September that anyone can access through my website, [centralmontanaprospectorscoalition.com](http://centralmontanaprospectorscoalition.com). Each year is described, logged, and elaborated on so anyone can share the experience. It's not fictitious, phony, or make believe; it is a real Montana adventure.

This website is a gift to those who would like to experience Montana's outdoor treasures. It is a non-profit organization designed to develop recreational prospecting and the pursuit of gold, gems, fossils, and other minerals. It is not commercial—it is totally an educational site.



Crystals on display at the T-Rex Agate Shop in Bynum. The shop features many Montana gems as well as fossils from around the State.

## Access to Ideas and Places to Prospect

Launching out with prospecting means fun. You are doing activities and going places you discover through networking and/or researching. Recording it means sharing it with others, which I have done by logging sites across Montana in search of gold, minerals, gems, and fossils. The first 2 years were logged with buttons that bring you to a write up of what to expect at those sites. The third year there was one write-up posted, and the last year was a quick summary of what to expect, including much happening in the month of April long before the main season started. It's all there for you to see.

## Looking for Gold

Just as our great State was founded driven by the search for gold by small parties of explorers, the penchant

for this search is still present today, only in different forms. A man in Montana who had some claims for 40 years teamed up with a few other folks, found a front-end loader and a Mine Lab 7000, went down 20 feet or so, and found \$5–10,000 worth of nuggets per day for 2 months this summer, netting them in the range of a few hundred thousand dollars in gold. Instead of filling buckets and panning the dirt, this mechanized method made their efforts worthwhile. Consideration of what tools to use and where to use them makes a huge difference in the results.

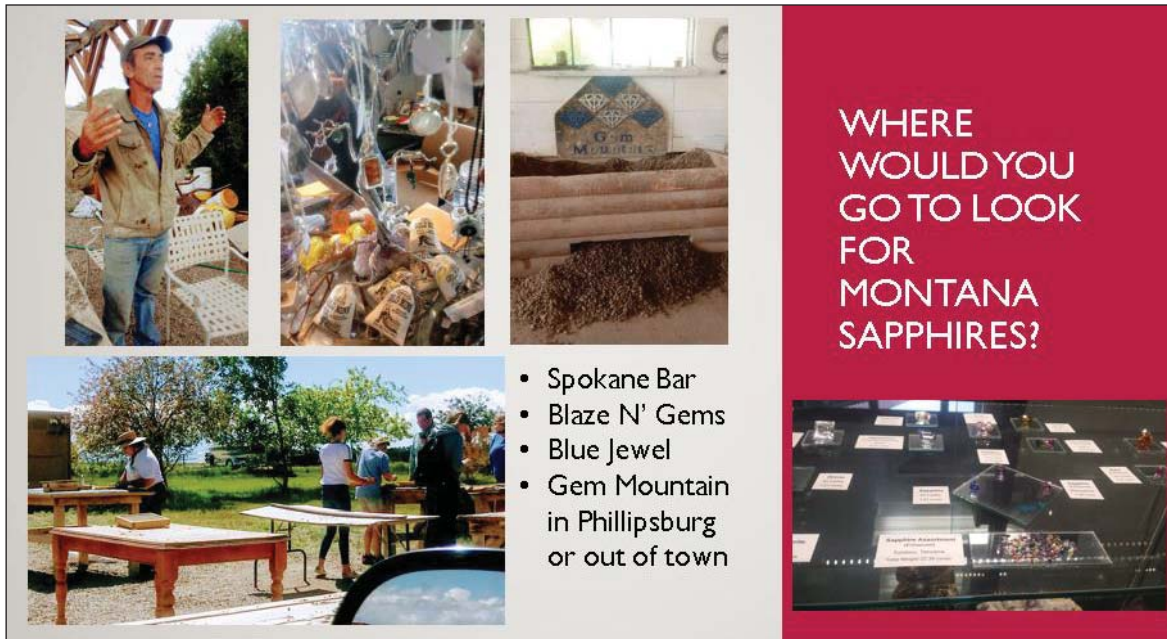
There are a wide variety of areas in Montana where the search for gold goes on every summer and people report finding success. The owner of the Gold Fox Company in Conrad has a huge stash of gold nuggets he found while prospecting in Zortman, in Phillips County, where he had access to the claims granted by the owners of the local hotel. People may gain access to these claims as people generously share their area.

Stories of local clubs that do similar sharing can be found within my website.

### The Search for Sapphires

There are a variety of places to go in search of sapphires in Montana. Spending money on buying bags or buckets of gravel doesn't necessarily net you some dandies. Using strategies in your search, luck, and carefully exploring places can work just as well. The El Dorado bar out of York in Lewis and Clark County was broken up into 20-acre plots for sale many years back. There are two active places with two different ways of obtaining the gravel yourself: Blaze N' Gems and The Blue Jewel. Reactions from visiting prospectors vary. Philipsburg in Granite County features many shops on its main street with information about sapphires, and there is a "mine" 12 miles outside of town that some have found to be be lucrative. These places are the go-to areas for beginners, visitors, and contacts. The Yogo sapphire site in Fergus County is tied up with legal and managerial issues, so it is not readily available unless you know the right person. All are worth exploring. See ideas on the treasure hunting areas on the website.

The origin of sapphires in Montana can at times be a controversial subject, as I quote on my website a Philipsburg staffer saying, "The sapphires in Philipsburg were created when a volcano spewed them into the sky and they fell down in their area, but the ones in the El Dorado bar were made from down under the earth evolving upward pushing the sapphires to the surface and makes them at the shore level, not up to the mountain."



WHERE  
WOULD YOU  
GO TO LOOK  
FOR  
MONTANA  
SAPPHIRES?

- Spokane Bar
- Blaze N' Gems
- Blue Jewel
- Gem Mountain in Phillipsburg or out of town

### Getting Garnets in Montana

You won't be finding many garnets out east or up north in Montana it seems. The place to go in search of garnets is the southwestern zone of our State. In the Alder area of Madison County, the general public can spot that red gem right on the ground at their feet, they are so plentiful. Bags of garnet gravel at the Red Rock Mine



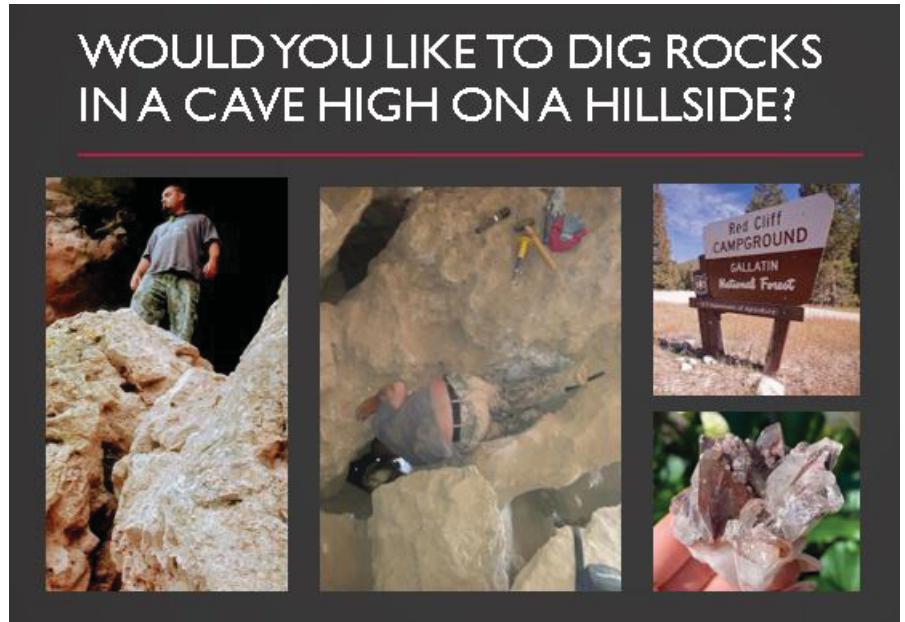
outside of Nevada City have more garnets than any place I have seen. They say they get it right from the bottom of the creek across the road. The roadside along the trail to Ruby Reservoir is said to be as plentiful. All along the shore of Ruby Reservoir the small, red pieces are common. The conditions for creating garnets from the earth are so prevalent in this area. Go southwest if you want garnet. Even though you can find them in your gravel wash in Philipsburg, the prospects for garneting is best out of Alder.

**Rockhounding for Other Minerals Also**

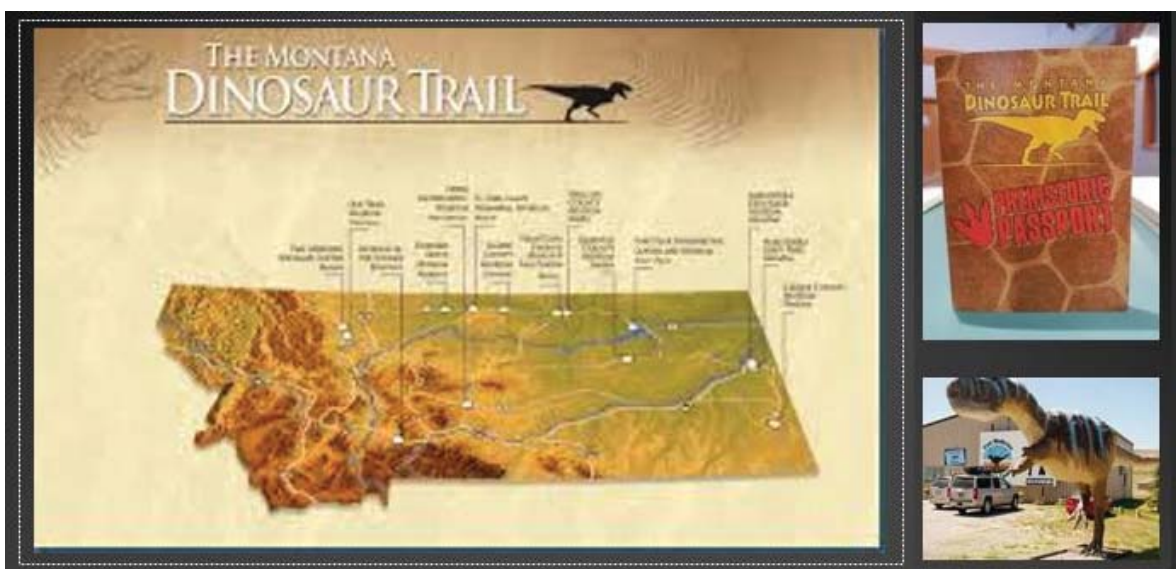
Finding self-taught folks who avidly rockhound is an invaluable resource. Andrew Luna on Facebook is a great one to contact because he knows so many sites that are lucrative, such as when you can find agates sticking right out of the hillside at Canyon Ferry Reservoir, dogtooth calcite from Red Cliffs Campground, or barite along the highway. The crystals he can pull out of their underground nest are found in many places across this land. He goes after fluorite too. It's all logged on my website.

**The Role of Fossils in Prospecting Searches**

The hot item at the gold dig in Zortman every year is more than the shiny mineral; it is what you can find at the local dump. The hillside that is awash every year with the runoff shores up large amounts of fossils of all sorts that are prizes for those with a keen eye. The finds show off a rich history of being underwater with the remnants of sea creatures and crystals. Such finding is fun, but so is the completion of the dinosaur trail booklet when one goes to all the dinosaur museums across the State. The result of your journey is the signature and letter from the Governor when you complete and submit it. So much geological and paleontological history can be found along the dinosaur trail. Bynum, Montana, in Teton County, is a perfect example of the knowledge that can be found, as well as at the Museum of the Rockies in Bozeman with its rich history of this State's former lives.



Red Cliff campground out of Big Sky offers an opportunity to hammer dogtooth calcite from a cave. Access to the entrance of the cave is by trail from the Red Cliff Campground.



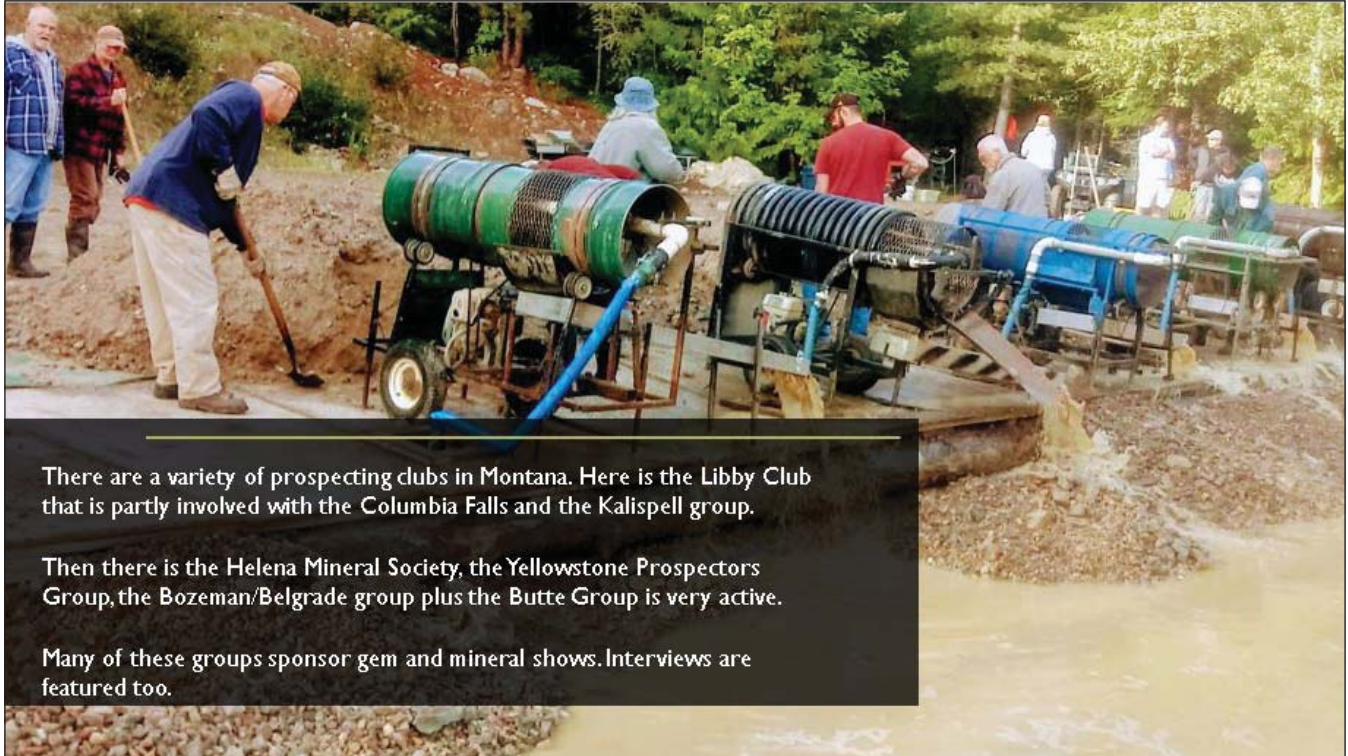
There is a "dinosaur passport" that anyone can get stamped by visiting Montana's dinosaur museums...and the Governor will sign it!



## Mining Networking

Shops, shows, museums, groups, and government are all sources for information. The experiences of other recreational prospecting people are shared during group digs. This is very helpful for progress in recreational mining pursuits. Even this symposium has generated ideas for future and possible sites for exploration.

GPAA and the Mining and Mineral Advisory Council will help in dealing with issues pertaining to claims and dealing with the government. Many resources can be found in a variety of areas on my webpage.



There are a variety of prospecting clubs in Montana. Here is the Libby Club that is partly involved with the Columbia Falls and the Kalispell group.

Then there is the Helena Mineral Society, the Yellowstone Prospectors Group, the Bozeman/Belgrade group plus the Butte Group is very active.

Many of these groups sponsor gem and mineral shows. Interviews are featured too.

## Governmental Participation

One time when Governor Steve Bullock came to Great Falls, I had the opportunity to talk with his advisor. I said to him, “Because you don’t designate recreational prospecting as a legitimate activity in Montana, even though the State owns Virginia City and Nevada City along with Crystal Park, which is all about recreational prospecting, you don’t keep track of the data as to the economic impact for the State. I went to Zortman with hundreds of ATVs, crawling all over the hilltops with people from all over the country. Recreational prospecting is a huge income for Montana.”

On my website one can see what was done with the legislature to try and change things in Montana. One year, when I explained to an out-of-state visitor that in order to do recreational prospecting one had to be lumped into commercial mining, he said to me, “That’s like asking a recreational fisherman to get a commercial fishing license to fish.” These are two completely different things, which many other states and Canada recognize, yet Montana doesn’t and refuses to consider. The general public accepts the differences, but not the infrastructure. The bill presented at the legislature is posted on the webpage.

At times, the Governor and his staff have been helpful in resolving cases of public access to claims and dealing with the illogical behavior of those in the U.S. Forest Service. Listed on the website are some of the issues.

National mining groups can help the recreational prospector, because things have changed elsewhere. With the Forest Service being under the Department of Agriculture, they want management over forest roads and the closing of them conflicts with access to claims which are guaranteed to the prospector.

## What Rocks Bring to Your Plate

When one works with the public regarding rocks, one finds out quickly that there is often a passion of connection. Many people hold rocks dear to their heart and go out in search of their favorite. There are a variety of topics on my webpage regarding rocks that I have found to be of interest to many, including kids, fossils, newsletters, making equipment, tools of the trade, state rock clubs and organizations, historical topics, prospecting stories, book reviews, some green prospecting information, and educational inserts.

Healing aspects of stones and minerals can also be found on my website. It is a popular source of information to many and I have found success with some of the information available there.

### Rock Love Launches Interests in a Variety of Areas

Take the map of Montana and see what you can do to find some of our great resources. Look around and talk with others. Set up a Farmer's Market booth, as such booths help disseminate good information about prospecting, and I have a kid I am sponsoring to do one next year.

I have done 5 years of one-person art shows at the Great Falls Public Library with lots of prospecting sculptures, photos, and displays regarding our Montana cultural heritage of recreational prospecting. I even did a crystal castle with a summer reading program tied to the levels that kids could participate in research about recreational prospecting. We have Urban Art Project windows in downtown Great Falls in which I have displayed many art installations promoting recreational prospecting. Lots of sources of advertising rocks are available in the public sector.

Prospecting can be an adventure in so many ways. People enjoy it and gain many benefits in their lives. Supporting it can bring much joy. Give yourself permission to explore with it.

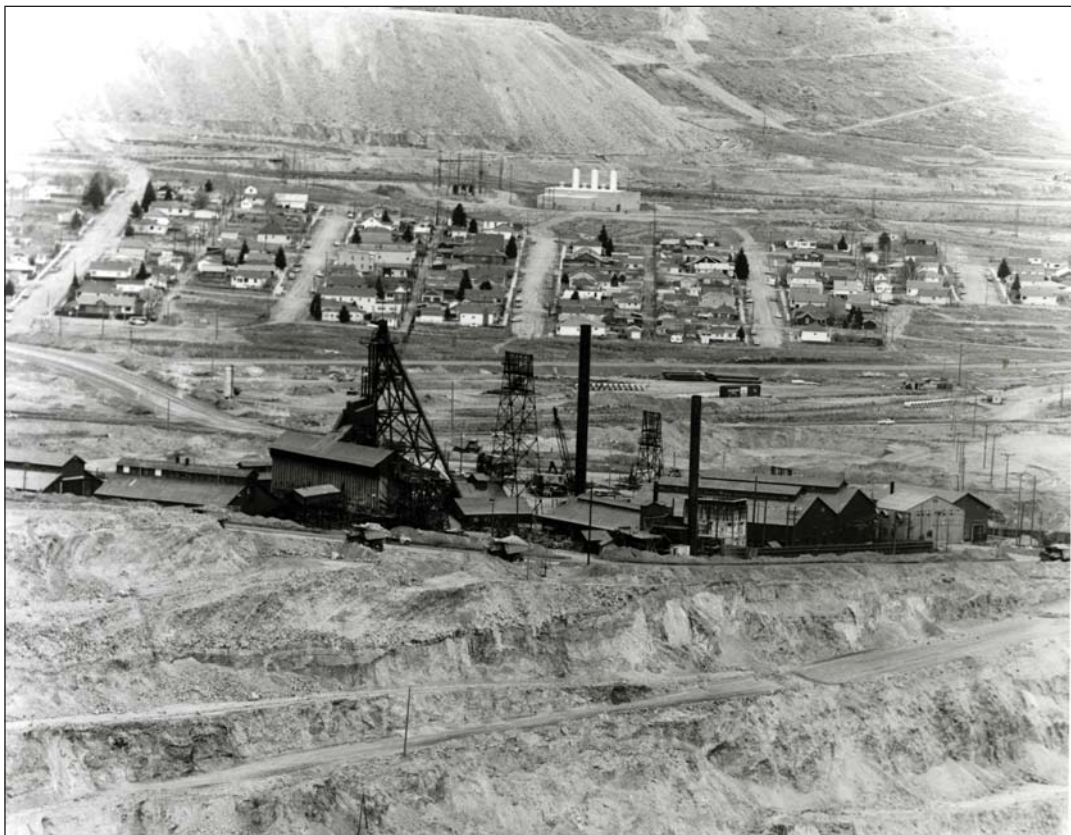


Calcite from Alzada; Carter County, MT. Courtesy of Michael J. Gobla.





The Golden Sunlight Mine located at the southern end of the Bull Mountains. Courtesy of Patrick E. Dawson.



East edge of Berkeley Pit 1956 and Meaderville in background. The mine in the photo, the Leonard, is in the process of being torn down for the Berkeley Pit. Courtesy of the World Museum of Mining; Butte, MT.



# Ultraviolet Fluorescence of Montana Sapphires

Bruce E. Cox<sup>1</sup> and Richard B. Berg<sup>2</sup>

<sup>1</sup>*Geologist/Consultant, Missoula, Montana*

<sup>2</sup>*Research Geologist Emeritus, Montana Bureau of Mines and Geology, Butte, Montana*

## Abstract

Corundum commonly displays fluorescence when exposed to ultraviolet light. This phenomenon has been described in gem and non-gem sapphires from mining districts worldwide, and Montana sapphires are no exception. Sapphires from three of Montana's principal sapphire mining districts were examined using a binocular microscope under incident white and long wave (365 nm) ultraviolet light sources (LW UV). Specimens were graded for ultraviolet color and intensity and submitted to a commercial lab for heat treatment. Analytical results indicate a high-intensity LW UV light source can be used to improve recognition of gem-quality sapphires in screen, sluice, and jig concentrates. Ultraviolet lamps may also have application for recognition of corundum-bearing bedrock source terrains.

## Ultraviolet Fluorescence Phenomena

Intense red ultraviolet fluorescence of ruby corundum is well documented in stones from worldwide localities and may be ubiquitous (figs. 1a,b). Chromium+2 is the probable elemental activator for this fluorescence, but magnesium and iron may have a contributing effect (Robbins, 1994). Fluorescent intensity may vary with the thickness (size), translucence, or crystallographic orientation of individual stones.

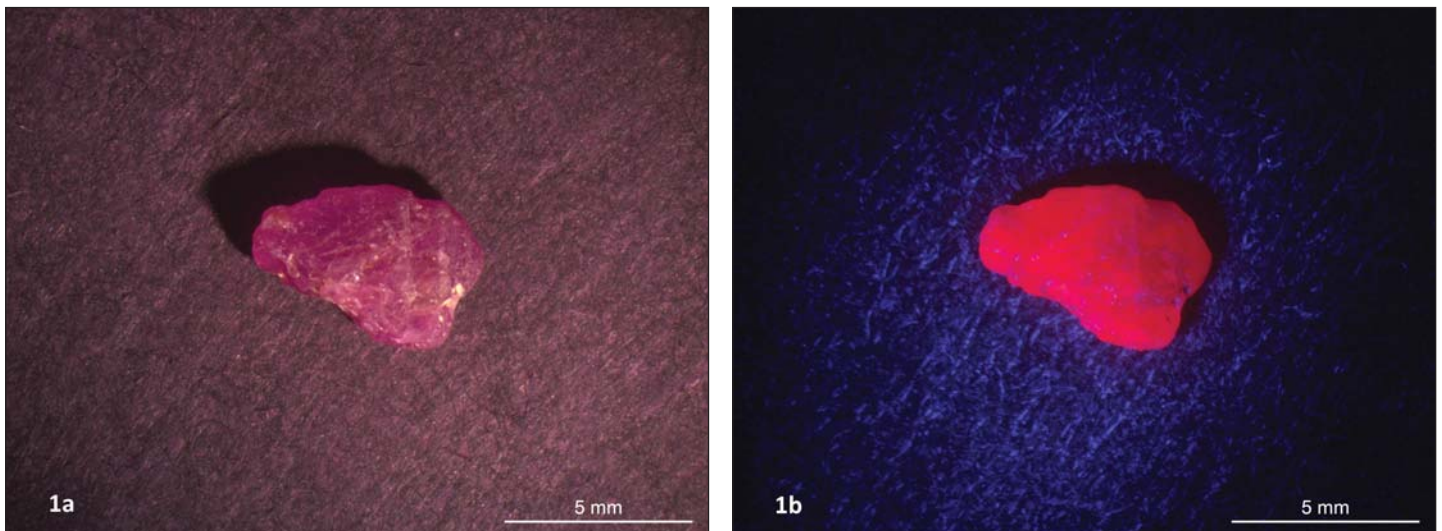


Figure 1. Sapphire from Quaternary alluvium, Cowee Valley, Franklin, North Carolina: (a) incident white illumination; (b) LW UV illumination.

## Montana Sapphire Mining Districts

Sapphires from the Rock Creek, Dry Cottonwood Creek, and Eldorado Bar mining districts (fig. 2) were examined for this study. The mining history and geologic context of these districts have been carefully described in numerous reports, most notably by Berg and Landry (2018) and Berg (2007, 2014). Suites of stones for each district were provided by current and historic mine operators from their sluice or jig concentrates. One suite from Eldorado Bar was collected from an active mine face in virgin ground.



Figure 2. Map of Montana showing location of principal sapphire mining districts.

### Study Objectives and Methods

Principal objectives were the following:

- Describe correlations, if any, between sapphire color under incident white light vs. LW UV fluorescent light.
- Describe the degree of UV color saturation, i.e., uniform color through the stone or color segregated into domains (possibly related to trace element concentrations and/or crystallographic orientation).
- Describe changes in UV color and intensity after heat treatment, if any.
- Compare/contrast above results between mining districts.
- Assess the utility of LW UV for grading mine-run concentrates and for exploration.

Each sapphire suite was examined and photographed using a Leica 164C binocular microscope under incident white and long wave (365 nm) UV illumination. The UV light source was a high-intensity Nichia Convoy flashlight, which was chosen for its compactness, intensity, and potential utility for examining mine run concentrates. Illumination under short wave (254 nm) UV was not addressed since compact high-intensity short wave lamps are not yet available.

Stones of each suite were selected to show the range of UV fluorescence prior to heat treatment. Five sapphire suites were heat treated in an oxidizing furnace between 1300 and 1500 degrees centigrade.

## Observations

Results of this study are empirical and qualitative to match the objective of serving the mine operator and explorationist for low-cost field recognition and grading of sapphires. Principal observations make reference to figures 3, 4 and 5 and are the following:

- Longwave ultraviolet fluorescence may aid recognition of sapphires in sluice or jig concentrates, especially small stones that might be otherwise discarded.
- A majority of sapphires from each district displayed moderate-to-strong fluorescence.
- Intensity of sapphire fluorescence has no apparent correlation with color enhancement after heat treatment.
- Sapphire fluorescence (at 365 nm) was not diminished by heat treatment.
- Fluorescence of non-gem-quality detrital corundum from the Ruby Range in Madison County suggests that UV fluorescence may aid exploration for sapphire source terrains.

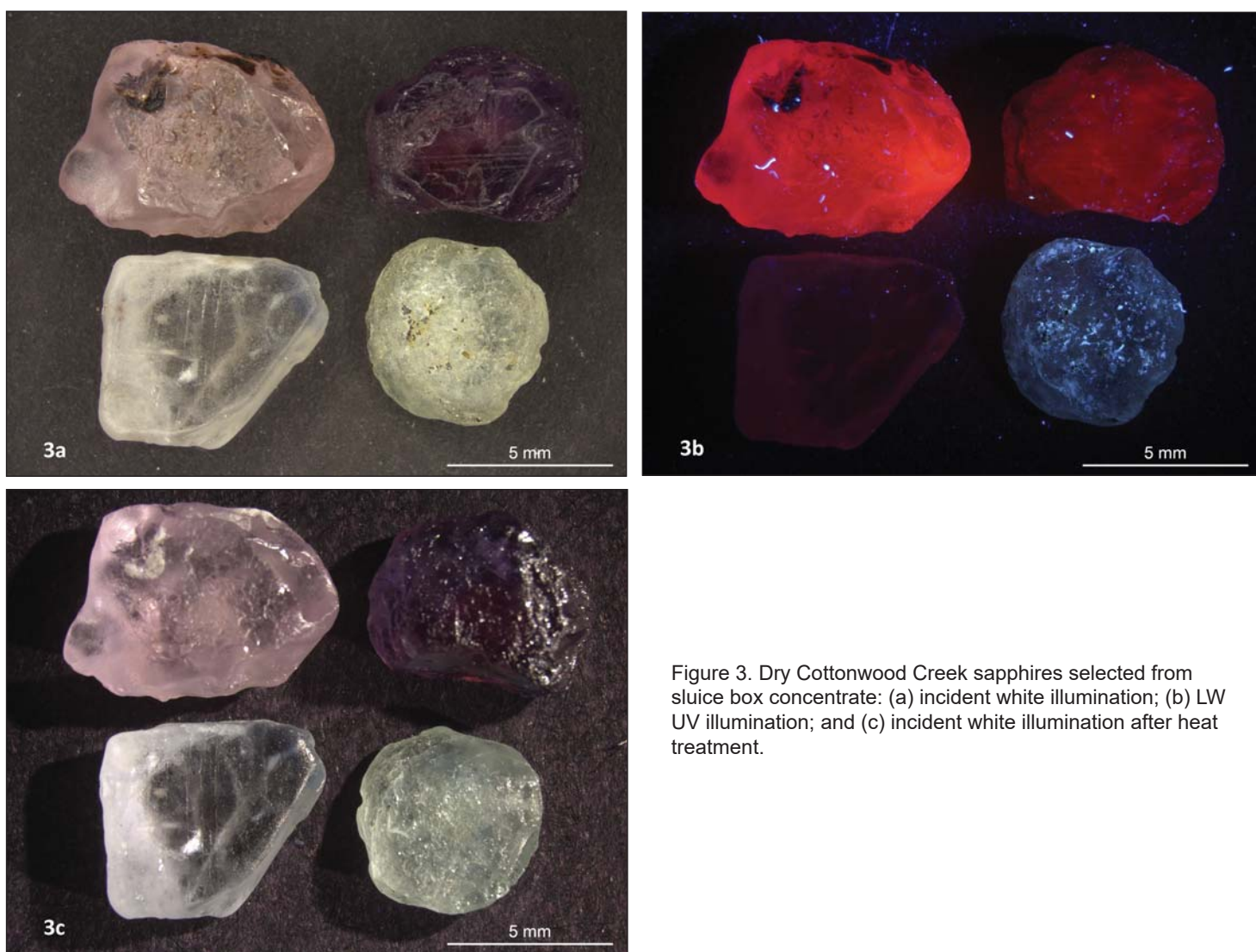


Figure 3. Dry Cottonwood Creek sapphires selected from sluice box concentrate: (a) incident white illumination; (b) LW UV illumination; and (c) incident white illumination after heat treatment.



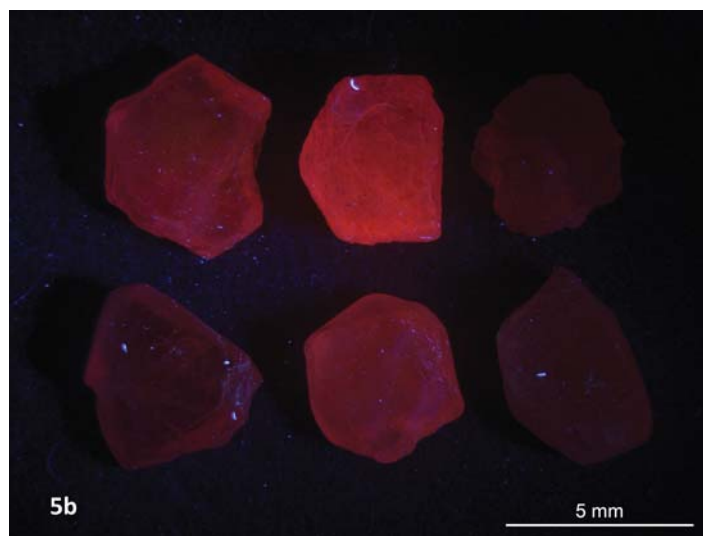
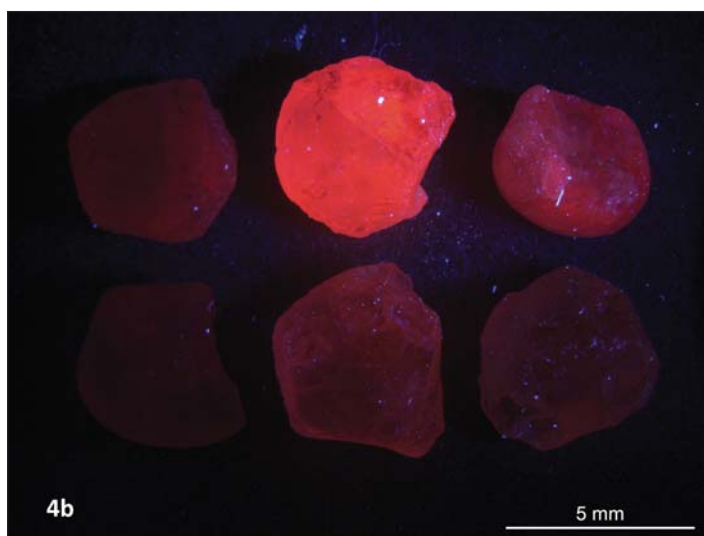


Figure 4. Rock Creek sapphires selected from jig concentrate: (a) incident white illumination, (b) LW UV illumination, (c) incident white illumination after heat treatment. The upper left and lower right stones yielded strong color change after heat treatment but did not display the strongest fluorescence.

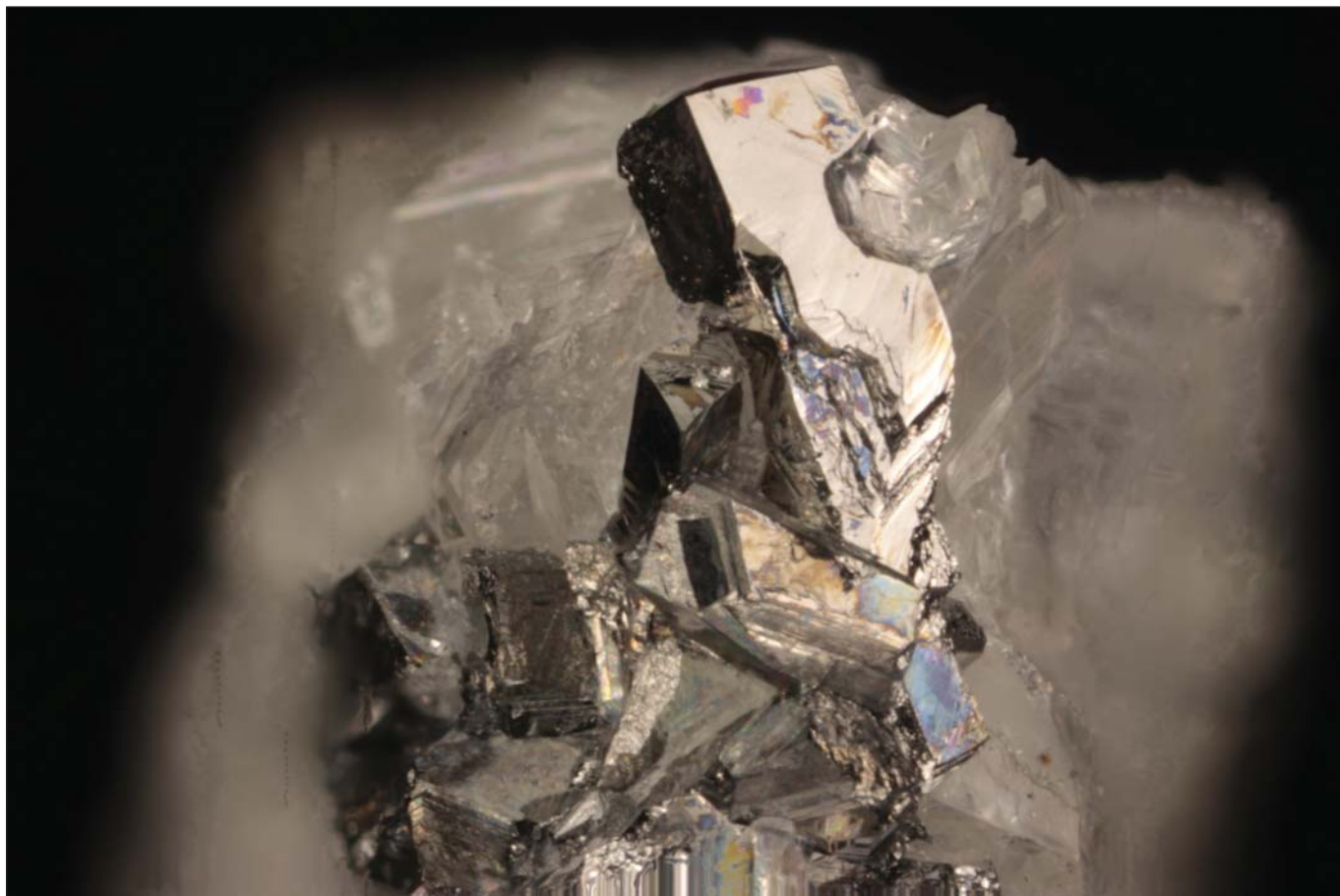
Figure 5. Rock Creek sapphires selected from jig concentrate: (a) incident white illumination; (b) LW UV illumination; (c) plain light illumination after heat treatment. Note the strong color change in the bottom center heat-treated stone.

### Acknowledgments

Neal Hurni and Blaze Wharton graciously provided access to their Eldorado Bar properties and sapphires for examination. Ted Antonioli provided Rock Creek sapphire concentrates from the family archive. Claudia Bielenberg Thorsrud and Peter Meistrick provided access to the Dry Cottonwood properties and samples, respectively. Gary Carlson provided access to concentrates from the Lowland Creek sapphire workings. Dale Siegford performed heat treatment on five selected suites and provided much insight on heat treatment methods and potential ambient color and ultraviolet color activator elements.

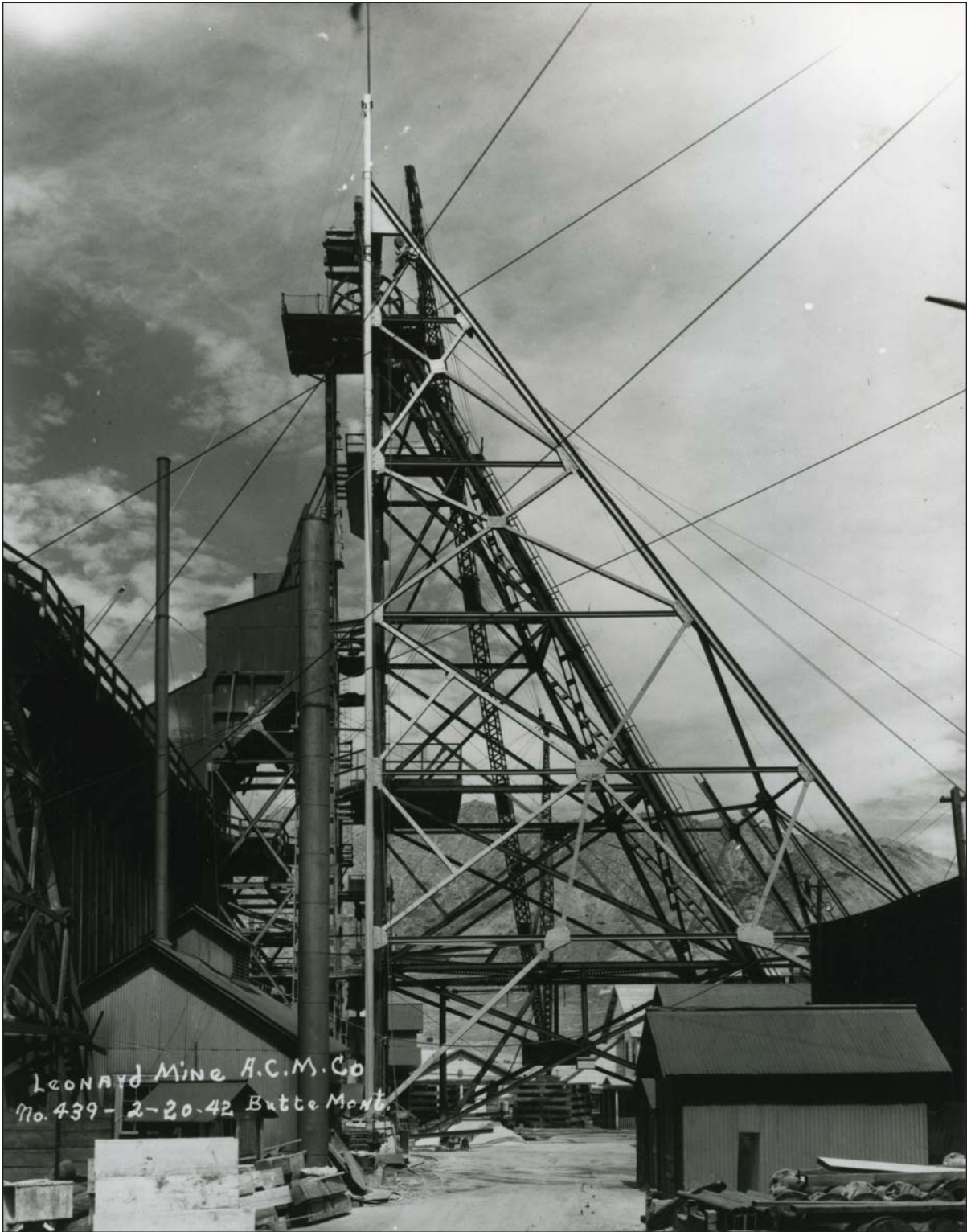
### References Cited

- Berg, Richard B., 2007, Sapphires in the Butte–Deer Lodge area, Montana: Montana Bureau of Mines and Geology Bulletin 134, 28 p.
- Berg, Richard B., 2014, Sapphires in the southwestern part of the Rock Creek sapphire district, Granite County, Montana: Montana Bureau of Mines and Geology Bulletin 135, 86 p.
- Berg, R.B., and Landry, M.T., 2018, Sapphire deposits along the Missouri River near Helena, Montana: Montana Bureau of Mines and Geology Bulletin 136, 52 p.
- Robbins, Manuel, 1994, Fluorescence: Gems and minerals under ultraviolet light; Geoscience Press, 384 p.



Arsenopyrite from the Emery Mine, MT. Courtesy of Michael J. Goble.





The Leonard #2 shaft headframe, 1942. Courtesy of the World Museum of Mining; Butte, MT.



## Green Pipestone North of Twin Bridges, Madison County, Montana

Ted Antonioli

*Geologist, Contact Mining Company, Philipsburg, Montana*

A narrative account and two maps by fur trappers and missionaries note a source of “green pipestone” a short distance north of Twin Bridges, Madison County, Montana (Ferris, 1940; De Smet, 1851; De Smet and Bridger, 1851). The narrative account is by fur trapper Warren Angus Ferris, written in the 1830s and published more than a hundred years later (Ferris, 1940). Ferris states that there is an occurrence of green pipestone located 15 miles north of Beaverhead Rock, on a bluff overlooking the Jefferson River. Ferris was not a surveyor and it appears his distance is short by approximately 5 miles. Maps made by Jim Bridger and Pierre De Smet, S.J., given to the U.S government in 1851 to use in treaty negotiations, and now available digitally from the Library of Congress collection, also show “green pipestone” just west of the Jefferson River, a short distance north of where the town of Twin Bridges, Montana, would be founded by later pioneers (fig. 1).

De Smet travelled through this part of the Jefferson River Valley in the early 1840s, but his published journals from this timeframe do not mention the green pipestone quarry. His fellow Jesuit, Nicolas Point, S.J., also traversed the Jefferson River Valley. His illustrated journal, which he created from notes and sketches made

during the early 1840s, contains a detailed discussion of the mixture of tobacco and kinnickinic smoked in peace pipes, as well as the ceremonial and social purposes of pipe smoking among several native tribes. His journal also contains numerous color paintings that include “calumets” or ceremonial pipes (Point and Donnelly, 1968). However, Point also does not note any quarry of green pipestone. It would appear the Jesuits, in particular Fr. De Smet, learned of the pipestone locality only after the period when he and Fr. Point were assigned to the Montana missions. His information source appears to be the sketch map provided him by Jim Bridger, a close personal friend of De Smet.

The term “pipestone” is used to refer to any rock used by the Native Americans to make peace pipes. The geology and geography of the area north and west of Twin Bridges indicates that the most likely source of the “green pipestone” is at or near the Golden Antler chlorite mine near Silver Star (fig. 2; O’Neill, 1996). At the Golden Antler mine, hydrothermal veins of massive green chlorite



Figure 1. Part of map by Pierre De Smet, S.J., 1851, retrieved from Library of Congress website. Jefferson River just west of site marked “Green Pipestone Rock. Just to south the “Stinking R” enters from the east.” The modern name of this river is the Ruby River, and the junction is at Twin Bridges, Montana.



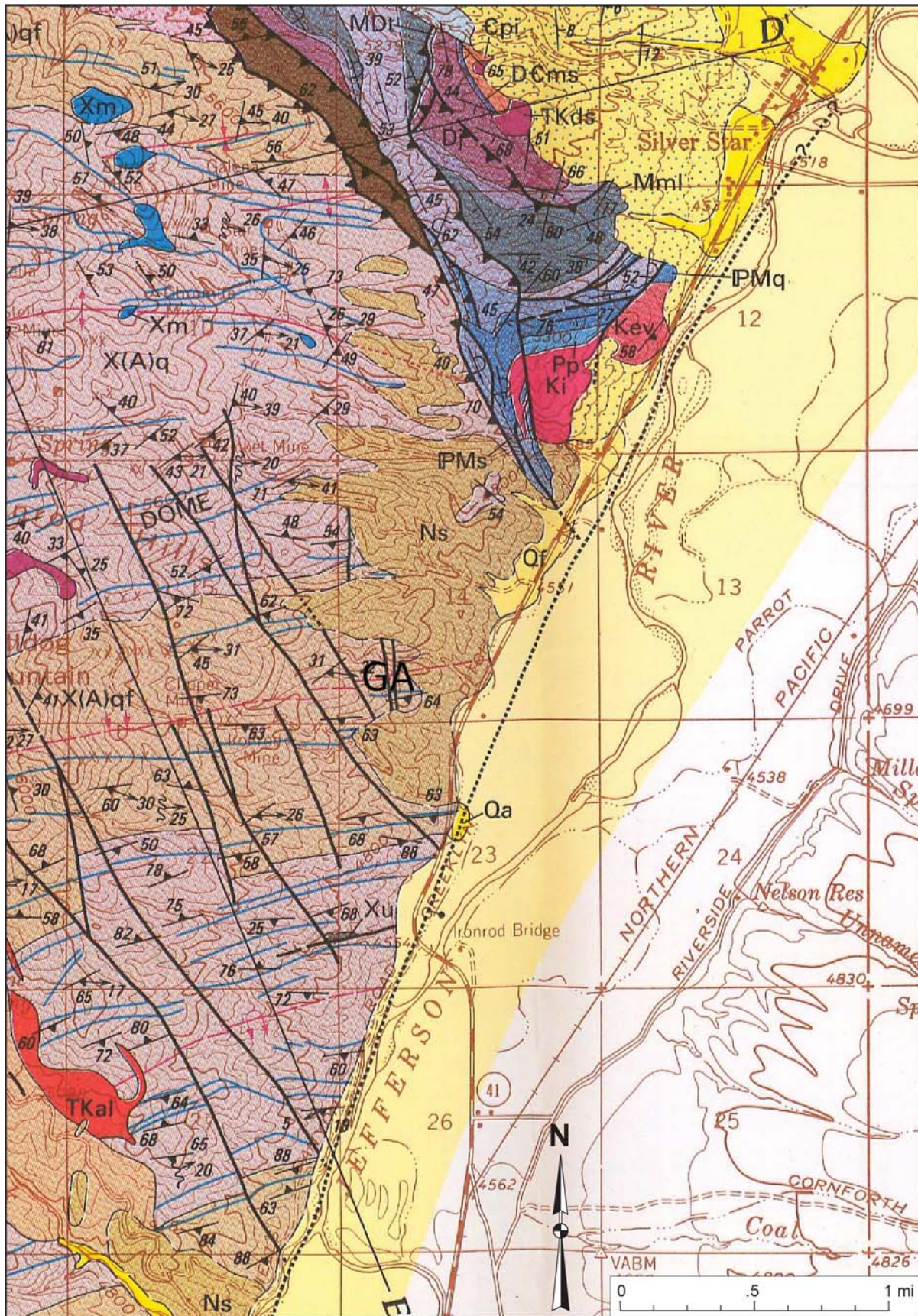


Figure 2. Map excerpt from O'Neill and others (1996), with position of Golden Antler mine marked "GA." Bedrock unit is Early Proterozoic and Archean quartz-feldspar-biotite gneiss.



were mined by Cyprus and processed at their Three Forks talc processing facility (Berg, 1979). A portion of the massive chlorite is carvable (fig. 3).



Figure 3. Pipe carved from Golden Antler chlorite by Bruce Cox, 2019.

A possibly related reference to a peace pipe appears in the Journals of Lewis and Clark (Lewis and others, 2002). In August 1805, when Meriwether Lewis met Cameahwait, the Shoshone chief who was Sacagawea's brother, they smoked a peace pipe made from a green translucent rock, which from the description could be chlorite such as that in the Golden Antler deposit. Thanks to Dick Berg, Bruce Cox, and Steve Antonioli for many useful discussions of this occurrence, and to Kaleb Scarberry and Susan Barth for help on the figures.

### References

- Berg, R.B., 1979, Talc and chlorite deposits in Montana: Montana Bureau of Mines and Geology Memoir 45, 66 p., 3 sheets.
- De Smet, P., 1851, Map of the upper Great Plains and Rocky Mountains region: Retrieved from the Library of Congress, <https://www.loc.gov/item/2005630226/> [Accessed February 2020].
- De Smet, P., and Bridger, J., 1851, Chart of the head of Yellow Stone: Jesuit Archives Digital Collections and Resources, <https://jesuitarchives.omeka.net/items/show/263> [Accessed February 2020].
- Ferris, Angus W., 1940, Life in the Rocky Mountains: A diary of wanderings on the sources of the rivers Missouri, Columbia, and Colorado from February, 1830, to November, 1835, Hathi Trust: Denver, Colo., F. A. Rosentstock, The Old West Publishing Company.
- Lewis, M., Clark, W., Moulton, G.E., and Dunlay, T.W., 2002, The definitive journals of Lewis & Clark: Through the Rockies to the Cascades: Lincoln, Nebr., University of Nebraska Press.
- O'Neill, J.M., Klepper, M.R., Smedes, H.W., Hanneman, D.L., Fraser, G.D, and Mehnert, H.H., 1996, Geologic map and cross sections of the central and southern Highland Mountains, southwestern Montana: U.S. Geological Survey Miscellaneous Investigations Map I-2525, scale 1:50,000.
- Point, N., and Donnelly, J.P., 1968, Wilderness kingdom: Indian life in the Rocky Mountains, 1840–1847: The journal & paintings of Nicholas Point, S.J.: London, Michael Joseph.





Montana sapphires. Courtesy of Alma Winberry.

# Mineralogy of Montana Iron Skarn Deposits

Michael J. Gobla

*Engineer, U.S. Department of the Interior, Bureau of Reclamation, Denver, Colorado*

The term “skarn” was originally used in a publication by Swedish geologist A.E. Tornebohm in 1875 in describing the silicate gangue associated with iron-ore bearing metal deposits formed in a calcareous iron formation. In modern usage, skarns are coarse-grained rocks containing calcium silicate minerals formed by a variety of metasomatic processes involving fluids of magmatic, metamorphic, meteoric, or marine origin. Although the modern use of the term allows for a broad manner of skarn formation in all types of rocks, the deposits from Montana described in this paper are metamorphic rocks formed at and near the contact of an igneous intrusion with a carbonate sedimentary rock such as limestone or dolomite. As the igneous rock cools, it releases heat and acidic fluids that thermally alter and chemically react with the intruded rocks forming the skarn minerals. Fracturing of the rocks and circulation of mineralized hydrothermal fluids are essential to mineral formation. Where the intrusions are dry, the carbonates are thermally converted to marble with little formation of other minerals. If fracturing is not extensive, the skarn deposits are small in extent.

## Types of Skarns

Skarns can form in both the igneous intrusive rock (endoskarn) and the adjacent carbonate sedimentary rock (exoskarn). Skarns can form economically important metal deposits and have been classified into seven economic types. From simple to complex, they are: iron, gold, copper, zinc, tungsten, molybdenum, and tin skarns. In Montana, iron, gold, copper, and tungsten skarns have been mined. Skarns can also be classified on the basis of the sedimentary rock as either calcic skarns derived from limestone or magnesian skarns derived from dolomites. The typical mineralogy of these two types of skarn are different (Meinert, 1992). In calcic iron skarns, the typical minerals include: andradite, anorthite, actinolite, clintonite, epidote, grossular, magnetite, muscovite, tremolite, and vesuvianite. In magnesian iron skarns, the typical minerals include: calcite, chlorite, chondrodite, clinocllore, diopside, fluorapatite, forsterite, hematite, humite, lizardite, ludwigite, magnetite, phlogopite, spinel, and talc, with minor amounts of galena, sphalerite, epidote, andradite, and grossular.

Skarns are also of great interest to mineralogists and mineral collectors due to the large grain size and well-formed crystals that typically occur. Montana has several skarns that are renowned by mineralogists for the prolific amount of crystals that have been produced and made their way into mineral collections. The best known are the Calvert tungsten mine, famous for large crystals of epidote, and the Crazy Spinx mine, which does not contain metals, but is known for its blue-colored octahedral crystals of spinel (Knudsen, 2011). Less well known are Montana’s iron skarn deposits, which also have produced interesting minerals.

## Rothfuss Iron Mine, Broadwater County, Montana

The Rothfuss Iron mine is located in sec 19, T. 5 N., R. 1 W., in the Radersburg district of Broadwater County. The mine, established on six unpatented claims called the North Star group, is located about 6 mi west of Radersburg. The mine was owned and operated by John Rothfuss of Boulder, Montana, who sent the ore to the Anaconda smelter for use as flux in smelting copper ore (DeMonk, 1956). The deposit was first worked in 1897 as a small underground gold mine. Rothfuss recognized its potential as an iron mine. It was initially developed by a 600-ft-long adit. The ore was extracted from underground stopes, some of which caved to the surface. There also were two small open cut excavations (fig. 1). Most of the production occurred from 1908 to 1910, when 75,000 tons of ore was produced from four ore zones. The total production of the mine is not known, and it last produced ore in 1929. The ore averaged 60% iron and contained \$1.50 per ton in gold along with about 1 oz of silver per ton and up to 4% copper (Reed, 1951).

It is a calcic iron skarn with massive magnetite formed in Cambrian limestone in contact with diorite dikes. The mineralogy is simple and is summarized in table 1. Interesting microcrystals of calcite, grossular (fig. 2), hematite, magnetite, malachite (fig. 3), and pseudomorphs of chrysocolla after malachite occur (fig. 4).





Figure 1. One of the open cut excavations at the Rothfuss Iron Mine, Broadwater County, Montana.

Table 1. Minerals of the Rothfuss Iron mine, Broadwater County, Montana

| Mineral Name | Formula  | Nature of Occurrence  |
|--------------|--|---|
| Calcite      | $\text{Ca}(\text{CO}_3)$   | As small masses and rarely as colorless transparent to opaque white scalenohedral microcrystals.  |
| Chrysocolla  | $(\text{Cu}_{2-x}\text{Al}_x)\text{H}_{2-x}\text{Si}_2\text{O}_5(\text{OH})_4 \cdot n\text{H}_2\text{O}$ | In massive magnetite, as small masses, thin fracture fillings, and pseudomorphs after malachite microcrystals with a radiating form.  |
| Diopside     | $\text{CaMgSi}_2\text{O}_6$  | Observed as small masses in the wall rocks of the deposit.  |
| Epidote      | $\text{Ca}_2(\text{Al}, \text{Fe}^{3+})[\text{Si}_2\text{O}_7][\text{SiO}_4]\text{O}(\text{OH})$         | Small fine-grained masses and microcrystals.  |
| Grossular    | $\text{Ca}_3\text{Al}_2(\text{SiO}_4)_3$   | Mostly massive grossular garnet is present in the wall rocks and occasionally occurs with the massive magnetite. Some orange-brown colored microcrystals occur in small vugs in the massive garnet. |
| Hematite     | $\text{Fe}_2\text{O}_3$  | As reddish-black colored masses with a platy texture, rare as microcrystals forming thin plates in calcite.   |
| Lizardite    | $\text{Mg}_3\text{Si}_2\text{O}_5(\text{OH})_4$  | Uncommon as small masses with magnetite.  |
| Magnetite    | $\text{Fe}^{+2}\text{Fe}^{+3}_2\text{O}_4$   | As masses, rarely as octahedral microcrystals, uncommon as masses with a platy texture.   |
| Malachite    | $\text{Cu}_2(\text{CO}_3)(\text{OH})_2$  | Thin crusts coating fractures in massive magnetite, rare as radiating aggregates of microcrystals.  |
| Pyrite       | $\text{FeS}_2$   | Massive grains of pyrite occur with magnetite and chrysocolla.  |
| Quartz       | $\text{SiO}_2$   | As small masses and microcrystals in the wall rocks associated with grossular.  |



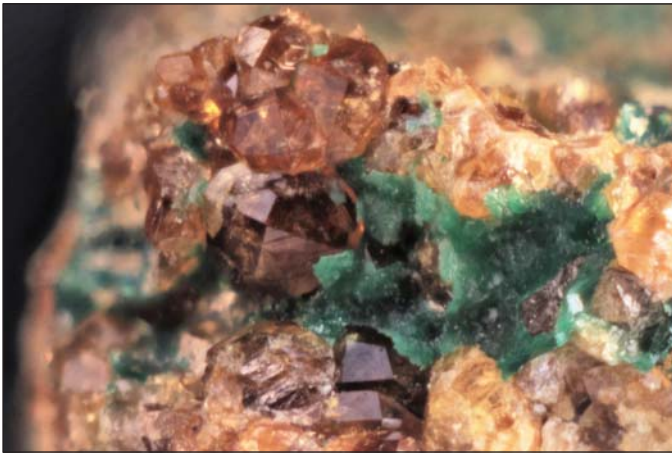


Figure 2. Grossular microcrystals with malachite, Rothfuss Iron Mine, Broadwater County, Montana.



Figure 3. Malachite microcrystals, Rothfuss Iron Mine, Broadwater County, Montana.



Figure 4. Blue-colored chrysocolla replacing green-colored malachite microcrystal aggregate, Rothfuss Iron Mine, Broadwater County, Montana.

### Pomeroy Mine, Deer Lodge County, Montana

The Pomeroy mine is located in sec. 9, T. 5 N., R. 13 W., in the Georgetown district about 1,400 ft southeast of the famous Southern Cross gold mine. The deposit consists of several patented claims that were discovered by a man named Pomeroy in 1866, with initial production of iron ore in 1870. Development was by an adit (now caved) using the glory hole method of extraction, which left three small open pits. A larger fourth pit, now partly backfilled, was created by surface excavation. A map of the mine is shown in figure 5, and a photograph of the number 2 pit is shown in figure 6. The mine was last operated in 1942 (Wimmler, 1946). The iron ore was shipped to the Anaconda smelter for use as flux in processing copper ore, but the total production is not known.

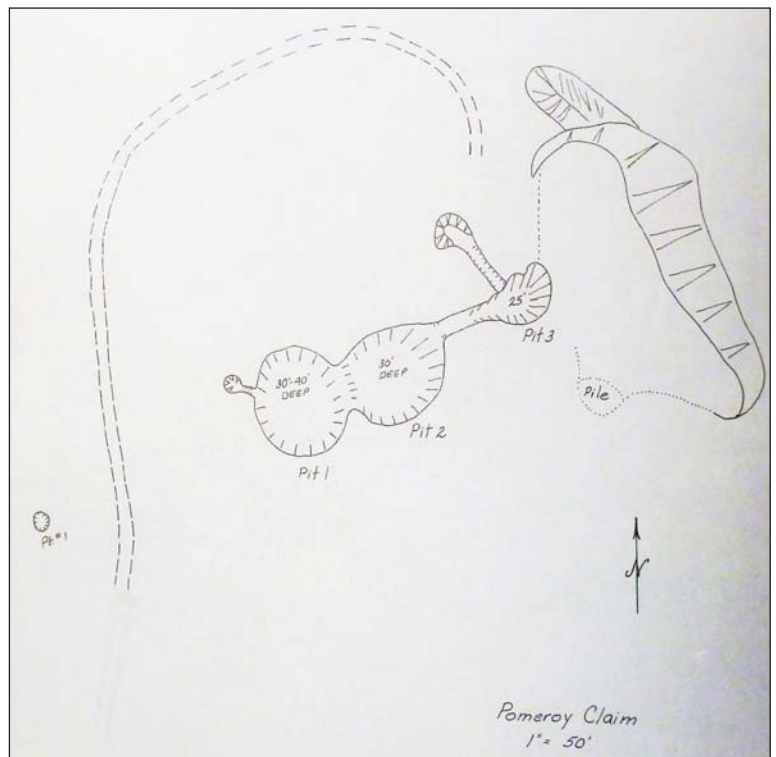


Figure 5. Plan view sketch map of the Pomeroy mine, Deer Lodge County, Montana, showing the arrangement of the pits.





Figure 6. The number 2 pit at the Pomeroy mine, Deer Lodge County, Montana, that produced the large crystals of magnetite.

The deposit at the Pomeroy mine is a magnesian iron skarn formed at the contact of the Cambrian-age Pilgrim dolomite that was intruded by the Cretaceous-age Uphill Creek granodiorite. The mineralogy is summarized in table 2. The mine is of great interest mineralogically because of the large crystals of magnetite that have been collected from the site (fig. 7) and because of the occurrence of the uncommon borate mineral ludwigite (fig. 8). Ludwigite was discovered in the early 1960s by Laszlo and Frank Dudas in a shallow roadcut in the mine access road (Dudas, 2015). It occurs in two thin black-colored bands in a white marble and varies from mostly magnetite with minor amounts of ludwigite to nearly solid aggregates of ludwigite crystals up to 5 cm long. Little of the ludwigite remains at the site. The mine also hosts crystals of clinocllore up to 1 cm in diameter (fig. 9), and a few specimens of lizardite, confirmed by x-ray diffraction analysis (fig. 10). Unique specimens of lizardite pseudomorphs after diopside on magnetite (fig. 11) have been recovered from the waste-rock dumps.



Figure 7. Large (2.5 to 3 cm) octahedral crystals of magnetite from the Pomeroy mine, Deer Lodge County, Montana.



Figure 8. Fan-shaped aggregates of prismatic microcrystals of ludwigite from the Pomeroy mine, Deer Lodge County, Montana.

Table 2. Minerals of the Pomeroy mine, Deer Lodge County, Montana.

| Mineral Name | Formula  | Nature of Occurrence   |
|--------------|--|--|
| Calcite      | $\text{Ca}(\text{CO}_3)$   | As massive white marble containing magnetite and other skarn minerals.   |
| Clinochlore  | $\text{Mg}_5\text{Al}(\text{AlSi}_3\text{O}_{10})(\text{OH})_8$      | Dark green micaceous crystals to 1 cm on magnetite in marble matrix.   |
| Humite       | Group Mineral<br>$\text{Mg}_7(\text{SiO}_4)_3(\text{F},\text{OH})_2$ | Tiny rounded grains in white marble matrix occurring in a band with magnetite near the ludwigite mineralization. The specific mineral species has not been identified. |
| Lizardite    | $\text{Mg}_3\text{Si}_2\text{O}_5(\text{OH})_4$                      | As small masses and pseudomorphs after diopside microcrystals.   |
| Ludwigite    | $\text{Mg}_2\text{Fe}^{3+}\text{O}_2(\text{BO}_3)$                   | Silky black acicular crystals in fan-shaped and radiating aggregates in marble with small grains of magnetite.   |
| Magnetite    | $\text{Fe}^{+2}\text{Fe}^{+3}_2\text{O}_4$                           | Large masses and rarely as rough octahedral crystals to 3 cm in diameter.  |

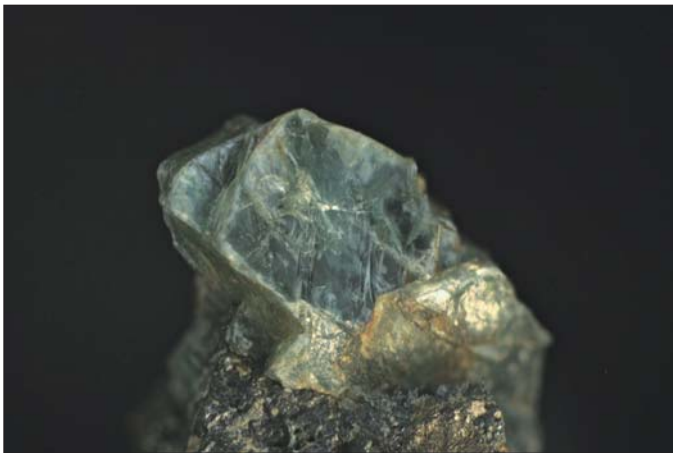


Figure 9. A 0.5 cm crystal of clinochlore on magnetite from the Pomeroy mine.



Figure 10. Fist-sized mass of lizardite showing slickenside texture from the Pomeroy mine, Deer Lodge County, Montana.



Figure 11. Green-colored pseudomorphs of lizardite after diopside on magnetite, Pomeroy mine, Deer Lodge County, Montana.



### Ludwigite in Montana

Ludwigite is a fairly uncommon mineral with 145 worldwide occurrences, 43 of which are in the United States. Montana has four of the known occurrences, all associated with skarn deposits. It was first found at the Redemption iron mine at Philipsburg (Schaller, 1911), where it occurs as aggregates of needle-shaped crystals intergrown with magnetite (figs. 12, 13). About 30 years later it was discovered in skarn deposits located in Colorado Gulch (fig. 14), west of Helena, that produced small amounts of iron ore (Knopf, 1942). The most recent find was underground in the Sourdough mine in the Elkhorn district in Jefferson County (Everson and Read, 1992), where it occurs as microcrystals with massive magnetite in skarn. Unfortunately, samples from the Sourdough mine have not been preserved.



Figure 12. Ludwigite from the Redemption iron mine, Philipsburg, Granite County, Montana.



Figure 13. Magnified view of ludwigite microcrystals from the Redemption iron mine, Philipsburg, Granite County, Montana.

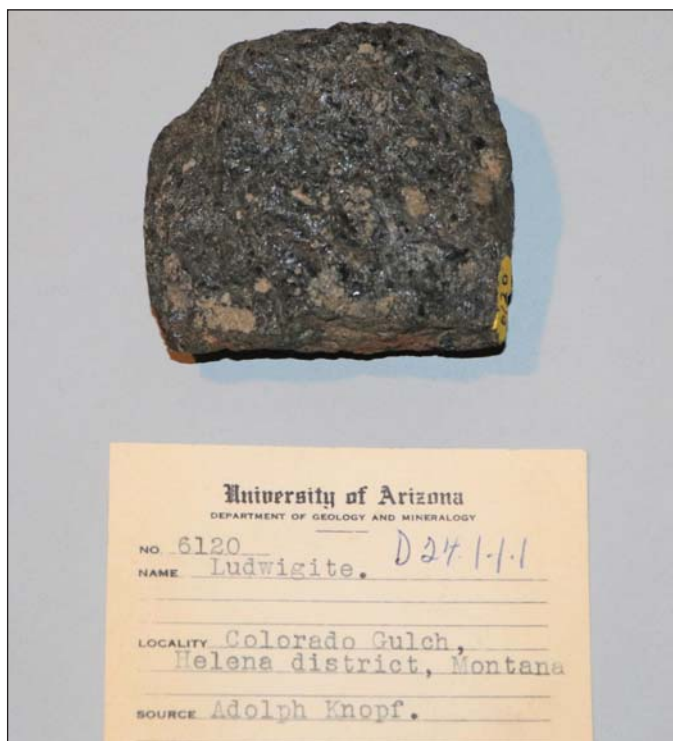


Figure 14. Specimen of ludwigite collected by Adolph Knopf from Colorado Gulch, Lewis and Clark County, Montana (ex. University of Arizona mineral collection now in the author's collection).

### Cable Mine, Deer Lodge County, Montana

The Cable mine is located 1 mi southeast of the Pomeroy mine in sec. 10, T. 5 N, R. 13 W., on private property consisting of 17 patented mining claims. The Cable mine is an example of a gold skarn that forms when the magmatic fluids are more chemically evolved than those that form an iron skarn deposit. Originally known as the Atlantic Cable mine, it produced the richest gold ore ever found in Montana, with one of the high-grade zones assaying over \$10,000 per ton. It also became world renowned for its spectacular specimens of native gold. The total production has been estimated at 165,127 oz of gold and 134,583 oz of silver, with 90% being produced before 1900 (Holms, 1982).

The Georgetown district, named by Salton Cameron in honor of his brother George, was established in 1865 when placer gold was discovered. The placers were difficult to work due to thick overburden. In 1866 Thomas Aiken, John Pearson, and Jonas Stough found fair placer ground to the southeast in the headwaters of Moose Creek (later renamed Cable Creek). They worked the deposit but, lacking sufficient water, they completed construction of a 4-mi-long ditch in the fall of 1866. The following year they found float rock rich in native gold. There was no visible outcrop, so they sunk an exploration shaft, and on June 13, 1867 they found bedrock studded with native gold. One partner traveled to Deer Lodge and recorded the Atlantic Cable claim on June 18, 1867 (*The Montana Post*, October 12, 1867, p. 4). The name Atlantic Cable was chosen because the three men had traveled from England to the United States on one of the ships that was carrying a portion of the actual cable that was being laid across the Atlantic Ocean in the 1850s to establish communication between London and New York.

Incredibly rich ore composed of coarse flakes of native gold in quartz was recovered from the upper levels of the mine. This created a sensation and a claim staking rush in the area, but the Cable claims already covered most of the valuable ground. The men constructed several arrastras to crush the ore to extract the gold (*The Montana Post*, October 12, 1867). After taking out a fortune in gold, Stough sold out to Aiken and Pearson.

In the fall of 1867, Captain George Plaisted arranged to gain control of the property by convincing Helena Banker William Nowlan to finance the development of the mine and construction of a 20-stamp mill. The mill (fig. 15) was erected in the winter of 1867 by Salton Cameron and Captain Plaisted at a cost of \$48,000. Nowlan provided the construction funds under a contract with Plaisted that required a supply of 10,000 tons per year of ore from the mine to be processed at the mill at a cost of \$11 per ton, all of the metal output to belong to Nowlan.

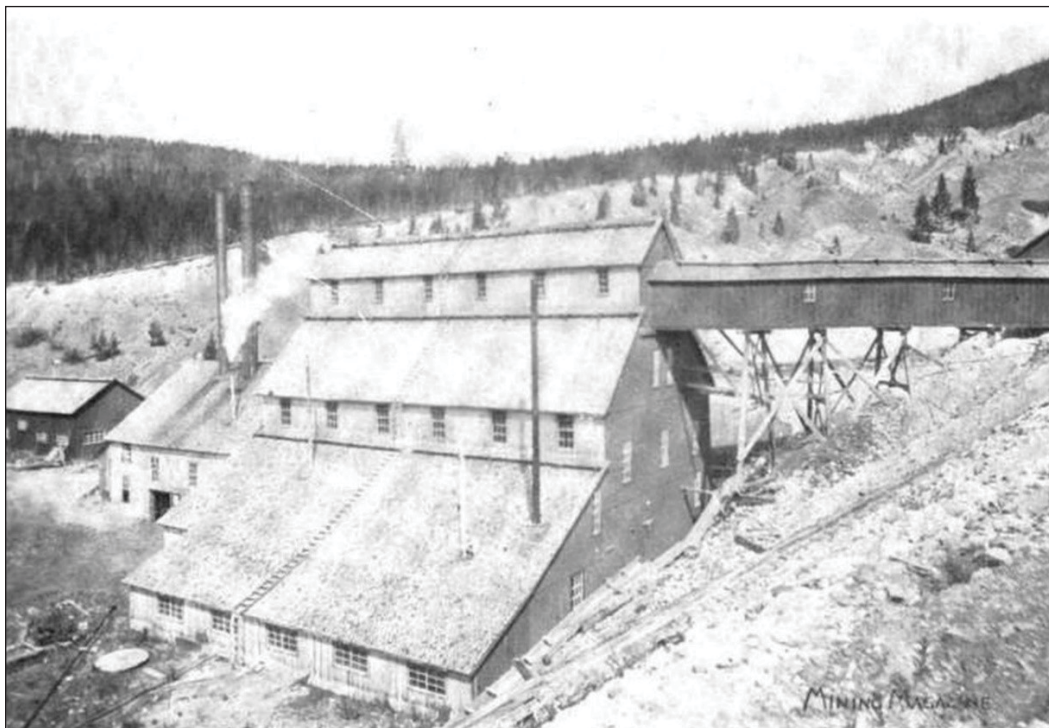


Figure 15. The Nolan Mill, constructed in 1867 at the Cable Mine, Deer Lodge County, Montana.



The mill produced its first gold in March 1868. The mine was developed by four shafts. Most of the ore was red colored and very crumbly. A level was run at a depth of 82 ft for a distance to the northeast of 300 ft. One shaft was deepened to 148 ft when the vein pinched down to a small seam. Mining was concentrated at the 82 ft level and below where the ore was mined in a large stope 80 ft deep and 45 to 55 ft wide. Below 85 ft the vein was full of loose boulders of limestone in soft ore. The stope, which had been poorly timbered, caved in for a length of 250 ft and a number of men were injured. The operation was closed down and claims for damages were made by the injured miners. At the time, near the end of 1868, a total of 9,200 tons had been processed, yielding \$172,000 in gold. Since only 9,200 tons (not 10,000 tons) were processed, Nowlan sued Plaisted for breach of contract. Several prominent mining men had invested with Nowlan, and more lawsuits entailed. In 1869 some attempts were made to extract ore from the other shafts, but only small amounts of gold ore were produced over the next few years. The operation closed down completely in 1872 as the lawsuits continued.

In 1870 Salton Cameron prospected ground adjacent to the Cable mine, finding placer gravels on an extension of the deposit, and he located a claim he called the North Pacific. He partnered with Conrad Kohrs, who helped finance construction of a ditch for \$10,000. By ground sluicing with hydraulic monitors to wash away the soil, \$18,000 in placer gold was recovered in 1871. The operation continued for 3 more years, yielding large profits. Around 1872 the sluicing operation uncovered some bedrock on what Cameron named the Thomas lode, which showed masses of white quartz seamed with gold (The Helena Independent, July 28, 1890). A total of 70 tons of rich float quartz was picked up at the tail race of the sluicing operation. Cameron leased the 20-stamp Hanauer mill at Georgetown to process ore from the mine. Cameron excavated into the bedrock, producing more gold ore for milling.

In the fall of 1873, Cameron struck a body of high-grade ore near the surface about 100 ft south from the original discovery. From this high-grade pocket he took out 100 tons that yielded \$20,000 in gold when processed at the Hanauer Mill; another two tons of high grade was processed by hand crushing, yielding \$8,000 (an incredible \$4,000 per ton), and he retained a collection of 200 pounds of the richest material showing large masses of crystalline gold. One specimen had a mass of pure gold projecting from the rock in the shape of a curved finger containing \$75 in gold (almost 4 oz), many specimens of pure gold weighing about an ounce each, and a large piece of nearly solid gold worth \$375 (over 19 oz of gold). Cameron stored the gold specimens in W.A. Clark's bank vault in Butte. After working out the high grade, Cameron closed down and went on to develop other mines in the district. The adjacent Cable mine remained closed until 1877 when Nowlan's brother-in-law J.C. Savery assumed Nowlan's debt and acquired the property. Savery had a new 30-stamp mill erected.

Savery had a lucrative business in New York City, so he only spent the summer months in Montana. He put the Cable mine back into operation and by July 1885 the mine was able to keep all 30 stamps at the mill in operation. Around 1886 a rich strike of high grade worth \$50,000 was encountered while Savery was back east. The gold was sold and all ten dishonest employees left with the money (Butte Inter Mountain, December 27, 1901, p. 3). When Savery returned he learned of the theft and went after them. Only one was captured; the others had fled the country. Afterwards he would only operate the mine when he was present and he had the mine superintendent enforce strict rules. Showers were installed. The men had to shower, change clothes, and were carefully searched as they left at the end of the work day. In July 1890 the mine shut down for want of ore. Savery then explored for placer in the flat below the mine like Salton Cameron did in the hill above the mine 20 years before. Some placer gold was produced, but thinking the mine worked out, Savery closed down the entire operation in 1891.

In 1900 the Bacorn Brothers (F.W. and H.C.) acquired the property and operated the mine and mill for 6 years. The mine was operated a few more times and to this day it is owned by a mining company that has continued exploration.

The deposit is a skarn formed by the intrusion of the Cable granodiorite stock into Cambrian-age Hasmark dolomitic limestone. The minerals of the Cable mine are summarized in table 3. The waste-rock dumps (fig. 16) contain interesting minerals such as magnetite (fig. 17), tremolite (fig. 18), actinolite (figs. 19, 20), and clinocllore (fig. 21).

Table 3. Minerals of the Cable Mine (Lincoln, 1911; Sharwood, 1911; Emmons and Calkins, 1913).

| Mineral Name | Formula  | Nature of Occurrence   |
|--------------|--|--|
| Actinolite   | $\text{Ca}_2(\text{Mg}, \text{Fe}^{2+})_5\text{Si}_8\text{O}_{22}(\text{OH})_2$                          | As intergrown aggregates of needle-like crystals in calcite and magnetite.   |
| Andradite    | $\text{Ca}_3\text{Fe}^{3+}_2(\text{SiO}_4)_3$  | Reported to occur on the 140 and 214 ft level as large blocks in calcite.  |
| Arsenopyrite | $\text{FeAsS}$   | As prismatic microcrystals and small masses in calcite.  |
| Azurite      | $\text{Cu}_3(\text{CO}_3)_2(\text{OH})_2$  | Small amounts of azurite occur in association with malachite.  |
| Baryte       | $\text{Ba}(\text{SO}_4)$   | Reported to occur.   |
| Bornite      | $\text{Cu}_5\text{FeS}_4$  | As coatings on pyrite and chalcopyrite.  |
| Calcite      | $\text{Ca}(\text{CO}_3)$   | As white colored masses often containing seams of native gold.   |
| Chalcocite   | $\text{Cu}_2\text{S}$  | As secondary films and coatings on pyrite and chalcopyrite in calcite.   |
| Chalcopyrite | $\text{CuFeS}_2$   | As small grains and masses associated with calcite.  |
| Chrysocolla  | $(\text{Cu}_{2-x}\text{Al}_x)\text{H}_{2-x}\text{Si}_2\text{O}_5(\text{OH})_4 \cdot n\text{H}_2\text{O}$ | As small masses.   |
| Clinochlore  | $\text{Mg}_5\text{Al}(\text{AlSi}_3\text{O}_{10})(\text{OH})_8$  | As dark green crystals in masses of intergrown actinolite and magnetite.   |
| Copper       | $\text{Cu}$  | A few small flakes of native copper were found by Bacorn in the upper mine workings of the mine.   |
| Cuprite      | $\text{Cu}_2\text{O}$  | Reported to occur.   |
| Diopside     | $\text{CaMgSi}_2\text{O}_6$  | As small colorless grains in white calcite marble.   |
| Dolomite     | $\text{CaMg}(\text{CO}_3)_2$   | As small crystals lining vugs in the upper part of the mine.   |
| Epidote      | $\text{Ca}_2(\text{Al}, \text{Fe}^{3+})[\text{Si}_2\text{O}_7][\text{SiO}_4]\text{O}(\text{OH})$         | As fine-grained masses.  |
| Galena       | $\text{PbS}$   | Reported to rarely occur.  |
| Goethite     | $\text{FeO}(\text{OH})$  | As an alteration of pyrite. Also mixed with limonite.  |
| Gold         | $\text{Au}$  | Finely disseminated in calcite, quartz, pyrite, pyrrhotite, and chalcopyrite, less commonly as coarse grains, often as thin sheets parallel to the cleavage of the calcite, rare as large crystalline grains and masses, intergrown with tetradymite in calcite. |



Table 3—Continued.

| Mineral Name | Formula   | Nature of Occurrence  |
|--------------|---|---|
| Hematite     | $\text{Fe}_2\text{O}_3$   | As small masses of specular hematite and as red earthy masses formed as an alteration of pyrite.  |
| Lizardite    | $\text{Mg}_3\text{Si}_2\text{O}_5(\text{OH})_4$   | As small masses intergrown with grains of magnetite.  |
| Magnetite    | $\text{Fe}^{+2}\text{Fe}^{+3}_2\text{O}_4$  | As large irregular bodies related to the bedding planes in the altered limestone. Mostly massive, uncommon as octahedral crystals. It also forms as small grains in calcite, in lizardite, tremolite, and other minerals. The magnetite carries little gold and is therefore plentiful on the waste rock dumps at the mine. |
| Malachite    | $\text{Cu}_2(\text{CO}_3)(\text{OH})_2$   | Common in oxidized ore as small botryoidal masses with limonite and small masses associated with chrysocolla and magnetite. Also as velvety green fibers lining vugs.   |
| Marcasite    | $\text{FeS}_2$  | Uncommon occurrence with pyrite in calcite.   |
| Meionite     | $\text{Ca}_4\text{Al}_6\text{Si}_6\text{O}_{24}(\text{CO}_3)$                                   | Reported to occur.  |
| Norbergite   | $\text{Mg}_3(\text{SiO}_4)(\text{F},\text{OH})_2$   | Colorless microscopic grains with a yellow-colored fluorescence under short-wave ultraviolet light occur in marble and are thought to be norbergite, but have not been confirmed by analysis.   |
| Pyrite       | $\text{FeS}_2$  | As irregular masses, often intergrown with pyrrhotite and less commonly chalcopyrite. Uncommon as pyritohedron-shaped microcrystals.  |
| Pyrrhotite   | $\text{Fe}_7\text{S}_8$   | As small masses and grains, less abundant than pyrite. It often is intergrown with gold.  |
| Quartz       | $\text{SiO}_2$  | As small masses and microcrystals. Some masses contain embedded gold.   |
| Siderite     | $\text{Fe}(\text{CO}_3)$  | Reported to occur.  |
| Sphalerite   | $\text{ZnS}$  | Reported to occur rarely.   |
| Tetradymite  | $\text{Bi}_2\text{Te}_2\text{S}$  | As massive grains in calcite often intergrown with native gold.   |
| Tetrahedrite | $\text{Cu}_6[\text{Cu}_4(\text{Fe},\text{Zn})_2]\text{Sb}_4\text{S}_{13}$                       | A small amount was found on the 200 ft level with chalcopyrite.   |
| Tremolite    | $\text{Ca}_2(\text{Mg}_{5.0-4.5}\text{Fe}^{2+}_{0.0-0.5})\text{Si}_8\text{O}_{22}(\text{OH})_2$ | As masses of intergrown radiating crystals aggregates.  |
| Wollastonite | $\text{CaSiO}_3$  | Reported to occur.  |



Figure 16. The waste rock dumps at the Cable mine, Deer Lodge County, Montana.



Figure 17. Massive magnetite with white tremolite from the Cable mine, Deer Lodge County, Montana.



Figure 18. A fist-sized mass of intergrown radiating aggregates of prismatic tremolite crystals, Cable mine, Deer Lodge County, Montana.



Figure 19. A specimen of magnetite with green actinolite, 18 in wide, Cable mine, Deer Lodge County, Montana.



Figure 20. A magnified view of actinolite crystals from the same specimen as figure 19, Cable mine, Deer Lodge County, Montana.



Figure 21. Clinocllore crystals to 2 cm in a matrix of magnetite and actinolite, Cable mine, Deer Lodge County, Montana.



### The Cable Mine Gold Specimens

Although the minerals found on the waste dumps are interesting, it was the native gold specimens that made headlines. In addition to Salton Cameron's famous specimens, around 1885 Savery also recovered some spectacular crystalized gold specimens from the mine. They were mostly in white calcite and much of the gold was intergrown with the bismuth-telluride mineral tetradymite. One piece was described as a boulder of calcite 2 ft across studded with coarse grains of gold and black-colored masses of tetradymite. Savery also exhibited his specimens at the various World's Fairs.

The famous Salton Cameron gold specimens had been displayed at many exhibitions in the United States and overseas. This started in 1876 when W.A. Clark paid to have them shipped to the Centennial Exhibition in Philadelphia. Cameron's samples were later exhibited in New Orleans, and were sent to London, to the 1893 Columbia Exposition in Chicago, and to the 1900 Paris Exposition.

When not on exhibit, they had been stored in the vault at W.A. Clark's bank in Butte. Clark would often take visiting dignitaries to the vault in the evening for a private viewing of the specimens, which contained about 500 oz of gold in total. W.A. Clark purchased the best of the Salton Cameron specimens, the big 19-oz chunk of gold, incorrectly reported as a "nugget" by many newspapers, for \$1,000. Cameron sold the remainder of the collection of specimens in March 1893 to John McCormick of Butte for \$10,000 (Butte Inter Mountain, August 6, 1902, p. 11). They were placed on display at Clark's Columbia Gardens (fig. 22), which hosted the International Mining Congress meeting in 1902 (Butte Inter Mountain, December 3, 1902, p. 3). It was said that there were two center cases in the mineral display containing over \$30,000 in gold specimens from all over Montana. W.A. Clark convinced mine owners from all over Montana to send specimens of their best crystals and rich ores to the Columbia Gardens mineral display. At the end of the mining conference he was successful in getting nearly all of the exhibitors to allow the specimens to remain on permanent display at Columbia Gardens. It was advertised as the largest mineral exhibit in the Pacific Northwest, and was the greatest assembly of crystals and rich ores from Montana ever assembled. Clark decided to have a fire sprinkler system installed in the building. Unfortunately, while the system was being installed, a pipe delivery was late, which delayed completion. The pavilion caught fire and was destroyed on October 28, 1907 (Butte Miner, 1907). The fire was so intense that the building burned to the ground. All the contents, including the mineral collections, and many Montana-related historical items, were lost. One impressive specimen from the Cable mine remains in existence. It is on display at the Montana Bureau of Mines and Geology Mineral Museum at Butte (fig. 23).

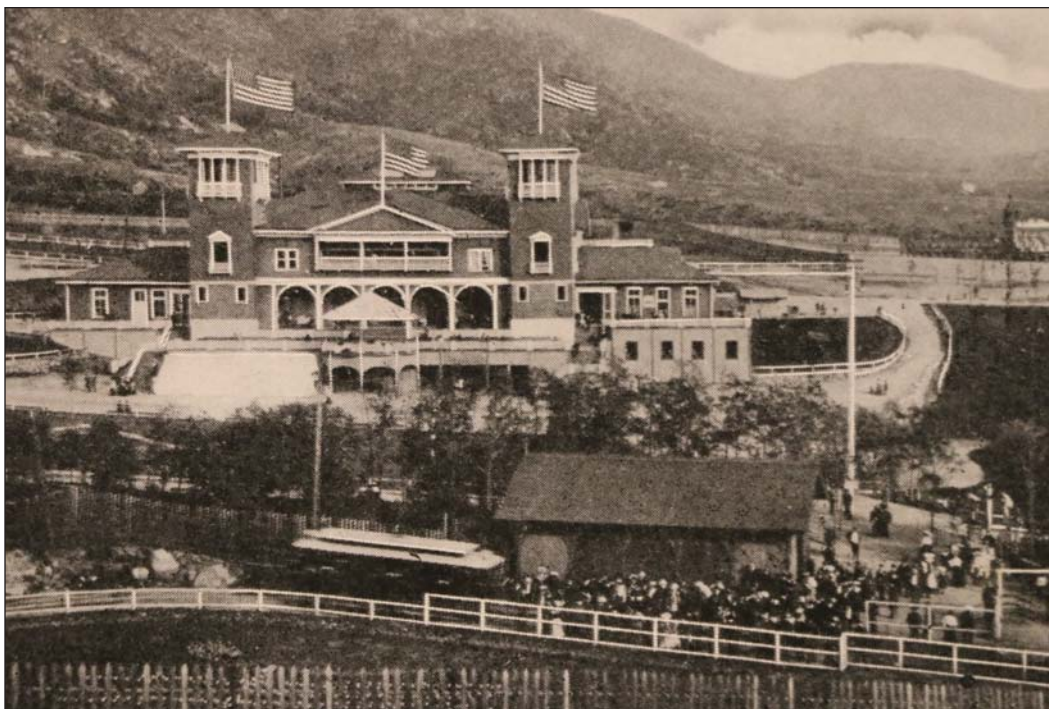


Figure 22. The pavilion at Columbia Gardens contained the mineral display that was created for the 1902 International Mining Congress so W.A. Clark could show off the wealth of Montana.



Figure 23. Photograph of a large specimen containing native gold and tetradymite in calcite from the Cable mine, Deer Lodge County, Montana, on display at the Montana Bureau of Mines and Geology's Mineral Museum in Butte. This may be J.C. Savery's "2-foot boulder of gold ore" from the Cable mine.

### References

- DeMunck, V.C., 1956, Iron deposits in Montana: Montana Bureau of Mines and Geology Information Circular 13, 55 p.
- Dudas, F., 2015, Ludwigite from the Pomeroy mine, Montana: *Mineral News*, v. 31, no. 9, pp. 1–2, 7–9.
- Emmons, W.H., and Calkins, F.C., 1913, Geology and ore deposits of the Philipsburg Quadrangle, Montana: U.S. Geological Survey Professional Paper 78, 271 p.
- Holms, M.A., 1982, Geology and mineralization of the mines around the Cable stock, Deer Lodge County, Montana: Butte, Montana Technological University, M.S. Thesis, 73 p.
- Knopf, A., 1942, Ludwigite from Colorado Gulch, near Helena, Montana: *American Mineralogist*, v. 27, p. 824–825.
- Knudsen, P., 2011, Vignettes of four Montana mineral localities (Crazy Sphinx mine, Sourdough mine, Bald Mountain, PC mine): Proceedings of the 32nd Annual New Mexico Mineral Symposium and 3rd Annual Mining Artifact Collectors Association Symposium, November 12–13, 2011, Socorro, New Mexico, 2 p.
- Lincoln, F.C., 1911, Some gold deposits of the northwest: *Engineering and Mining Journal* 92, p. 408–410.
- Meinert, L.D., 1992, Skarns and skarn deposits: *Geoscience Canada*, v. 19, no. 4, p. 145–162.
- Reed, G.C., 1951, Mines and mineral deposits (except fuels) Broadwater County, Montana: U.S. Bureau of Mines Information Circular 7592, 62 p.
- Schaller, W.T., 1911, Ludwigite from Montana, Paper in Mineralogical Notes Series 1: U.S. Geological Survey Bulletin 490, p. 28–32.
- Sharwood, W.J., 1911, Notes on tellurium-bearing gold ores: *Economic Geology*, v. 6, no. 1, p. 22–36.
- Wimmler, N.L., 1946, Exploration of Southern Cross iron deposits, Deer Lodge County, Montana: U.S. Bureau of Mines Report of Investigation 3979, 14 p.





Rock Man. Courtesy of Alma Winberry.



## Bull Mountain: Four Generations of Gold Seekers

Patrick E. Dawson<sup>1</sup> and James R. Gruber, Jr.<sup>2</sup>

<sup>1</sup>*Author, Journalist, patdawson@att.net*

<sup>2</sup>*Consulting Geologist, jimgruber406@gmail.com*

### Introduction

Bull Mountain, rising south of Boulder, in Jefferson County, Montana, occupies a large sector of the Boulder Batholith set among the historic mining districts of Butte, Comet, Basin, and Elkhorn. The north–south-trending mountain range has been geologically mapped over the years at different scales of accuracy. High elevations, dense stands of evergreen forest clogged with blowdown timber, and a historic lack of road access combined to limit exploration and mapping.

Most of the land area is in the Beaverhead–Deer Lodge National Forest. There are also approximately 9,858 acres of private checkerboard sections, originally from the Northern Pacific Railway land grant, and since shortly after World War II owned by the Bull Mountain Grazing Association, a local rancher cooperative.

Apart from the present-day Golden Sunlight Mine at the extreme southern end of the mountain range, and a few historic workings above the Whitetail Valley along the southwest slope of the mountain, relatively little exploration and mining have occurred on Bull Mountain.

The authors are descendants of John William “Jack” Dawson (1837–1922; fig. 1), a pioneer on the western mining frontier who settled in Boulder Valley. Jack Dawson filed his last claim in a drainage below Houghton Park on the southeast portion of Bull Mountain in 1918 when he was 80 years old. Prior to staking his claim, he had worked the site and built a log cabin. He died in 1922, at the age of 84.



Figure 1. Jack Dawson (with baby on lap) and his family.



Several years ago James Gruber, great-grandson of John W. Dawson and retired Department of Interior geologist, was doing genealogy research on his family roots and discovered that Jack Dawson was listed in the 1869 Territorial Census of Sweetwater County, Wyoming, in the South Pass–Atlantic City gold rush camp. That brought to mind the old man’s claim on Bull Mountain, which he had never seen. He asked his first cousin once removed, Patrick Dawson, grandson of John W. Dawson, about going to the claim on Bull Mountain.

Patrick Dawson assured his cousin that he knew the claim location, but had not been up to the site since helping to gather cattle about 30 years earlier when travel in the area was by either foot or horseback. In 2015 we cousins were able to travel on new logging roads on Bull Mountain Grazing Association lands. Initially disoriented by the logging activity, we eventually found the old diggings on a steep slope in dense timber.

Since that trip, we have conducted mineral exploration over portions of Bull Mountain, culminating so far with the filing of seven unpatented lode mining claims. This is the story of our family’s four generations on Bull Mountain.

### **Mining the Frontier**

Following Jack Dawson was never easy. He was born in Quebec, Canada, in 1837, and raised there. He and his brother Tom tried logging, but opportunities lured them west. Tom worked in the mines of the Butte area, and then, in 1879, filed a homestead in Boulder Valley. Meanwhile, Jack tried mining in Wyoming and then in the Dakotas. In April 1876 John and three partners staked the Clara Mine in the Black Hills, near what was to become the boom camp of Deadwood. Staked the same month as the soon-famous Homestake strike, the Clara was one of the first lode claims in the Black Hills. In the summer of 1876, James Butler Hickok, better known in history as Wild Bill, visited his old friend John Dawson. Not long after, Wild Bill was murdered during a now legendary poker game in the Number Ten Saloon in Deadwood.

Jack Dawson and partners developed the Clara prospect, an open cut with a shaft, and mined it for about 3 years. On 17 June, 1876, the Black Hills Weekly Pioneer reported that, “the Clara shaft is now 23 feet deep, about five feet wide and eighty feet long, with well-defined footwall. The quartz bears about the appearance of the Woolery lode, being of a reddish color, resembling half-burnt brick, is very much decomposed, and shows considerable free gold. It is easily worked and appears very rich.” Dawson made several trips out and back, usually by taking the Deadwood Stage south to Sidney, Nebraska, where he caught the Union Pacific train, or the stagecoach north to Bismarck to catch the Northern Pacific east. After the George Hearst Syndicate purchase of the Homestake and other properties, he too sold off his interests in the Clara claim in 1878 and 1879, to California operator Gen. J.W. Gashwiler, who was scheming to gain control of Deadwood properties in order to profit from Hearst’s ambitions. “I think the advent of Gashwiler into this camp has been the cause of nearly all our troubles,” Hearst wrote to his partners in 1878, adding that Gashwiler “has given outsiders confidence in thinking that they could at any time force us to pay out money, and I certainly think the effect of it all has been stupendous and outrageous.” The Caledonia Mine was also acquired by Gashwiler, and he hired Jack Dawson to be mine foreman. But Dawson soon grew restless, and perhaps weary of Gashwiler’s reputed shady dealings. He resigned the Caledonia after a warm testimonial sendoff from the loyal workers, and caught the Deadwood Stage one last time, bound for the new boom in the southwest. The exit was timely, as Gashwiler became insolvent in 1881.

Jack Dawson arrived in Tombstone, Arizona Territory, in the spring of 1881, a few months before the infamous Shootout at the OK Corral. In a letter to friends in Deadwood that was published in the newspaper, he observed that “Everything here is booming. I meet old timers here from every camp that I was ever in. The sporting fraternity run the town, twelve of them hired out yesterday at \$10 per day to take forcible possession of a mine and are now holding it. Old timers here say that there is plenty of killing to be done.” Dawson noted that two former Deadwood residents “are actually excited over the prospects they obtained from some rock they brought in from about 100 miles from here; none of it assaying less than \$200 per ton.... From what I have seen and can learn, southern Arizona and northern New Mexico is a rich country, although it seems too hot for a white man to live here.”

As summer came and temperatures soared, Jack Dawson reported back to Bob Cooper in Deadwood that after a prospecting trip outside of Tombstone, they did not find much. “Times here are looking down; that is the business portion, though the mines never looked better, the coach is loaded going out, and very few strangers coming in. Money is not near so plenty as when I first came here. The weather is very hot, the thermometer registering 110 in the shade about every day. This is a good camp to work in for wages, but too old for prospecting, as every foot of ground within a radius of 20 miles is monumented... Well, Bob, from my experience in the country, I would not advise anybody to come here... Do not write until you hear from me again, which will be as soon as I get to the Mogollon mountains.”

Jack Dawson journeyed into Sonora, Old Mexico, then up to the Mogollon and Black Mountains of New Mexico, then to Boulder City, Colorado. He passed through Butte in the summer of 1883, and was next heard from by folks in Deadwood in December 1883, when he was at the gold rush in the Couer d’Alenes of Idaho Territory. Once again, there was a nationwide stampede promoted by the Northern Pacific Railroad along its newly completed line, and by towns along the line boosting their outfitting stores. Many pilgrims hopped off the comfort of the trains at Superior or Sandpoint that winter and slogged through the dense, roadless forests and deep snows, dragging their gear on toboggans.

The Daily Deadwood Pioneer newspaper reluctantly reported Dawson in Eagle City, Idaho, in 1884. The paper quoted another former Deadwood miner saying that Deadwood residents should come to Idaho if they had nothing better going. It was a wild boom scene of characters, saloons, and a circus tent gambling hall run by Wyatt Earp and his brother. Later that summer, Jack Dawson and company were still there, working 35 feet down to bedrock and reportedly optimistic after having settled a drawn-out boundary dispute over their claims.

Jack Dawson ended up in the Boulder Valley of Jefferson County probably by 1884. In 1885, 4 years before Montana statehood, he began homesteading next to his younger brother, Tom. His mining days seemed far behind him when he began ranching, and in 1888 married the 18-year-old daughter of neighboring Confederate refugees. He was nearly 51. They had 13 children. But the gold bug wasn’t quite out of his system, and his diggings on south Bull Mountain were maybe his one last hope to strike it big again. He was assisted in the summers by at least two sons. When he officially filed his claim in 1918, he had lost his wife that fall when a gas lamp exploded and she died of severe burns. Many young children were still at home, and one son was in the World War One trenches of France. The severe drought, Spanish influenza epidemic, and killer winter of 1919 nearly ruined many small family ranches, but he held on. Some men he hired to work his claim on Bull Mountain reportedly “lost the lead,” and it languished for nearly a century, crumbling and overgrown with timber. Some of his sons and grandsons later searched Bull Mountain for a reputed but elusive 1870s silver prospect. Meanwhile, Jack Dawson died in 1922. According to probate records, he left his 12 surviving children a well-equipped ranch, including 7 work horses, 3 saddle horses, 10 range horses, and a Ford automobile. There were alfalfa acres, wild hay land, irrigated acres, dry farm land, and mostly pasturage. He was buried in the St. John’s Mission Catholic cemetery in Boulder Valley.

### **Mineral Reconnaissance**

Exploring family history began an odyssey by the authors of examining and testing the ancestral claim and following recent geologic mapping of Bull Mountain by the Montana Bureau of Mines and Geology (MBMG). Jack Dawson’s claim, it turned out, tapped into a mineralized short section of a lengthy andesite porphyry/rhyolitic tuff contact of the Cretaceous age Elkhorn Mountain Volcanics. Recent MBMG mapping and more recent logging roadcuts led us to a parallel mineralized contact composed of andesite porphyry and volcanogenic siltstone. These trends are mostly concealed for the better part of 4 miles. Rock that can be sampled without mechanized equipment and permitting has shown anomalous gold values, lending credence to John Dawson’s frontier prospecting.

From 2015 through 2019, the authors made several summer trips to Bull Mountain, camping out, field-checking and sampling recent MBMG mapping of sulfide zones (fig. 2). Logging of Bull Mountain Grazing Association sections aided reconnaissance by exposing previously uncharted rock and sulfide exposures.





Figure 2. Jim Gruber field-checks sulfide zones in the Wilson Park 7.5' quadrangle.

Dawson and Gruber's reconnaissance culminated in a decision. Inspired by the large-scale mapping of Weeks (1974), Scarberry (2017), and Scarberry and others (2017), the authors moved to the northeast slope of Bull Mountain. We staked four claims along a series of Paleozoic dolomitic marble outcrops and named these the JWD Lodes, in honor of the ancestor who passed on his obsession.

Fieldwork produced several assayed rock samples showing anomalous to high-grade sulfide mineralization and alteration at the JWD Lodes, along abandoned historic workings, including two claims dating back to 1920. The oldest prospecting evidence likely was pre-1890, based on square nails found with dilapidated log structures. The remains of the old-timers' hand labor, the subsided shafts, adit, re-forested dumps, and rotting wood artifacts made for an eerie graveyard of broken dreams.

The authors' knowledge of this deposit to date, the proximity of this mineralized carbonate unit to the Boulder Batholith, and the polymetallic style of mineralization suggest that metamorphism and mineralization occurred during emplacement of the Butte Granite pluton as described by numerous authors. Documented precious and base metals present in anomalous and ore grades suggest this deposit to be closely related genetically to ore deposits in the neighboring Elkhorn Mining District.

Inspired by the English translation from the Russian of *Geochemical Exploration Methods for Mineral Deposits* by Beus and Grigorian (1977), the authors in 2019 began a geochemical soils survey of the JWD Lodes claims. Beus and Grigorian addressed specific geological aspects rarely seen in other literature that the authors hope to apply to this unique zone on northeast Bull Mountain that contains known mineralized skarn and possibly a porphyry mineral deposit at depth.

Geochemical exploration to identify secondary dispersion halos are being conducted by means of systematic sampling of soils at optimal depths. To date, 60 samples have been collected in the field and analyzed by ALS Global in Reno, NV, for 50 elements using the aqua regia and ICP-MS super trace gold method. Sampling intervals are closely spaced (150 feet x 300 feet), and infilling may be necessary in some areas for better definition. The goals are to target what appear to be zoned skarn deposits of gold-silver, lead-zinc-silver, stibnite-molyb-

denum, and copper–manganese; to identify concealed faults and contacts; and find the favorable geochemistry related to blind porphyry ore.

Initial analyses are encouraging. Anomalous and overlapping concentrations of favorable suites of mineral elements have been found to be present.

### The Geology

Scarberry and others (2017) describe Bull Mountain as a Miocene Basin and Range horst block and remnant of the late Mesozoic Cordilleran arc (fig. 3). At the south end of Bull Mountain, near Whitehall, gold formed in rhyolite breccia at the Golden Sunlight Mine (GSM). Fifteen miles north of the mine, metallic minerals occur in dikes and sills that follow NE- and NS-striking fissures in the Elkhorn Mountain Volcanics.

Geologic relationships in the Wilson Park quadrangle (fig. 3) indicate that the ore setting of the GSM may extend northward where alkalic rocks intrude and brecciate middle member rhyolite of the Elkhorn Mountain Volcanic field (Scarberry (2017)).

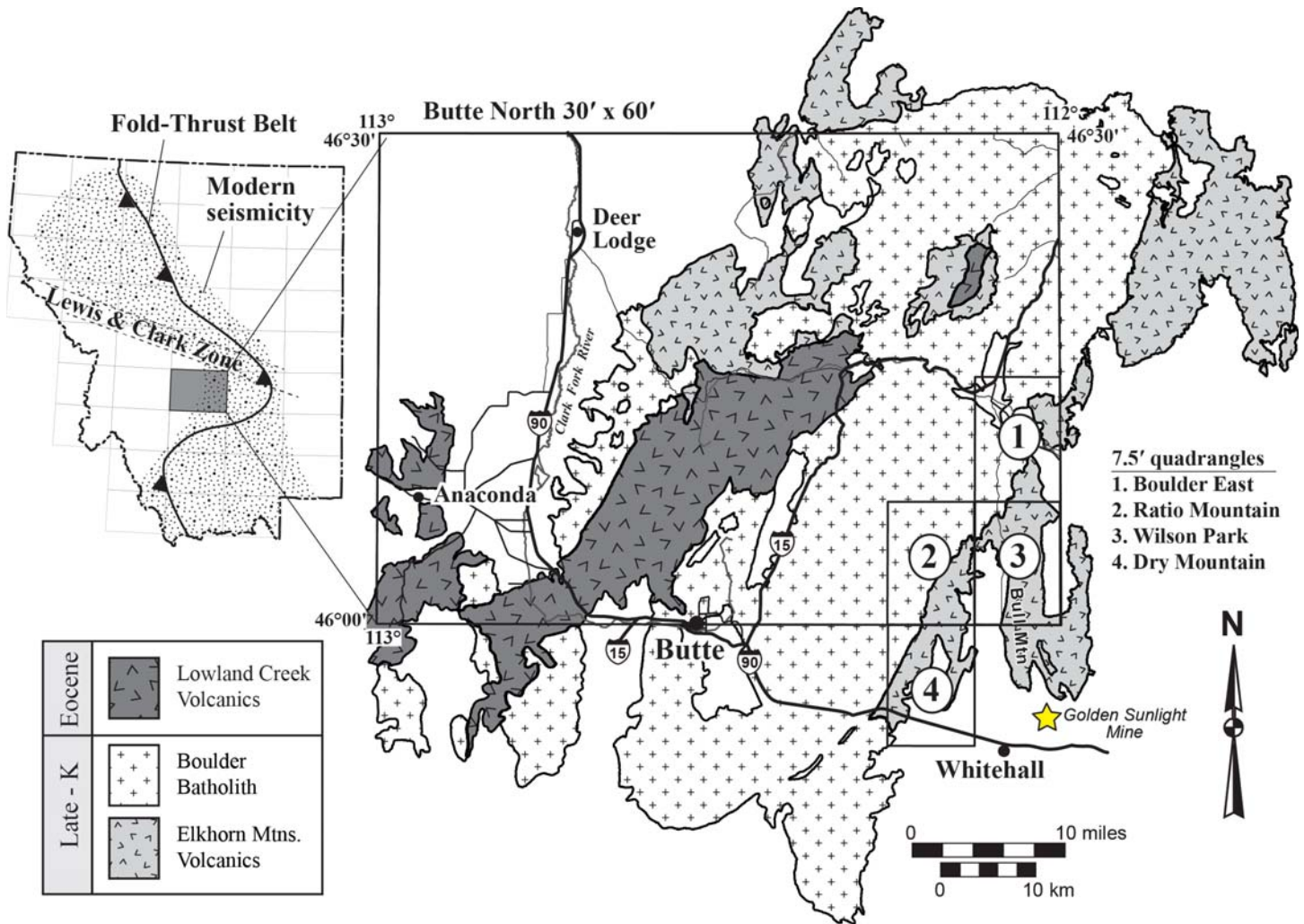


Figure 3. Location map shows Bull Mountain with respect to the Boulder Batholith–Elkhorn Mountains Volcanics magma system. 7.5' quadrangle locations and the Golden Sunlight Mine are also shown.

Klepper and others (1957) identify the Elkhorn mining district, to the north and adjacent to Bull Mountain, as the only place along the east margin of the batholith where Paleozoic carbonate rocks, which are favorable hosts for replacement ore deposits, crop out in contact with or close to the Boulder Batholith. Elsewhere along its east margin the batholith is in contact with Late Cretaceous volcanic rocks that overlie the Paleozoic and Mesozoic sedimentary rocks, and horizons that might contain replacement deposits are from several hundred to a few thousand feet beneath the surface. If any districts similar to the Elkhorn district occur at depth elsewhere along the intrusive contact, their presence may be indicated by an unusual amount of fracturing in the overlying



ing volcanic rock and by leakage of abnormal amounts of heavy metals into these fracture rocks (Klepper and others, 1957).

At the northeast corner of the Bull Mountain fault block, the authors have confirmed that veins in Paleozoic marble, containing galena, sphalerite, and pyrite, are mineralized and most likely related to skarn deposits in the adjacent Elkhorn mining district. This Paleozoic marble, which is probably the lower Amsden to upper Mission Canyon formation of Mississippian age (Weeks, 1974), crops out in numerous knobs for about 1 mile in a north–south direction and is overlain by cliff debris and alluvial sediments to the east and is in contact with Elkhorn Mountain Volcanics to the west.

### Need for Further Investigation

Geologic investigation and sampling of Bull Mountain by the authors from 2015 to 2019 using geologic mapping by Scarberry (2017), Scarberry and others (2017), Dixon and Wolfgram (1998), Weeks (1974), and Klepper and others (1957) target two areas for further study.

Of primary interest is the marble outcrop area near Rear Gulch and rock at Log Gulch (fig. 4) in the Boulder East 7.5' quadrangle, which suggests that carbonate rock underlies surface volcanics and is in contact with granitic pluton(s) at depth. Hydrothermal fluids related to emplacement of intrusive plutons are thought to be the source of mineralization that is present at the surface in Paleozoic marble skarn and highly fractured volcanic rock.

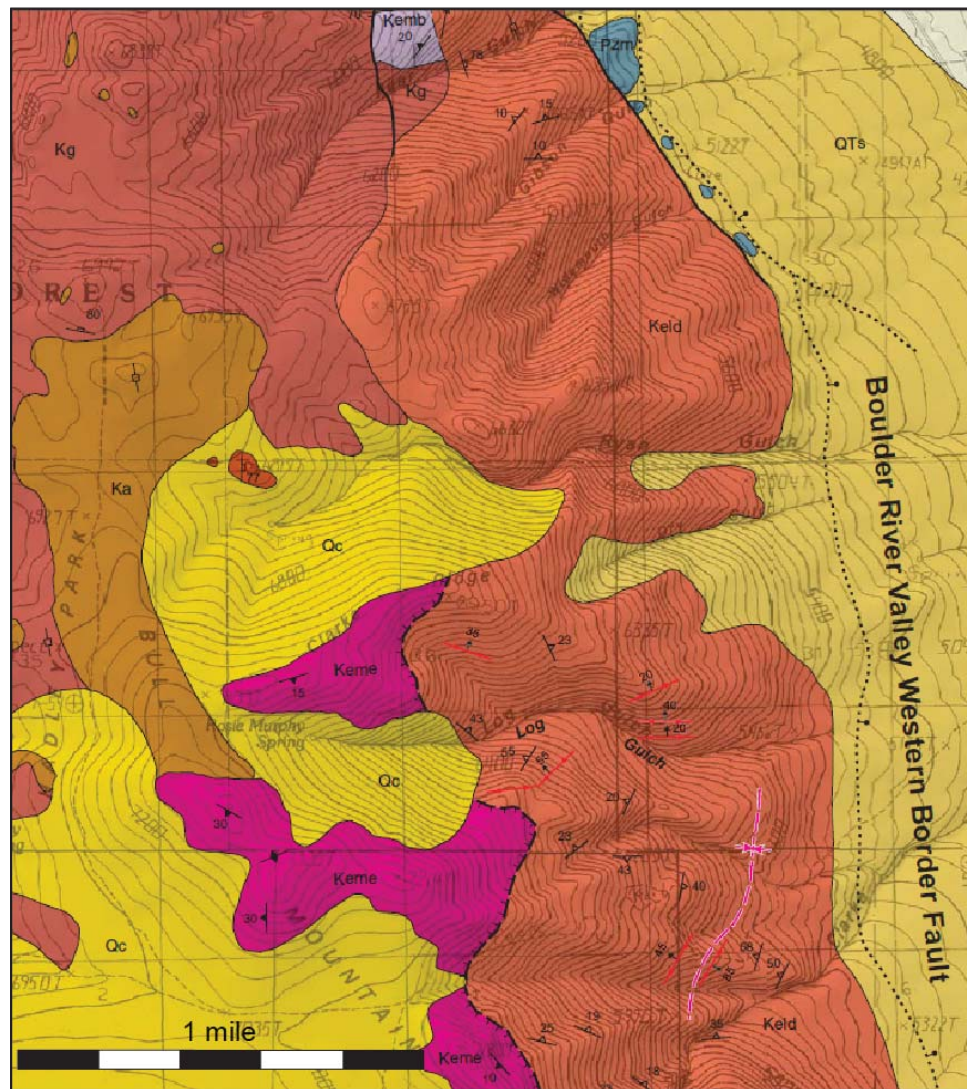


Figure 4. Geologic map of part of the Boulder East 7.5' quadrangle (see fig. 3 also) clipped from Scarberry and others (2017). Note outcrops of Paleozoic carbonate rocks (Pzm) along the margin of dacite flow-domes of the Elkhorn Mountains Volcanics (Keld) in the northeast map corner. Other rock units shown on the map include: Middle member rhyolite tuffs of the Elkhorn Mountains Volcanics (Kemb and Keme); Butte granite (Kg) and aplite (Ka) of the Boulder Batholith; Quaternary–Tertiary sediments (QTs) and Quaternary colluvium (Qc). The Boulder River Valley Western Border Fault is an active Basin and Range fault (Stickney and others, 2000).

Another area of interest follows the north to northwest trend of middle member rhyolites and andesites of the Elkhorn Mountain Volcanics (EMV). Scarberry (2017) mapped sulfide-bearing fissures that trend along this EMV middle member that extends to the south, at least to Cottonwood Creek below Houghton Park—the site of the John W. Dawson prospect where gold was discovered before 1918 and verified by the authors most recently.

### Acknowledgments

The authors wish to thank the following parties for their gracious cooperation, assistance, and encouragement in this project: Jack Dawson Ranch, Tom Dawson Ranch, Bull Mountain Grazing Association, Cooper Logging, Dr. Kaleb Scarberry, and the Montana Bureau of Mines and Geology.

### References

- Bamonte, T., and Bamonte, S., 2017, The Couer d’Alenes gold rush: Spokane, WA, Tornado Creek Publishing, p. 90–132.
- Beus, A.A., and Grigorian, S.V., 1977, Geochemical exploration methods for mineral deposits: Applied Publishing Ltd.
- Dixon, R.M., and Wolfgram, D., 1998, Bedrock geology of the Elkhorn Mountain volcanics in the southern Bull Mountain area, Jefferson County, Montana: Montana Bureau of Mines and Geology Open-File Report 374.
- Fielder, Mildred, 1969, The treasure of Homestake gold: Aberdeen, SD, The North Plains Press, p. 63–71.
- Klepper, M.R., Weeks, R.A., and Ruppel, E.T., 1957, Geology of the southern Elkhorn Mountains, Jefferson and Broadwater Counties, Montana: U.S. Geological Survey Professional Paper 292.
- Mitchell, Steven T., 2011, Nuggets to neutrinos: The Homestake story: Xlibris US, p. 73–81.
- Paul, Rodman Wilson, 1963, Mining frontiers of the far west 1848–1880: New York, Holt, Rinehart & Winston, 236 p.
- Scarberry, K.C., 2017, Geologic map of the Wilson Park 7.5’ quadrangle, southwest Montana: Montana Bureau of Mines and Geology Geologic Map 66.
- Scaberry, K.C., Kallio, I.M., and English, A.R., 2017, Geologic map of the Boulder East 7.5’ quadrangle, southwest Montana: Montana Bureau of Mines and Geology Geologic Map 68.
- Smalley, Eugene V., 1884, The Coeur d’Alene Stampede: The Century Magazine, XXVIII (October, 1884), p. 841–847.
- Stickney, M.C., Haller, K.M., and Machette, M.N., 2000, Quaternary faults and seismicity in western Montana: Montana Bureau of Mines and Geology Special Publication 114.
- Weed, W.H., 1901, Geology and ore deposits of the Elkhorn mining district, Jefferson County, Montana: Geological Survey Annual Report, v. 22, p. 399–510.
- Weeks, Robert A., 1974, Geologic map of the Bull Mountain area, Jefferson County, Montana: U.S. Geological Survey Open-File Report 74-354.

#### *Newspaper articles and obituary:*

- “The Clara,” The Black Hills Weekly Pioneer, June 17, 1876, p. 4.
- “Fatally Stabbed: Murder of John Hinch, First Homicide of the Diggings,” The Black Hills Pioneer, Deadwood, DT, July 15, 1876, p. 1.
- “Our Mining Review: Clara No. 1,” The Black Hills Weekly Pioneer, July 29, 1876, p. 4.
- “Hickok’s Assassin Acquitted; Wild Bill is Buried,” Lead Daily Call August 10, 1876, p. 1.
- “Arizona,” The Weekly Pioneer Times, Deadwood, DT, May 13, 1881 p. 3.
- “The Southern Bubble,” The Weekly Pioneer Times, Deadwood, DT, June 18, 1881, p. 1.



“Failure of J.W. Gashwiler,” *The Black Hills Weekly Times*, Deadwood, DT, July 18, 1881, p. 3.

“Innocents Abroad,” *The Daily Deadwood Times*, October 19, 1881, p. 2.

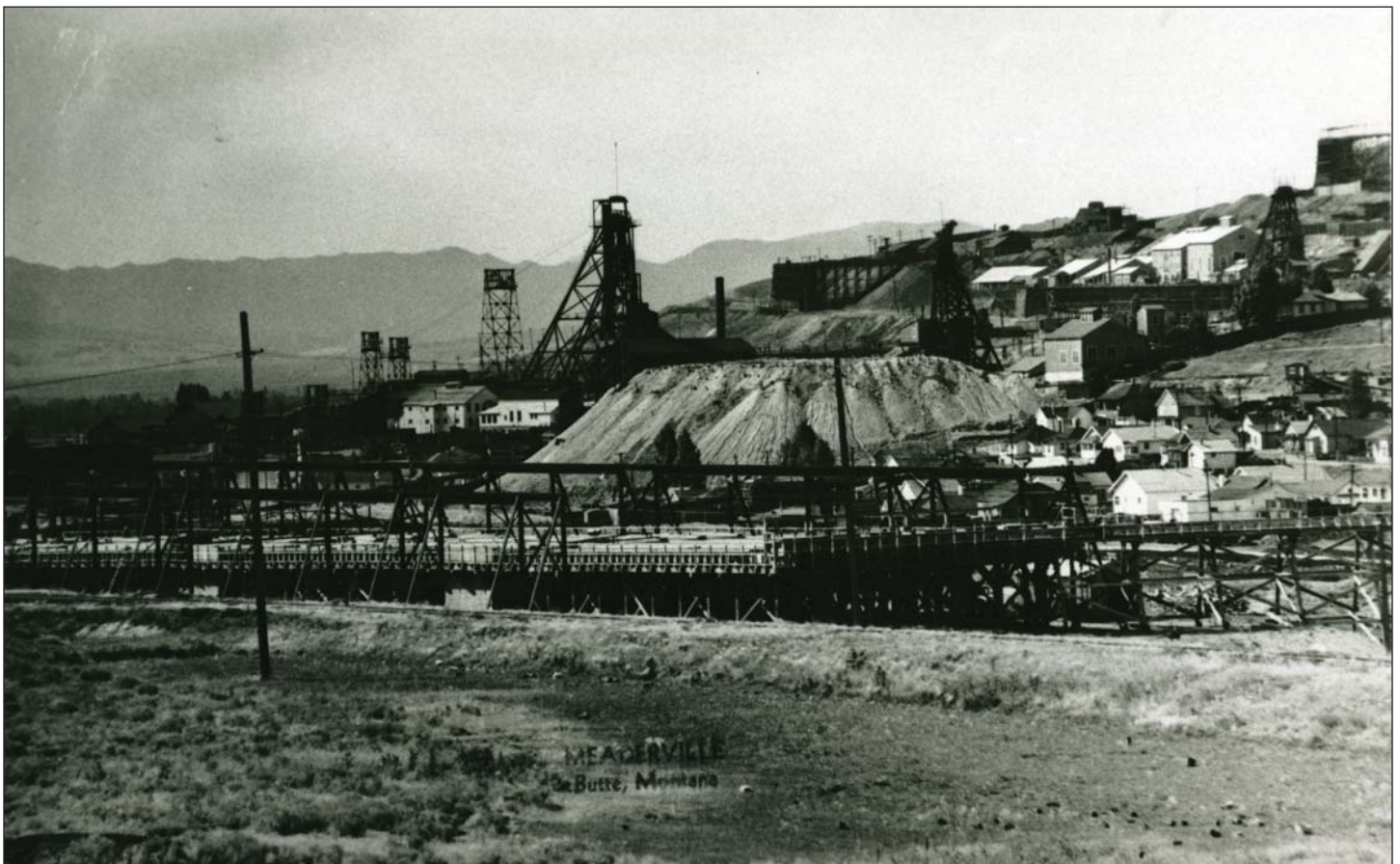
“Personal,” *The Butte Miner*, September 18, 1883, p. 4, “John Dawson of Boulder City is looking over the camp.”

“Heard From,” *The Black Hills Daily Times*, Deadwood, DT, December 22, 1883, p. 2.

“Couer d’Alene,” *The Daily Deadwood Pioneer*, February 28, 1884, p. 4.

“Personal Points,” *The Daily Deadwood Pioneer Times*, August 8, 1884, p. 2.

“James R. Haggin,” obituary, *Engineering & Mining Journal*, Vol. 8, Sept 19, 1914, p. 539



The Butte Hill viewed from the southeast circa 1950s. The Anaconda Company precipitation plant is in foreground. Courtesy of the World Museum of Mining; Butte, MT.

## J.K. Pardee, from Ohio Boyhood to Montana Mining

Anne Millbrooke

*Historian, Bozeman, Montana*



Figure 1. James K. Pardee, 1876. Pardee, formerly Superintendent of the Northwest Company, went East in the fall of 1876 to organize a new company to mine the Algonquin lode. He found investors in Philadelphia. This photograph was taken while he was in the East. (Photo: Pardee Family Collection, Mining Archives, Montana Bureau of Mines and Geology, Butte, Montana)

Working on a biography of geologist Joseph T. “Joe” Pardee (1871–1960), I am of course interested in people who influenced Joe. Perhaps the largest influence came from his father James Knox “J.K.” Pardee (1843–1914). J.K. Pardee (fig. 1) was known as a “mining man.” He worked in mine management—as an operator, superintendent, manager, investor, and a mining expert. He bought mines, or interests therein. He developed mines. He sold mines, or interests therein. He inspected mines for himself and for investors, and he reported on prospects good and bad. He specialized in silver mines, yet also considered gold, copper, carbons, and other minerals. His son Joe followed him into mining. Joe attended a mining school in Montana for 2 years and then studied mining at the University of California at Berkeley. Of an earlier time, J.K. had followed a different path into mining. J.K. went from Ohio potter to Utah smelter to Montana mining expert, a path linked by the common thread of furnaces being key to all the operations.

J.K. Pardee’s story began in 1843 when he was born in Wooster, Wayne County, Ohio, where his father Ebenezer Pardee worked as a bank bookkeeper. Ebenezer moved the family to nearby Wadsworth, Medina County, while he engaged in business with his brothers, and then to a farm just east of Wadsworth, in Western Star, Norton Township, Summit County. J.K. spent most of his youth on the Western Star farm. His father Ebenezer was one of seven brothers who had moved from Skaneateles in southern New York to the Wadsworth area in northern Ohio, so young J.K. grew up with uncles, aunts, and cousins in relatively close proximity (Pardee, 1896; Jacobus, 1927). In addition to any public schooling available, for 2 years J.K. and his younger brother, Joseph W. Pardee, attended the preparatory school at Western Reserve College in Hudson, in northeastern Summit County (later the college moved to Cleveland, but the preparatory school remained in Hudson and became Western Reserve Academy). The brothers boarded at a private home. They completed their studies in 1859 and returned to Western Star.

In April 1861, 18-year-old J.K. Pardee enlisted in Company G of the Ohio 19th Infantry Regiment. He received a medical discharge in late June, before his 3-month enlistment was up and without participating in combat. At the time he was in Clarksburg, Virginia. He traveled home, recovered his health, and later that summer enlisted again. From August 1861 to September 1865, Pardee served as a Private and later as a Sergeant with Company A of the Ohio 2nd Cavalry Regiment, which participated in campaigns in Kansas, Missouri, Kentucky, Tennessee, Virginia, and West Virginia. His unit had duty at Appomattox Court House, Virginia, on April 9, 1865; that was the date and place of Confederate General Robert E. Lee’s surrender. After a grand review in Washington, District of Columbia, his unit completed their service in Missouri. The regiment lost 267 men during the war, 83 to battle and 184 to disease (Historical Data Systems, 2009; Dyer, 1908). Pardee took pride in his military service. Later he served in the Philipsburg militia during the Nez Perce unrest in 1877, and, despite his disqualifying age, he tried to volunteer for the Spanish-American War. When the Grand Army of the



Republic, a veterans' organization, formed Montana chapters in the 1880s, he joined. He served as Commander of the Burnside Post in Philipsburg, and in 1895 as Aide-de-Camp for the Department of Montana. Later he became a member of Meade Post in Oregon City, Oregon.

### Potter

During the war Pardee's parents had moved to Rochester, Beaver County, Pennsylvania, and that is where he went to live after being discharged. But his mother, Almira Brace Pardee, died there in January 1866, and that August his father died while visiting a daughter (J.K.'s oldest sister, Harriet Loomis) in Wadsworth. Meanwhile, Pardee, who bought, operated, and sold a drug store in Rochester that year, developed an interest in the potteries of Rochester and elsewhere along the upper Ohio River (Gray, 2002). He also developed an interest in Maria A. Lukens, of an old Pennsylvania family. They married in her mother's home in Rochester in September 1866. That same autumn Pardee studied at Duff's Mercantile College in Pittsburgh. Established in 1840, the school was well known for its accounting course; Peter Duff's bookkeeping textbook was already in its eleventh edition at that time.

J.K. and Maria Pardee settled in Wadsworth. Pardee established the Wadsworth pottery works of Pardee & Co. He hired potters, apparently Jacob Tillze, an immigrant from Germany, and John Homer, an Ohio native; the 1870 Federal Census lists Pardee and those two as the three potters living in Wadsworth. Pardee managed the business, sold the product wholesale, and procured the fuel and other necessities for the pottery works. The product was stoneware, a salt-glazed rather than lead-glazed crockery, and it was fired at a relatively high

temperature. The result was a strong pottery resistant to breakage, strong enough to ship by rail without straw or other packing ("Crockery," *Minneapolis Star Tribune*, April 13, 1870, p. 4).

Pottery was still hand made in the 1860s, but the industry was in transition from small, local, and often short-lived potteries with one or a few kilns, to large pottery works with many kilns. At the time the Siemens regenerator furnace promised to enable potters to fire or burn pottery without enclosing each piece in fire-clay boxes called "saggers" (Patent No. 41-788, March 1, 1864, reissued as No. 3,265, January 12, 1869). Pardee and other potters continued to fire their ware in the traditional way (Barber, 1902), but the Siemens furnace was undergoing experimental use for metallurgical applications (*Chicago Tribune*, May 26, 1870, p. 2). Siemens was famous for, in the 1850s, developing the open-hearth furnace for processing steel, for regenerative preheating of fuel and air for combustion. The new Siemens furnace was also for metallurgy, but could be used for firing pottery. It was being tested at mines in Arizona. The fact that Pardee was, like other American potters, using traditional a furnaces in his kilns (fig. 2) rather than the experimental regenerative furnace, became important in hindsight, given his later work with furnaces.

The industrial revolution was reaching the American pottery industry, notably those potteries along the upper Ohio Valley which had river and rail transportation, plenty of native clays, local coal mines,

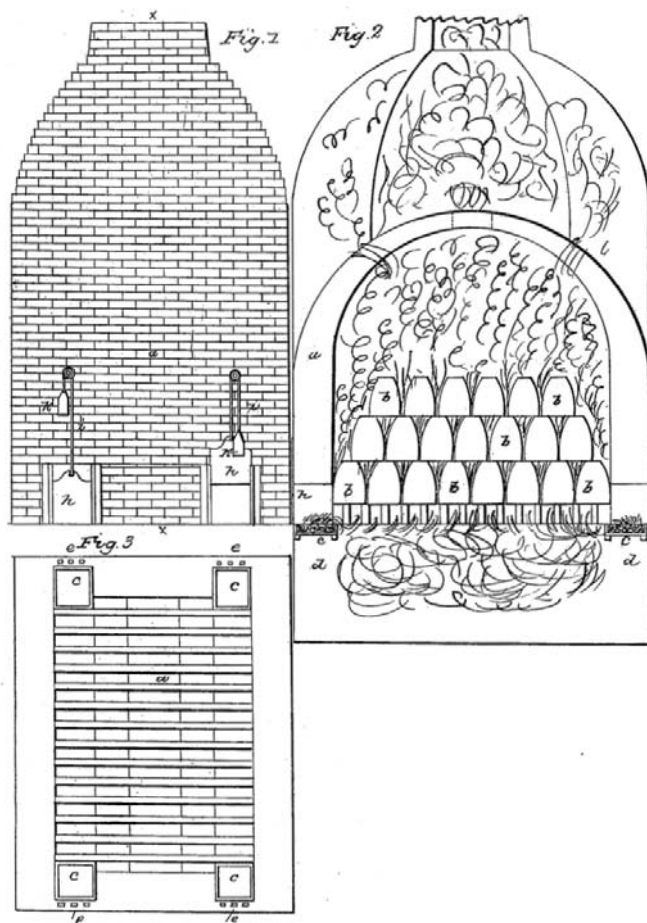


Figure 2. Pottery Kiln. The traditional kiln is shown, front view, in Fig. 1 in the image. Fig. 2 shows a vertical section, with pottery pieces in fire-clay boxes called "saggers" that protected the pottery from the flame and fuel. The Siemens regenerator furnace enabled potters to fire pottery without enclosing the clay in "saggers" (Patent No. 41-788, March 1, 1864, reissued as No. 3,265, January 12, 1869). Fig. 3 shows a base grate (Drawings: Patent 7,136, March 05, 1850).

and water; it took a lot of water to work clay. In 1869 Andrew Cheeseman received a patent for his “machine for making pottery,” an improvement on the jigger, which was a rotating table that held the mold being worked by the potter. The purpose of Cheeseman’s invention was “to dispense with the skilled labor required” to shape pottery by using an automated forming tool (Patent No. 93,966, August 24, 1869). Isaac Knowles’s 1870 invention of another “pottery machine” had a “former” or “pull down” to shape the pottery mold on the revolving jigger (Patent No. 108,157, October 04, 1870).

Pardee managed a traditional, standard pottery. He helped develop local coal resources as the furnace needed fuel. Traveling by train, he marketed the stoneware beyond Wadsworth and Ohio. He served on the local board of education, and he was elected to the village council. Pardee and his wife had a daughter, born in February 1869. Sadly for the young couple, little Mary A. Pardee died that September.

Pardee was in the news a lot in 1870 for one reason: he disappeared. He had gone to Chicago, visited friends, said farewell, and vanished. That was April 27, 1870. He was last seen on his way to a Chicago train station to start a marketing trip throughout the region. Family and friends searched for him. Police throughout the Midwest searched for him. Private detectives searched for him. The Medina County Gazette (June 03, 1870) soon reported, “If his friends are correct, in their opinion that he is dead—and we know not how any other conclusion can be reached—Wadsworth has lost one of her best and most active and energetic citizens.” And thus J.K. Pardee, stoneware merchant, community booster, and husband, was gone.

Then, from Colorado, Pardee sent a brother a telegraph with instructions to sell his properties. From Utah, Pardee telegraphed his wife Maria. He said to expect him home on August 17. When he arrived on that date, he fell ill and avoided public explanation of his long disappearance. What transpired between husband and wife at that reunion remains unknown. Within months, he and his wife left Ohio. In December 1870, just before Christmas, they were at the Townsend House hotel in Salt Lake City.

### Smelter

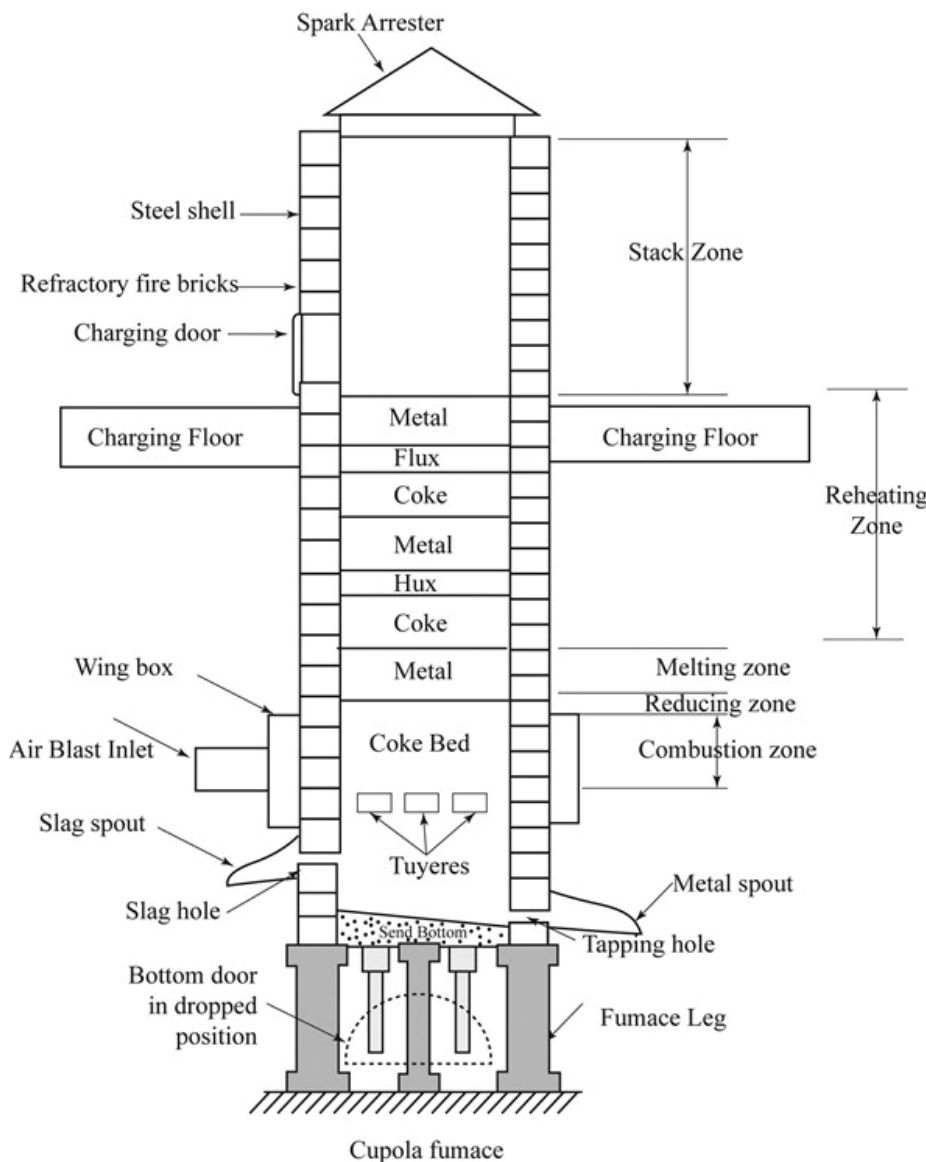
In Utah, Pardee formed a partnership with T.R. Jones (1833–1915), who had some foundry experience from his time in Virginia City, Nevada. The newspapers of the day referred to the partnership as Jones and Pardee, Pardee and Jones; Pardee, Jones and Co.; and Pardee & Co. In 1871 Pardee and Jones built a smelter at Tannersville on Tanner Flat near the mouth of the Little Cottonwood Canyon (fig. 3). Little Cottonwood was a booming mining district in the Wasatch Range on the eastern side of Salt Lake County. Silver and lead bullion were the



Figure 3. Little Cottonwood Canyon. In 1872 photographer William Henry Jackson of the U.S. Geological and Geographic Survey of the Territories took this picture of the head of Little Cottonwood Canyon in the Wasatch Mountains of Utah. (Photo: National Archives at College Park, Wikimedia Commons)



main products, and granite was being quarried for the Mormon temple then being built in Salt Lake City. The gross average of ore sold in the district for smelting ranged for silver from \$40 to \$120 per ton and for lead between 20 and 60 percent (Engelmann, 1873).



Pardee and Jones learned by doing and by copying. Their cupola and blast furnace (fig. 4) was a common type of the time and place. The cupola was a vertical furnace with a hollow shell. The upper section of the shell enclosed the stack or chimney for escaping smoke and gases. Fuel and ore entered via the charging opening above the charging plate, at the base of the stack. The charge was heated below the charging plate and above a base plate. The blast forced air through a nozzle called a tuyere; the tuyere carried the air through openings into the lower portion of the shell. Molten metal flowed out through a small opening in the bottom plate. Slag exited through a different opening. The cupola type enabled continuous or intermittent melting of ore. As the fuel was consumed and the metal melted, additional charges of fuel and ore could be added. Pardee and Jones used water from Little Cottonwood Creek to generate steam power for the smelter. Coal to fuel the furnace came from much farther away. The smelter could process ten tons of ore in 24 hours.

Figure 4. Cupola blast furnace. The vertical cupola blast furnace is basically a cylinder shell. At the top is the stack, where smoke and gases exit. The charging floor provides a base for loading the charge through an opening. The charge goes down through a heating zone, a melting zone, a reducing zone, and the combustion zone. Blast air enters openings at the combustion level. Slag and metal exit via taps near the base level. (Schematic: K.G. Budinski and M.K. Budinski, 2009, Engineering Materials, 9th ed., Chegg.com)

At the time, smelting was booming. Eighteen smelting furnaces, including the Pardee and Jones furnace, were built in Utah in 1870–1871 (Murphy, 1872). The Salt Lake Herald (November 3, 1871, p. 2) reported on “The Smelting and Mining Prospects

of Utah.” There seemed to be nearly as many problems as prospects. For smelters, there was the irregularity of ore deliveries; this suggested that a profitable smelter have its own mines, but even so, mines had uncertain futures. Fuel was expensive, as coal came from 60 miles or more away, sometimes from Nevada, and the railroads charged monopolistic shipping rates. After the cost and labor involved in producing bullion came the fees for commission, storage, shipping, and refining the bullion. Despite some fine ore, the bulk of the ores was low grade. A highlight of the article was “the splendid bullion (300, 400, and 500 ozs) of the Pardee furnace.”

In June the Pardee and Jones furnace was processing first- and second-class ore from the Emma silver mine, a fabulously rich mine that had the previous year sent its ore to New Jersey for smelting. The Emma was already under a cloud of fraud accusations regarding its ownership. The rich ore was quickly exhausted. Then the

mine became the subject of one of the most scandalous mining stock frauds in this nation's history, prompting investigations by both the United States Congress and the United Kingdom Parliament. The initial fraudsters were all in place when Pardee and Jones worked the Emma ore (Plazak, 2006; Spence, 1958). The Emma might have influenced Pardee, who throughout his mining career avoided mining stock markets. Pardee preferred tightly held companies that sold some stock locally, which was considered a courtesy to the local community of any mine, but sold stock mostly to major investors in a mining syndicate.

It was in 1871, while Pardee was engaged with the smelting works, that his son Joseph T. Pardee was born in nearby Salt Lake City, where Maria Pardee chose to live.

Pardee and Jones operated their smelting works through the end of the year. In addition to the Emma, the South Star (also called the Vallejo) and other mines sent ore to the smelter. In January 1872 Pardee and Jones sold the smelting works to David Buel, I.C. Bateman, and the associated Wellington Mining Company. The buyers operated the smelter while erecting new furnaces for ore from their Last Chance mine in Bingham Canyon and Flagstaff mine in Little Cottonwood. Smelting technology was quickly improving, making the early smelters obsolete. As soon as the new Buel and Bateman furnaces became operational at Sandy Station, they closed the Pardee smelter at Tannersville. It had been in operation for a total of 2 years.

After selling his interest in the smelter, Pardee explored mining prospects. He acquired an interest in the Vulcan mine, situated in Rush Valley District, Tooele County (he forfeited this interest in 1885). He became superintendent of the Vanderbilt mine, a new silver lode mine up the Little Cottonwood Canyon. The majority of mines in the Little Cottonwood district were new. While hundreds of claims had been filed since the ore discoveries of 1864, over 40 mines, including the Vanderbilt, had been located in the years 1870–1871. Near the Vanderbilt were the Miner's Dream, Dalton, and Lark. These were small, independent mines. At such independent mines miners had the potential to earn a share of the wealth, while the large companies that controlled both mining and milling paid only wages. The Vanderbilt did not incorporate until 1882, long after Pardee had moved to Montana (Whitley, 2006; Kantner, 1896).

### **Mining Expert**

In March 1874 Pardee traveled to Montana. In Deer Lodge the local New North-West newspaper (March 21, 1874, p. 3) referred to him as “a Utah quartz operator of repute.” He had paused in Deer Lodge on his way to examine quartz mines in the Philipsburg area. Pardee reported to eastern investors, who were apparently pleased, as Pardee became superintendent and manager of the North-West Company's Speckled Trout mine later that year. Pardee, his wife, and his son thus passed through Deer Lodge again that September, bound by coach to Philipsburg (fig. 5).

While Pardee is the focus of this discussion, each mine had multiple characters associated with it, including the locator, the incorporators, the investors, the people in management positions, and the mine and mill workers. The North-West Company had incorporated in Montana in January 1874. The incorporators were George W. Cass, President of the Northern Pacific Railroad; Charlemagne Tower, Thomas L. Jewett, William G. Moorhead, Jonathan K. Ewing, and General A.B. Nettleton. They were a Philadelphia syndicate. They were interested in Cole Saunders's Speckled Trout mine that Pardee had examined in the spring.

Below are some examples of diverse people affiliated with the Speckled Trout and Pardee. On behalf of the Philadelphia syndicate, General A.B. Nettleton toured the Trout (the Speckled Trout) mine in September. Alvred Bayard Nettleton (1838–1911) had hired Pardee. They had both served in the 2nd Ohio Cavalry during the Civil War. Nettleton had quickly risen through the ranks to Colonel, Commander of the 2nd Ohio Cavalry, and, briefly in 1865, Brevet Brigadier General; thereafter, in civilian life he used the title General. During his career Nettleton invested in mines, railroads, and newspapers. He had published a Chicago paper and managed the Philadelphia Inquirer. As an agent for the Northern Pacific Railroad, he helped bring the railroad to Montana. He was secretary of the new North-West Company. Accompanying Nettleton on his tour was Colonel J.A. Viall. Jasper A. Viall (1828–1910) acquired his military title by political appointment to the Iowa state militia in 1865, rather than in service during the Civil War. He had moved to Helena in 1870 when he became the Federal Superintendent of Indian Affairs, a post he held for 2 years. In 1873 he became an agent of the Northern Pacific





Figure 5. Philipsburg, Montana. From the 1870s to 1901, James K. and Maria A. Pardee lived in a house on Lower Broadway on the west side of downtown Philipsburg, the fenced lot center left in this 1887 picture. (Photo: Granite County Museum)

Railroad, and in 1874 he became also a general agent of the new North-West Company. Viall was temporarily the Trout manager, until Pardee arrived. A native of Missouri, Cole Saunders (1839–ca. 1913) came to Montana during the Virginia City gold rush. He became a mine developer, and he had a store in Helena. He helped publicize the area’s silver resources by writing a description of the Flint Creek District for Rossiter W. Raymond’s influential reports (1873a,b). Like Pardee, Saunders had erected a smelter to process silver ore. When costs threatened the smelter, Henry Schnepel of Philipsburg organized fellow workers to contribute capital, but that and other efforts could not save the smelter. The venture ended in bankruptcy. As a consequence, Saunders sold the Speckled Trout mine that he had begun to develop. Saunders helped arrange for North-West to acquire certain assets of the Imperial Silver Mining Company that had briefly leased the Trout mine. But Saunders emerged from the lengthy negotiations with both the five-stamp Imperial mill and the contract to reduce North-West ore. Before the end of 1874 Pardee had Saunders building the North-West Company mill. These are just a few of the names associated with the capitalization and management of the North-West Company as Pardee came upon the scene. The company soon modified the name from North-West to Northwest, and the name of the mining camp changed from Troutville to Tower, after board member Charlemagne Tower.

Pardee developed the Northwest Company’s mine and mill, and he moved on. In 1876 he became superintendent for the newly formed Algonquin Company, another Philadelphia syndicate. The Algonquin property was at the Hasmark camp, less than a mile from Tower. There Pardee developed the Algonquin mine and acquired the nearby Salmon mine. He oversaw construction of a large dry roasting-pan amalgamation mill with 20 stamps, which began operation in 1880. The mill’s furnace included an innovation patented by Pardee (Patent No. 235,800, December 21, 1880; Goodale, 1890).

Pardee described the basic rotary ore-roasting furnace (fig. 6) as having a capacity of one ton of silver ore an hour, with two fireplaces burning ten cords of wood every 24 hours. Tons of crushed silver ore mixed with

(No Model.)

J. K. PARDEE.  
Rotary Ore Roasting Furnace.

No. 235,800.

Patented Dec. 21, 1880.

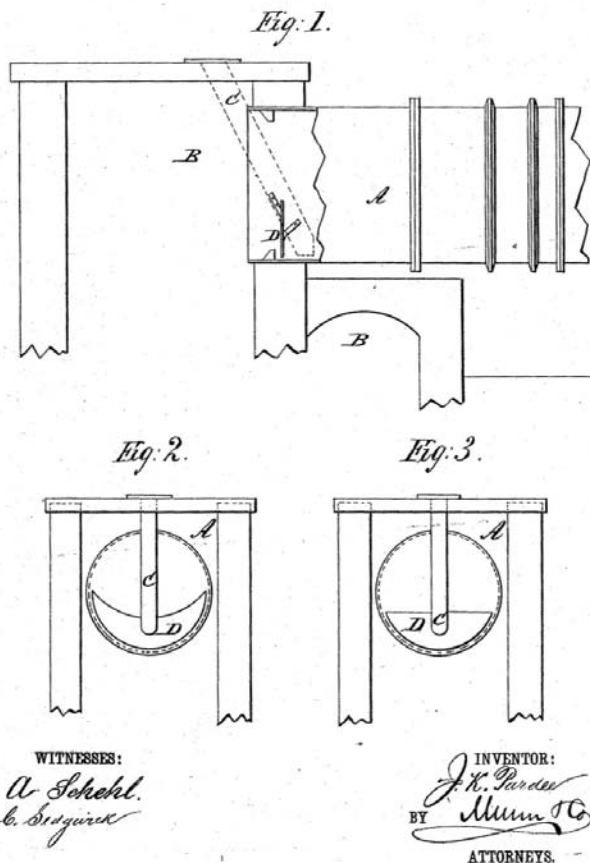


Figure 6. J.K. Pardee's improved furnace. According to Pardee's patent, "A represents the revolving cylinder or furnace; B, the fire-place and dust-chambers at the feed end of said furnace; C, the inclined feed-pipe, and D the diaphragm, partition, or plate fixed within said furnace A." Fig. 1 in diagram is a side elevation of the feed end of the rotary furnace. Fig. 2 is an end elevation of the furnace with the lune-shaped diaphragm. Fig. 3 is an end elevation with the diaphragm shaped like a segment of a circle. (Patent No. 235,800, December 21, 1880)

and metal-working machinery. Rumsey invented an improved diaphragm for the rotary furnaces at the Granite Mountain mills. His diaphragm was a ring-shaped piece with a projecting annular flange (fig. 7). He said that his invention was to eliminate the need for a second furnace and to reduce ore going into dust chambers. Rumsey received a patent for his improved furnace for roasting and chloridizing ores (Patent No. 343,731, June 15, 1886).

As illustrated by the cases of the Philadelphia syndicates owning the Northwest and Algonquin companies and the St. Louis syndicate owning Granite Mountain, it is clear that much of the profits from Philipsburg's silver mines went to out-of-state investors. But Pardee did well. When he, his wife, and son moved into their new home, the Philipsburg reporter for the county newspaper reported that the house was a "noticeable" improvement to the town (New North-West, February 9, 1877, p. 3). (The house, since renovated, is still on Lower Broadway in Philipsburg.) The county newspaper, the New North-West, called Pardee "efficient" (November 14, 1874, p. 3), "zealous" (September 03, 1875, p. 3), "the livest mining Superintendent we have ever had in Montana" (November 19, 1875, p. 3), "energetic" (June 9, 1876, p. 3), "one of the best of Montana miners"

salt entered the basic furnace through the feed pipe, but about a third of the ore did not go through the revolving cylinder to be roasted; rather, it fell into the dust chambers around the feed pipe's end. This ore had to be put into the feed again for roasting. That was the problem Pardee solved.

He designed a "diaphragm, partition, or plate" of boiler-plate iron, which could be cast iron or wrought iron. Shaped as a segment of a circle or as a lune, this piece of iron was attached either to the bottom end of the feed pipe where the ore fell out or to a frame holding it where the feed pipe discharged the ore. Ore entered the upper end of the feed pipe. At the bottom end the ore fell from the feed pipe. There the diaphragm allowed about a half inch of space below the plate through which the ore entered the furnace. With this improvement in place, more ore went into the furnace, less into the dust chambers. The improved furnace needed only one fireplace to burn (rather than two), used only 4 cords of wood (rather than 10) every 24 hours, and allowed only one twelfth of the ore (rather than one third) into the dust chambers. Furthermore, the invention allowed ore to be heated before the rotary movement carried it high enough to be dropped "through the moving current of flame and air," so the danger of ore dust being carried by the draft into the dust chambers was avoided, and the ore was more completely chloridized as it roasted.

Milling and milling technologies were competitive and changing. A local competitor made an additional improvement to the rotary furnace. L.M. Rumsey was president of the Granite Mountain Mining Company and thereby of the St. Louis syndicate owning that Granite Mountain mine and mills, which were only several miles from the Algonquin. Rumsey was also President of the L.M. Rumsey Manufacturing Company of St. Louis; the large Rumsey plant made wood-working



(No Model.)

L. M. RUMSEY.

FURNACE FOR ROASTING AND CHLORIDIZING ORES.

No. 343,731.

Patented June 15, 1886.

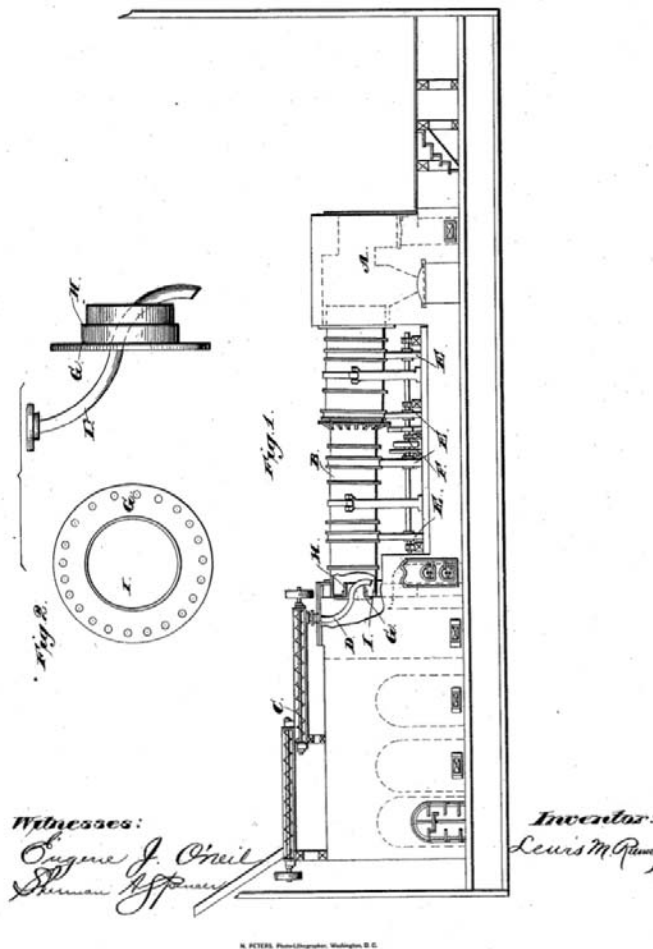


Figure 7. L.M. Rumsey's improved furnace. This illustration shows a slide elevation of a standard rotary furnace in Fig. 1 in the diagram. Pulverized ore enters feed mechanism C. Pipe D conveys the ore into the upper end of the rotary cylinder B. A is the fire chamber. Friction wheels E and driving mechanism F rotate the cylinder. Rumsey attached "a flanged annular piece, G," to the end of cylinder B. Rumsey's a ring-like plate G with its projecting flange H is shown in Fig. 2 in the diagram. The plate was to receive and hold fine ore dust in the internal dust chamber I until it was roasted or chloridized, at which stage it would fall with the heavier ore into the rotary cylinder. (Patent No. 343,731, June 15, 1886)

(October 6, 1876, p. 3), "competent and energetic and a good man to have in a community" (August 1, 1879, p. 3), and "a thorough miner, a progressive and systematic manager" (May 8, 1885, p. 3). The Butte Weekly Miner described Pardee as "a typical illustration of the daring, nerry, irrepressible miner" (July 31, 1886, p. 2) and "the erratic mining genius whose reputation is as broad as the continent" (January 15, 1891, p. 8). The Philipsburg Mail called Pardee "the mining magnate of the Flint Creek district" (May 9, 1889).

In 1882 Pardee organized the Princeton Mining Company to work the Princeton, Saranac, Mediterranean, Raritan, and Sandy Brown claims; he had bought the Saranac a few years earlier. The Princeton group of silver mines and Princeton mining camp were near Maxville, up the Boulder Creek canyon at the mouth of Princeton Gulch. The Princeton group of mines was in the Boulder mining district, north of Philipsburg and its Flint Creek mining district. Pardee profitably developed the Princeton claims and expanded the operations to include the Tigress, Crowned Prince, and Clear Creek claims. Trouble with French investors led the Princeton company to close temporarily in 1885 and thereafter to lease the mines.

Pardee, usually in conjunction with other investors, became involved in many mining ventures, including in 1885 the coal mines at Cinnabar in southern Park County (the mining camp of Horr was later renamed Aldridge). In 1886 he helped organize and became general manager of the West Granite Mountain Mining Company, which in 1889 was acquired by the Elizabeth mining syndicate of the Granite Mountain and Bi-Metallic companies. He organized the Pearl Silver Mining Company in 1888 (fig. 8). Late that year he investigated new claims prospectors had filed on the Iron Mountain, northwest of Missoula. He quickly bonded the properties and organized the Iron Mountain mining company. Despite having to build a 20-mile wagon road to the mine and having to ship ore on the Missoula River (now Clark Fork) to reach the railhead at Paradise, the mine soon became a regular shipper of ore to the Helena smelter. In recognition of Pardee's role in developing that mining district, the miners chose to name their camp Pardee (Butte Daily Post, July 15, 1889, p. 4). In 1889 Pardee also joined a Helena syndicate formed to operate the Fourth of July mine in Washington. In 1890 he organized the East Granite Mining Company (fig. 9; Wolle, 1963; Emmons and Calkins, 1913; Domine, 2008, 2009, 2012).

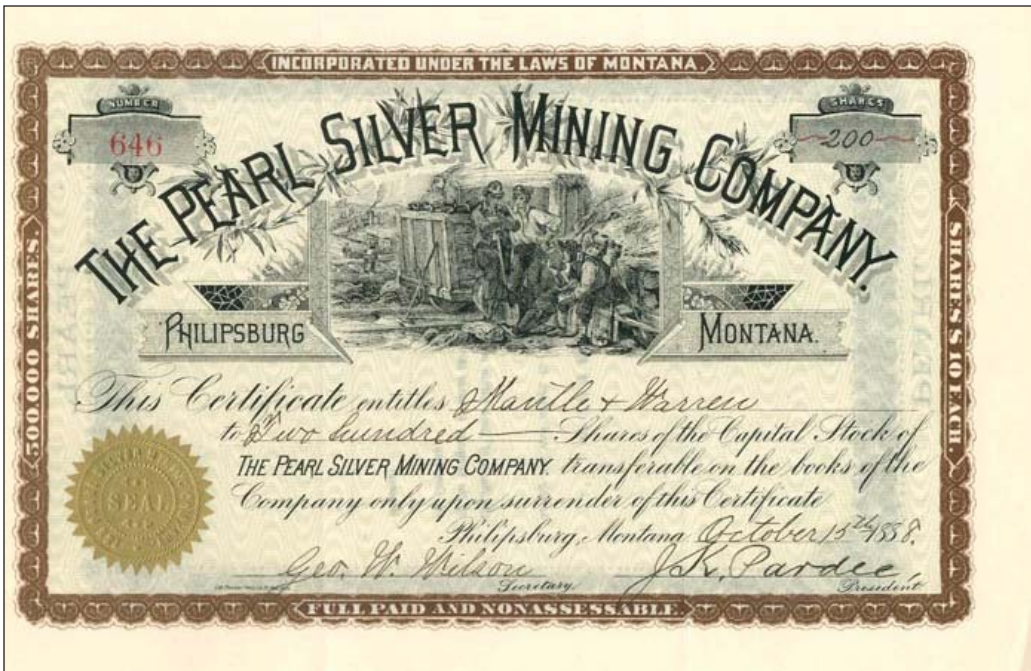


Figure 8. The Pearl Silver Mining Company. J.K. Pardee, President, signed this stock certificate for Mantle & Warren. Lee Mantle and Charles S. Warren, both of Butte, were mine investors. (Photo: Michael Gobra Collection)



Figure 9. The East Granite Company. J.K. Pardee, President, signed this certificate for East Granite stock. (Photo: Michael Gobra Collection)



Samuel T. Hauser (1833–1914), Helena banker and capitalist, invested in several of Pardee's ventures, including the Iron Mountain and Fourth of July mines. Among the Hauser papers at the Montana Historical Society are letters from Pardee concerning mines. He reported on the Maginnis Mining Company, the Jefferson copper lode, the Pleasant View mine, and the San Francisco mine, all in western Montana; the Blue Jacket and Fourth of July mines in Washington; and litho-carbon deposits in Texas. Meanwhile, Pardee was also an incorporator of the Philipsburg & Drummond Railroad Company and the Philipsburg Real Estate & Water Company. He also represented Deer Lodge County in the territorial House (1881) and the territorial Council (1887).

Mining involved conflicting claims, labor disputes, court cases, investor interference, partner disagreements, bank frauds, and competitor challenges. Pardee's arrest in 1888 provides an example. In a case of disputed right-of-way, the courts had ruled against Pardee and his West Granite mine cohorts. Not ready to concede, Pardee planted explosive charges among the rocks along the right-of-way in dispute. Railroad workers building a branch line to the competitor's property safely removed the explosives. To stop the work on the line, Pardee shouted a warning, then threw a stick or multiple sticks of Giant powder (a brand of dynamite) at the railroad workers. Newspaper accounts vary. In one account, the railroad workers responded by getting dynamite and returning fire. Whatever the actual details, Pardee was arrested. The case came before a probate judge obviously friendly to Pardee. The judge overlooked the initial sabotage of hiding charges along the right-of-way. The judge accepted the explanation that only one stick of dynamite had been thrown and that no one had been in danger because the railroad men had time to flee. Case dismissed. Among the newspapers that carried the story were the Helena Weekly Herald ("Pardee Arrested," September 6, 1888, p. 7), Deer Lodge's New North-West ("Philipsburg Giant Powder" and "Summons," September 7, 1888, p. 3), the Great Falls Tribune ("Lively Times Near the Granite Mountain Mine," September 9, 1888, page 1), the Butte Semi-Weekly Miner ("Pardee Discharged," September 8, 1888, p. 1), and Fort Benton's River Press ("A Serious Charge," September 12, 1888, p. 1).

The good times for Pardee and silver mining throughout the mining west came abruptly to an end in the Panic of 1893. The Sherman Silver Purchase Act of 1890 had increased the amount of silver the government was required to purchase with notes backed by gold. This was good for mine owners and miners. Silver mining boomed. So much silver came out of the western mines that inflation became a national problem. That was good for farmers in debt, who like the miners supported free silver or a high statutory limit on the government's purchase of silver as provided in the 1890 law. The commercial price of silver crashed in 1893, but the government had to buy silver at the legally set price—until the repeal of the silver purchase act that November. As the price of silver fell, mining companies cut wages and, when that was not sufficient, they closed the mines. Entire mining camps, such as the once bustling community of Granite on Granite Mountain, essentially closed as the population, the miners, businessmen, and their families moved away.

According to historians and economists, the Panic of 1893 and subsequent depression were as bad as the crash and Great Depression of the next century (Petrik, 2009). Before the economy improved from the Panic of 1893, the nation ran into the Panic of 1896. Over half the chartered banks in Montana disappeared through merger or closure. Helena, the financial center of the State and the entire region, lost four of its seven banks. The Second National Bank closed; the Helena National Bank merged with the First National Bank, which then closed; and Merchants National Bank also closed—all in a 5-year period. These Helena banks had invested heavily in mines, but their banking practices were very poor according to the bank examiners over the years. The banks routinely provided unsecured loans, including loans to the bankers themselves. S.T. Hauser was the founder of First National, a former governor, a popular capitalist, and sometimes colleague of J.K. Pardee, but he was also a careless banker who borrowed freely from First National till it closed.

Pardee personally suffered by poor banking practices at the First National Bank in Butte, part of the S.T. Hauser & Co.'s banking network. An employee blurred the line between personal and bank business. In April 1881 Pardee sold mining stock to a bank employee in Butte, A.J. Davis. Pardee received the payment from the bank and gave an \$11,000 promissory note in return. He understood that Davis would pay the sum on the note to the bank. The transaction was supposedly finalized with payment in August 1883, but the bank did not receive the money from Davis till mid-December, after the deadline stated in the note. The bank sued Pardee for

missing the payment deadline. A jury trial yielded a judgment for the bank. Pardee appealed. Finally, in 1895, the Montana Supreme Court settled the case. Pardee was held personally responsible for the debt, and the bank could foreclose on the deed of trust (promissory note), despite the fact that Davis should have credited the payment in August. The court said, “There is nothing in the case to authorize holding of the bank responsible for the failure of Davis to pay the money at the time claimed to have been agreed upon between him and the defendant” (Maddox, 1895).

The national depression hit Philipsburg and other silver mining communities particularly hard. The Iron Mountain Mine, once “Pardee’s Bonanza” (Helena Independent, January 9, 1889, p. 4), but no longer one of Pardee’s interests, was one of the few silver mines to survive. Its miners did go on strike when wages dropped in late 1893, but Iron Mountain recovered. The mine continued operations and even regularly paid dividends (Missoulian, November 25, 1895, p. 4). But, like other mines of the period, Iron Mountain experienced workplace injuries, management squabbles, union activities, claim cases, funding shortages, transportation issues, and weather headaches. Moreover, a fire destroyed its mining camp of Pardee, which was rebuilt, and the mining company banked in Helena at First National, which closed.

The Silver Issue was a leading political topic of the long depression. Pardee joined the Silver Republicans, splitting from the main Republican Party that supported the gold standard rather than bimetallism (silver and gold). William Jennings Bryan won the Democratic nomination for President in 1896 based largely on his support of bimetallism, which he expressed eloquently in his now famous Cross of Gold speech given at the party’s convention that summer. Free silver was free on restriction of silver coinage; it was coinage on demand, or, as Bryan advocated, almost-free silver at the high weight ratio to gold of 16 to 1. Bryan won the vote in Montana, four to one, but lost the election; he visited Montana in 1897, already campaigning for the 1900 election. During this period, Pardee was actively opposing the American Protective Association’s anti-Catholic, anti-immigrant campaign and attempt to take over the Republican Party at the local level as well as the national level. At the Granite County Republican convention of 1896, he led a walk-out and organized a separate convention for like-minded Republicans. His son Joe participated in this alternate convention. That year Pardee ran as Silver Republican Candidate for Granite County Treasurer. He won. He served a 2-year term. In the next election, he lost the position.

Pardee continued to explore mining opportunities. He convinced his son Joe to join him in acquiring two adjacent gold mining claims in the Greenhorn Mountains of northeastern Oregon. With Charles S. Warren of Butte, they organized a Montana syndicate, the Pardee syndicate, to back their Diadem Gold Mining Company. This was Pardee’s last big attempt to become a capitalist rather than to work for capitalists. But limited personal resources after the long depression, ill health, and the failure to find a major vein led Pardee to exit that short-lived venture, and his son soon thereafter extricated himself from the Diadem venture. Both were gone by the time Montana’s former U.S. Senator Lee Mantle, a major investor, sued the Diadem company and acquired the then-closed mine.

### **In the Shadow of Mines**

In the autumn of 1901 the Pardees—J.K., Maria, and Joe—left Philipsburg. They moved into a fine house on East Front Street in Missoula. Joe had purchased the house from the pioneer Catlin family. Although Joe married and moved to Stevensville in 1904, J.K. and Maria Pardee continued to live in Missoula. J.K. continued to hold interests in various mining properties and to consider mining propositions. Political patronage at that time controlled the appointment of postmasters and led to Pardee’s appointment as postmaster of Plains, Montana, as well as to his subsequent replacement. J.K. and Maria lived in Plains from late 1905 to the start of 1908. They then moved to Stevensville to live with their son Joe, his wife Ruby, and their little daughter Mary Jo. The extended family moved to Gladstone, Oregon, in 1909. The following year Joe and his wife and daughter moved to Washington, D.C., where Joe had taken a job with the federal Geological Survey. J.K. and Maria stayed at Joe’s place in Gladstone. J.K. Pardee was among the petitioners behind incorporating Gladstone in 1910. He served as city treasurer for 2 years. He later ran unsuccessfully for Clackamas County treasurer.





Figure 10. James K. Pardee, 1914. Pardee used this photograph on his campaign card for the Republican nomination for County Treasurer of Clackamas County, Oregon. He campaigned on his Civil War record, on having given “the best 3 1/2 years of my life to save what is now this great and glorious nation.” He lost in the primary election, and days later, on May 18, 1914, he died at his home in Gladstone, Oregon. (Card: Pardee Family Collection, Mining Archives, Montana Bureau of Mines and Geology, Butte, Montana)

Maria died of sclerosis on March 25, 1914. J.K. Pardee (fig. 10) died by self-inflicted gunshot on May 18, 1914. The press blamed his suicide on grief over losing his wife and on his loss in the recent Republican primary race for county treasurer, but his health must also be considered a factor. He had a long history of periodic illness serious enough to make the newspapers. The Philipsburg Mail on January 12, 1883, for example, reported that Pardee was “quite ill” and on May 18 that he was “ill” but “convalescent” at the Warm Springs Hotel. On October 3, 1900, for a later example, the Sumpter Miner in Oregon had reported that Pardee had gone back to Philipsburg, “his health utterly wrecked.” Other than a couple mentions of rheumatism, the newspapers did not say what ailed him. Metal poisoning was common among pottery, smelting, mining, and mill workers of that period. Lead poisoning, for example, caused potter’s paralysis, but the Wadsworth pottery had produced stoneware not requiring the glazing and decorating sources of lead. Smelting and milling were more likely sources if Pardee was poisoned, but other explanations could be offered based on the limited evidence at hand at this date.

Pardee still held interests in multiple mining properties at the time of his death. His interest in the Princeton mine was the last of his estate to be settled by his son, who forfeited that interest when an opportunity arose in the early 1940s.

### References

- Barber, E.A., 1902, *The pottery and porcelain of the United States*: New York, G.P. Putnam’s Sons.
- Domine, L.M., 2008, 2009, 2012. *Mettle of Granite County*, 3 volumes: Helena, Mont., KAIOS Books and Loraine M. Domine.
- Dyer, F.H., 1908, *A compendium of the War of the Rebellion*. Des Moines, IA: Dyer Publishing Company, <https://archive.org/details/08697590.3359.emory.edu/> [Accessed February 2020]
- (The Ohio regimental histories copied from Dyer are online at the Civil War Archive, <http://www.civil-wararchive.com/unionoh.htm/> [Accessed February 2020].)
- Emmons, W.H., and Calkins, F.C., 1913, *Geology and ore deposits of the Philipsburg Quadrangle, Montana*: U.S. Geological Survey Professional Paper 78: Washington, D.C., Government Printing Office.
- Engelmann, H., 1873, *Observations on the mines and ores of Little Cottonwood Canyon, Utah*: The Engineering and Mining Journal, v. 15, p. 145–147.
- Goodale, C.W., 1890, *Notes on the additional diaphragm in the Howell roasting furnace*: Transactions of the American Institute of Mining Engineers, v. 18.
- Gray, P.L., 2002, *Ohio Valley pottery towns*: Images of America series: Charleston, S.C., Arcadia Publishing.
- Historical Data Systems, 2009, *U.S. Civil War soldier records and profiles, 1861–1865* [database online]: Provo, Utah, Ancestry.com Operations Inc.
- Jacobus, D.L., ed., 1927, *The Pardee genealogy*: New Haven, Conn., New Haven Colony Historical Society.

- Kantner, H.W.B., 1896, A hand book of the mines, miners, and minerals of Utah: Salt Lake City, Utah, R.W. Sloan.
- Maddox, F., 1895, Reports of cases argued and determined in the Supreme Court of the State of Montana, embracing a portion of the March term, 1895, and the June term, 1895: First National Bank of Butte v. Pardee: Montana Reports, v. XVI: San Francisco, Calif., Bancroft-Whitney Co., 1896, p. 390–393.
- Murphy, J.R., 1872, The mineral resources of the Territory of Utah, with mining statistics and maps: Salt Lake City, Utah, James Dwyer, and San Francisco, Calif., A.L. Bancroft & Co.
- Pardee, A., 1896, Genealogy of one line of the Pardee family, and some memoirs: Wadsworth, Ohio.
- Petrik, P., 2009, Parading as millionaires: Montana bankers and the Panic of 1893: Enterprise & Society, v. 10, no. 4, December 2009, p. 729–762.
- Plazak, D., 2006, A hole in the ground with a liar at the top: Fraud and deceit in the golden age of American mining: Salt Lake City, Utah, University of Utah Press.
- Raymond, R.W., 1873a, Mineral resources of the states and territories west of the Rocky Mountains: Washington, D.C., Government Printing Office.
- Raymond, R.W., 1873b, Silver and gold: An account of the mining and metallurgical industry of the United States: New York: J.B. Ford and Company.
- Spence, C.C., 1958, British investments and the American mining frontier, 1860–1901: Ithaca, N.Y., Cornell University Press for American Historical Association.
- Wolle, M.S., 1963, Montana pay dirt: A guide to the mining camps of the Treasure State: Denver, Colo., Sage Books.
- Whitley, C., ed., 2006, From the ground up: The history of mining in Utah: Logan, Utah, Utah State University Press.



Pyrite from Butte, MT. Courtesy of Michael J. Goble.





Bull Mountains. Courtesy of Patrick E. Dawson.



Elkhorn Mountains Volcanics pyroclastic lag breccia deposits at MacDonald Pass, MT. Courtesy of Kaleb C. Scarberry.

# Two-Event Genesis of Butte Lode Veins: Geologic and Geochronologic Evidence from Ore Veins, Dikes, and Host Plutons

Karen Lund,<sup>1</sup> Ryan J. McAleer,<sup>2</sup> John N. Aleinikoff,<sup>1</sup> and Michael A. Cosca<sup>1</sup>

<sup>1</sup>*U.S. Geological Survey, Denver, Colorado*

<sup>2</sup>*U.S. Geological Survey, Reston, Virginia*

## Abstract

The long-standing ore-genesis model for world-class deposits of the Butte mining district, Montana, is of deep pre-Main Stage porphyry Cu-Mo and overlying Main Stage Ag-Zn-Cu-zoned lode veins—formed from discrete hydrothermal systems related to rhyolite dikes. The lode-specific model describes metals zones that formed in the lode veins as hydrothermal processes diminished in intensity (changing temperature and chemical characteristics) outward from the district center. New geologic and multi-method geochronologic studies provide new timing constraints on the lode veins and reevaluation of geologic relations (Lund and others, 2018), leading to a new model for formation of the lode veins and their relations to stockwork Cu-Mo deposits and igneous events.

Our geochronologic studies yield three major constraints: (1) Dates on samples of the Butte granite country rock indicate that, after its emplacement at  $76.9 \pm 0.8$  Ma (SHRIMP U-Pb), it cooled relatively quickly to 350–400°C in <4 m.y. ( $^{40}\text{Ar}/^{39}\text{Ar}$ ). (2) Dates on cross-cutting quartz porphyry rhyolite dikes (SHRIMP U-Pb) indicate that the five main dikes and a small stock were emplaced into the cooled Butte granite at  $66.3 \pm 1.3$  to  $65.1 \pm 0.9$  Ma (six ages overlap within uncertainty) as a single event; the youngest E–W rhyolite dike was emplaced at  $60.3 \pm 0.7$  Ma. Emplacement of the dikes did not sufficiently reheat the country rocks to reset host-rock  $^{40}\text{Ar}/^{39}\text{Ar}$  ages more than about a meter from dike contacts. (3)  $^{40}\text{Ar}/^{39}\text{Ar}$  ages were acquired for 58 white mica and K-feldspar samples from alteration envelopes associated with lode veins across the district and at various depths. Ag-Au-polymetallic lode veins in outer parts of the district yield ages of  $73.7 \pm 0.5$  to  $72.3 \pm 0.4$  Ma, Zn plus Cu lodes in intermediate areas yield complex age spectra most in the range of 69–65 Ma, and Cu-rich lodes in the district center yield ages of  $64.8 \pm 0.3$  to  $63.8 \pm 0.4$  Ma. Summary data are in figure 1.

Petrographic data for the dated minerals facilitate interpretation of the  $^{40}\text{Ar}/^{39}\text{Ar}$  ages. Backscattered electron (BSE) and panchromatic cathode-luminescent (CL) images and electron microprobe (EMP) analyses of K-feldspar reveal different degrees of K-feldspar replacement with proximity to veins. Primary igneous K-feldspar is more completely replaced and recrystallized by secondary hydrothermal K-feldspar closer to veins, and the alteration corresponds to progressively younger K-feldspar  $^{40}\text{Ar}/^{39}\text{Ar}$  ages. EMP analyses and BSE images of the white mica mineral separates identify three morphological types. Clear, monocrystalline, white mica was a primary hydrothermal alteration mineral and predominates in samples from the Ag-rich lode veins (with ages of about 74–70 Ma). Two other white mica types are those containing numerous rutile grains, which replaced igneous biotite, and others composed of muscovite–kaolinite–pyrophyllite composites, which replaced igneous plagioclase. These secondary white micas predominate in the Zn plus Cu lode veins and produced complex 69–65 Ma ages. A mixed population of white mica morphologies are present in the intensely altered rocks of the central Cu area where white mica uniformly produced 65–64 Ma ages.

Early descriptive studies of the district presented geologic evidence of overprinted mineralizing phases. However, the general lack of age constraints in the district resulted in misinterpretation of which mineralizing phases were separated by significant amounts of time and which had close temporal ties. The destruction of critical exposures by continued mining, the change from underground to open-pit mining, and ensuing research emphasis on the stockwork Cu-Mo deposits all resulted in entrenched shorthand geologic descriptions that matched the well-accepted deposit model.



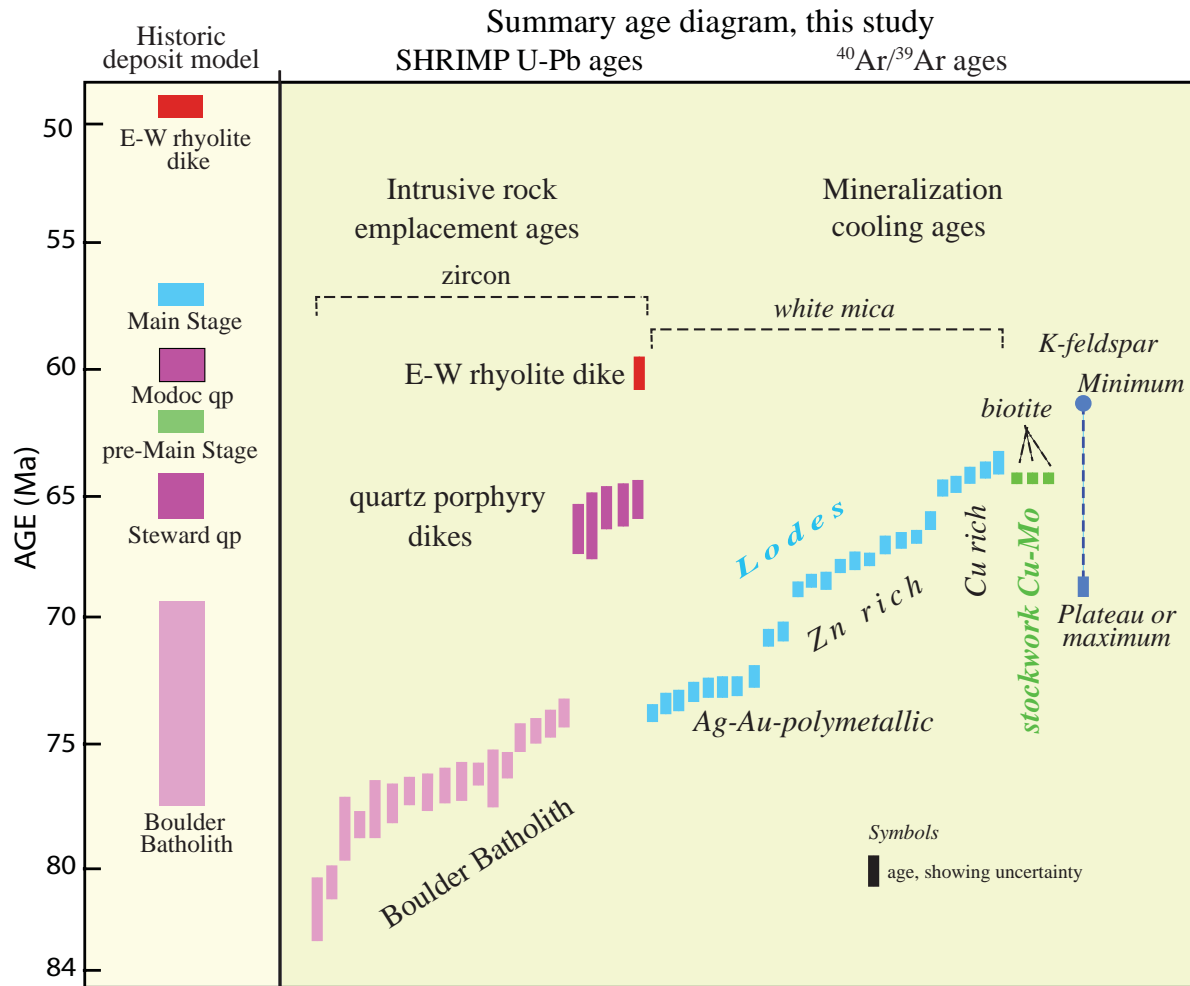


Figure 1. Summary age diagram showing SHRIMP U-Pb ages for intrusive rocks and  $^{40}\text{Ar}/^{39}\text{Ar}$  cooling ages for mineralization systems. qp, quartz porphyry dike.

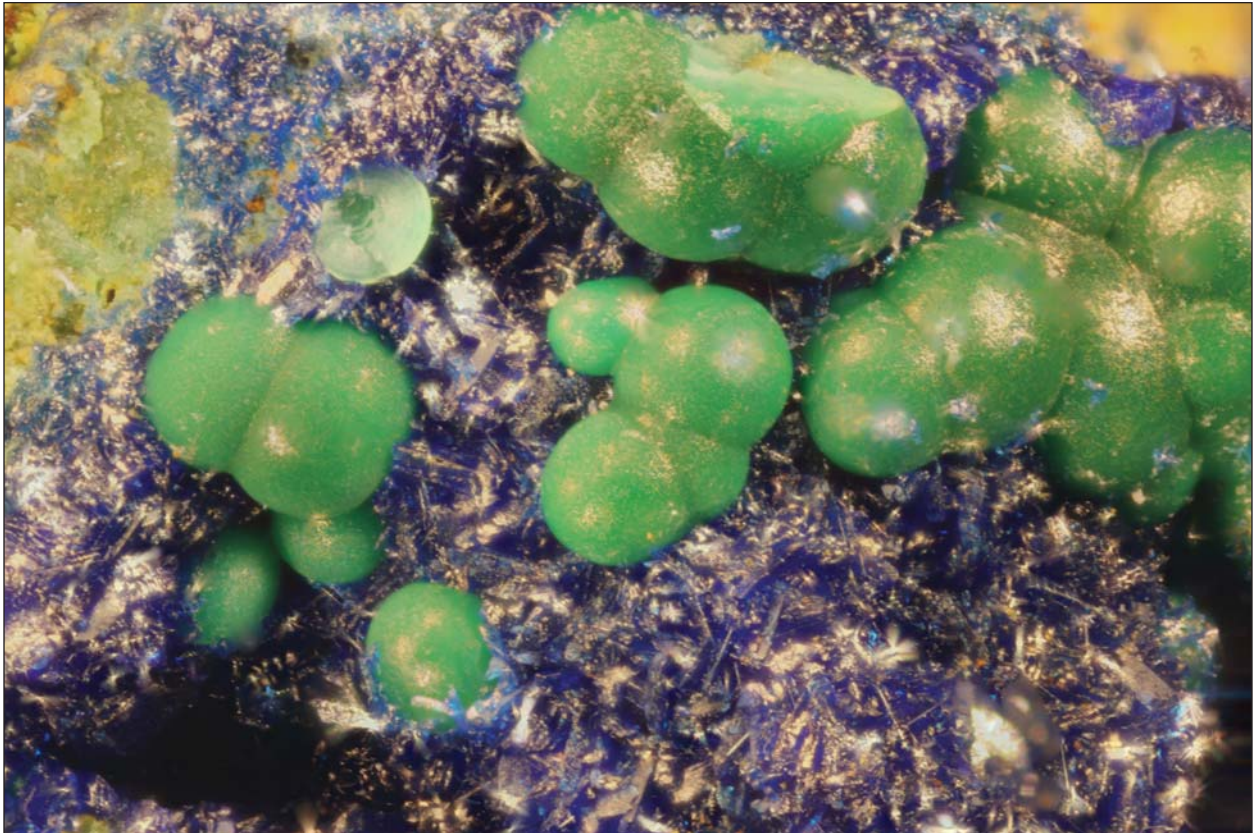
The sequence and timing of events that formed the Butte ore deposits are revised through synthesis of the geologic, microchemical-petrographic, and geochronologic data. Large Ag-Au-polymetallic lodes occupied cross-district fractures by about 73 Ma, forming the greater Butte mining district (91 km<sup>2</sup> in area). At 67–65 Ma, minor quartz porphyry dikes were emplaced into central and eastern parts of the rejuvenated fracture system, but in the absence of related cupola or volcanic rocks or of thermal disturbance in the country rock. At  $64.5 \pm 0.2$  Ma, overlapping hydrothermal cells formed two stockwork Cu-Mo domes in deep parts of the preexisting fracture system. At 64.8–63.8 Ma and closely related to the stockwork Cu-Mo deposit, a penecontemporaneous hydrothermal pulse (thus, within the margin of error for dating but with cross-cutting relations at the depths where the systems overlap) formed a high-sulfidation hydrothermal plume. The high-sulfidation plume (1) utilized the large reopened earlier fractures to cannibalize and remobilize Cu from autologous, stockwork, and older Ag-Au-polymetallic lode veins of the central district, (2) deposited the rich, high-sulfidation Cu lodes in the district center, and (3) mobilized metals from early Ag-Au-polymetallic lode veins in the central district, transported the metals outward, and redeposited them in the intermediate Zn plus Cu areas to revise and enrich early Ag-Au polymetallic lode veins.

Metals zones in lodes of the Butte district are the result of an intensely focused, Cu-rich hydrothermal plume that variably reworked the center of a significantly larger, 10 m.y. older, Ag-Au-polymetallic lode system.

**References Cited**

- du Bray, E.A., Aleinikoff, J.N., and Lund, K., 2012, Synthesis of petrographic, geochemical, and isotopic data for the Boulder Batholith, southwest Montana: U.S. Geological Survey Professional Paper 1793, 46 p., <http://pubs.usgs.gov/pp/1793> [Accessed February 2020].
- Houston, R.A., and Dilles, J.H., 2013, Structural geologic evolution of the Butte district, Montana: *Economic Geology*, v. 108, p. 1397–1424, doi: [doi.org/10.1144/SP378.9](https://doi.org/10.1144/SP378.9) [Accessed February 2020].
- Lund, K., Aleinikoff, J.N., Kunk, M.J., Unruh, D.M., Hodges, W.C., du Bray, E.A., O'Neill, J.M., and Zeihen, G., 2002, SHRIMP U-Pb and  $^{40}\text{Ar}/^{39}\text{Ar}$  age constraints for timing of mineralization in the Boulder Batholith region, Montana: *Economic Geology*, v. 97, p. 241–267, doi: <https://doi.org/10.2113/97.2.241> [Accessed February 2020].
- Lund, K., McAleer, R.J., Aleinikoff, J.N., Cosca, M.A., and Kunk, M.J., 2018, Two-event lode-ore deposition at Butte, USA:  $^{40}\text{Ar}/^{39}\text{Ar}$  and U-Pb documentation of Ag-Au-polymetallic lodes overprinted by younger stockwork Cu-Mo ores and penecontemporaneous Cu lodes: *Ore Geology Reviews*, v. 102, p. 666–700, doi: <https://doi.org/10.1016/j.oregeorev.2018.05.018> [Accessed February 2020].
- Meyer, C., Shea, E.P., Goddard, C.C., Jr., Zeihen, L.G., Guilbert, J.M., Miller, R.N., McAleer, J.F., Brox, G.B., Ingersoll, R.G., Jr., Burns, G.J., and Wigal, T., 1968, Ore deposits at Butte, Montana, in Ridge, J.D., ed., *Ore deposits of the United States, 1933–1967, Graton-Sales Volume II*, American Institute of Mining and Metallurgical Engineers, p. 1373–1416.
- Miller, R.N., 1973, Production history of the Butte district and geological function, past and present, in Miller, R.N., ed., *Guidebook for the Butte field meeting of Society of Economic Geologists, 1973*, Butte, Montana: Society of Economic Geologists, p. F1–F10.
- Tilling, R.I., Klepper, M.R., and Obradovich, J.D., 1968, K-Ar ages and time span of emplacement of the Boulder Batholith, Montana: *American Journal of Science*, v. 266, p. 671–689.
- Woakes, M., 1960, Potassium-argon dates on the mineralization at Butte, Montana: Berkeley, University of California Berkeley, Master's thesis, 42 p.





Malachite and azurite from the Rosetta Mine, MT. Courtesy of Michael J. Gobl.



Pseudobrookite from Sierra County, NM. Courtesy of Michael J. Gobl.

# Butte Main Stage Veins: Control of Fracturing by the Central Gray Sericitic Zone

Mark H. Reed

*University of Oregon, Eugene, Oregon*

## Abstract

The Butte ore deposit contains two porphyry copper–molybdenum centers and a superimposed system of large Main Stage veins spanning more than 5 km east–west and extending more than 2 km in depth. The Main Stage veins are well developed in the western part of the district, but they are mostly absent in the center of the district, which is occupied by a large pre-Main Stage dome-shaped body of stockwork pyrite veins with intense gray sericitic alteration. Large throughgoing fractures propagated through the brittle rock of the western district, but failed to form in the ductile rock of the central gray sericitic zone. At the transition from the central gray sericitic zone and the brittle granite beyond to the west, the granite fractured into sets of en echelon openings that formed the famous horsetail ores of the Butte Main Stage in the Leonard mine. Much of the Butte advanced argillic alteration, characterized by topaz, pyrophyllite, kaolinite, sericite, and quartz, formed where Main Stage fluids reacted with gray sericitic wallrock.

## Introduction

The Butte porphyry copper mineralization is defined by the Anaconda and Pittsmont domes, which are each 2 km in diameter (fig. 1), aligned along a series of quartz porphyry dikes. Between the two domes is the central gray sericitic (GS) zone, a 1.2 x 1.8 km domical body of pyrite–quartz veins with pervasive sericite–pyrite–quartz alteration. Superimposed on the porphyry copper vein stockworks that make up the domes and the central GS zone are the Main Stage veins (fig. 1), whose high-grade copper, silver, and zinc lodes were the object of underground mining in Butte for the first 100 years of operation. The Main Stage fracture pattern (fig. 1) was shaped by a regional stress regime (Houston and Dilles, 2013) superimposed on the relatively ductile body of rock of the central GS zone.

## Butte Pre-Main Stage Alteration

### *Anaconda and Pittsmont Domes*

The Anaconda and Pittsmont domes consist of overlapping concentric shells of millimeter- to centimeter-scale stockwork veinlets of the potassic series (Reed and others, 2013), all with alteration envelopes that gradationally change upward and outward over a radial span of about 1 km. The alteration in all contain sericite, and all but GS contain newly formed K-feldspar. The deepest contain biotite and distinctive andalusite (Roberts, 1975; Brimhall, 1977), giving way upward to chlorite-bearing assemblages surrounding magnetite-rich veinlets, then shallow sericite–pyrite–quartz (GS) envelopes with peripheral dark green chlorite–sericite (DGS), followed outward by veins with sericite, chlorite, and epidote (propylitic assemblage). The magnetite veinlets lie within a well-defined shell in each of the two domes (fig. 1; Reed, 1979, 1981). Chalcopyrite occurs within the veinlets and alteration of the potassic series veins, which are cut by centimeter-scale quartz molybdenite veins that are distributed in the same domical volumes.

### *Central Gray Sericitic Alteration Zone*

In the geometric center of the Butte district, deep drill holes 1 and 7 (fig. 1) encountered approximately 400 m thicknesses of pervasive GS alteration in a stockwork of 5- to 15-mm-thick pyrite-dominated veins with minor quartz and chalcopyrite. Bulk rock iron assays in the GS alteration average more than 6.4 wt% Fe, reflecting the abundance of pyrite in veins and disseminations, compared to less than 4.5 wt% in non-GS-altered rock above and below the GS interval. The pyrite-rich pervasively GS-altered granite is quite dense,  $\sim 2.93$  g/cm<sup>3</sup>, relative to 2.72 g/cm<sup>3</sup> in the non-GS-altered rock above and below it, which gives rise to a gravity high (Wightman, 1979) centered on the central GS zone (fig. 2A). The gravity high was recognized after DH-1 was





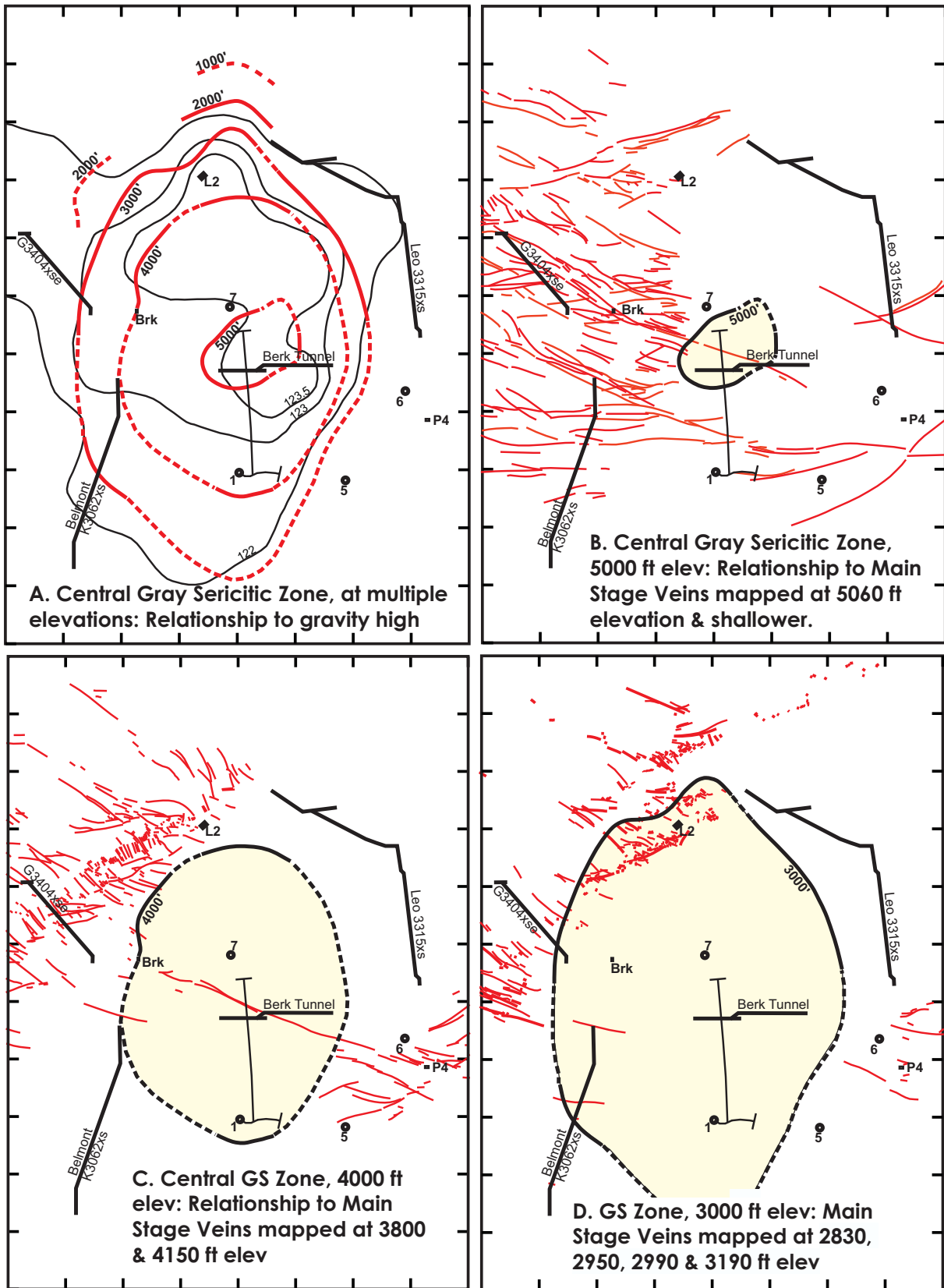


Figure 2. Main Stage veins in proximity to the central gray sericitic zone. (A) Gravity contours (black solid line, milligals; Wightman, 1979) based on surface measurements, revealing a broad gravity high. Red curves are elevation contours (ft) on the top surface the central GS zone, shown as solid lines where fixed by direct observation in deep drill holes (small circles), historic hand samples, and drill core from underground crosscuts on the 3400, 3300, and 3000 mine levels (elevations 2830', ~2900', and ~3200' respectively), and the Berkeley Tunnel (5000'); drill holes 1 and 1A are marked with lines showing their projections to a horizontal plane; GS contours are dashed where approximately located (Reed, 1979), on the basis of distant samples and gravity contours. (B) Main Stage veins near 5000' elevation shown in relation to the top of the GS zone. Veins traverse through unsericitized ground above the GS zone, which expands beneath 5000'. (C) Veins near 4000' elevation, which are numerous to the west of the GS zone and in the Pittsmont mine to the east, but only the Windlass cuts through the zone, where it contains minerals of the high-sulfur assemblage (pyrite, enargite, digenite, covellite) and is bordered by advanced argillic alteration. (D) Veins near 3000' elevation, where they are largely absent from the GS zone but numerous to the west and east.



underway, and prompted us to determine rock densities in DH-1 and subsequent holes by weighing core boxes and measuring the length of core in each box.

Gray sericitic alteration of the central GS zone contains the same minerals and destroyed texture as the gray sericitic alteration of GS/DGS veins above the Anaconda and Pittsmont domes, but the central zone GS veins cut quartz–molybdenite veins, whereas the GS/DGS veins are part of the potassic series that is cut by quartz–molybdenite veins. The pyrite/GS veins are cut by Main Stage veins, establishing the pre-Main Stage timing of the central GS zone.

### **Relationship of Main Stage Veins and Advanced Argillic Alteration to the Central GS Zone**

The geometric center of the Butte district is sparsely traversed by large Main Stage veins only at shallow depth veins such as the Windlass (fig. 2), characterized by enargite–pyrite and bordered by topaz-bearing advanced argillic alteration. Main Stage veins such as the Anaconda-Steward, Syndicate, and Edith May are thick and long in the western and northern parts of the district, but most veins and workings on them end eastward where they intersect the central GS zone (figs. 1, 2). On the east side of the GS zone, Main Stage veins reappear in the Pittsmont mine (fig. 2). The response of Main Stage vein extent and horsetail fractures (see below) to the central GS zone makes it clear that Main Stage fracturing came after the GS alteration zone formed.

Veins within the GS zone such as the Windlass (fig. 1) and horsetails of the deep Leonard (fig. 2) are bordered by intense advanced argillic alteration characterized by topaz, pyrophyllite, kaolinite, sericite, and quartz (Howard, 1972). In earlier studies, the location of this advanced argillic alteration was credited to pervasive Main Stage sericitic alteration around the horsetail ores, but with the recognition of the central GS zone, it now appears that much of the advanced argillic alteration is a consequence of acidic Main Stage fluids reacting with already sericitized rock of the GS zone, which failed to neutralize the acidity. That same acidity yields the high-sulfur-ore mineral assemblages, covellite–digenite–enargite–pyrite, of Sales' "central zone" (Sales, 1914), as pointed out by Meyer and others (1968). The occurrences of the high-sulfur assemblage and topaz alteration in and bordering Main Stage veins in deep drill holes 1 and 7, which penetrate the full thickness of pervasive GS alteration (fig. 1), reflect the chemical association of advanced argillic alteration with high-sulfur minerals recognized in the Leonard mine and in high-sulfidation epithermal deposits worldwide (e.g., Saunders and others, 2014).

The horsetail veins of the Leonard and Tramway mines are small, closely spaced, southeast-striking fractures that break away from east–northeast-striking large veins, forming an en echelon vein set (Meyer and others, 1968; figs. 2C,2D). The elongate direction of the horsetail veins as a set strikes in about the same direction as the east–northeast large veins. At the time of Main Stage fracturing, relatively ductile rock of the central GS zone was surrounded on all sides by fresh granite and pre-Main Stage-altered granite, both of which were feldspar-rich, making them brittle. It is likely that the particular location of horsetail veins was fixed by the transition in rock mechanical properties along the northwest flank of the central GS zone (fig. 2) where ductile GS-altered rock transitions to brittle fresh granite (Reed, 1979, 1981). Horsetail fractures formed where throughgoing fissures in brittle rock broke into a series of en echelon tears near the GS boundary because the shear strain focused in the large vein fracture was spread over a large volume in the ductile GS zone.

The strikes of horsetail veins and those of large veins are east–west and west–northwest in the more southerly veins on the west side of the GS zone; then strikes swing to nearly north–south in the north (figs. 2C,2D). The swing in vein strikes probably reflects the effect of the curving interface of weak GS rock against strong granite and the consequent rock mechanical effect on stress orientation.

The macroscopically ductile behavior of the GS-altered granite at <350°C in Main Stage time occurs in the form of inter-grain slip in massive sericite, and strain on closely spaced brittle fractures that produced millimeter-to-centimeter-scale veinlets of chalcocite, bornite, or enargite within the pervasive GS alteration, some of which are bordered by topaz alteration; this is to say, the macroscopic ductile behavior did not occur at a microscopic scale by intragranular strain and thus was not responsive to the common brittle–ductile transition temperature (>400°C) in quartz-rich rock. Main Stage hydrothermal fluids also permeated the GS-altered rock at the grain scale, revealed by bornite and chalcocite dissemination, much of which replaces and rims original disseminated GS chalcopyrite.

## References

- Brimhall, G.H., 1977, Early fracture-controlled disseminated mineralization at Butte, Montana: *Economic Geology*, v. 72, p. 37–59.
- Houston, R.A., and Dilles, J.H., 2013, Structural geologic evolution of the Butte District, Montana: *Economic Geology*: v. 108, p. 1397–1424, doi:10.2113/econgeo.108.6.1397
- Howard, K., 1972, Pyrophyllite–topaz alteration in the ore deposit at Butte, Montana: Berkeley, University of California, Ph.D. thesis.
- Meyer, C., Shea, E., Goddard, C., and staff, 1968, Ore deposits at Butte, Montana, in Ridge, J.D., ed., *Ore deposits of the United States 1933–1967, The Graton-Sales Volume*: New York, American Institute of Mining, Metallurgical, and Petroleum Engineers, v. 2, p. 1363–1416.
- Reed, M.H., 1979, Butte district early stage geology synthesis: Unpublished Anaconda Company Report, 42 p.
- Reed, M.H., 1981, Summary of recent developments in the interpretation of Butte geology: Unpublished Anaconda Company Report, 28 p.
- Reed, M., Rusk, B., and Palandri, J., 2013, The Butte magmatic-hydrothermal system: One fluid yields all alteration and veins: *Economic Geology*, v. 108, p. 1379–1396.
- Roberts, S., 1975, Early hydrothermal alteration and mineralization in the Butte district, Montana: Cambridge, Mass., Harvard University, Unpublished Ph.D. dissertation, 157 p.
- Sales, R.H., 1914, Ore deposits at Butte, Montana: *Transactions of the American Institute of Mining, Metallurgical and Petroleum Engineers*, v. 46, p. 3–109.
- Saunders, J.A., Hofstra, A.H., Goldfarb, R.J., and Reed, M.H., 2014, Geochemistry of hydrothermal gold deposits, in Holland, H.D., and Turekian, K.K., eds., *Treatise on Geochemistry, Second Edition*: Oxford, Elsevier, v. 13, p. 383–424.
- Wightman, E., 1979, Butte aeromagnetic and gravity surveys, Anaconda Company Report.





Digenite from the Leonard Mine; Butte, MT. Courtesy of Michael J. Goble.



Microcline on epidote. Jefferson County, MT. Courtesy of Michael J. Goble.

# Mineralogical Investigation of the Sheep Creek Nb-REE Carbonatite Deposits, Southern Ravalli County, Montana

Christopher H. Gammons

Department of Geological Engineering, Montana Tech, Butte, Montana

## Introduction

The Sheep Creek carbonatite deposits are located 38 mi south of Darby, Montana, on the north side of Sheep Creek, a small tributary to the headwaters of the West Fork of the Bitterroot River (fig. 1). Following the first discovery of columbite at Sheep Creek in 1953 (Sahinen, 1957), more detailed studies of the district were conducted by Crowley (1960) and Heinrich and Levinson (1961). Minor production of niobium and rare earth elements (REE) took place in the late 1950s by the Sheep Creek Mining Company, a subsidiary of the Continental Columbian Corporation of California (Heinrich and Levinson, 1961). Immediately to the south, in the Mineral Hill district of Idaho, a similar set of Nb- and REE-rich carbonate “vein-dikes” were explored and described in the 1950s and 1960s (Kaiser, 1956; Abbott, 1958; Anderson, 1960), with small-scale production. Jaffe and others (1959) reported lead-alpha dates for monazite from the Mineral Hill district, while Powell (1965) examined the  $^{87}\text{Sr}/^{86}\text{Sr}$  composition of the veins. Spence (1984) described the petrology of the host rocks in the Mineral Hill district, and produced a geologic map. However, since the mid-1960s, little published work exists on the REE-rich deposits themselves in either the Sheep Creek or Mineral Hill districts, which was a motivation for this study.

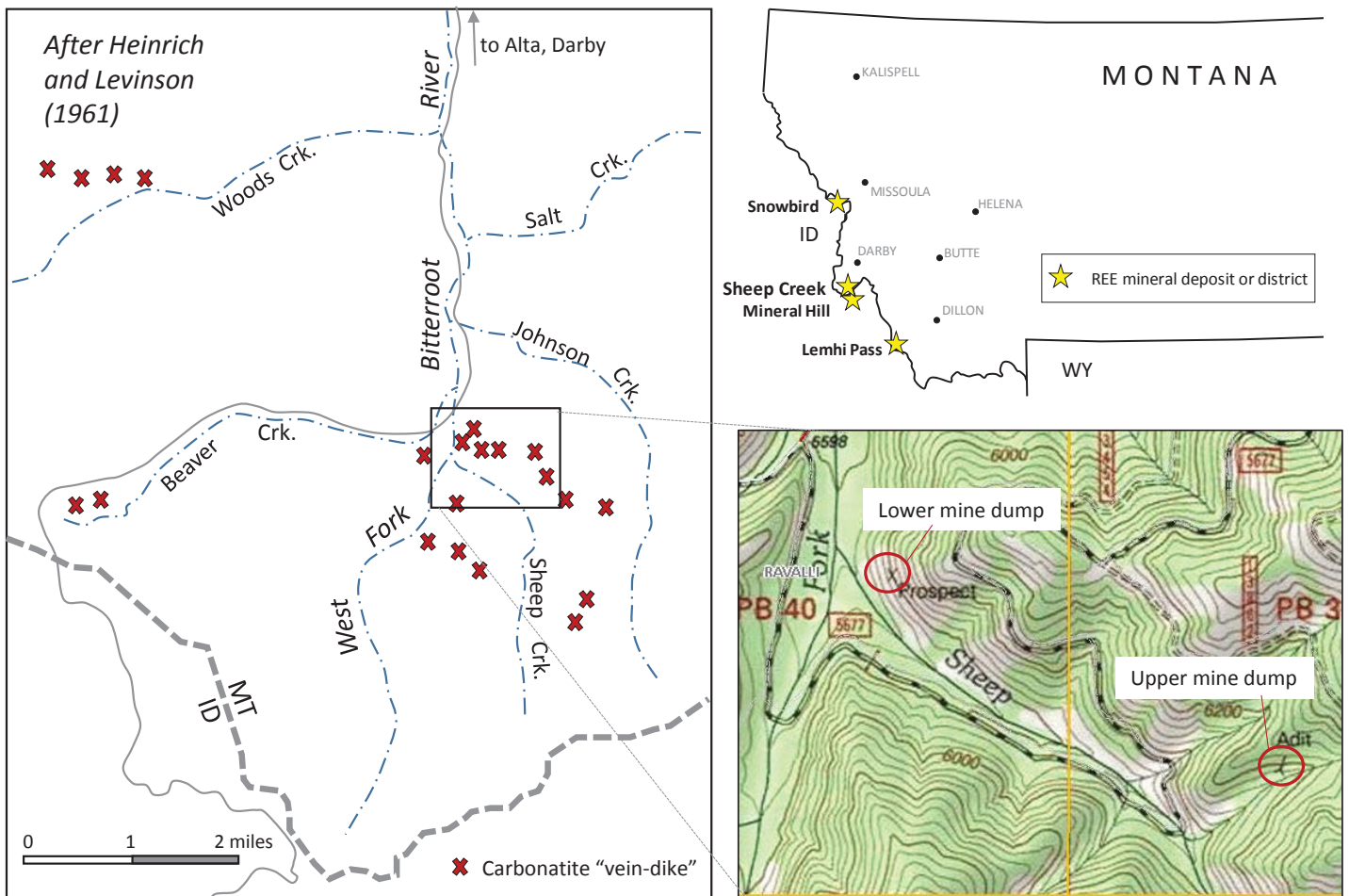


Figure 1. Location maps of the Sheep Creek district with sample collection sites (lower right panel).



The geology of southern Ravalli County was described by Berg (1977). Bedrock in the area includes metamorphosed sediments of the mid-Proterozoic Belt Basin (mica schist, impure quartzite), amphibolite and hornblende gneiss, augen gneiss, and meta-gabbro. In the vicinity of Sheep Creek, amphibolite is the most common rock type. According to Heinrich and Levinson (1961), the Nb-REE-rich deposits of interest range from a few inches to 10 ft in width, with strike lengths of <10 ft to >450 ft. The veins are crudely parallel to the NW-striking and NE-dipping metamorphic foliation, but locally cross-cut the foliation at a low angle. At least 20 veins of this type are scattered over an area that extends from Woods Creek to the north to Beaver Creek and the headwaters of the West Fork of the Bitterroot River to the south (fig. 1). Including the Mineral Hill district, REE- and Nb-rich veins have been found in a NW-trending belt that is at least 18 mi long (Heinrich and Levinson, 1961).

### Methods

All of the samples described in this study were collected from abandoned mine dumps. None of the historic mine workings are accessible, and outcrops are scarce in the vicinity of the major prospects. The upper Sheep Creek dump was sampled in July 2017, and the lower Sheep Creek dump was sampled in May 2018 (see fig. 1 for locations). A portable X-ray fluorescence meter (XRF) proved useful to find samples rich in rare metals. Hand samples were sawn, trimmed, set in 1-in-diameter epoxy mounts, and polished. In all, roughly 30 polished plugs were made, all of which were examined by reflected light microscopy. Of these, 12 plugs were examined by scanning electron microscopy-energy dispersive X-ray spectroscopy (SEM-EDS) using the LEO SEM at the Center for Advanced Mineral and Materials Processing (CAMP) lab at Montana Tech. Many of the samples containing matrix carbonate and barite were examined by X-ray diffraction using an Olympus Terra XRD (Co source).

### Results

The carbonatite deposits of Sheep Creek are mineralogically complex, with interesting banded textures and zones that locally appear deformed (fig. 2). The dominant matrix minerals are white to tan calcite and dolomite, although barite is locally abundant and apatite is typically present. Monazite and ancylite are easy to spot in the field, being honey-brown or brick-pink, respectively, whereas allanite and the Nb-rich minerals are black. Beyond these generalities, accurate mineral identification is not possible without XRD, optical microscopy, or SEM-EDS. A complete list of minerals identified is given in table 1. For the most part, the mineral list is similar to that reported by previous workers (Crowley, 1960; Heinrich and Levinson, 1961). New phases found in this study include the REE-rich minerals parisite, bastnäsite, synchysite, and chevkenite, the sulfide minerals siegenite, cobaltite, and galena, as well as pyrochlore, thorite, and Ba-rich K-feldspar.

Selected SEM photographs of polished plugs from the lower Sheep Creek mine dump are shown in figure 3. Panels 3A and 3B, from the same sample, show mutual inclusion textures between monazite and calcite, where the included mineral has rounded outlines. The monazite is invaded along cracks by a younger generation of calcite. Coarse barite and magnetite are locally intergrown with calcite and monazite (figs. 3D,E). Parisite and bastnäsite occur as fine-grained crystals with a distinct bladed or feathery habit (figs. 3C,E,F), whereas ancylite forms fine granules with more or less equidimensional shape (fig. 3F). Bastnäsite blades overgrow ancylite (fig. 3F) and fill cracks in chalcopyrite (fig. 3E), indicating that bastnäsite and the Ca-REE fluorocarbonates (parisite, synchysite) are relatively late in the paragenesis. Similar textures are displayed by samples from the upper mine site (fig. 4), with the addition of allanite. A few tiny grains of thorite (fig. 4F) and galena (fig. 4D) can also be seen.

Mineral textures in the black, Nb-rich sections of the Sheep Creek veins are especially complex, with fine intergrowths of allanite, columbite, Nb-rich rutile, monazite, Nb-baotite, and aeschynite in a matrix of dolomite, calcite, actinolite, and apatite (fig. 5). Although described by early workers (Hess and Trumppour, 1959), fersmite was not found in this study. Allanite is perhaps the most abundant mineral in the black zones, and has a large range in composition (table 2), due to variations in the relative abundances of Al, Ca, Fe, and the REE. In a single zoned crystal (fig. 6), Ce abundance grades from 22 wt% in the core—where monazite is also present—to 7.5 wt% in the rims (table 2). Figure 5F shows allanite grains that appear resorbed associated with fine-grained REE phases including monazite, chevkinite, and aeschynite. It is possible that the REE minerals formed at the

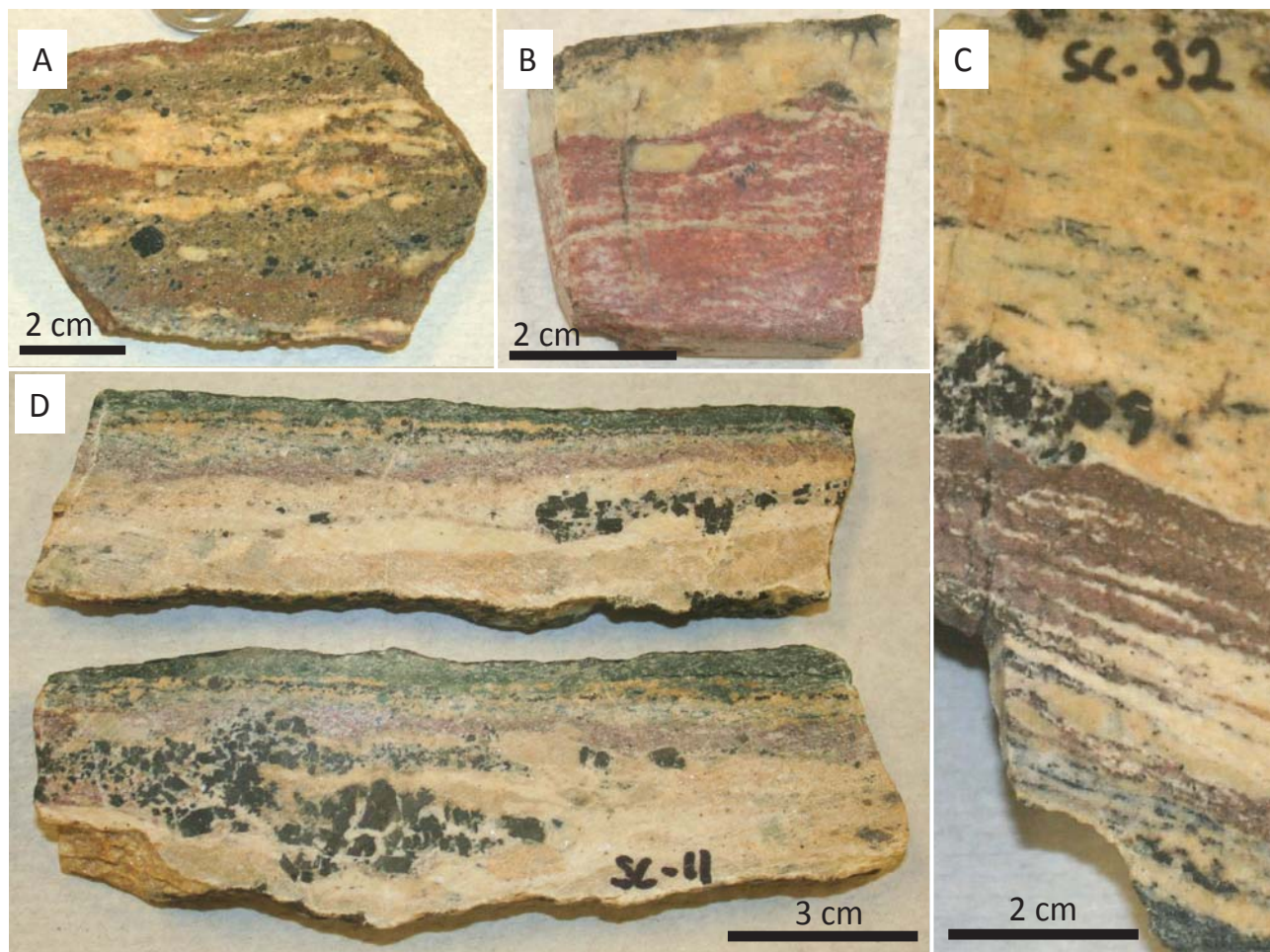


Figure 2. Photographs of sawn hand samples from Sheep Creek (upper prospect). Pink-brown is mostly ancylite, monazite, and quartz. Black is allanite, columbite, aeschynite, and Nb-rich rutile. White-tan is calcite, dolomite, and barite.

Table 1. List of minerals found in the Sheep Creek deposits.

| Mineral Name | Formula  | Ref.  | Mineral Name  | Formula  | Ref.  |
|--------------|--|-------|---------------|--|-------|
| Allanite     | {CaREE}{Al <sub>2</sub> Fe <sup>2+</sup> }(Si <sub>2</sub> O <sub>7</sub> )(SiO <sub>4</sub> )O(OH)      | 1,2,3 | Fluorite      | CaF <sub>2</sub>                                       | 2     |
| Ancylite     | (REE)Sr(CO <sub>3</sub> ) <sub>2</sub> (OH)·H <sub>2</sub> O   | 1,2,3 | Apatite       | Ca <sub>5</sub> (PO <sub>4</sub> ) <sub>3</sub> (OH,F) | 1,2   |
| Monazite     | (REE)PO <sub>4</sub>   | 1,2,3 | Barite        | BaSO <sub>4</sub>                                      | 1,2,3 |
| Bastnäsite   | REE(CO <sub>3</sub> )(F,OH)  | 1     | Calcite       | (Ca,Sr)CO <sub>3</sub>                                 | 1,2,3 |
| Parisite     | Ca(REE) <sub>2</sub> (CO <sub>3</sub> ) <sub>3</sub> (F,OH) <sub>2</sub>                                 | 1     | Dolomite      | Ca(Mg,Fe)(CO <sub>3</sub> ) <sub>2</sub>               | 1,2   |
| Synchysite   | Ca(REE)(CO <sub>3</sub> ) <sub>2</sub> (F,OH)  | 1     | Siderite      | FeCO <sub>3</sub>                                      | 1,3   |
| Chevkinite   | (REE,Ca) <sub>4</sub> (Ti,Fe) <sub>5</sub> (Si <sub>2</sub> O <sub>7</sub> ) <sub>2</sub> O <sub>8</sub> | 1     | Quartz        | SiO <sub>2</sub>                                       | 1,2,3 |
| Nb-          | (REE,Fe)(Nb,Ti) <sub>2</sub> (O,OH) <sub>6</sub>   | 1,2,3 | Hematite      | Fe <sub>2</sub> O <sub>3</sub>                         | 1,2   |
| Aeschynite   |  |       | Magnetite     | Fe <sub>3</sub> O <sub>4</sub>                         | 1,2,3 |
| Fersmite     | (Ca,REE)(Nb,Ti) <sub>2</sub> (O,OH,F) <sub>6</sub>   | 2,3   | Ilmenite      | FeTiO <sub>3</sub>                                     | 2,3   |
| Baotite      | Ba <sub>4</sub> (Ti,Nb,Fe) <sub>8</sub> Si <sub>4</sub> O <sub>28</sub> Cl                               | 1,4   | Thorite       | (Th,U)SiO <sub>4</sub>                                 | 1     |
| Columbite    | Fe(Nb,Ti,Y) <sub>2</sub> O <sub>6</sub>  | 1,2,3 | Nb-rutile     | (Ti,Nb,Fe)O <sub>2</sub>                               | 1,2,3 |
| Pyrochlore   | (Ca,REE) <sub>2</sub> (Nb,Ti) <sub>2</sub> O <sub>6</sub> (O,OH)   | 1     | Albite        | NaAlSi <sub>3</sub> O <sub>8</sub>                     | 1,2   |
| Pyrite       | FeS <sub>2</sub>   | 1,2,3 | Actinolite    |  | 1,2,3 |
| Marcasite    | FeS <sub>2</sub>   | 1     | Chlorite      | Fe-rich  | 1,2   |
| Chalcopyrite | CuFeS <sub>2</sub>   | 1,2,3 | Biotite       |  | 1,2   |
| Galena       | PbS  | 1     | Andradite     |  | 2     |
| Molybdenite  | MoS <sub>2</sub>   | 1,2,3 | Glaucophanite |  | 2     |
| Pyrrhotite   | FeS  | 1,2,3 | Wollastonite  |  | 2     |
| Siegenite    | (Ni,Co) <sub>3</sub> S <sub>4</sub>  | 1     | Ba-rich K-    | (K,Ba)AlSi <sub>3</sub> O <sub>8</sub>                 | 1     |
| Cobaltite    | (Co,Ni)AsS   | 1     | feldspar      |  |       |

References: (1) this study; (2) Heinrich and Levinson, 1961; (3) Hess and Trumpour, 1959; Crowley, 1960; (4) Heinrich and others, 1962.



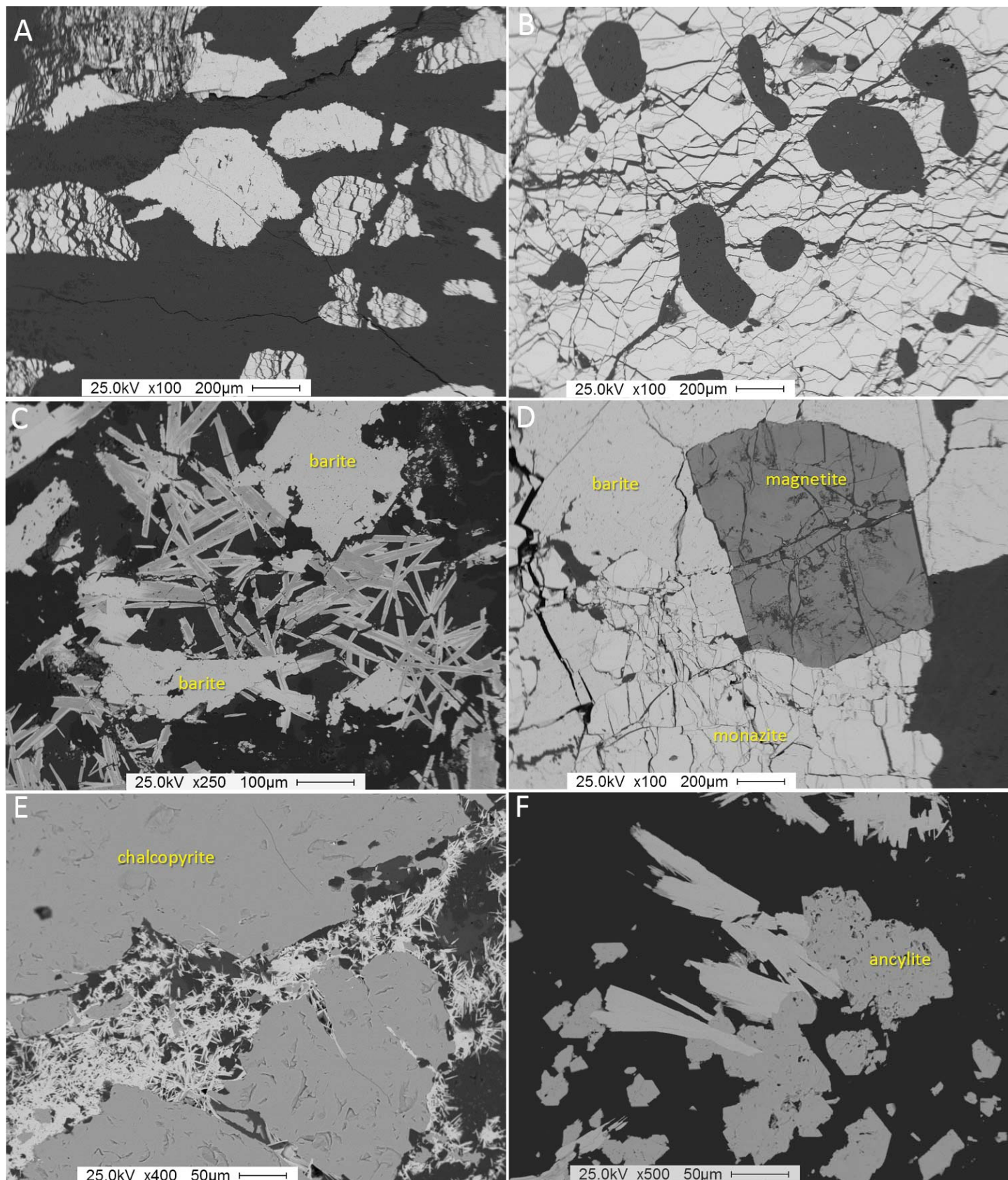


Figure 3. SEM-BSE photographs of REE-rich minerals from lower Sheep Creek. (A) Rounded crystals of monazite (cracked) and barite (bright, uncracked) in a calcite matrix (a later generation of calcite fills the cracks in monazite); (B) large monazite grain with rounded inclusions of calcite (dark); (C) bladed crystals of parisite (medium gray) rimmed and replaced by bastnäsite (bright rims), with barite, in a calcite matrix; (D) coarse intergrowth of monazite, barite, magnetite; (E) bastnäsite (bright) and quartz (black) filling a crack in chalcopyrite; (F) Blades of bastnäsite (bright) growing on ancylite in a quartz matrix.



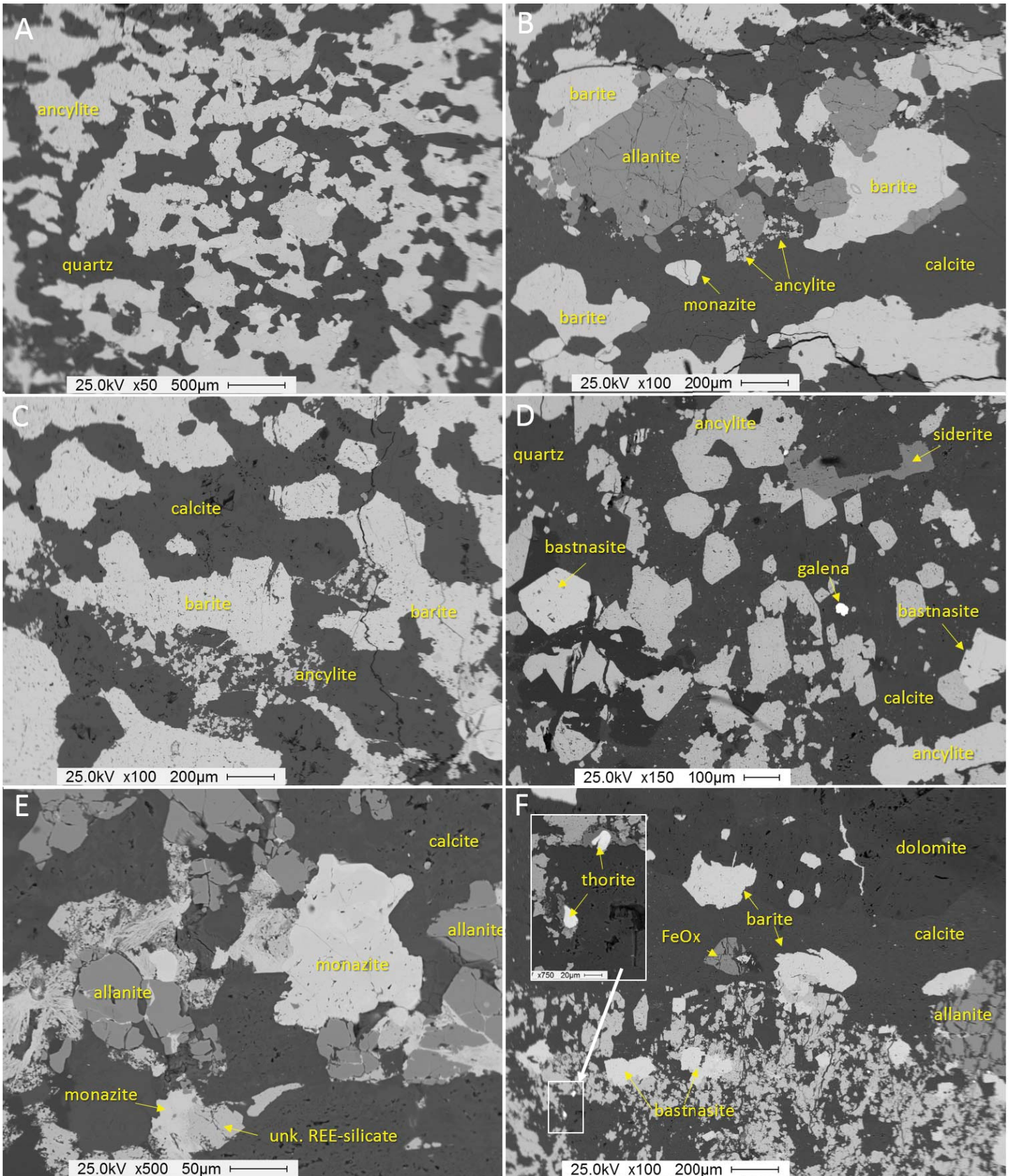


Figure 4. SEM-BSE photographs of REE-rich minerals from the upper prospect. (A) Fine-grained intergrowth of ancylite (?) and quartz; (B and C) ancylite, barite, calcite and allanite; (D) ancylite with a few grains of OH-bastnasite, galena, and siderite; (E) monazite, allanite, calcite, and unknown REE-silicate phases; (F) ancylite (light gray minerals in bottom half of image) with bastnasite, allanite, barite, calcite and dolomite. The inset shows two small crystals of thorite.



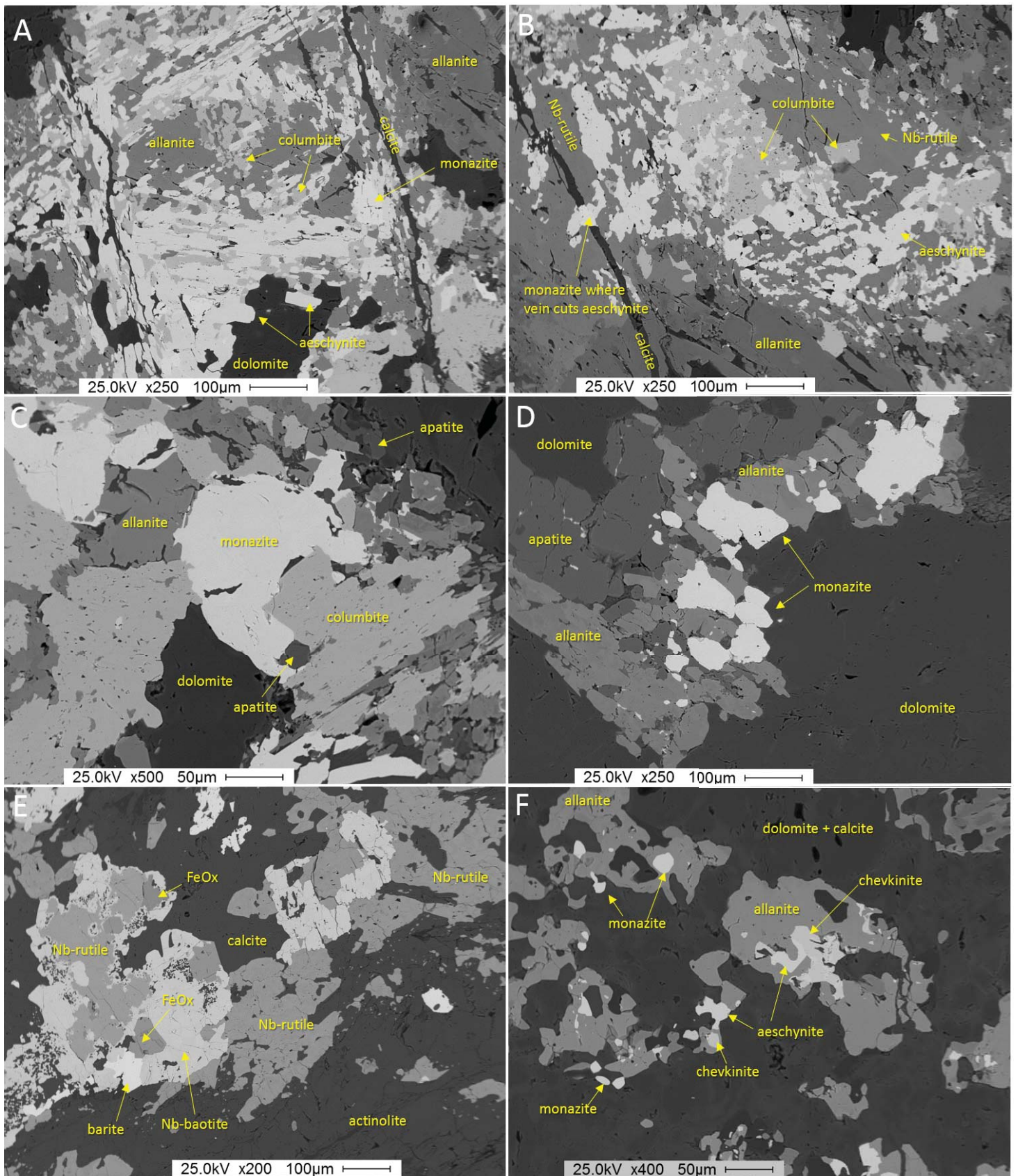


Figure 5. SEM-BSE photographs of niobium-rich minerals. (A, B) Complex, fine-grained intergrowths of aegschynite, columbite, Nb-rich rutile, and allanite in carbonate gangue (SC18-13X); (C, D) same assemblage, with monazite and apatite (SC18-13X); (E) Nb-rutile rimmed by biotite and Fe-oxide (hematite?). Note actinolite gangue at bottom (SC18-33); (F) cellular (resorbed?) allanite with inclusions of aegschynite, chevkinite, and monazite (SC18-22).



Table 2. Allanite compositions (wt %), based on SEM-EDS (see fig. 6 for locations of each analysis).

| Spot | O    | Al   | Si   | Ca   | Fe   | Mg  | La   | Ce   | Nd  |
|------|------|------|------|------|------|-----|------|------|-----|
| 1    | 20.3 | 4.3  | 17.7 | 6.8  | 22.0 | 0.8 | 12.0 | 13.3 | 2.9 |
| 2    | 25.2 | 13.3 | 21.7 | 12.9 | 11.6 | 0.6 | 5.7  | 7.5  | 1.5 |
| 3    | 19.6 | 5.9  | 16.2 | 3.7  | 9.5  |     | 16.5 | 21.9 | 4.8 |
| 4    | 17.7 | 3.9  | 17.7 | 6.8  | 22.1 | 0.7 | 12.3 | 12.9 | 2.5 |
| 5    | 19.3 | 6.6  | 16.1 | 3.7  | 8.3  | 0.8 | 16.5 | 22.0 | 5.0 |

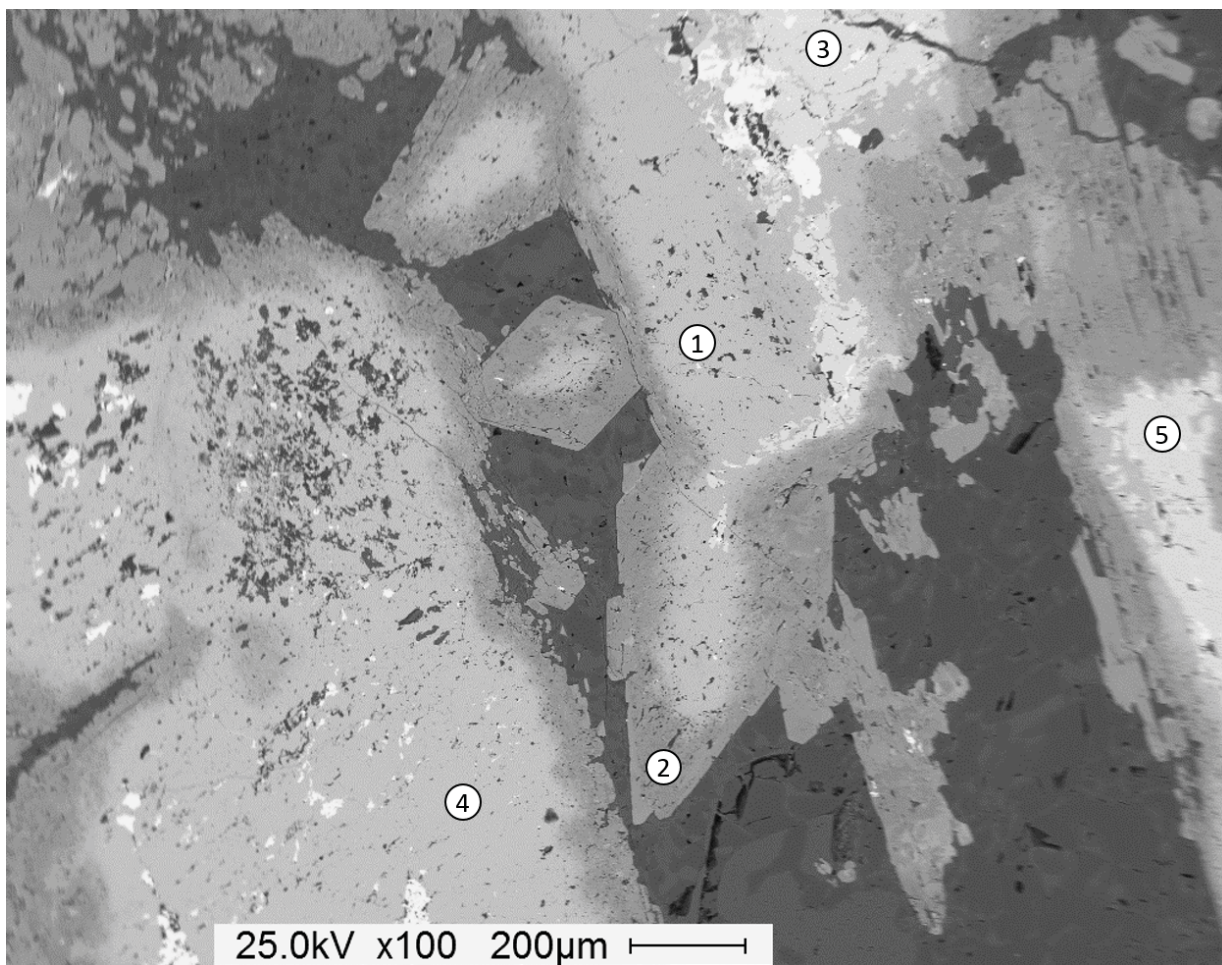


Figure 6. SEM-BSE photograph of zoned allanite crystals (SC18-14). Brightest spots are monazite; dark is calcite + dolomite gangue; all of the rest is allanite with variable REE composition. See table 2 for compositions of allanites 1 through 5.



expense of REE-rich allanite. All of the allanite and monazite grains examined by SEM-EDS in this study ( $n = 31$ ) had undetectable concentrations of uranium and low to undetectable concentrations of thorium.

Table 3 gives SEM-EDS compositions for other minerals of interest. The average composition obtained in this study for ancylite is similar to the chemistry reported by Heinrich and Levinson (1961) based on XRF analysis of an impure mineral separate. Following the general model for ancylite derived by Dal Negro and others (1975), Sheep Creek ancylite has an average formula:  $(\text{REE})_{1.3}(\text{Sr,Ca})_{0.7}(\text{CO}_3)_2(\text{OH})_{1.3} \cdot 0.7\text{H}_2\text{O}$ . Thus, although there are two metal cations per formula unit, the ratio of REE to  $(\text{Sr} + \text{Ca})$  is not 1:1, but closer to 1.3:0.7. Synchysite, parisite, and bastnäsitate have similar REE contents, differing mainly in the amount of Ca.

One interesting feature noted at the lower Sheep Creek dump was a boulder of massive carbonatite that was cut by an irregular, 2- to 4-cm-wide mafic dike with a deep green color (fig. 7). Under the SEM, this rock proved to be rich in Fe-chlorite (chamosite) and Barich K-feldspar, as well as barite and dolomite. The alkali feldspar averaged 15 wt% Ba, and has the approximate formula  $(\text{K}_{0.7}\text{Ba}_{0.3}\text{Al}_{1.3})\text{Si}_{2.7}\text{O}_8$ .

A number of samples at the lower adit contained fresh sulfide minerals (fig. 8). Pyrite forms euhedral cubes or octahedra up to 0.5 cm in diameter. Chalcopyrite is sometimes found with pyrite, and sometimes on its own or with magnetite. Pyrite locally contains many small inclusions of chalcopyrite or pyrrhotite (fig. 8F). Molybdenite was found in hand sample and polished section (fig. 8E). Small amounts of galena are locally intergrown with siegenite  $(\text{Ni,Cu})_3\text{S}_4$  and cobaltite  $(\text{Co,Ni})\text{AsS}$ . These sulfide minerals are surrounded by calcite and appear to be part of the main carbonatite assemblage. In contrast, secondary, fine-grained marcasite is associated with a later generation of quartz and Nb-baotite (fig. 8D). Marcasite is a lower temperature mineral that commonly forms by retrograde alteration of pyrrhotite. It is possible that the marcasite in the Sheep Creek carbonatite sample formed in this way.

## Discussion

Because of the bewildering array of textures observed in this study, it is a challenge to decipher a mineral paragenesis for the Sheep Creek deposits. Calcite, dolomite, and barite are the main matrix minerals in the veins, although apatite and magnetite are locally abundant. With respect to the REE-rich minerals, monazite and allanite appear early, with ancylite (most often intergrown with fine-grained quartz) intermediate, and the fluorocarbonates synchysite, parisite and bastnäsitate late in the sequence. Of the Nb-rich minerals, columbite,

Table 3. Average compositions<sup>1</sup> for miscellaneous minerals based on SEM-EDS analysis.

|                     |      |      |      |      |      |      |      |      |     |
|---------------------|------|------|------|------|------|------|------|------|-----|
| <b>Baotite</b>      | O    | Si   | Nb   | Ti   | Fe   | Ba   | Cl   |      |     |
| wt% (1)             | 15.2 | 9.2  | 17.1 | 13.6 | 4.8  | 37.4 | 2.6  |      |     |
| at% (1)             | 43.7 | 15.0 | 8.4  | 13.0 | 4.0  | 12.5 | 3.4  |      |     |
| <b>Chevkinite</b>   | O    | Si   | Nb   | Ti   | Fe   | Ca   | La   | Ce   | Nd  |
| wt% (1)             | 14.7 | 10.8 | 1.4  | 9.8  | 10.4 | 0.8  | 15.8 | 25.3 | 6.7 |
| at% (1)             | 42.4 | 17.7 | 0.7  | 9.4  | 8.5  | 0.9  | 5.2  | 8.3  | 2.1 |
| <b>Aeschynite</b>   | O    | Nb   | Ti   | Ca   | Fe   | Y    | Ce   | Nd   |     |
| wt% (3)             | 15.0 | 39.9 | 11.6 | 4.5  | 1.3  | 2.0  | 13.4 | 10.8 |     |
| at% (3)             | 47.9 | 22.0 | 12.4 | 5.7  | 1.2  | 1.2  | 4.9  | 3.8  |     |
| <b>Columbite</b>    | O    | Nb   | Ti   | Fe   | Y    | Mn   |      |      |     |
| wt% (6)             | 15.6 | 61.1 | 3.2  | 16.7 | 1.9  | 1.1  |      |      |     |
| at% (6)             | 47.4 | 31.8 | 3.3  | 14.5 | 1.1  | 1.0  |      |      |     |
| <b>Ancylite</b>     | C    | O    | Sr   | Ca   | Ce   | La   | Pr   | Nd   |     |
| wt% (14)            | 6.3  | 19.6 | 16.0 | 0.9  | 28.0 | 22.8 | 2.3  | 6.1  |     |
| at% (14)            | 22.2 | 51.9 | 7.8  | 1.0  | 8.5  | 6.7  | 0.7  | 1.8  |     |
| <b>Synchysite</b>   | O    | C    | F    | Ca   | La   | Ce   | Pr   | Nd   |     |
| wt% (2)             | 18.1 | 6.8  | 3.3  | 14.7 | 21.2 | 27.4 | 2.2  | 6.4  |     |
| at% (2)             | 42.7 | 21.6 | 6.6  | 13.9 | 5.8  | 7.4  | 0.6  | 1.7  |     |
| <b>Parisite</b>     | O    | C    | F    | Ca   | La   | Ce   | Pr   | Nd   |     |
| wt% (1)             | 16.4 | 5.99 | 3.5  | 7.4  | 23.8 | 33.3 | 2.6  | 7    |     |
| at% (1)             | 43.3 | 21   | 7.8  | 7.8  | 7.2  | 10   | 0.78 | 2.1  |     |
| <b>Bastnäsitate</b> | O    | C    | F    | Ca   | La   | Ce   | Pr   | Nd   | Sr  |
| wt% (6)             | 15.9 | 5.9  | 2.5  | 0.6  | 27.6 | 33.9 | 3.2  | 9.1  | 1.8 |
| at% (6)             | 48.4 | 22.7 | 6.3  | 0.7  | 9.7  | 12.3 | 1.1  | 3.1  | 1.0 |
| <b>Siegenite</b>    | Co   | Ni   | S    |      |      |      |      |      |     |
| wt% (5)             | 48.4 | 22.7 | 41.9 |      |      |      |      |      |     |
| at% (5)             | 15.6 | 26.5 | 56.9 |      |      |      |      |      |     |
| <b>Cobaltite</b>    | Co   | Ni   | As   | S    |      |      |      |      |     |
| wt% (4)             | 26.4 | 8.8  | 41.5 | 22.0 |      |      |      |      |     |
| at% (4)             | 24.0 | 8.2  | 29.8 | 36.8 |      |      |      |      |     |

<sup>1</sup>Numbers in parentheses refer to number of analyses.

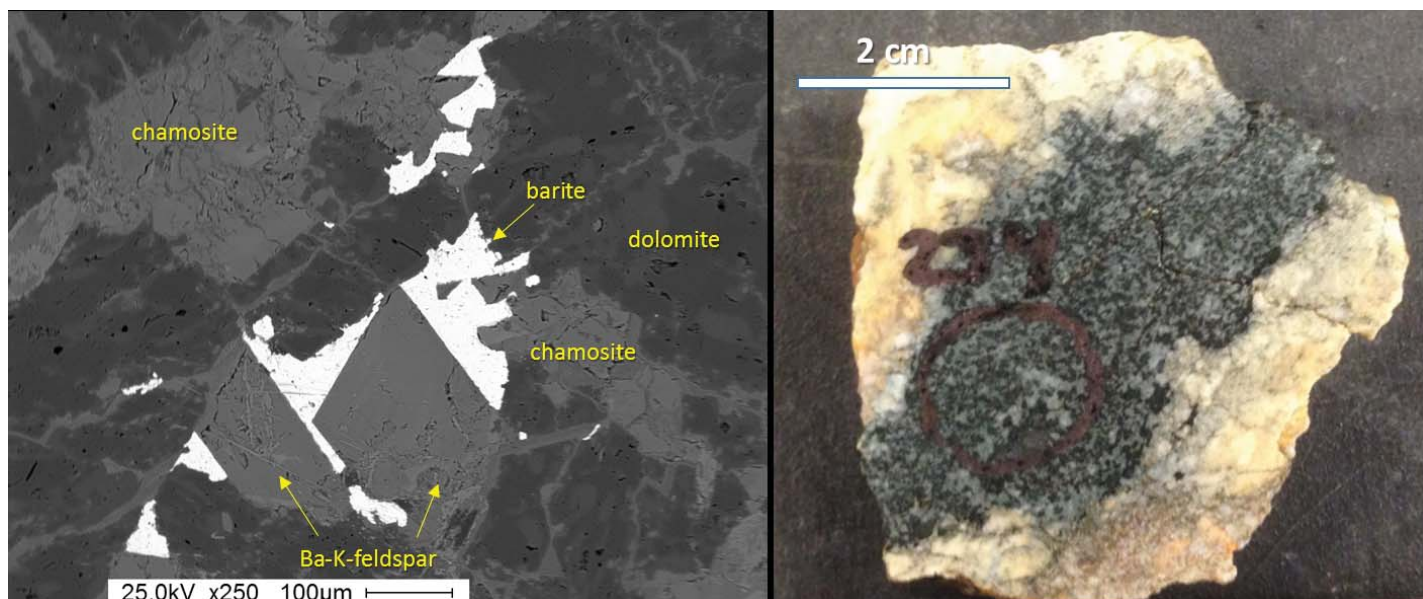


Figure 7. SEM-BSE image (left) and hand sample of a chlorite-rich “dikelet” cutting carbonatite.

aeschnite, and Nb-rutile appear first, with Nb-baotite appearing late. Most of the sulfide minerals crystallized early (e.g., contemporaneous with calcite, barite, monazite, and magnetite), although marcasite is clearly late, possibly forming as a retrograde alteration of primary pyrrhotite, synchronous with baotite. The occurrence of the Ni-Co sulfide minerals siegenite and cobaltite at Sheep Creek is of interest, and may somehow tie into the presence of gersdorffite (NiAsS) at the Snowbird fluorite deposit (Metz and others, 1985), a pegmatitic, quartz-carbonate vein rich in parisite located west of Missoula near the Montana–Idaho border.

Although mineralogically interesting and locally of high grade, the Nb-REE carbonatite dikes in the Sheep Creek district are too small to be of major economic importance. An important question, then, is whether the dikes could be the shallower expression of a more massive carbonatite pluton at depth. Powell (1965) argued, on the basis of  $^{87}\text{Sr}/^{86}\text{Sr}$  isotopes, that the carbonate “vein-dikes” of Sheep Creek and the neighboring Mineral Hill district of Idaho were not derived from carbonatitic magmas, but rather from hydrothermal fluids associated with basaltic or alkalic magmas related to the Idaho Batholith. The  $^{87}\text{Sr}/^{86}\text{Sr}$  ratio of three samples from southern Ravalli County fell in the range 0.7048 to 0.7059, significantly higher than the mean for 21 carbonatite samples of 0.7035 (Powell and others, 1965). However, more recent work has shown that carbonatites worldwide have more variation in  $^{87}\text{Sr}/^{86}\text{Sr}$  than was known in the 1960s. For example, in a recent review of >500 analyses (Rukhlov and others, 2015), carbonatites have been found with initial  $^{87}\text{Sr}/^{86}\text{Sr}$  values as low as 0.702 and as high as 0.711. This range easily overlaps with the values obtained from the Sheep Creek area.

The mineral associations documented in this paper and by previous workers are strongly suggestive of a magmatic origin for the Nb-REE-rich carbonate dikes of Sheep Creek and the surrounding area. The Sheep Creek/Mineral Hill carbonatites are part of the poorly recognized “Montana–Idaho Alkalic Belt” (see the companion paper of Gammons, 2020) that extends northward and links up with the well-established “British Columbia Alkalic Province.” The B.C. province includes many carbonatite deposits, some of which are enriched in REE and Nb (BCGS, 2016). A major question remains as to the age of the REE mineralization in southwest Montana and neighboring Idaho. Jaffe and others (1959) obtained three lead-alpha dates for monazite from the Mineral Hill district that ranged from 90 to 99 Ma. However, these dates have a high uncertainty as assumptions needed to be made about the U/Th ratio of the host monazite. Jercinovic and others (2002) reported two age groupings of 800–1100 Ma and 200–400 Ma for U-Th-Pb dates on monazites from the Lemhi Pass district, Idaho–Montana, which is considered by some to be a southeastern extension of the Sheep Creek/Mineral Hill district (fig. 1). Metz and others (1985) published a date of  $71.1 \pm 1.0$  Ma for parisite from the Snowbird deposit. More detailed work on the REE-rich veins and dikes near the Montana–Idaho state line is needed to build a better picture of the age of these understudied but geologically interesting deposits.



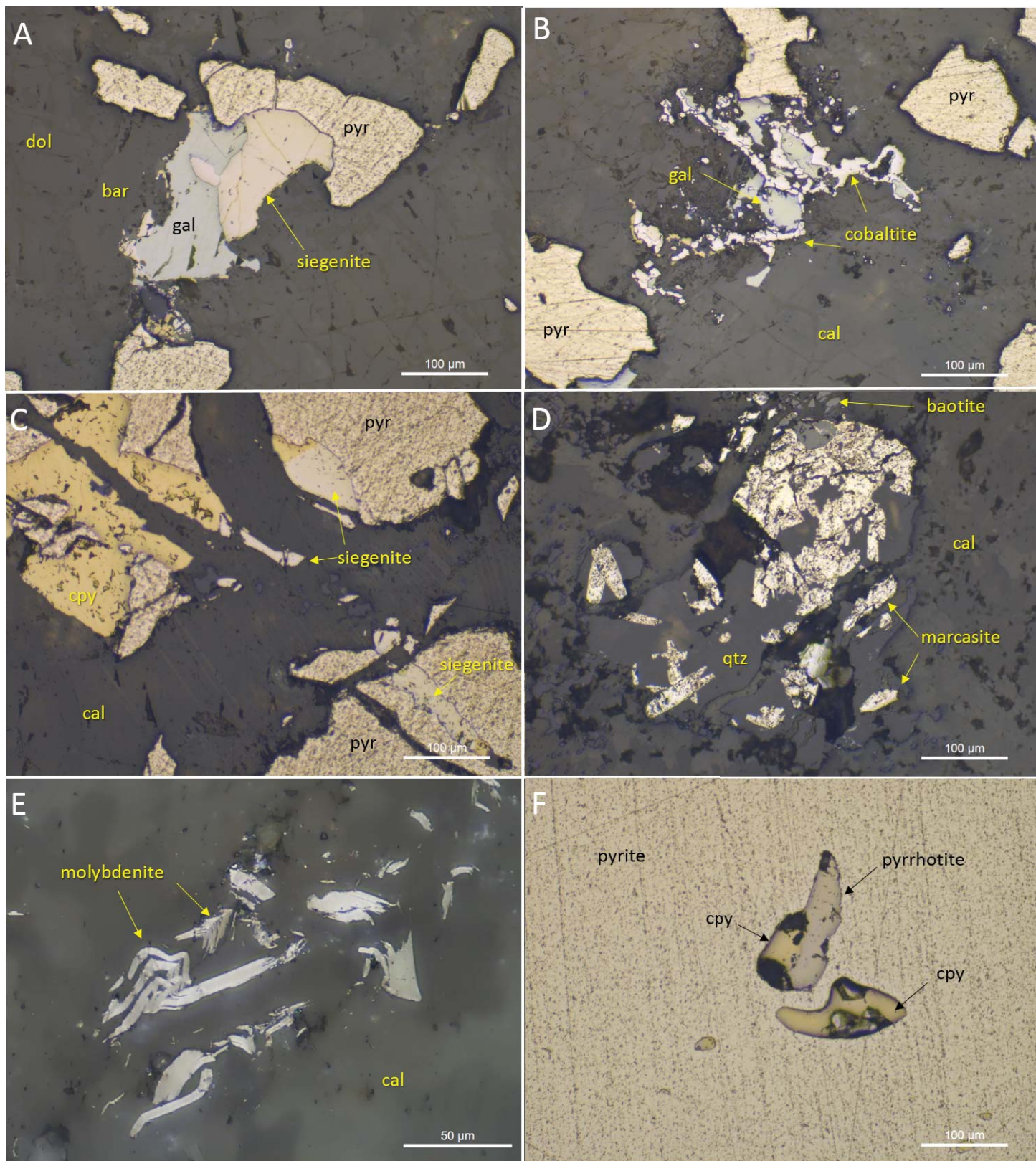


Figure 8. Reflected light photos of sulfide minerals from Sheep Creek: (A) pyrite, galena, and siegenite; (B) galena-cobaltite intergrowths; (C) chalcopyrite, pyrite, and siegenite; (D) late marcasite in association with baotite; (E) molybdenite in calcite; (F) small inclusions of chalcopyrite and pyrrhotite in coarse-grained pyrite.

## Acknowledgments

Funding for this study came from the Stan and Joyce Lesar Foundation at Montana Tech. The author thanks Francis Grondin for helping with field work in 2018, and Dick Berg for his ideas and geologic knowledge.

## References Cited

- Abbott, A.T., 1958, Monazite deposits in calcareous rocks, northern Lemhi County, Idaho: Idaho Bureau of Mines and Geology Pamphlet 99, 25 p.
- Anderson, A.L., 1960, Genetic aspects of the monazite and columbium-bearing rutile deposits in northern Lemhi County, Idaho: *Economic Geology*, v. 55, p. 1179–1201.
- BCGS, 2016, Rare metal deposits in British Columbia: British Columbia Geological Survey Information Circular 2016-4, 2 p.
- Berg, R.B., 1977, Reconnaissance geology of southernmost Ravalli County, Montana: Montana Bureau of Mines and Geology Memoir 44, 39 p.
- Crowley, F.A., 1960, Columbium-rare-earth deposits, southern Ravalli County, Montana: Montana Bureau of Mines and Geology Bulletin 18, 47 p.
- Dal Negro, A., Rossi, G., and Tazzoli, V., 1975, The crystal structure of ancylite,  $(RE)_x(Ca,Sr)_{2-x}(CO_3)_2(OH)_{x(2-x)}H_2O$ : *American Mineralogist*, v. 60, p. 280–284.
- Gammons, C.H., 2020, The Montana–Idaho Alkalic Belt: An exploration target for critical metals and industrial minerals: Proceedings 2019 Montana Mining and Minerals Conference, in press.
- Heinrich, E.W., and Levinson, A.A., 1961, Carbonatic niobium-rare earth deposits, Ravalli County, Montana: *American Mineralogist*, v. 46, p. 1424–1447.
- Heinrich, E.W., Boyer, W.H., and Crowley, F.A., 1962, Baotite (pao-t'ou-k'uang) from Ravalli County, Montana: *American Mineralogist*, v. 47, p. 987–993.
- Hess, H.D., and Trumpour, H.J., 1959, Second occurrence of fersmite: *American Mineralogist*, v. 44, p. 1–8.
- Jaffe, H.W., Gottfried, D., Waring, C.L., and Worthing, H.W., 1959, Lead-alpha age determinations of accessory minerals of igneous rocks (1952–1957): U.S. Geological Survey Bulletin 1097-B, p. 65–148.
- Jercinovic, M.J., Gillerman, V.S., and Stein, H.J., 2002, Application of microprobe geochronology to hydrothermal monazite and thorite, Lemhi Pass district, Idaho: Geological Society of America, Abstracts with Programs, v. 34, p. 172.
- Kaiser, E.P., 1956, Preliminary report on the geology and deposits of monazite, thorite, and niobium-bearing rutile of the Mineral Hill district, Lemhi County, Idaho: U.S. Geological Survey Open-File Report 390, 41 p.
- Metz, M.C., Brookins, D.G., Rosenberg, P.E., and Zartman, R.E., 1985, Geology and geochemistry of the Snowbird deposit, Mineral County, Montana: *Economic Geology*, v. 80, p. 394–409.
- Powell, J.L., 1965, Isotopic composition of strontium in four carbonate vein-dikes: *American Mineralogist*, v. 50, p. 1921–1928.
- Rukhlov, A.S., Bell, K., and Amelin, Y., 2015, Carbonatites, isotopes and evolution of the subcontinental mantle: An overview, in Simandl, G.J. and Neetz, M., eds.: Symposium on critical and strategic materials: British Columbia Geological Survey Paper 2015-3, p. 39–64.
- Sahinen, U.M., 1957, Mines and mineral deposits of Missoula and Ravalli counties, Montana: Montana Bureau of Mines and Geology Bulletin 8, 63 p.
- Spence, J.G., 1984, Geology of the Mineral Hill interlayered amphibolite-augen gneiss complex, Lemhi County, Idaho: M.S. Thesis, University of Idaho, 239 p.





Gold from Montana prospecting. Courtesy of Alma Winberry.

## Antimony, a Strategic Metal, and USAC

John C. Lawrence

*CEO, USAC, Thompson Falls, Montana*

### Abstract

Antimony is a strategic metal that is used to harden lead alloys in bullets, lead acid batteries, and other alloys. Antimony oxide is used as a flame retardant in most plastics, many textiles, and as a catalyst in PET. Sodium antimonate is used as a flame retardant in plastics, as a fining agent in glass, and as an opacifier. Antimony trisulfide is used in primers for all center-fired ordnance and as a lubricant in friction brakes on aircraft and vehicles. During World War II, the War Department received antimony from the Stibnite Hill Mine (now owned by USAC), and the Sunshine Mine and the Yellow Pine District, both in Idaho. They could not keep up with the demand, and they ended up buying the bulk of the antimony from three mines in Mexico, the Wadley, Soyatal, and Guadalupe. Following the war, the U.S. Government bought 40,000 tons of antimony metal, primarily from the Wadley smelter, to create a strategic stockpile. By 2003, all of the metal had been sold from the strategic stockpile. Approximately 92% of all the antimony in the world is now supplied by the Chinese. China is the main supplier of antimony trisulfide. This has placed the United States in a very vulnerable position.

USAC began mining and smelting the ore from the Stibnite Hill Mine in Montana in 1969 and continued until 1983, when prices forced its closure. According to the U.S. Geological Survey, the mine production and reserves were estimated at 15,400 metric tons or 33,950,840 pounds of antimony. After the mine closed in 1983, smelter operations continued with raw materials from North America and around the world, and it has now become one of two significant antimony smelters in North America (the other smelter is owned by USAC in Mexico). USAC produces all of the four strategic products. The company has developed the technology to remove impurities such as arsenic, lead, and bismuth and recover precious metals.

To become a viable supplier of antimony, USAC had to have its own mine reserves. The Company attempted to reopen the Stibnite Hill Mine, but new permitting requirements preempted the plans. USAC turned to Mexico where it had previously mined antimony. Ironically, USAC now has the three top producing Mexican mines that had produced during World War II. All of them are classic Mexican manto deposits. Wadley produced 57,613 tons by 1943 and has produced an estimated 25,000 tons since that time. Soyatal had produced 25,630 tons by 1943 and probably another 20,000 tons since that time. Sierra Guadalupe has no recorded production, but its production is comparable to the other two deposits. All three properties were mined and smelted by the Cookson Group of England, which changed ownership many times and ended up as Great Lakes Chemical.

### Antimony Strategic Products

**Antimony Metal** is used to harden lead in bullets and in lead/acid deep-cycle batteries for vehicles, tanks, and heavy equipment

**Antimony Oxide** is used as a flame retardant in many plastic products, including vehicle and aircraft interiors; all insulation for wire; textiles, including canvas for tents; carpeting; and as a catalyst to make PET.

**Sodium Antimonate** is used as a flame retardant in high-impact thermoset plastics and also as a fining agent to remove bubbles from optical glass and cathode ray tubes.

**Antimony Trisulfide** is used as a component in all center-fired ordnance and rockets. It is also used as a lubricant in heavy duty brakes on aircraft and vehicles.



### Antimony: A Strategic Metal in the United States

During World War II, the War Department produced antimony from the Stibnite Hill Mine (now USAC's mine), the Sunshine Mine in Idaho, and from the Yellow Pine District in central Idaho. The domestic mines were not adequate, and most of the antimony was mined in Mexico. The U.S. Geological Survey was sent to Mexico to evaluate the mines and prepare USGS Bulletins. The important mines included the Wadley, Soyatal District, Sierra Guadalupe, and three other areas of lesser importance.

Following the War, the National Defense Stockpile was built by the United States Government, containing 37,498 short tons of metal. Most of the metal was produced from the Wadley Mine. By 2003, the U.S. Government had sold the last of the stockpile. Chinese mines purchase raw materials and smelt about 92% of the world supply of antimony. For many years several domestic companies bought concentrates, direct shipping ore (DSO), crude oxide, and metal primarily from China and produced antimony oxide. They have all ceased production.

USAC started production at the Stibnite Hill Mine in western Montana in 1969. Mining continued from 23 adits until 1983, when it was closed due to low prices. Subsequently, the smelter has been in continuous production utilizing raw materials from around the world.

The U.S. Geological Survey (Seal and others, 2017) states: "The U.S. Antimony Mine in western Montana is the second largest simple quartz-stibnite vein deposit in the United States. It had significant production in the past, but was closed in 1983; the mine's production and reserves are estimated to be nearly 15,400 metric tons of antimony (33,951,183 pounds of antimony)"

When antimony prices recovered after 1983, USAC attempted to reopen the Stibnite Hill Mine. They were told that it would require an EI., a zero discharge tailings pond, and bonding. Knowing that an EIS would be extremely expensive and could take more than 30 years without any certainty that a "not likely to adversely impact the environment" decision would ever be established, and realizing that bonding would be large and require cash, the reopening of the mine looked bleak. The authorities added that even if we obtained a successful EIS and were able to bond, the next event would likely include numerous lawsuits filed to stop the project. USAC made the prudent decision to not try to reopen the mine but to source raw materials from Mexico. Ironically, USAC ended up mining the same mines that were mined during World War II and one additional mine, the Los Juarez.

### Antimony Deposits and Production of the World

Table 1. As of 12 May 2016, estimated sources of world supply of antimony.

| Source                  | Metric tons/year | Pounds per year |
|-------------------------|------------------|-----------------|
| Secondary lead smelters | 50,000           | 110,200,000     |
| Primary lead smelters   | 30,000           | 66,120,000      |
| China non-Hunan         | 25,000           | 55,350,000      |
| China Minmet Hunan      | 15,000           | 33,060,000      |
| China private Hunan     | 15,000           | 33,060,000      |
| Mandalay                | 7,000            | 15,428,000      |
| Siberia                 | 7,000            | 15,428,000      |
| Tajikistan              | 6,000            | 13,224,000      |
| Myanmar                 | 5,000            | 11,020,000      |
| Turkey                  | 2,000            | 4,409,000       |
| Bolivia                 | 1,500            | 3,306,000       |
| Mexico                  | 1,000            | 2,204,000       |
| Peru                    | 500              | 1,102,000       |
| Total world production  | 165,000          | 363,911,000     |

Note. The annual supply of antimony was 160,000–200,000 metric tons (352,640,000–440,800,000 ppy).

## Historic Pricing

Table 2. Metal prices bulletin: average monthly metal price per metric ton CIF, USA.

| Month   | 2011   | 2012   | 2013   | 2014   | 2015  | 2016  | 2017  | 2018  | 2019  | Month   |
|---------|--------|--------|--------|--------|-------|-------|-------|-------|-------|---------|
| Jan     | 14,027 | 11,850 | 11,492 | 9,877  | 8,543 | 5,456 | 7,683 | 8,609 | 7,922 | Jan     |
| Feb     | 14,950 | 11,960 | 10,803 | 10,072 | 7,937 | 5,374 | 7,650 | 8,688 | 7,975 | Feb     |
| Mar     | 16,452 | 13,051 | 10,626 | 10,141 | 8,234 | 5,511 | 8,653 | 8,813 | 7,799 | Mar     |
| Apr     | 17,879 | 13,503 | 10,458 | 9,866  | 8,488 | 5,585 | 8,945 | 8,736 | 7,302 | Apr     |
| May     | 16,769 | 13,917 | 10,351 | 9,711  | 8,616 | 6,283 | 8,763 | 8,228 | 6,911 | May     |
| Jun     | 15,997 | 13,977 | 10,183 | 9,755  | 8,300 | 6,504 | 8,548 | 8,361 | 6,713 | Jun     |
| Jul     | 14,815 | 13,531 | 9,893  | 9,797  | 7,824 | 6,724 | 7,937 | 8,294 | 6,008 | Jul     |
| Aug     | 14,991 | 12,886 | 10,086 | 9,755  | 7,330 | 7,176 | 8,351 | 8,014 |       | Aug     |
| Sep     | 15,454 | 12,814 | 10,417 | 9,659  | 6,790 | 7,634 | 8,460 | 8,625 |       | Sep     |
| Oct     | 15,419 | 12,911 | 10,472 | 9,469  | 6,462 | 7,785 | 8,157 | 8,611 |       | Oct     |
| Nov     | 14,509 | 12,732 | 10,340 | 9,281  | 6,049 | 7,584 | 8,226 | 8,175 |       | Nov     |
| Dec     | 13,062 | 12,125 | 9,893  | 9,039  | 5,677 | 7,606 | 8,510 | 7,910 |       | Dec     |
| High    | 17,879 | 13,977 | 11,492 | 10,141 | 8,616 | 7,785 | 8,954 | 8,813 |       | High    |
| Low     | 13,062 | 11,850 | 9,893  | 9,039  | 5,677 | 5,374 | 7,650 | 7,910 |       | Low     |
| Avg/MT  | 15,360 | 12,938 | 10,418 | 9,702  | 7,521 | 6,602 | 8,324 | 8,422 |       | Avg/MT  |
| Avg/lb. | 6.97   | 5.87   | 4.725  | 4.40   | 3.41  | 2.99  | 3.775 | 3.82  |       | Avg/lb. |

## History of USAC Production

**25 November 1969.** USAC purchased the Stibnite Hill Mine at Thompson Falls, Montana.

**December 1969.** The price of antimony metal increased from \$0.52/pound to more than \$4.00/pound.

**1970–1975.** USAC core drilled part of the property and built a mill with a heavy media separator and 50 tpd flotation mill. The concentrates were initially sold to a smelter. Thereafter, furnaces were installed and antimony metal was produced by the English precipitation method and sold to the lead/acid battery market.

**1975–1983.** The maintenance-free calcium lead storage battery was developed and by 1975 the demand for antimony metal fell sharply. USAC decided to sell antimony oxide at a better price. The problem was that the Stibnite Hill antimony contained too much arsenic. To eliminate the arsenic, USAC built a caustic leach plant and initially made sodium antimonate to be converted to antimony oxide that could be sold as a chemical intermediate to make an arsenic-free antimony oxide. Meanwhile, it was discovered that there was a market for sodium antimonate as a fining agent (degasser to remove bubbles from glass) and radiation shield for TV bulbs. For years USAC sold sodium antimonate to the TV bulb manufacturers. Early in the 1980s, the flat screen TV took over the market, and sodium antimonate had little value. At this point, USAC produced antimony metal by electro-winning. The mines were shut down in 1983.

**1983–Present.** USAC produces all antimony oxide products from raw materials from around the world. Currently, 42% comes from North America and the balance comes from USAC's Mexican mines.



### Mexican Mines

**Wadley Mine, San Luis Potosi.** Wadley was historically the largest producer of antimony in Mexico. By 1943 the mine had produced 57,512 tons of antimony, and since 1943 it has probably shipped another 40,000 tons. During World War II with up to 2,500 miners they shipped as much as 500,000 pounds per month. The mine has more than 600 kilometers of tunnels, a mill, railroad siding, living quarters, stores, hospital, assay laboratories, and warehouses. Wadley is a classic manto deposit where the ore zones are layered in limestone with multiple horizons. Because of an agreement with the Huichol Indians, explosives are not used. USAC has 40 to 90 workers mining on a contract basis.

**Sierra Guadalupe, Zatecas.** Historically the Sierra Guadalupe shipped ore to the Wadley or to the Laredo Smelter of National Lead. There are no production records or maps. The areal extent and number of workings is extensive and the deposit is a typical manto similar to Wadley except there are many more sulfides. Flotation concentrates at the Puerto Blanco mill have assayed 60–68% antimony.

**Soyatal, Queretaro.** The Soyatal deposit was the third largest producer in Mexico. By 1943 it had shipped 25,630 tons, and since that time it has probably shipped another 25,000 tons.

**Los Juarez, Queretaro.** Unlike the manto deposits, Los Juarez (fig. 1) is a deep-seated jasperoid pipe deposit with good gold, silver, and antimony values to a depth of more than 400 m. The deposit is 3.5 km in length and over 1 km in width (fig. 2). It has all the signature elements of the Carlin gold mine and the Robert's Mountain overthrust belt in Nevada. The deposit has been owned by two major mining companies but has never gone into production due to the complex metallurgy. USAC has solved the metallurgical problem with the flotation product by adding an alkaline leach circuit for the flotation concentrates and a cyanide leach for the mill tailings.

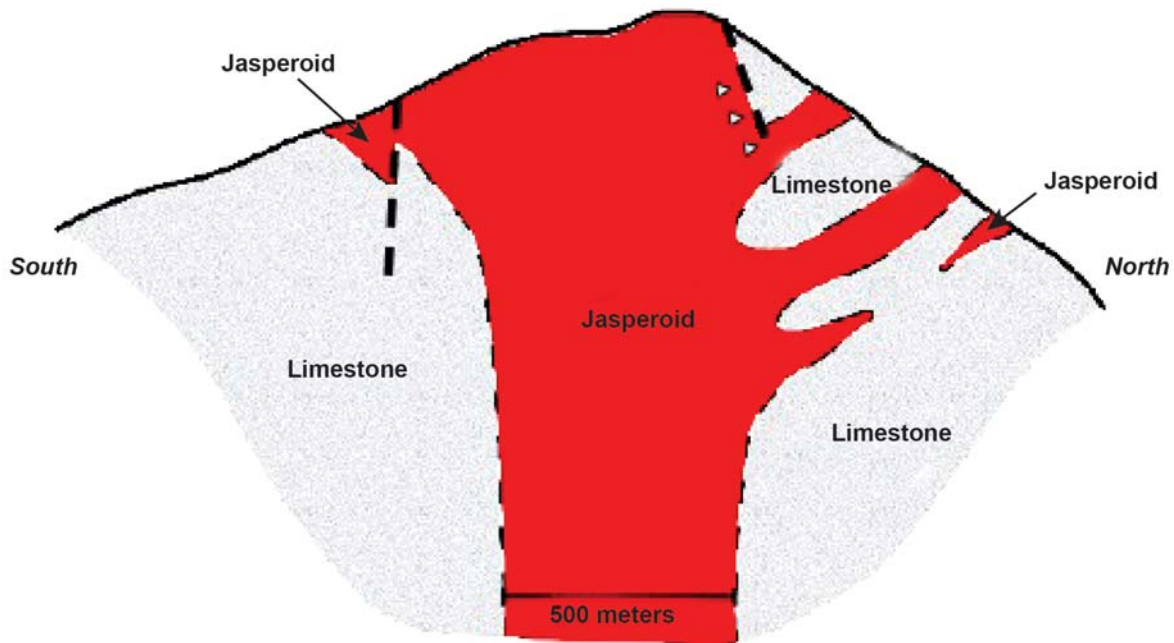


Figure 1. Los Juarez Project. Diagrammatic cross section looking west.

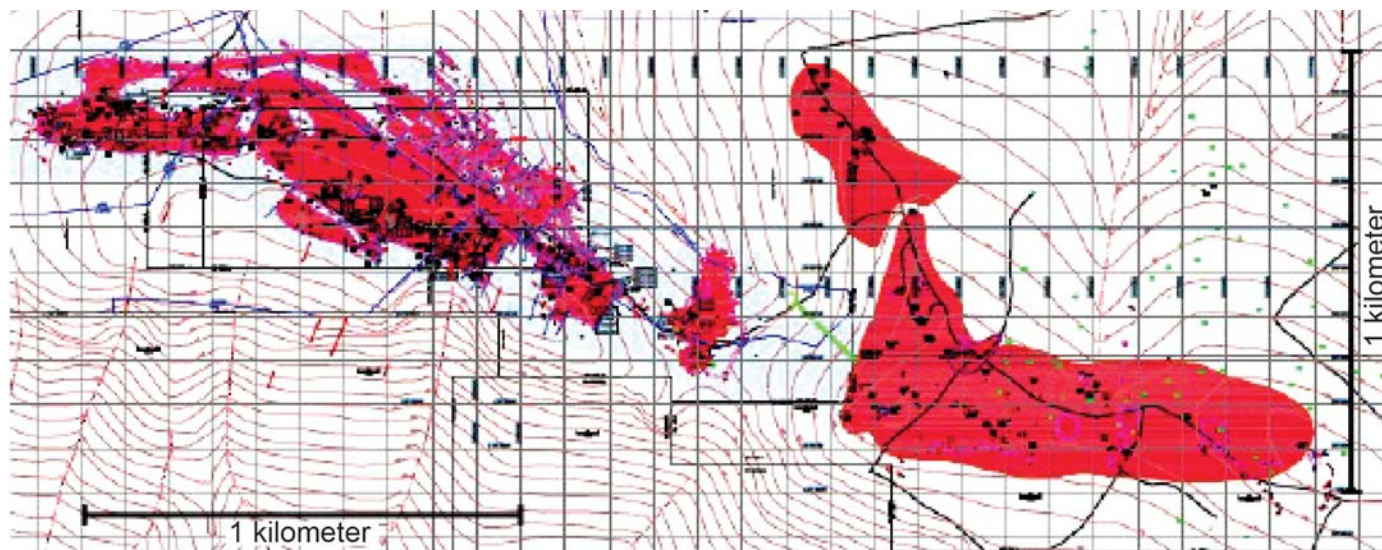


Figure 2. Deposit map with mineralization areas in red.

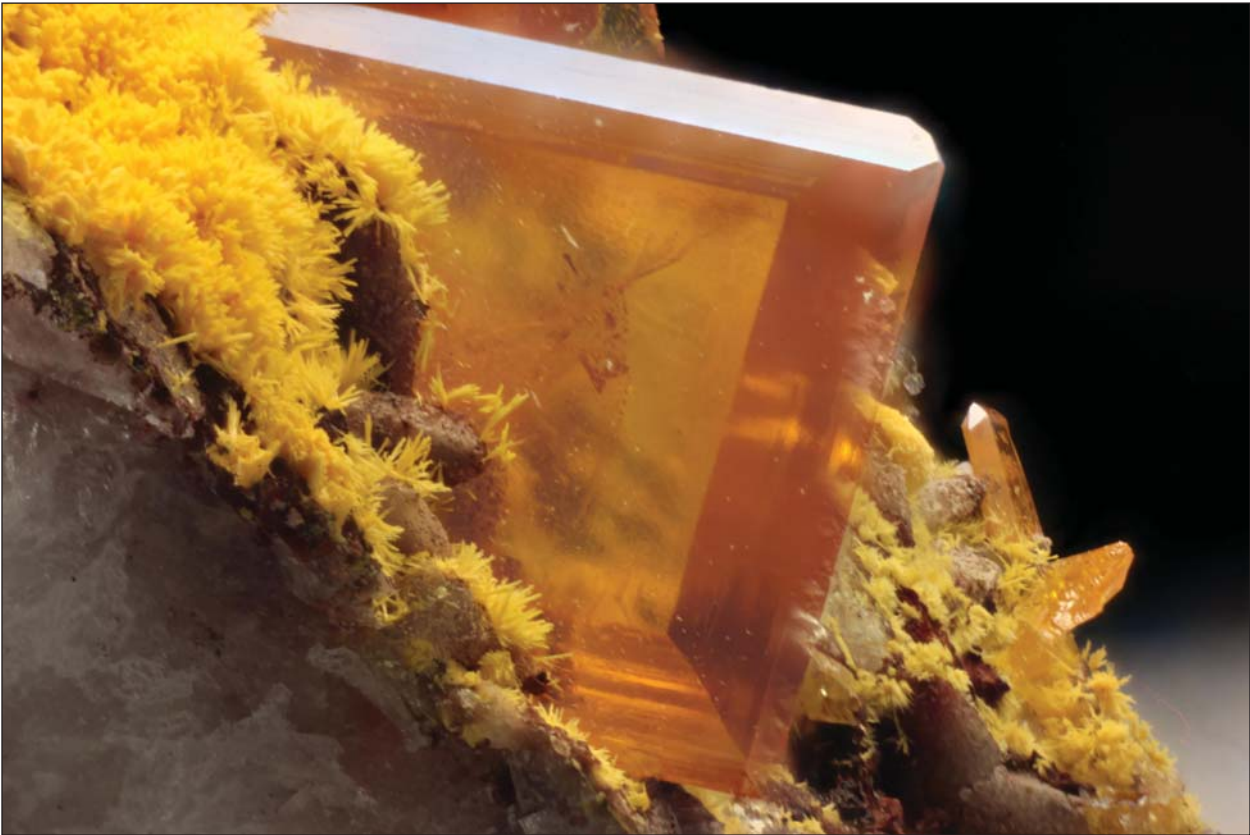
### References

Seal, R.R. II, Schulz, K.J., and DeYoung, J.H., Jr., 2017, Antimony, chap. C of Schulz, K.J., DeYoung, J.H., Jr., Seal, R.R., II, and Bradley, D.C., eds., *Critical mineral resources of the United States—Economic and environmental geology and prospects for future supply*: U.S. Geological Survey Professional Paper 1802, p. C1–C17, doi: <https://doi.org/10.3133/pp1802C>.





Pyrite from the Troy Mine, MT. Courtesy of Michael J. Gobla.



Wulfenite and mimetite from the Rowley Mine, AZ. Courtesy of Michael J. Gobla.

# New Studies on the Oro Fino Mining District, Deer Lodge County, Montana: Metals, Boron, and Heavy Isotopic Sulfur Sourced in the Revett Formation

Stanley L. Korzeb and Kaleb C. Scarberry

*Montana Bureau of Mines and Geology, Butte, Montana*

## Introduction

The Oro Fino mining district is located 6 mi east of Galen and extends south to the boundary between Deer Lodge and Silver Bow Counties. This investigation generated new and updated geologic data on the known mineral resources and assessed the future exploration potential for the district. New data were generated using advanced investigative techniques, including stable isotope, trace element and whole rock geochemistry, geochronology, identifying alteration types, fluid inclusion studies, mineralogy, and cathodoluminescence analysis of quartz veins.

## History

Gold was discovered and mined in 1867 from placers along Caribou, Oro Fino, and Dry Cottonwood Creeks. Placer mining started to decline by 1870 in favor of the newly discovered lode veins (Williams, 1951). Sapphires were discovered in 1889 and commercial operations began in 1907 on the upper portion of Dry Cottonwood Creek (Berg, 2007). The first operating mine was the Champion mine located at the head of Oro Fino Creek. The Champion mine started operations in 1886 and closed in 1888 when operations proved to be unprofitable (Pardee and Schrader, 1933). Mining did not begin again until 1916 when the Independence mine opened, producing a small quantity of gold–silver ore and oxide copper ore that was shipped in 1918 and 1919. Interest was renewed at the Champion mine in 1919 with the construction of a flotation mill in 1920. Since the Champion mine was predominantly a silver producer, it was shut down in 1926 due to low silver prices (Pardee and Schrader, 1933). The Cashier and Independence mines were in production from 1924 to 1931, and by 1933 the Independence mine was the only mine producing in the district (Williams, 1951). The Champion mine was reopened in 1938, and by 1940 the American, Cashier, Grizzly Bear, Independence, and Champion mines were operating (Williams, 1951). In 1941, the Champion and Independence were the only mines in production. Mining shut down throughout the district during World War II, with no reported production from 1943 to 1946 (table 1), and resumed in 1947. After 1947, the Champion was still producing and continued up to 1975 when operations ended (Korzeb and Scarberry, in preparation).

Table 1. Oro Fino production from 1933 to 1948 summarized by Williams (1951) from the Mineral Yearbook for the years 1933 to 1950.

| Year | Producing Mines | Tons of Ore | Oz. Gold | Oz. Silver | Lbs. Copper | Lbs. Lead |
|------|-----------------|-------------|----------|------------|-------------|-----------|
| 1933 | 3               | 68          | 21       | 1,053      | 64          | -         |
| 1934 | 3               | 22          | 9        | 2,183      | 16          | -         |
| 1935 | 2               | 8           | 2        | 280        | -           | -         |
| 1936 | 8               | 158         | 83       | 3,854      | 265         | 200       |
| 1937 | -               | -           | -        | -          | -           | -         |
| 1938 | 3               | 105         | 21       | 1,383      | 112         | -         |
| 1939 | 4               | 346         | 161      | 4,262      | -           | -         |
| 1940 | 4               | 1,429       | 131      | 16,252     | -           | -         |
| 1941 | 2               | 1,176       | 55       | 17,564     | -           | -         |
| 1942 | 2               | 518         | 10       | 4,815      | 1,000       | -         |
| 1947 | 2               | 15          | 1        | 378        | -           | -         |
| 1948 | 1               | 3           | -        | 94         | -           | -         |



## Production

Production from 1867 to 1870 came from gold placers and is estimated to have a value of \$80,000 (1800s gold price of \$20.67; Williams, 1951) and is calculated to be approximately 3,870 oz. Production has not been recorded from 1866 to 1911, but both lode and placer mines were operating. From 1916 to 1926, production was reported by Williams (1951) to be from the Champion, Independence, and Cashier Group mines and was estimated to total \$350,000 (based on early 1900s prices for gold, silver, lead, zinc, and copper). Accurate production records were not reported until after 1933 and are summarized in table 1.

## Regional Geology

The mining district is within the Boulder Batholith (fig. 1). The Boulder Batholith and Elkhorn Mountains volcanic field concurrently formed during crustal shortening near the end of Mesozoic Cordillera arc magmatism between about 85 and 76 Ma (Mahoney and others, 2015; Rutland and others, 1989). The eruption of the Elkhorn Mountains volcanic field was the first magmatic event during continental arc magmatism and is pre-

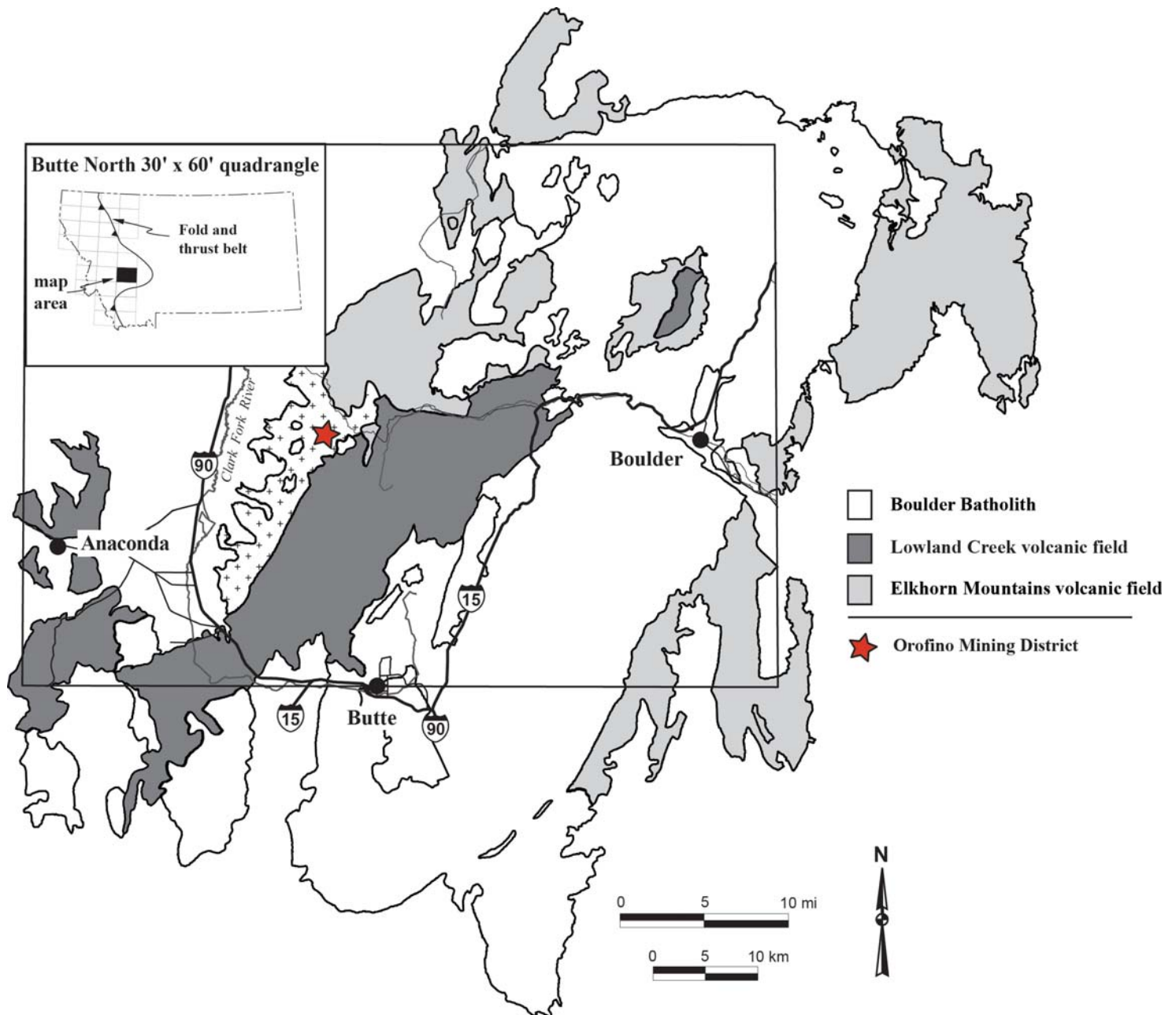


Figure 1. Generalized geologic map of the Boulder Batholith showing location of the Oro Fino Mining district and volcanic field locations.

served along the west and east flanks of the Boulder Batholith (fig. 1). Plutonic intrusions that developed the Boulder Batholith began approximately 81 Ma and continued until approximately 74 Ma (Lund and others, 2002).

After the Boulder Batholith was emplaced, a combination of Laramide, Eocene crustal extension, and Basin and Range faulting caused the Elkhorn Mountains volcanic field and Boulder Batholith to be uplifted, eroded, and exhumed. Between about 65 and 55 Ma, post Laramide crustal shortening from the west occurred, forming grabens in the upper plate of the Anaconda Metamorphic Core Complex detachment. The grabens were later filled with the Lowland Creek volcanic field between 53 and 49 Ma (Scarberry and others, 2015; Dudás and others, 2010).

Back-arc volcanism started during the early Eocene caused by the steepening of the subducting Farallon plate under the North American plate (Feely, 2003), leading to the eruption of the Lowland Creek volcanic field. The Lowland Creek volcanic field was erupted in a northeast–southwest-trending half graben traversing the Boulder Batholith (fig. 1; Sillitoe and others, 1985; Dudás and others, 2010).

During and after the Lowland Creek volcanic field developed, extension related to core complex formation continued until about 35 Ma (Lonn and Elliott, 2010). Basin sedimentation began near the close of Lowland Creek volcanism, 50 Ma (Portner and others, 2011). The Lowland Creek volcanic field is overlain by lacustrine and fluvial sedimentary rocks in the Deer Lodge and Warm Springs Creek valleys and is locally unconformable with the volcanic rocks (Dudás and others, 2010).

### District Geology

The entire district lies within the Butte Granite of the Boulder Batholith, which is the host rock for the epithermal veins (fig. 2). On top of Cottonwood Mountain, Orofino Mountain, and at the head of Oro Fino Creek, the Butte Granite is overlain by rhyolite that is attributed to the  $40.62 \pm 0.16$  and  $40.8 \pm 0.17$  Ma Avon volcanic event (Hargrave, 1990; Hargrave and Berg, 2013; Mosolf, 2015). The veins occupy east–northeast- to west–southwest- and north–south-trending faults and fractures in the Butte Granite (fig. 2). Development of these faults and fractures probably coincides with the formation of the northeast-trending partial graben and the eruption of the Lowland Creek volcanic field. The veins show evidence of the original faults being open fractures filled with brecciated Butte granite. Epithermal veins adjacent to aplite dikes contain both brecciated aplite and Butte granite.

### *Geochronology*

Hydrothermal muscovite (sericite) from altered Butte granite host rock adjacent to a vein exposed in the Banker mine, at location OF-31, was dated by  $^{40}\text{Ar}/^{39}\text{Ar}$  methods. Sericite analysis was conducted at the Oregon State University Argon Geochronology Laboratory, Corvallis, OR. Analysis was completed by standard incremental heating at 77-sec intervals using an Argus-VI-D instrument. The  $^{40}\text{Ar}/^{39}\text{Ar}$  plateau date for OF-31 was  $45.26 \pm 0.11$  Ma, and is represented by more than five concordant heating steps .

### *Wall rock alteration*

Alteration of the Butte granite is directly related to vein development and is found adjacent to the quartz veins. From field observations, SEM-EDS analysis, X-ray diffraction analysis, and examination of hand specimens and thin sections, silicic and sericitic-argillic alteration were identified. The SEM-EDS analysis was performed at the Center for Advanced Mineral and Metallurgical Processing, Montana Tech. X-ray diffraction analysis was performed at the College of Oceanic and Atmospheric Sciences, Oregon State University.

Sericitic-argillic alteration is superimposed on silicic alteration, suggesting they are simultaneous events (Korzeb and Scarberry, in preparation). Sericitic-argillic alteration is characterized by hydrothermally crystallized muscovite (sericite), illite, kaolinite, adularia, and montmorillonite. Adjacent to the veins, disseminated pyrite is concentrated in the sericitic-argillic alteration along with silicified wall rock. Both sericitic-argillic and silicic alteration decreases in intensity outward from the veins into unaltered granite. Adjacent to the veins, silic-



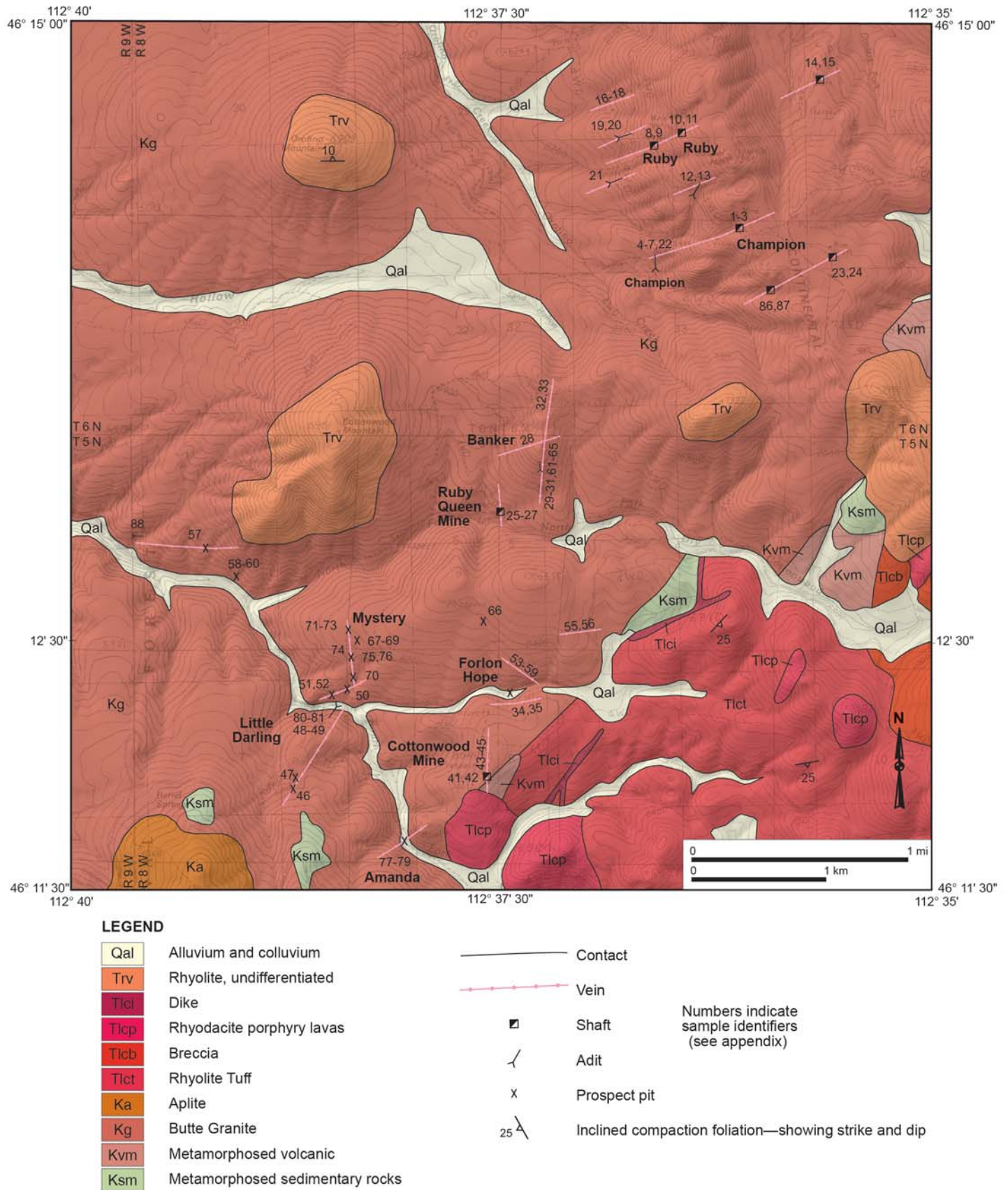


Figure 2. Geologic map of the Oro Fino mining district showing sample and vein locations and rock types.

ic alteration is strongest and is characterized by fine-grained quartz and disseminated pyrite replacing the granite host. Granite breccia fragments that were assimilated into the quartz veins were likewise altered and replaced by fine-grained quartz.

#### *Alteration trace elements*

Trace-element associations for epithermal vein systems and modern hot springs are geochemically unique (Mosier and others, 1987; Silberman and Berger, 1985; Simmons and Brown, 2000). In comparison to trace element averages for unaltered granite, silicic alteration shows an enrichment in Ag, As, Bi, Cs, Li, Mo, Sb, Tl, W, and Zn. Sericitic-argillic alteration shows enrichment in the same elements as silicic alteration with the exception of Li and Mo, which show a depletion compared to unaltered granite. Silicic alteration shows a depletion in Al, Ba, Ca, Co, Cu, Fe, K, Mg, Mn, Na, Ni, and Pb compared to unaltered granite. Sericitic-argillic alteration shows a depletion in the same elements as silicic alteration with the exception of Al and K, which have the same concentration as unaltered granite.

The trace elements Au, Ag, As, Sb, Tl, Pb, and Zn are characteristic of hydrothermal systems that are classified as epithermal (Silberman and Berger, 1985). Discharge waters from geothermal wells in New Zealand contain Au, Ag, As, Bi, Li, Mo, Pb, Sb, Tl, W, and Zn (Weissberg, 1969; Ewers and Keays, 1977; Simmons and Browne, 2000; Simmons and others, 2016). The suite of enriched trace elements found in the Oro Fino mining district altered rocks are the same as those found in active geothermal fields and are characteristic of epithermal systems. The exception is the enrichment of Cs, which is not known to be a characteristic trace element in epithermal systems.

### **Vein Paragenesis**

The veins in the district are characterized by massive white quartz with breccia fragments of altered granite host rock, disseminated sulfide minerals, and vugs lined with quartz crystals and late stage sulfide minerals. Vein widths varied from less than 1 ft to over 6 ft and were mined to depths up to 900 ft at the Champion mine. The host granite was replaced along the vein contacts by quartz and disseminated pyrite. Schorl associated with the silicified host rock occurs along the contact between the veins and host granite at isolated locations. When present, schorl occurs as inclusions in early quartz veins, indicating early crystallization. Where the veins are exposed in shaft collars and prospect pits, host rock alteration extends about 3 ft distal from the vein contacts.

A series of mineralizing events developed the Oro Fino veins, consisting of host rock alteration, base metal, silver-gold, and late-stage mineralization followed by supergene alteration (Korzeb and Scarberry, in preparation). Base metal mineralization took place in conjunction with host rock alteration and is characterized by pyrite, arsenopyrite, chalcopyrite, sphalerite, and galena. Silver-gold mineralization overprints and followed base metal mineralization. Native silver and gold along with silver sulfosalt minerals identify the silver-gold mineralization stage. The gangue minerals fluorite, barite, ankerite, and calcite were deposited during a late-stage mineralizing event. Following hydrothermal mineralization, supergene mineralization caused primary minerals to be replaced with secondary minerals such as scorodite and hematite.

#### *Fluid inclusions*

To gain an understanding of the temporal evolution of the hydrothermal veins, microthermometric measurements of fluid inclusions were conducted by Jarred Zimmerman. Examination of fluid inclusions in thin section showed a variety of types and were classified as type I, type II, liquid, vapor, and three phase inclusions. Type I inclusions are the most common and are two-phase, consisting of a liquid-rich phase and a vapor bubble. In type I inclusions, the vapor phase is less than 50% of the inclusion volume. Other two-phase inclusions are of type II and consist of liquid and vapor phases where the vapor phase volume exceeds the liquid volume. Some type II inclusions have a vapor phase that is 70% or greater with a thin outer rim of liquid. Single-phase inclusions consisting of all liquid or vapor were common. Three-phase inclusions with a halite daughter mineral, liquid, and vapor were also present but are rare and were found to be associated with schorl.



Salinity and homogenization temperatures suggest the hydrothermal fluids underwent four major changes during vein mineralization (Korzeb and Scarberry, in preparation). The hydrothermal fluids evolved from an early magmatic phase followed by boiling phases and late magmatic fluid mixing at the close of mineralization. Fluid inclusion results are summarized in table 2. When temperature is plotted against salinity (fig. 3), four distinct fields emerge representing salinity changes for the hydrothermal fluid and equivalent temperatures. The field with the highest salinity (early magmatic fluid, fig. 3), ranging from 30.34 to 37.66 wt% NaCl eq (table 2), is interpreted to represent a fluid with a magmatic origin (Lang and others, 2000). This magmatic derived hydrothermal fluid was the first fluid pulse that began developing the veins and was trapped before boiling took place. After the first pulse of magmatic fluid, boiling took place, causing phase separation of the early magmatic fluids, generating a less saline hydrothermal fluid (boiling magmatic fluid, fig. 3).

Table 2. Summary of fluid inclusion data for 176 homogenization temperatures and wt% NaCl equivalent determinations from throughout the Oro Fino district.

| Mineralizing Fluid Phases  | Host Mineral             | Th°C Range  | Th°C Average | Tm°C Halite Range | Tm°C Halite Average | Tm°C Ice Range | Tm°C Ice Average |
|----------------------------|--------------------------|-------------|--------------|-------------------|---------------------|----------------|------------------|
| Early magmatic             | Quartz                   | 197.1–362.7 | 273.5        | 166.0–293.4       | 212.4               |                |                  |
| Boiling phase              | Quartz                   | 175.2–314.7 | 232.9        |                   |                     | -5.7 to -11.9  | -8.4             |
| Boiling phase              | Quartz                   | 192.9–346.5 | 244.4        |                   |                     | 0.0 to -4.1    | -1.1             |
| Late magmatic fluid mixing | Barite, fluorite, quartz | 129.6–189.5 | 167.6        |                   |                     | 0.0 to -1.4    | -0.4             |

| Mineralizing Fluid Phases  | Host Mineral             | Wt% NaCl eq Range | Wt% NaCl eq Average | <i>n</i> for All Averages |
|----------------------------|--------------------------|-------------------|---------------------|---------------------------|
| Early magmatic             | Quartz                   | 30.34–37.66       | 32.70               | 17                        |
| Boiling phase              | Quartz                   | 8.81–15.99        | 12.18               | 16                        |
| Boiling phase              | Quartz                   | 0.0–6.58          | 1.5                 | 87                        |
| Late magmatic fluid mixing | Barite, fluorite, quartz | 0.0–2.4           | 0.65                | 56                        |

*Note.* Th°C, temperature of homogenization to liquid in degrees centigrade; Tm°C halite, melting temperature for halite in degrees centigrade; Tm°C ice, melting temperature for ice in degrees centigrade. *n*, number of inclusions used for averages.

Assemblages of fluid inclusions show boiling was a common event during mineralization and most two-phase inclusions were trapped during boiling. The presence of bladed calcite, quartz replacing bladed calcite, and colloform quartz banding is physical evidence boiling was taking place during vein development (Simmons and Browne, 2000; Moncada and others, 2012). Groups of type I and II inclusions with similar Th with associated liquid and vapor inclusions suggest boiling was taking place and were most likely trapped along the boiling curve. Most fluid inclusions were trapped at a temperature ranging from 193° to 347°C with salinities varying from 0 to 6.50 wt% NaCl eq averaging 1.6 wt% NaCl eq. Liquid inclusions had a salinity varying from 0.18 to 8.13 wt% NaCl eq. Using the average salinity and temperature range, fluid densities determined from a diagram in Roedder (1984) ranged from 0.60 to 0.90 g/cm<sup>3</sup>. After applying these densities to the boiling curve on a diagram from Fisher (1976), a pressure of near 0 to 150 bars was determined. This assumes NaCl was the only salt present in the fluid inclusions.

### Cathodoluminescence

Quartz is the most common gangue mineral in the Oro Fino veins and is found throughout the district. Examination of hand specimens, cut slabs, and thin sections show quartz forming multiple generations. Breciated host rock is replaced by quartz and multiple generations of quartz fills open spaces in the silicified granite. Quartz forms comb structures on vein margins, replaces bladed calcite, and occurs as free-forming crystals

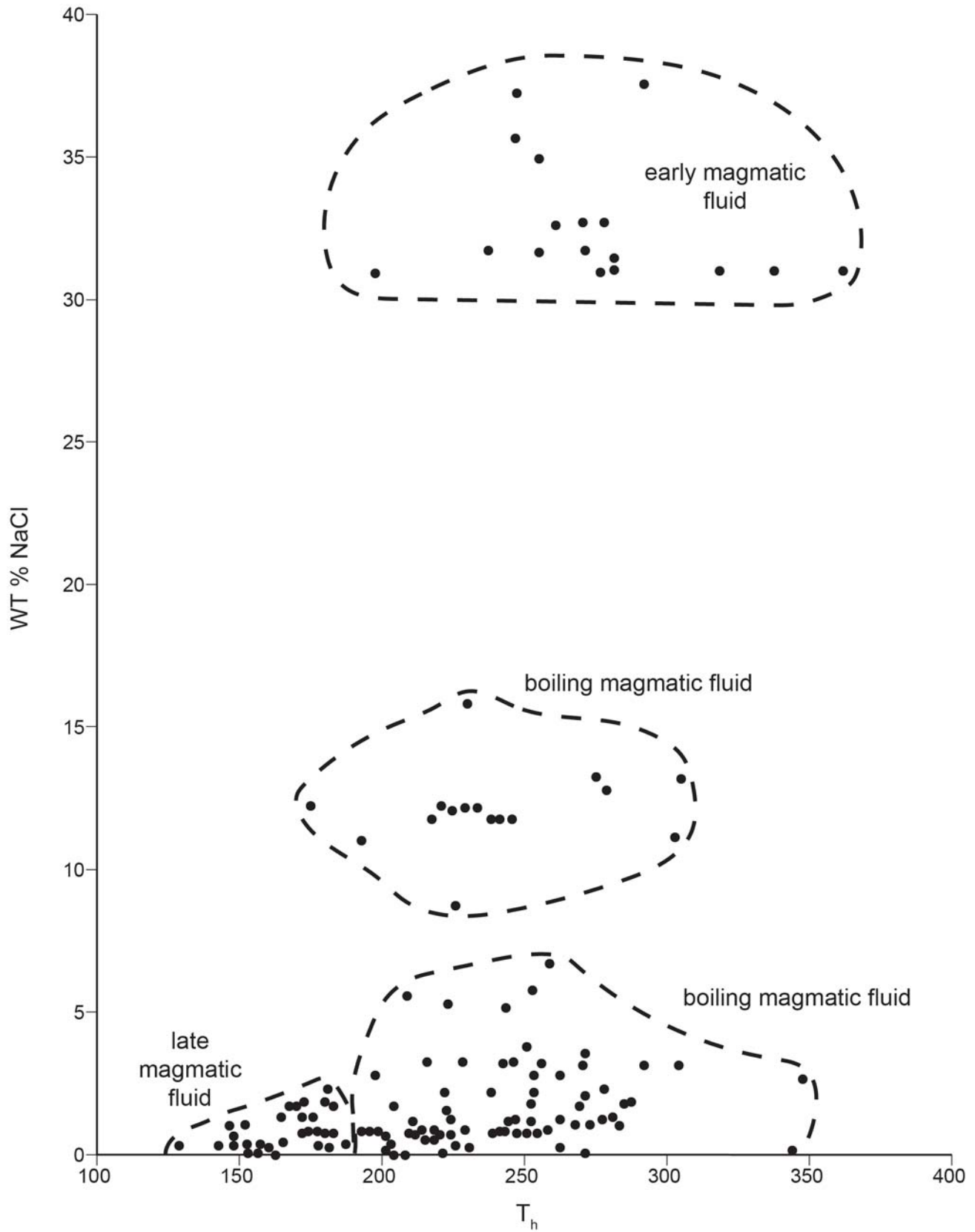


Figure 3. Plot of fluid inclusion homogenization temperature versus weight % equivalent NaCl showing different fields representing changes from a magmatic to meteoric fluid. Th, homogenization temperature. WT% NaCl, weight % equivalent NaCl



in open vugs and chalcedony bands. The paragenetic sequence and trace elements of these quartz generations are used to trace the physical and chemical changes that took place during vein development. From the cathodoluminescence images, four quartz generations were identified (Korzeb and Scarberry, in preparation). The first two quartz generations are related to the alteration of the granite host rock and fill fractures in brecciated primary quartz. The third generation fills open spaces and is related to base metal mineralization and in some locations replaces bladed calcite. Quartz-hosted fluid inclusions are related to this third generation. The fourth quartz generation represents recrystallized colloform quartz and is related to silver-gold mineralization.

Electron micro probe (EMP) analysis of the four quartz generations showed a variable Al content. The first quartz generation had the highest Al content, ranging from 11,802 to 4,752 ppm. Aluminum concentration of the second generation varied from 3,835 to 1,888 ppm. The third quartz generation had the widest Al variations, ranging from 3,441 to 57 ppm. Aluminum was not detected in the fourth quartz generation (Korzeb and Scarberry, in preparation).

### Sulfur Isotopes

Sulfur isotope analysis was performed on 29 sulfide samples from different veins in the Oro Fino mining district (Korzeb and Scarberry, in preparation). Sulfur isotopic data for 27 pyrite and two chalcopyrite samples are illustrated on a histogram plot shown in figure 4. The sulfur isotope data show a wide variation from -2.7 to 8.5‰, but the highest population varies from 3.6 to 8.5‰. The histogram plot shows two different  $\delta^{34}\text{S}$  populations: one that varies from -3 to 2‰ and another that varies from 3 to 9‰. The population that varies from -3 to 2‰ is from locations that have pyrite associated with schorl and three-phase fluid inclusions with halite daughter minerals. Pyrite and chalcopyrite associated with schorl is brecciated with quartz filling open spaces between breccia fragments. The brecciated sulfides represent an early sulfide phase in the paragenetic sequence and crystallized during or shortly after schorl crystallization. Pyrite and chalcopyrite samples from the rest of the vein locations yielded  $\delta^{34}\text{S}$  values within the 3 to 9‰ population. Sulfide minerals from these locations are later stage than for those of the -3 to 2‰ population and represent main stage vein development.

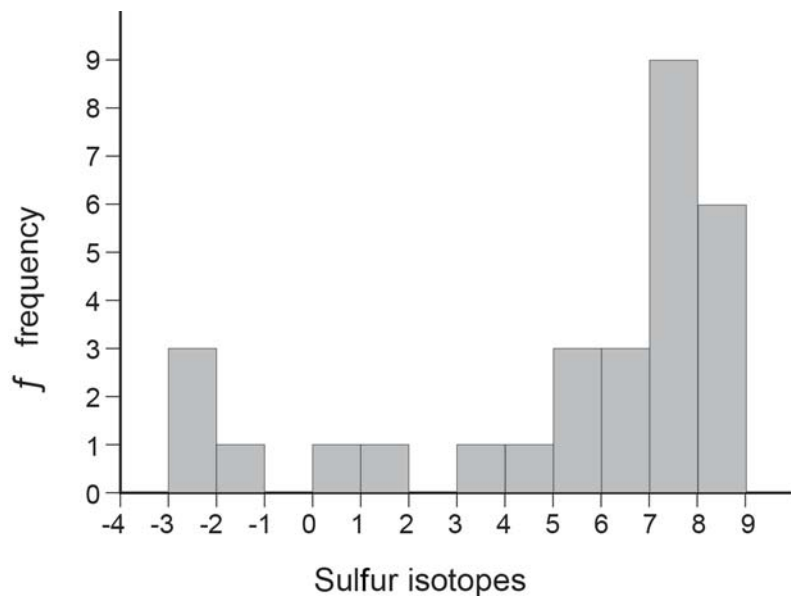


Figure 4. Histogram plots for sulfur isotope values (‰ relative to CDT standard) for pyrite and chalcopyrite.

### Discussion

Fluid inclusion, sulfur isotope, cathodoluminescence, and EMP-analysis data, along with alteration and vein mineralogy, suggest the veins developed from a changing and evolving hydrothermal fluid (Korzeb and Scarberry, in preparation). Fluid inclusion data imply the initial hydrothermal fluids had a high salinity (26.24 to 37.44 wt% NaCl eq) and moderate temperatures (197.1° to 362.7°C). These fluid inclusions are hosted by quartz associated with schorl, pyrite, and minor chalcopyrite, which crystallized near the contacts of the veins with the granite host rock. EMP analysis of early quartz veins revealed a high Al concentration (up to 11,802 ppm), suggesting the quartz crystallized from an Al-saturated aqueous fluid with an acid pH (Rusk and others, 2008). Sulfur isotope data from pyrite and chalcopyrite associated with schorl showed a depletion to minor enrichment in  $\delta^{34}\text{S}$  (-2.7‰ to 1.2‰). Fluids that crystallized schorl had a high boron and aluminum concentration. The high salinity, depletion to minor enrichment of  $\delta^{34}\text{S}$  in associated pyrite and chalcopyrite, and high boron concentration suggest these early hydrothermal fluids had a magmatic origin originating from a cooling pluton that followed Lowland Creek volcanism (Korzeb and Scarberry, in preparation). The initial magmatic-derived hydrothermal fluids evolved into a fluid with lower Al saturation and moderate salinity, and approached a moderately acidic to neutral pH.

Sulfur isotopes show an enrichment in  $\delta^{34}\text{S}$  (3.6‰ to 8.5‰), averaging 6.9‰, suggesting the veins developed from a hydrothermal fluid influenced by crustal contamination. An inferred source for the enrichment in  $\delta^{34}\text{S}$  could be Proterozoic Belt Supergroup formations, which are known to be enriched in heavy isotopic sulfur. Diagenetic pyrite from the Newland Formation has an average  $\delta^{34}\text{S}$  value of 7.6‰ (Lyons and others, 2000), and barite can have a  $\delta^{34}\text{S}$  values ranging from 13.6‰ to 18.3‰ (Strauss and Schieber, 1990). Hydrothermal fluids sourced from the Revett Formation developed the Spar Lake Cu-Ag-Co deposit. Sulfides precipitated from these hydrothermal fluids have  $\delta^{34}\text{S}$  values ranging from 3‰ to 23‰, suggesting the  $\delta^{34}\text{S}$  and metal source was the Revett Formation (Hayes and Einaudi, 1986; Hayes and others, 1989). The Belt Supergroup underlies the Boulder Batholith and Oro Fino mining district (Harrison, 1972), and could have served as a source of heavy isotopic sulfur and metals found in the Oro Fino veins.

The veins exposed on the surface in the Oro Fino district represent the lower section of an epithermal system that formed about 0.8 km below the surface (based on pressure estimates from fluid inclusions; Korzeb and Scarberry, in preparation). The top portion of the veins were removed by erosion developing the gold placer deposits found in drainages and streams throughout the district. Epithermal systems are vertically and laterally zoned reflecting the geochemical and physical conditions of the hydrothermal fluids that crystallized the veins (Simmons and others, 2005).

### Geologic Model

A geologic model for the development of the low to intermediate-sulfidation epithermal veins was derived from sulfur isotope, fluid inclusion, trace element, and geologic data obtained from this investigation (Korzeb and Scarberry, in preparation). The Oro Fino mining district developed during back arc magmatism that erupted the Eocene Lowland Creek volcanic field. Sulfur isotope, trace element, and fluid inclusion data suggest the Oro Fino veins had a magmatic origin and developed during the cooling and release of volatile components from an intrusive body. The presence of schorl in the veins indicates the early mineralizing fluids contained boron, most likely sourced from crustal rocks being assimilated into an intrusive body that generated the mineralizing fluids. The enrichment of  $\delta^{34}\text{S}$  (3.6‰ to 8.5‰) in the veins further suggest the intrusive that generated the mineralizing fluids assimilated crustal rocks or Proterozoic Belt Supergroup formations.

### Conclusion

The Oro Fino mining district veins are hosted by the Butte granite of the Boulder Batholith, and age dating suggests they formed after Eocene Lowland Creek volcanism. The hydrothermal system that developed the veins could have been driven by intrusions following the last volcanic event that developed the Lowland Creek volcanic field. Fractures in the Butte granite provided channel ways for hydrothermal fluids to vent to the surface, thus leading to vein development under shallow low-pressure conditions indicated by the fluid inclusions.

The veins in the Oro Fino mining district have many features found in both epithermal low and intermediate sulfidation systems and can be classified as low to intermediate sulfidation. Alteration associated with the Oro Fino veins is characterized by variable amounts of adularia, sericite, illite, kaolinite, and disseminated pyrite with quartz and chalcedony, which are characteristic of low and intermediate sulfidation veins (Cooke and Simmons, 2000). Silicification of the host granite, and the Al content of quartz veins, indicate periodic acidic conditions during vein development, indicating higher sulfidation levels than low sulfidation systems.

It is inferred that a porphyry deposit served as a fluid source for the Oro Fino epithermal veins. Sillitoe (2010) suggests intermediate sulfidation vein systems can be peripheral or overlie porphyry deposits. Since the Oro Fino veins have features related to both low-and intermediate-sulfidation epithermal veins, they could overlie or are peripheral to a deep-seated porphyry deposit. Deep geophysical surveys within and adjacent to the district will be required to locate potential drill targets underlying or hosted by the Butte granite.

In addition to porphyry system exploration, the veins themselves can be exploration targets. Epithermal veins are known to be highly variable in form, caused by variations in vein permeability and structural controls of the hydrothermal fluids (Hedenquist and others, 2000). Due to the variability of epithermal veins, the past producing mines were developed on silver-gold, base metal bonanza ore shoots with barren sections of quartz



veins between the shoots. It is possible additional ore shoots can occur along strike and at depth in the past producing mines. At depth, below the silver-gold mineralization, a base metal horizon could be present that developed from a retreating boiling front.

### References

- Berg, R.B., 2007, Sapphires in the Butte–Deer Lodge area, Montana: Montana Bureau of Mines and Geology Bulletin 134, 59 p.
- Cooke, D.R., and Simmons, S.F., 2000, Characteristics and genesis of epithermal gold deposits, in Hagemann, S.G., and Brown, P.E., eds.: *Gold in 2000, Reviews in Economic Geology*, v. 13, p. 221–224.
- Dudás, F.O., Ispolatov, V.O., Harlan, S.S., and Snee, L.W., 2010,  $^{40}\text{Ar}/^{39}\text{Ar}$  geochronology and geochemical reconnaissance of the Eocene Lowland Creek volcanic field, west-central Montana: *Journal of Geology*, v. 118, p. 295–304.
- Ewers, G.R., and Keays, R.R., 1977, Volatile and precious metal zoning in the Broadlands geothermal field, New Zealand: *Economic Geology*, v. 72, p. 1337–1354.
- Feely, T.C., 2003, Origin and tectonic implications of across-strike Geochemical variations in the Eocene Absaroka Volcanic Province, United States: *Journal of Geology*, v. 111 p. 329–346.
- Fisher, J.R., 1976, The volumetric properties of H<sub>2</sub>O—A graphical portrayal: *Journal of Research, U.S. Geological Survey* v. 4, no. 2, p. 189–193.
- Hargrave, P.A., 1990, Geology of the Browns Gulch and Flume Gulch area, Deer Lodge, Jefferson and Silver Bow Counties, Montana: Butte, Montana Tech, M.S. thesis, 95 p., scale 1:24,000.
- Hargrave, P.A., and Berg, R.B., 2013, Geologic map of the Lockhart Meadows 7.5' quadrangle, west central Montana: Montana Bureau of Mines and Geology Open-File Report 629, 1 sheet, scale 1:24,000..
- Harrison, J.E., 1972, Precambrian Belt Basin of northwestern United States: Its geometry, sedimentation, and copper occurrences: *Geological Society of America Bulletin*, v. 83, p. 1215–1240.
- Hayes, T.S., and Einaudi, M.T., 1986, Genesis of the Spar Lake strata-bound copper-silver deposit, Montana: Part I: Controls inherited from sedimentation diagenesis: *Economic Geology*, v. 81, p. 1899–1931.
- Hayes, T.S., Rye, R.O., Whelan, J.F., and Landis, G.P., 1989, Geology and sulfur isotope geothermometry of the Spar Lake strata-bound Cu-Ag deposit in the Belt Supergroup, Montana, in Boyle, R.W., Brown, A.C., Jowett, E.C., and Kirkham, R.V., eds.: *Sediment-hosted strata-bound copper deposits*, v. 36, Special Paper, Geological Association of Canada, p. 319–338.
- Hedenquist, J.W., Arribas, R.A., and Gonzalez-Urien, Eliseo, 2000, Exploration for epithermal gold deposits, in Hagemann, S.G., and Brown, P.E., eds.: *Gold on 2000, Reviews in Economic Geology*, Society of Economic Geologists, Inc., v. 13, p. 245–277.
- Korzeb, S.L., and Scarberry, K.C., in preparation, Genesis and exploration potential for Eocene age veins of the Oro Fino mining district, Deer Lodge County, Montana: Montana Bureau of Mines and Geology Bulletin.
- Lang, J.R., Baker, T., Hart, C.J.R., and Mortensen, J.K., 2000, An exploration model for intrusion-related gold systems: *Society of Economic Geologists Newsletter*, no. 40, p. 1, 6–15.
- Lonn, J.D., and Elliott, C., 2010, A walking tour of the Eocene Anaconda detachment fault on Stucky Ridge near Anaconda, Montana: *Northwest Geology*, v. 39, p. 81–90.
- Lund, K., Aleinikoff, J.N., Kunk, M.J., Unruh, D.M., Zeihen, G.D., Hodges, W.C., Du Bray, E.A., and O'Neill, J.M., 2002, SHRIMP U-Pb and  $^{40}\text{Ar}/^{39}\text{Ar}$  age constraints for relating plutonism and mineralization in the Boulder Batholith region, Montana: *Economic Geology*, v. 97, p. 241–267.
- Lyons, T.W., Luepke, J.J., Madeline, E.S., and Zieg, G.A., 2000, Sulfur geochemical constraints on Mesoproterozoic restricted marine deposition: Lower Belt Supergroup, northwestern United States: *Geochimica et Cosmochimica Acta* v. 64, p. 427–437.

- Mahoney, J.B., Pignotta, G.S., Ihinger, P.D., Wittkop, C., Balgord, E.A., Potter, J.J., and Leistikow, A., 2015, Geologic relationships in the northern Helena salient, Montana: *Geology of the Elliston region: Northwest Geology*, v. 44, p. 109–135.
- Moncada, D., Mutchler, S., Nieto, A., Reynolds, T.J., Rimstidt, J.D., and Bodnar, R.J., 2012, Mineral textures and fluid inclusion petrography of the epithermal Ag-Au deposits at Guanajuato, Mexico: Application to exploration: *Journal of Geochemical Exploration*, v. 114, p. 20–35.
- Mosier, D.L., Sato, T., Page, N.J., Singer, D.A., and Berger, B.R., 1987, Descriptive model of Creede epithermal veins, in Cox, D.P. and Singer, D.A., eds.: *Mineral deposit models: U.S. Geological Survey Bulletin 1693*, p. 145–149.
- Mosolf, J.G., 2015, Geologic field guide to the Tertiary volcanic rocks in the Elliston 30' X 60' quadrangle, west-central Montana, in Mosolf, J.G. and McDonald, C., eds.: *Northwest Geology, 40th annual field conference, Geology of the Elliston area, Montana and other papers, Tobacco Root Geological Society, Inc.* v. 44, p. 213–231.
- Pardee, J.T., and Schrader, F.C., 1933, Metalliferous deposits of the greater Helena mining region, Montana: *U.S. Geological Survey Bulletin 842*, 318 p.
- Portner, R.A., Hendrix, M.S., Stalker, J.C., Miggins, D.P., and Sheriff, S.D., 2011, Sedimentary response to orogenic exhumation in the Northern Rocky Mountain Basin and Range province, Flint Creek basin, west-central Montana: *Canadian Journal of Earth Sciences*, v. 48, p. 1131–1153.
- Roedder, Edwin., 1984, Fluid inclusions: *Mineralogical Society of America, Reviews in Mineralogy*, v. 12, 646 p.
- Rusk, B.G., Lowers, H.A., and Reed, M.H., 2008, Trace elements in hydrothermal quartz: Relationships to cathodoluminescent textures and insights into vein formation: *Geology*, v. 36, p. 547–550.
- Rutland, C., Smedes, H., Tilling, R., and Greenwood, W., 1989, Volcanism and plutonism at shallow crustal levels: The Elkhorn Mountains Volcanics and the Boulder Batholith, southwestern Montana, in Henshaw, P., ed.: *Volcanism and plutonism of western North America; v. 2, Cordilleran volcanism, plutonism, and magma generation at various crustal levels, Montana and Idaho, Field trips for the 28th International Geological Congress: American Geophysical Union Monograph*, p. 16–31.
- Scarberry, K.C., Korzeb, S.L., and Smith, M.G., 2015, Origin of Eocene volcanic rocks at the south end of the Deer Lodge Valley, Montana, in Mosolf, J., and McDonald, C., eds.: *40th annual field conference Geology of the Elliston area, Montana and other papers, Northwest Geology*, v. 44, p. 201–212.
- Silberman, M.L., and Berger, B.R., 1985, Relationship of trace-element patterns to alteration and morphology in epithermal precious-metal deposits, in Berger, B.R. and Bethke, P.M., eds.: *Geology and geochemistry of epithermal systems, Reviews in Economic Geology*, v. 2, p. 203–232.
- Sillitoe, R.H., Graubeger, G.L., and Elliott, J.E., 1985, A diatreme-hosted gold deposit at Montana Tunnels, Montana: *Economic Geology* v. 80, p. 1707–1721.
- Sillitoe, R.H., 2010, Porphyry copper systems: *Economic Geology*, v. 105, p. 3–41.
- Simmons, S.F., Brown, K.F., and Tutolo, B.M., 2016, Hydrothermal transport of Ag, Au, Cu, Pb, Te, Zn, and other metals and metalloids in New Zealand geothermal systems: Spatial patterns, fluid-mineral equilibria, and implications for epithermal mineralization: *Economic Geology*, v. 111, p. 589–618.
- Simmons, S.F., and Browne, P.R.L., 2000, Hydrothermal minerals and precious metals in the Broadlands-Ohaaki geothermal system: Implications for understanding low-sulfidation epithermal environments: *Economic Geology*, v. 95, p. 971–999.
- Simmons, S.F., White, N.C., and John, D.A., 2005, Geologic characteristics of epithermal precious and base metal deposits, in Hedenquist, J.W., Thompson, J.F.H., Goldfarb, R.J., and Richards, J.P., eds.: *Economic Geology One Hundredth Anniversary Volume: Society of Economic Geologists*, p. 485–522.



Strauss, H., and Schieber, J., 1990, A sulfur isotope study of pyrite genesis: The mid-Proterozoic Newland Formation, Belt Supergroup, Montana: *Geochimica et Cosmochimica Acta*, v. 54, p. 197–204.

Weissberg, B.G., 1969, Gold-silver ore grade precipitates from New Zealand thermal waters: *Economic Geology*, v.64, p. 95–108.

Williams, H.G., 1951, Geology and ore deposits of an area east of Warm Springs, Montana: Butte, Montana Tech, M.S. thesis, 64 p.



Descloizite from the Summit Mine; Radersburg, MT. Courtesy of Michael J. Gobl.

# Black Butte Copper: A High-Grade Underground Movable Copper Deposit in Meagher County, Montana

Eric LeLacheur and G.A. Zieg

*Sandfire Resources America, White Sulphur Springs, Montana*

The Black Butte Project is a high-grade sediment-hosted copper deposit. The project is in west central Montana, about 17 miles (27 km) north of White Sulphur Springs, Montana, on the south flank of the Little Belt Mountains.

The deposit formed on the north margin of the Helena Embayment, a Mesoproterozoic E–W-oriented basin that formed as an east extension of the generally N–S-oriented Belt Basin (fig. 1). The Helena Embayment contains significantly more carbonate rocks than the main part of the basin and was likely somewhat hydrologically restricted from the main basin (Godlewski and Zieg, 1984).

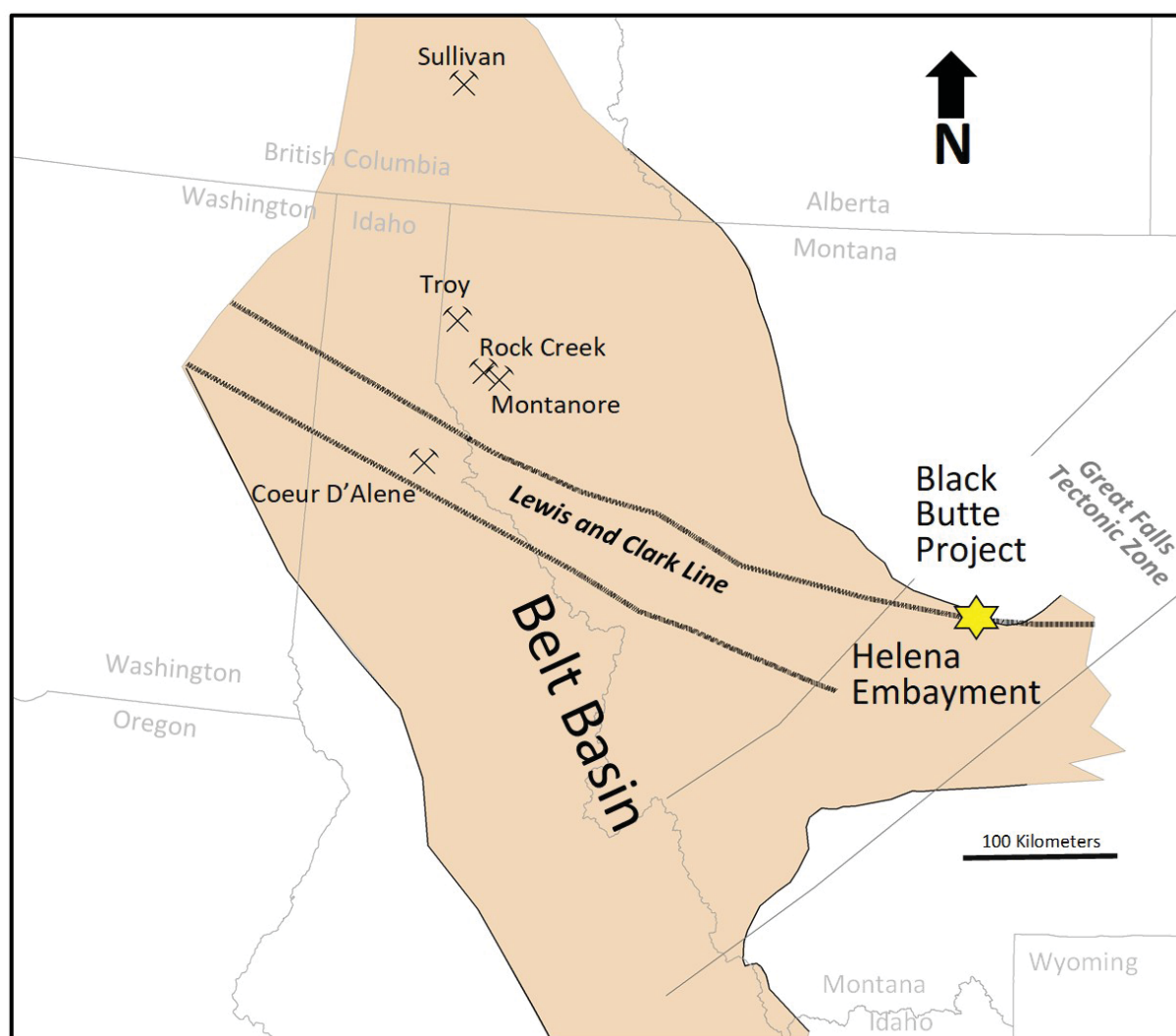


Figure 1. Outcrop area of the Belt Supergroup with Belt age sediment hosted deposits located (Sandfire Resources, 2019).

During the deposition of silty shales, dolomitic shales, and interspersed carbonate beds of the Lower Newland Formation, hydrothermal hot springs utilized basin-bounding faults near the basin's northern margin and deposited large volumes of sulfide, largely pyrite, on the sea floor. Shortly after burial, copper sulfides, mainly chalcopyrite, but also minor tennantite, chalcocite, and bornite, replaced parts of the pyrite beds (fig. 2). The hydrothermal activity also introduced cobalt, lead, zinc, silver, and gold into basin muds. Syn-depositional sulfides occur in a sedimentary column over a kilometer thick, indicating a very long-lived hydrothermal system.





Figure 2. Drill core illustrating pyrite largely replaced by chalcopyrite from the Johnny Lee Lower zone.

The general east–west compression of the Laramide orogeny reactivated and inverted many of the Proterozoic faults in the western U.S. (Marshak and others, 2000), and at Black Butte resulted in NE-directed thrusting along the north margin of the Helena embayment, displacing Proterozoic basin sedimentary rocks up along the Proterozoic basin margin (figs. 3, 4).

Modern exploration for sedimentary metal deposits began in the early 1970s with several operators acquiring and drilling prospects, including Anaconda, Exxon, Homestake, Kennecott, Utah International, and Cominco. The deposit was discovered by a Cominco American Inc.– Utah International Inc. joint venture in 1985. In 2010, Tintina Resources Inc. leased the mineral rights containing the Johnny Lee and Lowry deposits and began drilling with the intention of establishing a resource for mine planning. Drilling has continued into 2019 when the company, now doing business as Sandfire Resources America, Inc., completed a 23-hole program to provide resource, geotechnical, and metallurgical data to support a feasibility study.

The current resource, updated October 25, 2019, is shown in table 1.

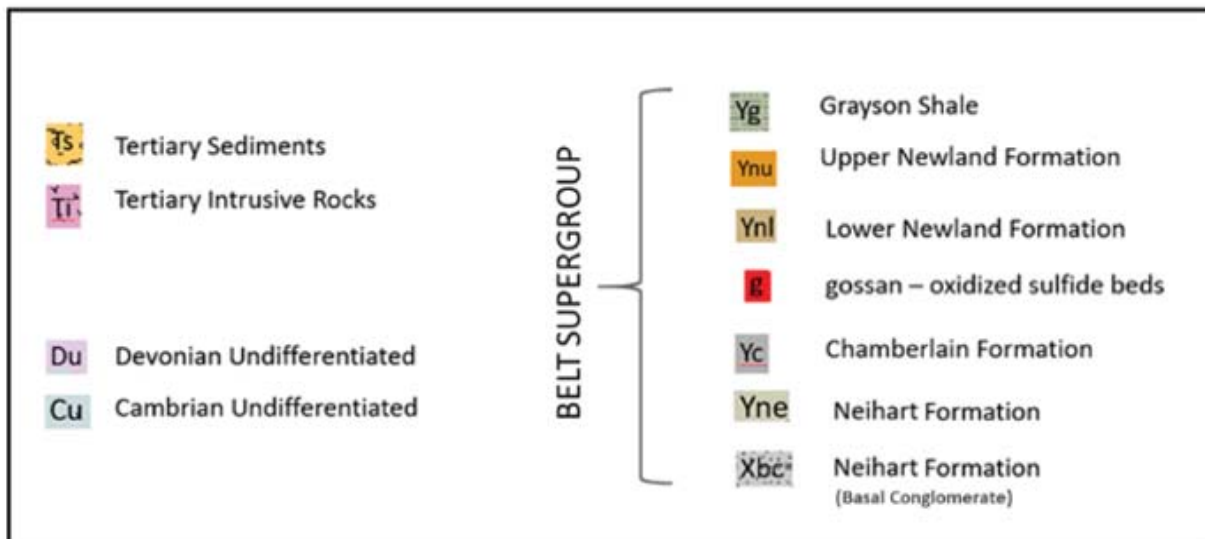
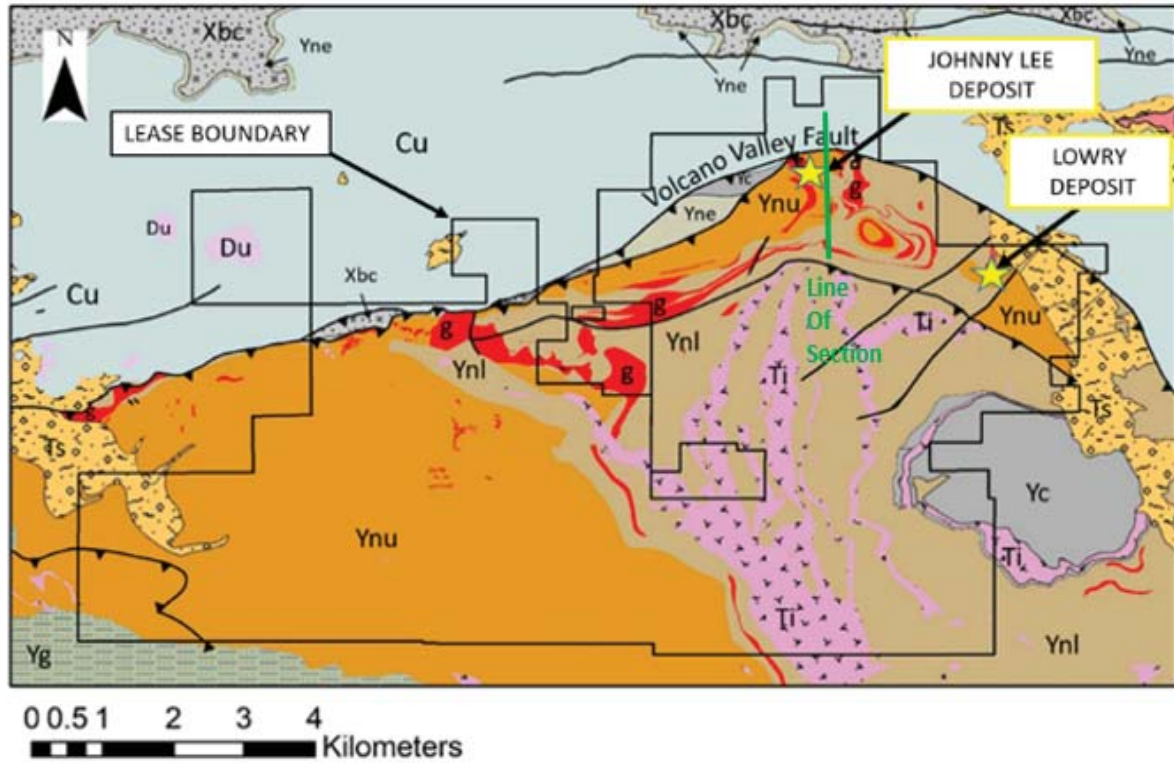


Figure 3. Generalized geologic map of the Black Butte Project area. From Ronald and Malhotra (2019).



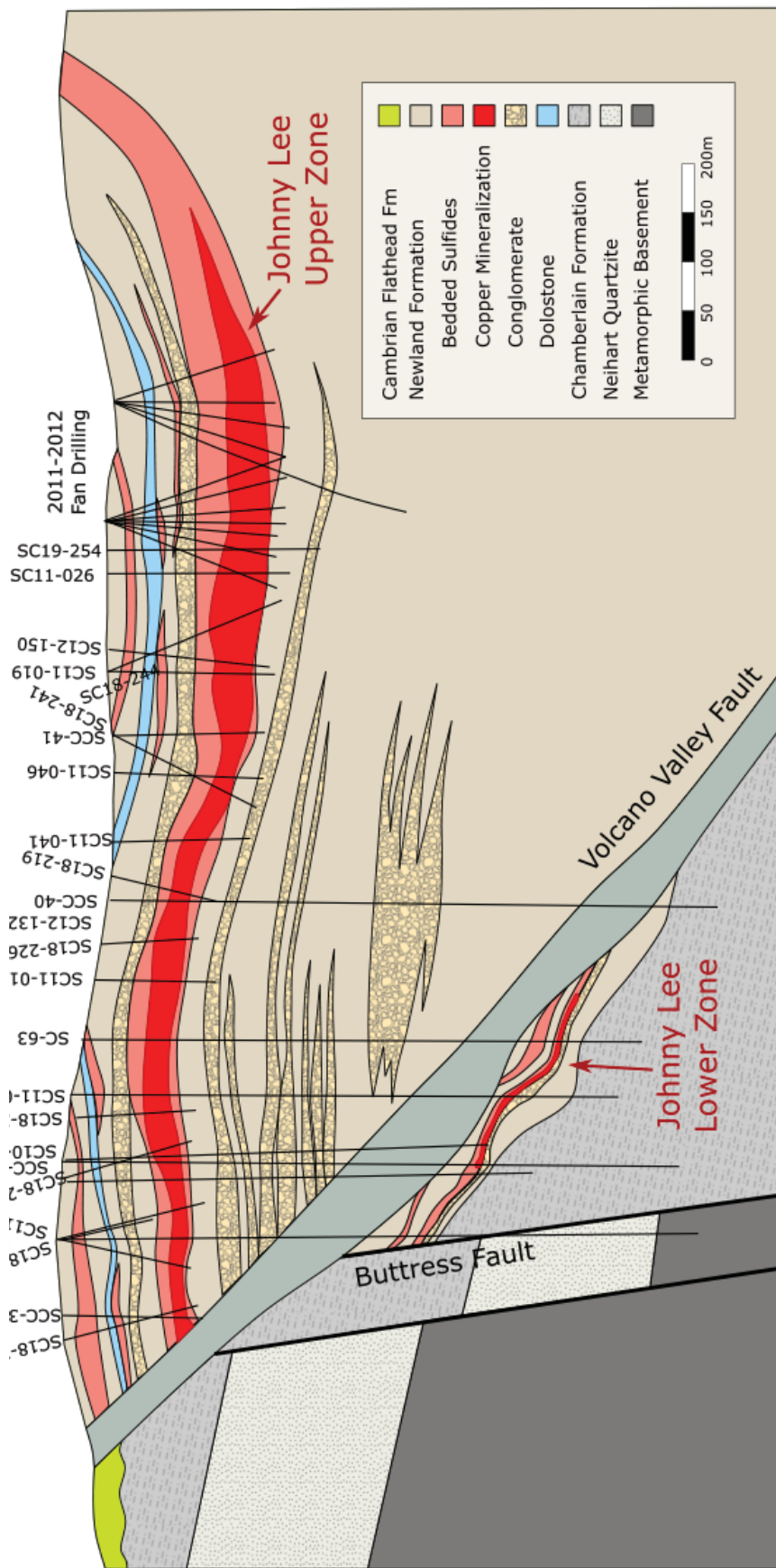


Figure 4. Cross section through the Johnny Lee deposit. View to the east (Sandfire Resources America, unpublished, 2019).



Table 1. Black Butte Copper Project mineral resource estimate for the Johnny Lee deposit as of October 15, 2019 (from Ronald and Malhotra, 2019).

| Johnny Lee Upper Copper Zone              |                   |      |                  |
|---|-------------------|------|------------------|
| Category                                  | Tonnes (millions) | Cu%  | Total Metal (MT) |
| Measured                                  | 1.4               | 2.6% | 36.2             |
| Indicated                                 | 8.3               | 2.3% | 191.3            |
| Measured and Indicated                    | 9.7               | 2.4% | 227.5            |
| Inferred                                  | 2.2               | 2.2% | 49.5             |
| Johnny Lee Lower Zone                     |                   |      |                  |
| Category                                  | Tonnes (millions) | Cu%  | Total Metal (MT) |
| Measured                                  | 0.6               | 5.7% | 32.9             |
| Indicated                                 | 0.6               | 7.9% | 50.5             |
| Measured and Indicated                    | 1.2               | 6.8% | 83.4             |
| Inferred                                  | 0.5               | 6.3% | 30.3             |
| Combined Johnny Lee Upper and Lower Zones |                   |      |                  |
| Category                                  | Tonnes (millions) | Cu%  | Total Metal (MT) |
| Measured                                  | 2.0               | 3.5% | 69.1             |
| Indicated                                 | 8.9               | 2.7% | 241.8            |
| Measured and Indicated                    | 10.9              | 2.9% | 310.9            |
| Inferred                                  | 2.7               | 3.0% | 79.7             |

*Note.* The effective date for this Mineral Resource is October 15, 2019. All significant figures are rounded to reflect the relative accuracy of the estimates. Copper assay values were capped where appropriate.

- Mineral Resources are not Mineral Reserves and do not have demonstrated economic viability. Inferred Mineral Resources have a high degree of uncertainty as to their economic and technical feasibility. It cannot be assumed that all or any part of an Inferred Mineral Resource can be upgraded to Measured or Indicated Mineral Resource;
- Metallurgical recovery of copper has been estimated on a block basis in the Upper Copper Zone, averaging 77.4%, with a consistent 94.0% Cu recovery applied to the Lower Copper Zone;
- To demonstrate reasonable prospects for eventual economic extraction of Mineral Resources, a cut-off grade of 1.00% copper based on metal recoverability assumptions, long-term copper price assumptions of \$3.20/lb, mining costs, processing costs, General & Administrative costs totaling \$71/t;
- There are no known legal, political, environmental, or other risks that could materially affect the potential development of the Mineral Resources other than those outlined in the Management Discussion and Analyses of the June 2019 Company Quarterly Report. All Mineral Resources are located within land currently under control or lease to Sandfire Resources America Inc.

Sandfire America is planning to mine underground with a cut-and-fill style operation at Black Butte. The anticipated mining rate of 3,300 metric tons per day will produce about 400 metric tons of copper concentrate per day. Surface disturbance will be about 311 acres and will include a portal pad, a surface tailing storage facility, a process plant facility, and various road and water storage ponds. All surface disturbance will be reclaimed to livestock pasture at the end of mining.

Mining is designed to minimize environmental impacts by: (1) Placing surface activities on private lands, away from surface waters, (2) About 45% of the mill tailings will be returned underground as paste backfill, to backfill the ore openings underground, (3) Remaining tailings will be placed as a cemented paste into a double-lined surface impoundment, and (4) water encountered on site will be treated using reverse osmosis and be returned to the groundwater via infiltration. There will be no surface discharge, and no water treatment at the end of mining (fig. 5).

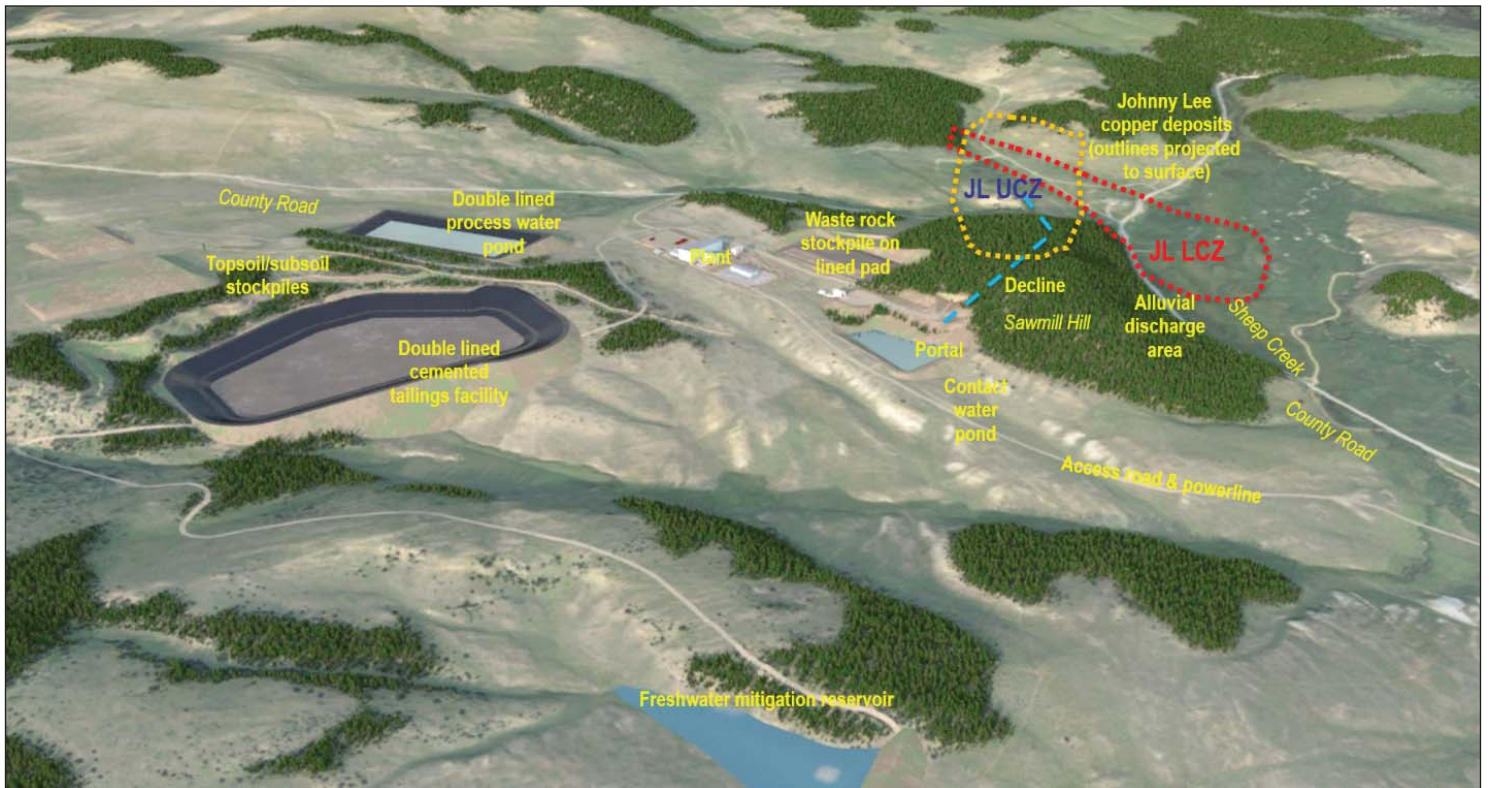


Figure 5. Site layout as proposed in the Black Butte Mine Operating Plan (from Sandfire America Resources, 2019).

The operating permit application was submitted in December 2015, and was deemed complete and compliant in August 2017. An Environmental Impact Study (EIS) has been in preparation since then, with the draft EIS published in March 2019. Publication of the final EIS and a Record of Decision (ROD) is expected soon. A Feasibility Study is also expected to be completed shortly after the ROD is released.

### References

- Godlewski, D.W., and Zieg, G.A., 1984, Stratigraphy and depositional setting of the Precambrian Newland Limestone, in Hobbs, S.W., ed., *The Belt: Abstracts with summaries*, Belt Symposium II, 1983: Montana Bureau of Mines and Geology Special Publication 90, p. 2–4.
- Marshak, S., Karlstrom, K., and Timmons, J.M., 2000, Inversion of Proterozoic extensional faults: An explanation for the pattern of Laramide and Ancestral Rockies intracratonic deformation, *United States: Geology*, v. 28, p. 735–738.
- Ronald, E., and Malhotra, D., 2019, NI 43-101 Technical report on mineral resources, Black Butte Copper Project in White Sulphur Springs, Montana, USA, report to Sandfire Resources America, Inc., SRK Consulting, Denver, 240 p.

# Supporting the Transition to Deep Porphyry Copper Exploration: SHRIMP U/Pb Radiometric Dating of Titanite (CaTiSiO<sub>6</sub>) in the Distal and Superjacent Orbicular Alteration Zone of the Clementine Prospect, Southwest Montana

George Brimhall<sup>1</sup> and Mark Fanning<sup>2</sup>

<sup>1</sup>*Clementine Exploration, Wise River, Montana*

<sup>2</sup>*Arise Geosciences Pty Ltd, Australian National University, Canberra ACT, Australia*

## Abstract

The projected increase in world requirements for copper, even considering recycling, will require mining more copper over the next three decades than was mined in all prior human history. Since there are no good substitutes for copper's ubiquitous electrical uses, the failure over the past decade to discover more than a few new shallow porphyry copper deposits (PCD) and some near-mine, brownfields discoveries, a pressing need exists for a decisive change in how the search for new deeper orebodies is designed and prospects are scientifically evaluated. This is a daunting challenge as many ore bodies with their tops located 1 km or more below surface are unlikely to exhibit the traditional signs on the surface that have guided past exploration, which applied the extant porphyry copper genetic paradigm. The intent of this work on orbicular alteration is revising the distal and upper reaches of the geo-spatial patterns of the PCD paradigm and providing new field methods that help support the transition to deep PCD exploration. First, exploring through the tops of prospective new deep porphyry copper deposits means confronting the realities of a largely unfamiliar geological domain above the current tops of the porphyry copper paradigms, based on mined ore deposits whose surface exposures intersected the surface within ore grade levels. Deeper targets are different in that their tops are 500 to 1,000 m above ore grade levels. This report describes our efforts on the Clementine prospect to extend the porphyry copper paradigm upwards to include the tops of potential deep orebodies, where their distal wall rock alteration is likely to be encountered first in exploration as the outermost ring of concentric features. We describe low-grade disseminated chalcopyrite zones within orbicular alteration zones representing a cupola at the upper and outer edge of hydro-fractured stockworks where advective flow slowed and spherical actinolite-calcite-titanite orbs formed by diffusion under low chemical Peclet Number conditions. Orb alteration makes this subtle physical boundary feature macroscopically visible and contributes a powerful new mapping tool in lithologies where orbs are likely to form as in sedimentary and other wall rocks with connected pore space, allowing intergranular diffusion, rather than in non-porous rocks with interlocking grains. Nevertheless, we have observed and mapped orbs in gabbro sills. In comparison to strongly advective flow vein systems with planar, vein-parallel wall rock alteration zones like Mainstage Butte veins, distal orb growth involved alteration fronts that are functionally wrapped into 1- to 3-cm-diameter spheres at crack tips forming nested semi-spherical reaction fronts that slowly migrated outwards, with inner reaction fronts replacing outer fronts. In order to determine the age of the hydrothermal titanite, we used *in situ* ion probe methods in which single grains offer multiple independent analysis spots. Using the Tera-Wasserburg plotting method, we determined a U/Pb SHRIMP date of hydrothermal titanite of 70.7 million years, which is similar to the plutonic age range of the Boulder and Pioneer Batholiths, thus eliminating concern that orbs are merely a strange regional metamorphic effect. Similarly, this new age date supports the hydrothermal origin of the orbs that alter many different rock formations and are axially-symmetrically aligned with respect to vein gossans, breccias, and felsic plutons at the center of the zoning pattern. Furthermore, the normality of orbicular alteration within the PCD model is further established by describing the close geochemical conditions of the titanite-ilmenite-chalcopyrite assemblage with potassic biotite-bearing alteration and early high-temperature mineralization. Orb mapping and radiometric dating of titanite can assist in targeting large, deep porphyry copper deposits during early exploration through properly interpreting the orbicular zonation surrounding the typical alteration halo around large intrusive systems as the exterior of the system's fracture pattern, thus providing a bullseye to focus follow up exploration. Our approach offers new unequivocal



geological evidence that may prove more trustworthy in discerning the large, deep chalcopyrite-bornite PCD targets than amassing a host of conventional geochemical data on late vein systems that can be offset from the early stage mineralization.

## Introduction

Axially symmetric vein gossans, breccias, and felsic plutons surrounded by distal actinolite-calcite-titanite-filled orbicular alteration with disseminated pyrrhotite, chalcopyrite, and ilmenite between orbs were described by Brimhall at the Clementine prospect of southwest Montana (Brimhall, 2018). The Clementine system was interpreted as the top of a possible deep porphyry copper deposit (PCD) emplaced with clear regional structural control near the axial crest of a doubly plunging anticline (fig. 1), confined by the overlying Grasshopper thrust plate. Brimhall (2018) interpreted the orbs in plan and cross section as describing a cupola formed at the outer and upper edge of hydro-fractured stockworks. Here, the advective flow rate slowed considerably at the fringes of the magmatically heated convective system such that spherical hydrothermal orbs formed by in situ diffusion from the outermost and uppermost crack tips or crack intersections as aqueous ions migrated over short distances after arriving at this distal position by convective fluid flow. Using the chemical Peclet number, which describes the relative importance of advective transport and diffusion in a continuum, Brimhall (2018) showed that the orb zones define the advective/diffusive boundary of a large hydrothermal system 2 by 6 km centered on the vein gossans, breccias, and felsic plutons. The utility of orb cupolas as a targeting tool in PCD exploration then stems from the assertion that orbicular zones mark the position of a key hydrodynamic boundary: the peripheral edge of the mineralized fracture permeability network at the time of coupled wall rock alteration and copper mineralization, since disseminated chalcopyrite occurs in the rock matrix between the orbs. Orb alteration makes this subtle physical boundary feature macroscopically visible and contributes a powerful new mapping tool in lithologies where orbs are likely to form in sedimentary and other rocks with connected pore space, allowing intergranular diffusion, rather than in non-porous rocks with interlocking grains. The orbicular alteration described in Brimhall (2018) was viewed as an innovation that can assist targeting large, deep porphyry copper deposits during early exploration through properly interpreting the orbicular zonation surrounding the typical alteration halo around these large intrusive systems as the exterior of the system's fracture pattern, providing a bullseye to focus follow-up exploration (Shaffer, 2019). Similarly, since it has now been shown at the Clementine prospect that springs today occur near the orb bands (fig. 1), it is inferred that the gross permeability of the hornfels altered rocks inside the orb cupola is lower than those outside the cupola in unaltered formations. Hence, the spatial association of springs with orb bands provide another exploration tool of using mapped springs from U.S. Geological Survey topographic maps to: (1) help find and map orbicular alteration and associated disseminated sulfide mineralization in new districts, and (2) infer on a potential district scale, the position, size, and orientation of a new prospective region of interest.

The Clementine zonation pattern is the first complete geologically mapped orbicular actinolite alteration cupola since such alteration was first described in logged diamond drill core from the contact metamorphic aureole at Carr Fork, Bingham, Utah (Atkinson and Einaudi, 1978) over 40 years ago. Since their insightful descriptions of orbs, orbs have been described, though not mapped, at three deposits in Chile: Caspiche, La Escondida, and El Hueso (Sillitoe and others, 2013); Cajamarca in Peru; Morenci and Fortitude Copper Canyon in the U.S.; Cananea in Mexico; and Oyu Tolgoi in Mongolia (Marco Einaudi, written commun., 2019). During the past four decades, opportunities to discover shallow porphyry copper orebodies have diminished significantly throughout much of the world (Wood, 2016), as reflected in the falling discovery rate of major orebodies from the early 1970s onward, while expenditures have continued to rise (Schodde, 2013). Sillitoe and others (2016) summarized the current discovery climate using traditional methods and the application of the Sillitoe (2010) porphyry copper deposit model: "in the past decade, deep exploration for porphyry copper deposits completely concealed beneath extensive lithocaps has become increasingly common as near-surface mineralization becomes scarcer, but with rare exceptions there have been few successes." Wood and Hedenquist (2019) go further in stating that overall, "exploration efforts since 2010 have been wealth destructive." Consequently, a compelling need exists to embrace deep exploration (Schodde, 2013) rather than continuing a traditional surface to near-surface target approach searching for exposed ore bodies. However, deeper ore bodies with their tops located 500 to 1,000

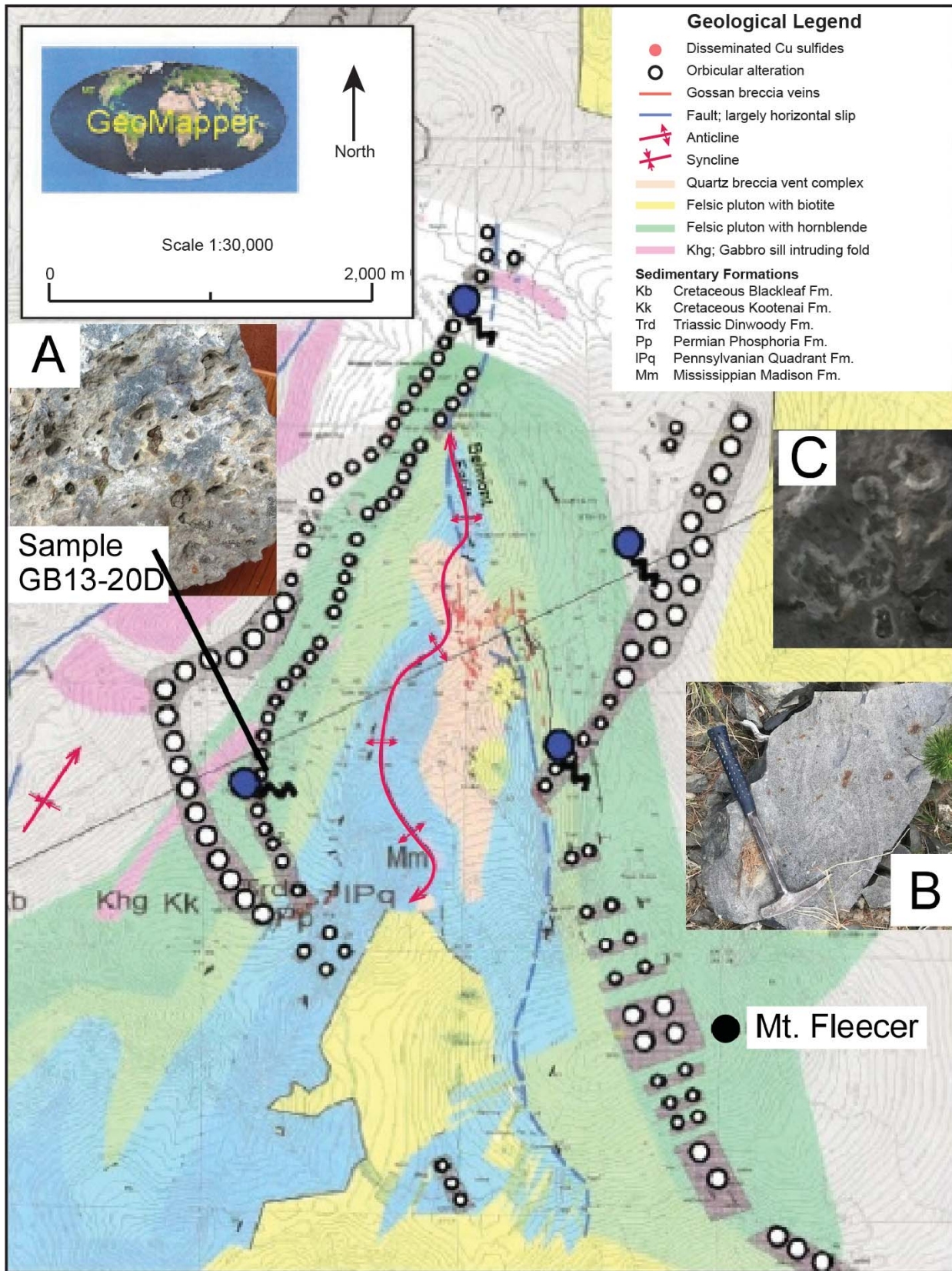


Figure 1. Bedrock geological plan map of Clementine (Brimhall, 2018). Formation abbreviations are: Mm (Mississippian Madison), IPq (Pennsylvanian Quadrant), Trd (Triassic Dinwoody), Kk (Cretaceous Kootenai), Khg (hornblende gabbro sills), and Kb (Cretaceous Blackleaf). Four groundwater-derived springs are shown with blue circles. (A) The orbicular alteration sampled for analysis in this study (sample GB13-20D). Mapping this alteration zone is possible largely due to four factors: (1) the surficial chemical weathering of the orbs where minerals are leached out, leaving vacuous cavities etched on exposed rock surfaces that are readily recognized while mapping; (2) the silicified nature of the alteration makes these rocks outcrop even under dense tree canopy; (3) the fact that disseminated pyrrhotite and ilmenite with ferrous iron oxidize and leave a rust-like ferric oxide surface coating (B); and (4) the orbs are often surrounded by white rings where biotite in the surrounding hornfels has been removed during orb growth diffusion (C).



m or more below surface are unlikely to exhibit the obvious signs on the surface which for decades was based on comparing new prospect mapping with models published by Lowell and Guilbert (1970) and Gustafson and Hunt (1975) on outcropping ore bodies exposed at their midsection levels, not their tops nor upper edges relevant now to deep exploration (John and others, 2010). In contrast, the orbicular cupola discovered and mapped at Clementine may prove useful in helping to fill in the nature and architecture of the vertical gap between the top of current porphyry copper paradigm (Sillitoe, 2010) and the superjacent region that is now the prime prospective region: the tops of deep porphyry copper deposits thus rendering this frontier less prone to misinterpretation and misallocation of exploration resources. The focus here is on helping to illuminate the unfamiliar superjacent zone through fieldwork and laboratory analysis. The work described here seeks to further demonstrate that orbicular alteration is indeed an integral part of porphyry copper alteration and not a mere petrological rarity, nor are orbs a strange metamorphic effect entirely unrelated to mineralization processes. Similarly, it is vital to not confuse actinolite-calcite-titanite orbs with orbicular granites, as the processes of formation are fundamentally different: fracture and diffusion-controlled hydrothermal alteration in contrast to solidification of magma.

With the regional geological patterns now described (fig. 1) proving the epigenetic hydrothermal origin of the orbs that crosscut and alter many different rock formations (Blackleaf, Kootenai, Dinwoody, Phosphoria, Quadrant, and gabbroic sills) and are axially-symmetrically aligned with respect to vein gossans, breccias, and felsic plutons, the goal here is to provide unequivocal answers to a key question at the pre-pilot drilling phase of exploration, specifically: What is the age of the orbicular actinolite-calcite-titanite alteration-disseminated chalcopyrite mineralization? Since junior exploration companies are expected to account for about 70 percent of porphyry copper discoveries over the next few decades (Schaffer, 2018) and the high cost of deep pilot hole drilling usually requires co-investment by larger mining companies, establishing the age of the mapped orb zones may help further understanding of the superjacent zone and perhaps motivate partnerships with major corporations. Towards that end, we intend that by radiometrically dating the orbs, we can demonstrate that orbicular alteration is in fact clearly related to axially-symmetric vein gossans, breccias, and felsic plutons surrounded by distal actinolite-calcite-titanite-filled orbicular alteration and can thus enhance the efficacy of the porphyry-copper paradigm used in exploration. Ideally, an orb ring would appear circular in plan view like a bullseye target. However, with the strong structural anticlinal control at Clementine, the bullseye is flattened into an ellipse.

### **Regional Geological Context**

The Clementine prospect is shown in figure 2A in relation to well-known regional structures of the western U.S. comprising the ancient southwest Laurentia continent and major ore deposits including Butte, Bingham, Tintic, Henderson, and Questa (Pettke and others, 2010). Within the regional context that is believed to have influenced its formation and geochemical character, the Clementine prospect may represent the top of a new deep porphyry copper deposit situated at the intersection of the Great Falls and the Farmington tectonic zones, which are Proterozoic accretionary tectonic suture zones formed where early Proterozoic subduction zones and ancient oceans closed as the continental fragments coalesced and Laurentia (North America) was assembled. The Great Falls tectonic zone then originated at a convergent margin that developed during the closure of an ocean basin along the northwestern margin of the Wyoming craton ca. 1.9 Ga (Mueller and others, 2002). Today, much of the evidence of these ancient rocks is buried beneath Phanerozoic cover.

Clementine also occurs within the frontal fold of the Sevier Fold and Thrust Belt (fig. 2B) along the crest of a doubly plunging regional anticline that also contains the older mining districts and ore deposits at Quartz Hill, Cannivan Gulch, Hecla, and Argenta (fig. 2C). Along this north-south-trending anticlinorium, Clementine, Quartz Hill, and Hecla occur at doubly plunging anticlines or domes, revealing a clear local structural control in addition to the large-scale structures along which the parental magmas came up from depth.

A vertical cross section through Clementine is shown in figure 3. Our interpretation asserts that in southwestern Montana similar thrust sheet anticlines were the loci of magma ascent (Kalakay and others, 2001), mineralization, and alteration processes in syncompressional environments at the top of frontal thrust ramps



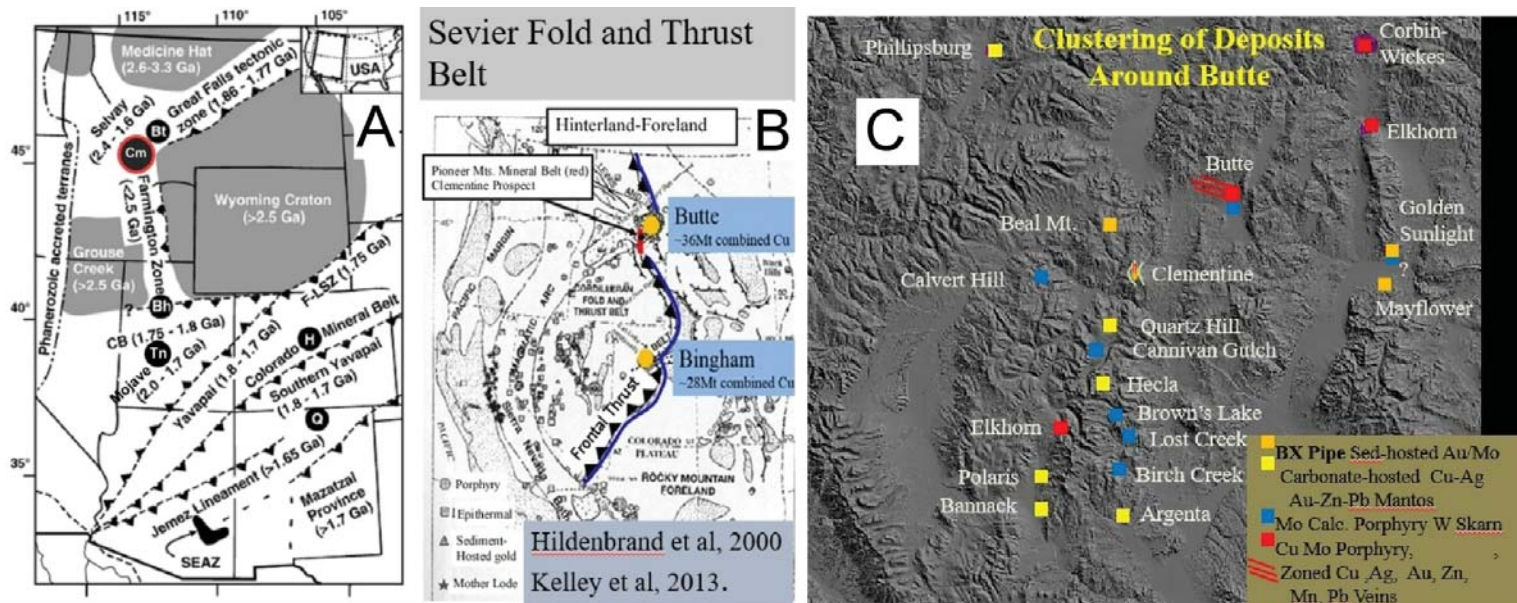


Figure 2. (A) Sketch of SW Laurentia (W USA) identifying major crustal segments (modified from Karlstrom and others, 2004; Foster and others, 2006). Archean crustal blocks (gray) are delimited by Proterozoic accretionary tectonic zones. Segments to the south of the Cheyenne Belt (CB) are terranes accreted during assembly of Laurentia, and sutures represent early Proterozoic subduction zones. The dash-dotted line separates terranes accreted to the Laurentian crustal block in the Phanerozoic. Filled black circles denote Clementine (Cm), Bingham (Bh), situated on the Uinta Axis, Butte (Bt), Henderson (H) in the Colorado Mineral Belt, Questa (Q) on the eastern rim of the Cenozoic Rio Grande Rift (omitted for clarity), and the northern SE Arizona (SEAZ) ore district. F-L SZ refers to the Farewell Mt.–Lester Mt. Suture Zone. (B) The relationship between the Cordilleran foreland thrust belt and the Clementine prospect, after Hildenbrand et al, 2000, and Brimhall (2017). (C) Clustering of ore deposits around the Butte district.

where “releasing steps” at ramp tops served as initial points of emplacement, subsequent pluton growth, and exceptional levels of chemical differentiation within underlying laccoliths (Brimhall and Marsh, 2017). Besides facilitating magma ascent, these localized lower pressure zones may also provide a mechanism inducing magmatic water saturation, driving magmatic-hydrothermal mineralization, and thus explaining the ubiquitous mineralization and alteration of many of the plutons in the Butte–Pioneer Mineral Belt (Brimhall and Marsh, 2017).

### Analytical Methods

A large fresh rock sample (GB13-20D) of a well-exposed actinolite-calcite-titanite orbicular zone shown on the west side of the orb cupola (figs. 1, 3) was broken into pieces as free of surficial oxidation effects as possible. The freshest of these pieces were sawn into parallel slabs 1 cm thick using a Barranca Diamond BD-10 diamond saw cooled by water-soluble synthetic cutting fluid as lubricant so as to retain most of the mineral filling contained in the intact orbs. A polished thin section blank was cut to size and sent to Wagner Petrographic, where the final 30- $\mu\text{m}$ -thick polished thin section slide was prepared (fig. 4). At the Australian National University the polished thin section was cut into small millimeter-scale pieces containing titanite grains and set in epoxy mounts for Sensitive High Resolution Ion MicroProbe (SHRIMP) analysis, which is a play on words as the SHRIMP analysis instrumentation is unusually large (Froude and others, 1983; Williams, 1997). The size is necessary in order have the high sensitivity and resolution capacity to analyze individual mineral grains with many distinct in situ spots so as to acquire statistics necessary to offer an accurate radiometric U/Pb age date and where possible explore the range of common lead isotopes as well.

Typically titanite ( $\text{CaTiSiO}_5$ ) is known as a common accessory mineral in felsic granitoid rocks. However, thin section petrography of the orbicular alteration at Clementine revealed that titanite appeared to be a mineral phase formed by hydrothermal alteration, not igneous processes. As such, titanite, which contains  $\text{U}^{4+}$  substituting for  $\text{Ti}^{4+}$ , affords an opportunity to ascertain the radiometric age of titanite and hence the age of hydrothermal formation of the orb cupola. We can also infer the likely age of the associated chalcopyrite and perhaps much of the hydrothermal and magmatic processes inside of the cupola, including veins, breccias, and felsic plutons to a first approximation.

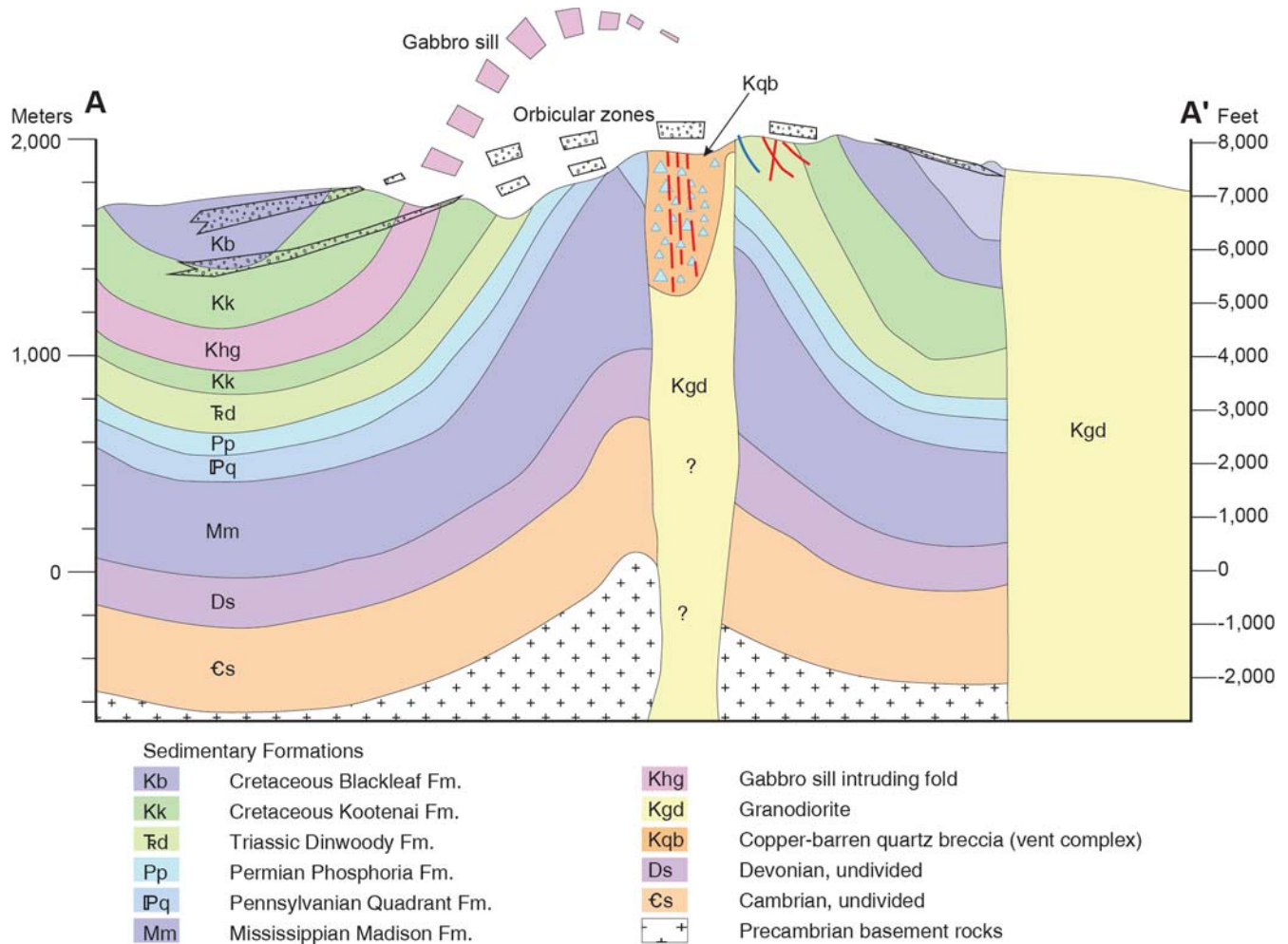


Figure 3. Interpretive vertical geological cross section of Clementine based entirely upon: (1) surface digital geological mapping and (2) approximate formation thickness. Notice the gentle outward dips of the orbicular zones and their upward closure near the present surface. The apparent dips shown here are based on the "V" patterns where mapped orbs cross steep canyons. Also, notice that the copper-barren breccia, with quartzite fragments occurring along the axial plane of the anticline, plots in the vertical vicinity of the orbicular zone projection. We interpret this to mean that fragmentation of the Quadrant Formation was related to formation of the steeply dipping, tabular copper-barren breccia zones. The location of the orbicular alteration sampled for analysis in this study is shown as Sample GB13-20D.

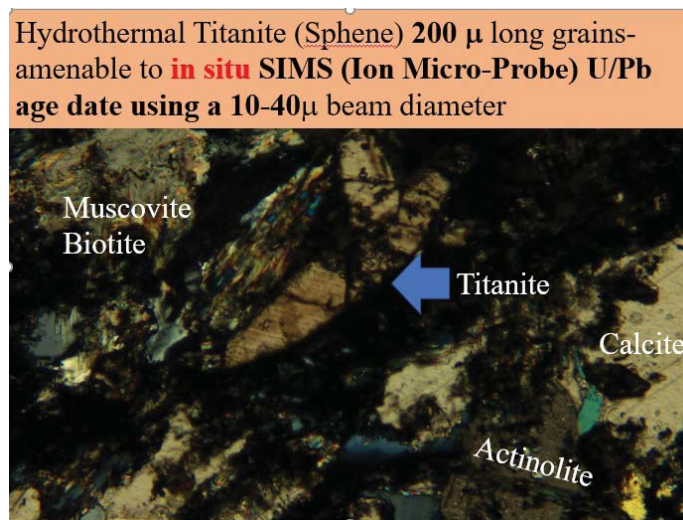


Figure 4. Photomicrograph in crossed polarizers of sample GB13-20D actinolite-calcite-titanite (sphene), biotite, muscovite, and quartz. All minerals identified optically have been verified using a Zeiss EVO-10 Variable Vacuum SEM using both secondary electron and backscattered electron imaging and qualitative chemical analyses using an energy-dispersive EDAX system.



Table 1. Summary of SHRIMP U-Pb results for Titanite from sample GB13-20D.

| Area.<br>spot | U<br>(ppm) | Th<br>(ppm) | Th/U | <sup>206</sup> Pb*<br>(ppm) | <sup>204</sup> Pb/<br><sup>206</sup> Pb | ±        | f <sub>206</sub><br>% | Total                                  |       |   |        | Radiogenic                             |         | Age (Ma)                               |      |
|---------------|------------|-------------|------|-----------------------------|---|----------|-----------------------|--|-------|---|--------|--|---------|--|------|
|               |            |             |      |                             |   |          |                       | <sup>238</sup> U/<br><sup>206</sup> Pb | ±     | <sup>207</sup> Pb/<br><sup>206</sup> Pb | ±      | <sup>206</sup> Pb/<br><sup>238</sup> U | ±       | <sup>206</sup> Pb/<br><sup>238</sup> U | ±    |
| 1.1           | 98         | 7.3         | 0.07 | 7.2                         | 0.048228                                | 0.001030 | 85.7                  | 11.691                                 | 0.298 | 0.7309                                  | 0.0202 | 0.01220                                | 0.00260 | 78.1                                   | 16.5 |
| 1.2           | 35         | 2.7         | 0.08 | 8.8                         | 0.053168                                | 0.001455 | 91.9                  | 3.395                                  | 0.159 | 0.7928                                  | 0.0131 | 0.02394                                | 0.00705 | 152.5                                  | 44.4 |
| 1.3           | 104        | 6.2         | 0.06 | 1.7                         | 0.018417                                | 0.001770 | 40.1                  | 53.720                                 | 0.904 | 0.3658                                  | 0.0190 | 0.01114                                | 0.00050 | 71.4                                   | 3.2  |
| 1.4           | 12         | 0.4         | 0.03 | 3.9                         | 0.052841                                | 0.001730 | 94.7                  | 2.700                                  | 0.110 | 0.8177                                  | 0.0169 | 0.01946                                | 0.01013 | 124.3                                  | 64.0 |
| 5.1           | 55         | 144.9       | 2.65 | 3.3                         | 0.044431                                | 0.002132 | 79.2                  | 14.398                                 | 0.296 | 0.6792                                  | 0.0094 | 0.01442                                | 0.00136 | 92.3                                   | 8.6  |
| 6.1           | 79         | 2.9         | 0.04 | 1.2                         | 0.026294                                | 0.002026 | 40.13                 | 55.404                                 | 0.993 | 0.3657                                  | 0.0062 | 0.01081                                | 0.00028 | 69.3                                   | 1.8  |
| 7.1           | 52         | 5.5         | 0.11 | 0.9                         | 0.025643                                | 0.002238 | 45.0                  | 49.222                                 | 0.999 | 0.4040                                  | 0.0092 | 0.01118                                | 0.00037 | 71.7                                   | 2.4  |
| 7.2           | 82         | 9.2         | 0.11 | 1.5                         | 0.028674                                | 0.003383 | 44.1                  | 47.186                                 | 2.203 | 0.3978                                  | 0.0042 | 0.01184                                | 0.00059 | 75.9                                   | 3.8  |
| 7.3           | 45         | 3.5         | 0.08 | 1.1                         | 0.031268                                | 0.002215 | 60.1                  | 36.104                                 | 0.765 | 0.5245                                  | 0.0111 | 0.01105                                | 0.00055 | 70.8                                   | 3.5  |
| 7.4           | 50         | 1.7         | 0.03 | 1.3                         | 0.032822                                | 0.005110 | 68.5                  | 32.791                                 | 2.731 | 0.5909                                  | 0.0438 | 0.00960                                | 0.00191 | 61.6                                   | 12.2 |
| 8a.1          | 41         | 8.6         | 0.21 | 1.5                         | 0.040849                                | 0.002171 | 75.29                 | 24.048                                 | 0.731 | 0.6453                                  | 0.0199 | 0.01027                                | 0.00124 | 65.9                                   | 7.9  |
| 8.1           | 56         | 9.5         | 0.17 | 1.0                         | 0.029106                                | 0.003717 | 48.3                  | 48.759                                 | 1.063 | 0.4307                                  | 0.0139 | 0.01060                                | 0.00047 | 68.0                                   | 3.0  |
| 8.2           | 35         | 8.2         | 0.24 | 2.0                         | 0.047472                                | 0.002174 | 80.8                  | 15.045                                 | 0.632 | 0.6913                                  | 0.0068 | 0.01273                                | 0.00128 | 81.6                                   | 8.2  |
| 8.3           | 47         | 7.5         | 0.16 | 1.9                         | 0.039721                                | 0.002047 | 77.2                  | 21.294                                 | 0.437 | 0.6612                                  | 0.0091 | 0.01069                                | 0.00090 | 68.5                                   | 5.7  |
| 8.4           | 56         | 9.9         | 0.18 | 2.2                         | 0.041668                                | 0.002292 | 73.97                 | 21.548                                 | 0.415 | 0.6356                                  | 0.0101 | 0.01208                                | 0.00091 | 77.4                                   | 5.8  |
| 8.5           | 42         | 7.5         | 0.18 | 1.8                         | 0.043405                                | 0.002561 | 76.8                  | 20.319                                 | 0.459 | 0.6584                                  | 0.0145 | 0.01139                                | 0.00118 | 73.0                                   | 7.5  |
| 8.6           | 79         | 13.2        | 0.17 | 2.8                         | 0.039025                                | 0.001437 | 72.7                  | 24.391                                 | 0.444 | 0.6252                                  | 0.0123 | 0.01118                                | 0.00087 | 71.7                                   | 5.6  |
| 8.7           | 74         | 13.9        | 0.19 | 1.3                         | 0.027578                                | 0.001892 | 48.7                  | 47.017                                 | 0.848 | 0.4339                                  | 0.0134 | 0.01091                                | 0.00045 | 69.9                                   | 2.9  |
| 9.1           | 64         | 9.4         | 0.15 | 1.1                         | 0.021482                                | 0.002137 | 45.6                  | 49.223                                 | 0.932 | 0.4095                                  | 0.0202 | 0.01104                                | 0.00059 | 70.8                                   | 3.7  |
| 10.1          | 181        | 27.6        | 0.15 | 1.9                         | 0.004553                                | 0.000715 | 10.10                 | 80.399                                 | 1.186 | 0.1276                                  | 0.0032 | 0.01118                                | 0.00017 | 71.7                                   | 1.1  |
| 10.2          | 111        | 16.5        | 0.15 | 1.3                         | 0.008245                                | 0.001232 | 17.7                  | 74.370                                 | 1.264 | 0.1876                                  | 0.0063 | 0.01107                                | 0.00022 | 71.0                                   | 1.4  |
| 11.1          | 112        | 18.7        | 0.17 | 2.1                         | 0.027608                                | 0.002796 | 50.2                  | 45.138                                 | 0.753 | 0.4460                                  | 0.0288 | 0.01103                                | 0.00085 | 70.7                                   | 5.4  |

## Results

The SHRIMP data and related errors are summarized in table 1 for the 22 spots analyzed under the ion beam.

A central concept to using the data in table 1 is that <sup>238</sup>U decays to <sup>206</sup>Pb with a half-life of 4.468 x 10<sup>9</sup> years and <sup>235</sup>U decays to <sup>207</sup>Pb with a half-life of 0.707 x 10<sup>9</sup> years. <sup>238</sup>U is the more abundant U isotope in the earth, amounting to about 99.2745%, while <sup>235</sup>U constitutes only about 0.72%. <sup>204</sup>Pb is a stable non-radiogenic isotope of Pb that is used to normalize the <sup>206</sup>Pb and <sup>207</sup>Pb measurements as shown in equations 1 and 2 for <sup>238</sup>U decay to <sup>206</sup>Pb and <sup>235</sup>U decay to <sup>207</sup>Pb, respectively. λ<sup>238</sup> and λ<sup>235</sup> are the radiometric decay rate constants for <sup>238</sup>U and <sup>235</sup>U, respectively, and *t* is time. λ<sup>238</sup> is 1.55125 x 10<sup>-10</sup> and λ<sup>235</sup> is 9.8485 x 10<sup>-10</sup> (Steiger and Jäger, 1977).

$$\left(\frac{{}^{206}\text{Pb}}{{}^{204}\text{Pb}}\right) = \left(\frac{{}^{206}\text{Pb}}{{}^{204}\text{Pb}}\right)_0 + \left(\frac{{}^{238}\text{U}}{{}^{204}\text{Pb}}\right) (e^{\lambda^{238}t} - 1) \quad 1$$

$$\left(\frac{{}^{207}\text{Pb}}{{}^{204}\text{Pb}}\right) = \left(\frac{{}^{207}\text{Pb}}{{}^{204}\text{Pb}}\right)_0 + \left(\frac{{}^{235}\text{U}}{{}^{204}\text{Pb}}\right) (e^{\lambda^{235}t} - 1) \quad 2$$

Notice that both equations 1 and 2 are of the form  $y = a_0 + X_m$ , where  $a_0$  is the y-intercept where  $x$  equals zero,  $x$  is <sup>238</sup>U/<sup>204</sup>Pb (equation 1) or <sup>235</sup>U/<sup>204</sup>Pb (equation 2), and the terms with  $(e^{\lambda^{238}t}-1)$  or  $(e^{\lambda^{235}t}-1)$  are the slope,  $m$ . The y-intercept values  $({}^{206}\text{Pb}/{}^{204}\text{Pb})_0$  and  $({}^{207}\text{Pb}/{}^{204}\text{Pb})_0$  are called initial Pb or common lead in contrast to radiogenic Pb formed by U decay after the titanite formed, which is the fraction used in radiometric dating. Common Pb can pose a serious challenge to accurate radiometric dating so minerals like zircon are usually sought out as their structure precludes inclusion of much Pb while having a very high U/Pb ratio. Titanite may have substantial common or initial Pb so that special care must be taken to acquire an accurate radiometric age. The initial Pb ratio can be determined by making Isochron plots as commonly done in Rb/Sr dating. Here

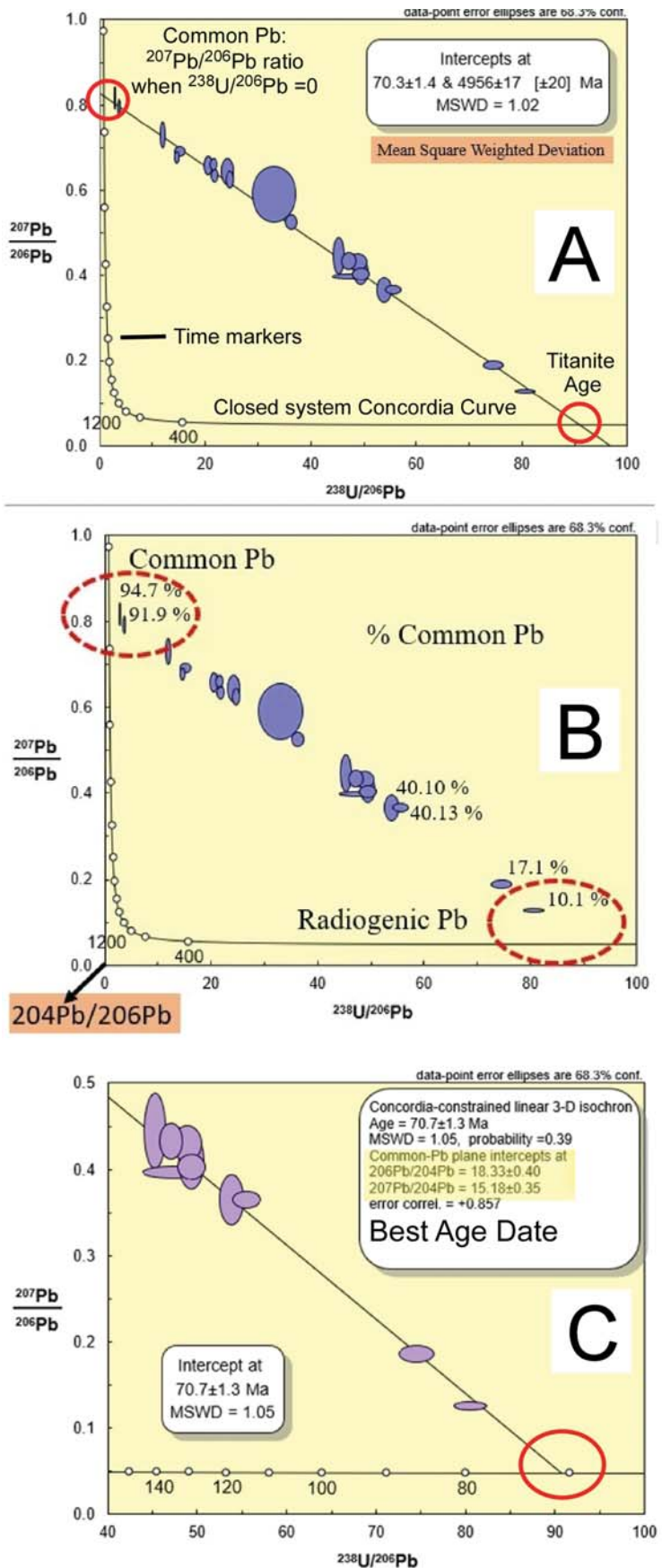


instead, the **ratio** of the common initial Pb values was determined by using a method derived and described by Tera and Wasserburg (1972), working with lunar samples and making no assumption about the magnitude of initial or common lead ratios, that is the y-intercepts in equations 1 and 2. Instead, measured **total**  $^{207}\text{Pb}/^{206}\text{Pb}$  ratios are plotted against  $^{238}\text{U}/^{206}\text{Pb}$  ratios. Ratios are not corrected for initial or common Pb. A series of *in situ* sample spots with different U/Pb values containing common Pb will plot along a straight line that intercepts the closed system 'concordia' curve at a point where  $^{207}\text{Pb}/^{206}\text{Pb}$  and  $^{238}\text{U}/^{206}\text{Pb}$  ages are equal. The intercept of the regression line is the initial  $^{207}\text{Pb}/^{206}\text{Pb}$  because a sample with a  $^{238}\text{U}/^{206}\text{Pb}$  ratio of 0 will retain its initial Pb isotopic composition. In simple cases multiple analyses define a discordia line whose intersections with the Concordia curve indicates both the time of formation of the titanite and the composition of the common lead. The Tera–Wasserburg coordinate system has now been tested for almost 50 years on a wide variety of complex sample types with detailed assessment of errors (Lugwig, 1998). The Tera–Wasserburg plot can be expanded into a three-dimensional plot where the third axis is defined by  $^{204}\text{Pb}/^{206}\text{Pb}$ . This 3-D plot allows dealing with samples comprising substantial amounts of common Pb without requiring *a priori* correction. The data, uncorrected for common Pb, are generally visualized as projections on the  $^{207}\text{Pb}/^{206}\text{Pb}$  and  $^{238}\text{U}/^{206}\text{Pb}$  plane, and for concordant populations having different proportions of radiogenic to common Pb they define a line whose intersection with Concordia yields the age of crystallization. A version of the plot reduced to 2-D is used occasionally to visualize and interpret high common Pb data without measuring  $^{204}\text{Pb}/^{206}\text{Pb}$ .

In figure 5A, a Tera–Wasserburg plot for the 22 titanite SHRIMP analysis spots in Sample GB13-20D is shown in relation to the Concordia closed system curve in black with age ticks. Notice that the data shown with their error ellipses define a linear relationship from the upper left intercept with Concordia showing the

Figure 5. (A) Tera–Wasserburg plots of discordant U/Pb data on titanite (sphene) in sample GB13-20D actinolite-calcite-titanite orbicules shown in figures 1A and 3. The linear discordia line intersects the Wetherill concordia curve in two places: the lower right intersection gives the radiometric age of the hydrothermal titanite. The upper left intercepts provide the common Pb composition. (B)

The percent common lead in each SHRIMP analysis spot, from 94.7% in the upper left down to 10.1% in the lower right, which is mostly radiogenic Pb formed *in situ* after the titanite crystallized from the ore-forming hydrothermal solution and became a closed isotopic system. Notice that the  $^{207}\text{Pb}/^{206}\text{Pb}$  ratio of the common lead is about 0.80 on the Y-axis. (C) The best age of 70.7 Ma, where the discordia line intersects the concordia curve and almost all the Pb is radiogenic. In addition to the radiometric age determination, the common Pb plane intercepts yield a  $^{207}\text{Pb}/^{206}\text{Pb}$  ratio 0.8282 on the Y-axis by regression.



common Pb ratio  $^{207}\text{Pb}/^{206}\text{Pb}$  near a value of 0.8 down to lower right where the radiometric age of 70.3 million years (Ma) is shown. In figure 5B the percent common lead in each SHRIMP analysis spot is shown varying from 94.7% in the upper left down to 10.1% in the lower right, which is mostly radiogenic Pb formed in situ after the titanite crystallized from the ore-forming hydrothermal solution and became a closed isotopic system. Notice that the y-intercept  $^{207}\text{Pb}/^{206}\text{Pb}$  ratio of the common lead is about 0.80 on the y-axis. Figure 5C shows the best regressed age of the titanite 70.7 Ma where the Discordia line intersects the Concordia curve and almost all the Pb is radiogenic. In addition, two fundamental Pb isotope ratios central to our work are shown in figure 5C: regressions in the common Pb plane yield intercepts with the  $^{206}\text{Pb}/^{204}\text{Pb}$  ratio at 18.33 with an error of 0.40 and a  $^{207}\text{Pb}/^{204}\text{Pb}$  ratio of 15.18 with an error of 0.35. The ratio of  $^{207}\text{Pb}/^{204}\text{Pb}$  and  $^{206}\text{Pb}/^{204}\text{Pb}$ , which is 15.18/18.33, is 0.8282.

### Comparison of SHRIMP Age of Clementine with Plutons and Ore Deposit Ages Nearby

In figure 6, the radiometric age of Clementine (70.7 Ma) is shown in relation to ages of ore deposits in the surrounding area. Clementine, with its U/Pb age of 70.7 Ma, occurs within the general outline of the Boulder Batholith and as such is clearly north of the Pioneer Batholith. Zen (1996a), based on Rb/Sr isotopic difference, asserted that the boundary between the two batholiths was the Sawmill Gulch Fault south of the Big Hole River Canyon pluton. The Butte pre-Mainstage is shown as 68–66 Ma, with the Mainstage as 62.5 Ma (Houston and Dilles, 2013). Dates on the Big Hole Canyon pluton immediately south of Clementine are shown as 75.4 to 74.7 Ma for the inclusion-bearing granodiorite biotite (Zinter and others, 1983), although these dates are younger than the earlier, more mafic phases. Dates on rocks south of the Sawmill Canyon Fault, including Cannivan Gulch, are shown as 68 to 66.8 Ma (Schmidt and others, 1979). Fresh pluton ages reported by Zen (1988) are shown as 72 Ma for the Uphill Creek granodiorite, 74.8 Ma for the Stine Creek pluton, and 64 Ma for the leucogranite of Bobs Lake. The Pioneer Batholith has multiple groupings of ages (Snee and others, 1983): Group 1 (83–80 Ma), 2 (79–76 Ma), 3 (76.5–74.5 Ma), 4 (74.5–72.0 Ma), 5 (72–69.5 Ma), 6 (72–69.5 Ma), and 7 (67–66

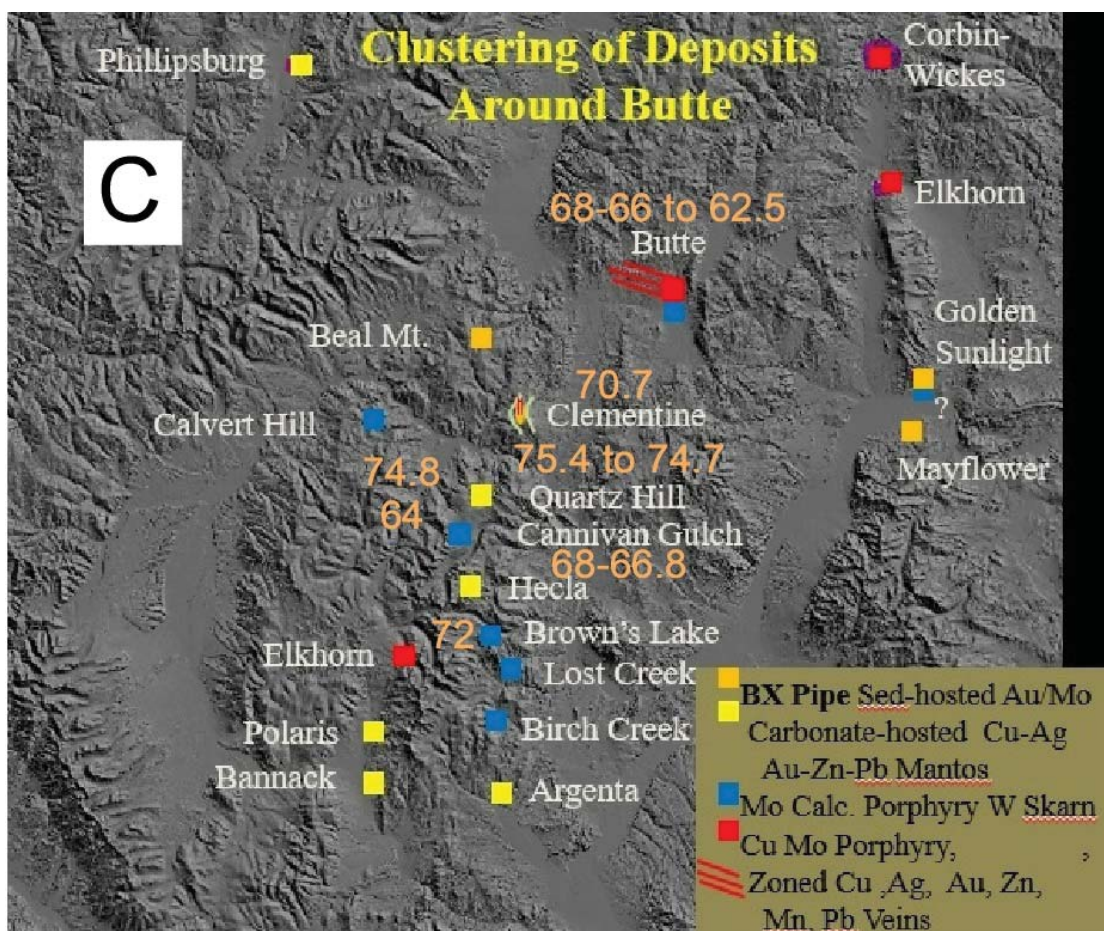


Figure 6. Radiometric (K-Ar,  $^{40}\text{Ar}/^{39}\text{Ar}$  dates of plutons and mineralization.



Ma). Snee and others (1983) notes that these age ranges are  $^{40}\text{Ar}/^{39}\text{Ar}$  cooling stages and not necessarily pluton crystallization ages.

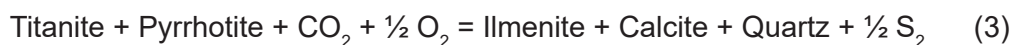
Zen (1996a,b) asserts that the initial Sr (iSr) values of the Pioneer Batholith stand in contrast to those of the Boulder Batholith situated to the north–northeast. Among the highest iSr ratios measured are porphyry dikes near Hecla (Zen, 1996b). Rocks of the two batholiths are petrographically and chemically similar; they have the same age range and share comparable tectonic setting and history. However, the Boulder Batholith (both the “Main Series” and the “Sodic Series” of Tilling, 1973) has much lower values of iSr (Doe and others, 1968), ranging from 0.7055 to 0.7092; an isopleth of 0.710 fully separates the two batholiths, and this boundary is in fact mappable, at the current level of erosion, as the north–northwest-striking Sawmill

Gulch–Trusty Gulch fault system (fig. 1; Zen, 1988; Arth and others, 1986). Comparing the Clementine SHRIMP titanite age of 70.7 Ma with the variety of ages shown in figure 6 shows that the hydrothermal processes by which the orbicular alteration formed and the titanite precipitated from high-temperature aqueous solutions are clearly well within the age ranges of the plutons and alteration ages of large and minor ore deposits.

### **Titanite Stability in Relation to Potassic Alteration and Carbon Dioxide Content of the Fluid**

Given the importance of potassic alteration associated with high-temperature mineralization in porphyry copper genesis and in textures observed at Clementine (fig. 1A) where a white bleached zone surrounds actinolite-filled orbs with titanite and calcite (fig. 1C), thermodynamic phase equilibria help explain the textures (fig. 7). While the most abundant mineral within orbicular alteration is actinolite, the titanite, calcite, pyrrhotite, chalcopyrite, ilmenite, quartz, and the annite component in biotite ( $\text{KFe}_3\text{AlSi}_3\text{O}_{10}(\text{OH})_2$ ) are more accurately represented in phase diagrams, given the broad solid solution range of actinolite, which is a complex amphibole with wide solid solution ranges and hence complex and largely unknown thermodynamic values. A new equilibrium phase diagram shown in figure 7 was calculated here using computer program SUPCRIT, which was developed at U.C. Berkeley by H.C. Helgeson and students (Johnson and others, 1992) and revised by Zimmer and others (2016) with improvements in the thermodynamic data, specifically the addition of ilmenite (Holland and Powell, 2011), which is critical for this study and lacking in the earlier data set. The version of SUPCRITBL (for Bloomington, Indiana) used here can be accessed at: <https://www.indiana.edu/~hydrogeo/supcrtbl.html>.

One of the phase boundaries, shown as a heavy red line 1 in figure 7, is equation 3:



In reaction 3, the stoichiometric coefficients are written so as to conserve moles of elements in solid phases and use only  $\text{O}_2$ ,  $\text{S}_2$ , and  $\text{CO}_2$  to balance the total moles of the solid phases. Using this convention (Holland, 1959) and composing the equilibrium constant, then taking its log yields equation 4, which is the algebraic equation for the heavy red line 1:

$$\log f_{\text{S}_2} = 2\log K + \log f_{\text{O}_2} + 2\log f_{\text{CO}_2} \quad (4)$$

Biotite-bearing hornfels wall rock formed as the earliest manifestation of alteration in the regions near the orbs at the diffusive/advective boundary. Many orbs studied in this section have a microscopic biotite crackle veinlet that appears to have been the feeder channel for the orbs. With the start of orb growth, the fluids reaching the area probably were in equilibrium with biotite (annite) with a fugacity of  $\text{CO}_2$  such that biotite was stable inside the orbs as well. However, figure 7 shows that titanite–ilmenite boundaries are sensitive to  $\text{CO}_2$  fugacity and move accordingly, and under specific conditions may migrate outside the biotite stability field. What process caused the selective destruction of fine-grained biotite in the white ring surrounding the actinolite-titanite-calcite-quartz orb apparently involved elevating the fugacity of  $\text{CO}_2$  slightly outside the biotite stability



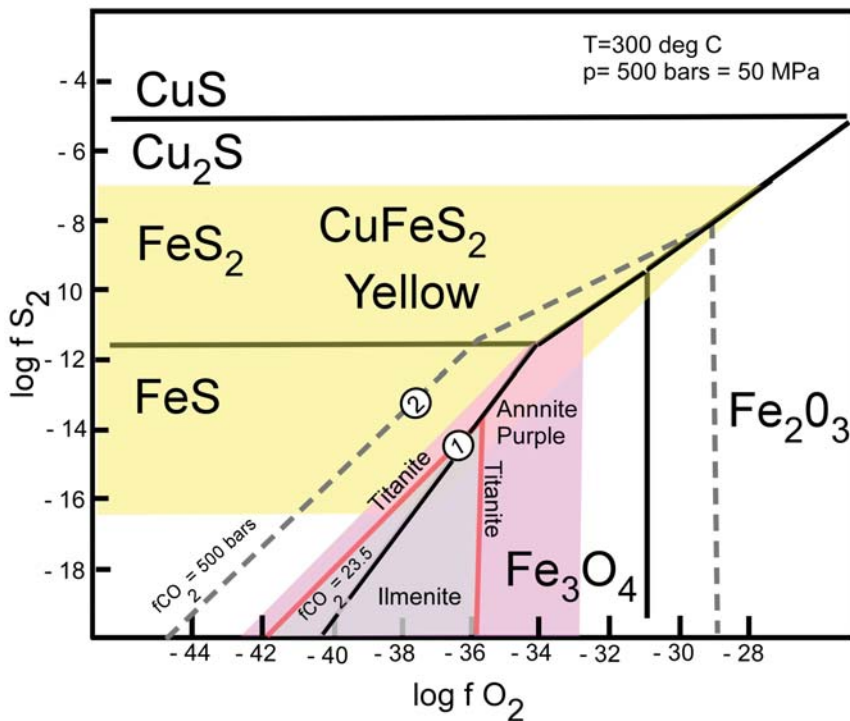


Figure 7. The heavy solid lines define the stability fields of pyrrhotite (FeS), pyrite (FeS<sub>2</sub>), magnetite (Fe<sub>3</sub>O<sub>4</sub>), hematite (Fe<sub>2</sub>O<sub>3</sub>), covellite (CuS), and chalcocite (Cu<sub>2</sub>S; Holland, 1959, 1965; Meyer and Hemley, 1967). The chalcopyrite field is shown in yellow surrounded by bornite (Cu<sub>5</sub>FeS<sub>4</sub>; Brimhall, 1980). The annite component of biotite yields outwards to orthoclase in purple (Brimhall, 1980), where all the mineral–solution–gas equilibrium are presented for this phase diagram. Here, ilmenite in gray is added surrounded by titanite shown in purple. The mineral assemblage in rock sample GB13-20D consisting of titanite, pyrrhotite, chalcopyrite, ilmenite, calcite, quartz with biotite (annite, heavy red line 1) represents the main orbicule mineralogy. A small partial pressure of CO<sub>2</sub> gas of 23.5 bars (out of 500 bars total pressure) is necessary for titanite and ilmenite to have equilibrated with both pyrrhotite and chalcopyrite. At lower CO<sub>2</sub> pressure less than 23.5 bars the titanite–ilmenite boundary would not be at equilibrium with chalcopyrite at the conditions shown of 300°C and 500 bars (50 Mpa). As the CO<sub>2</sub> pressure increases, the ilmenite stability field expands at the expense of titanite until at the fugacity of CO<sub>2</sub> equal to the total pressure of 500 bars (heavy dashed gray line 2), titanite and ilmenite are stable well outside the biotite (annite) field. We interpret the white rings surrounding the orbs shown in figure 1C as having formed with slightly elevated CO<sub>2</sub> pressures above about 30 bars so that biotite in the surrounding hornfels was destroyed.

with clear regional structural control near the axial crest of a doubly plunging anticline confined by the overlying Grasshopper thrust plate. The entire system was emplaced between Archean crustal blocks, which are delimited by Proterozoic accretionary tectonic zones interpreted as sutures representing early Proterozoic subduction zones where oceans disappeared. Major ore deposits sharing this crustal heritage include Butte, Bingham, Henderson, and Questa. On a smaller scale, the clustering of ore deposits around the Butte district shows that Clementine occurs within a north–south-striking belt of old mining districts (Quartz Hill, Cannivan Gulch, Hecla), all of which occur along the crest of a regional anticlinorium. Furthermore, each district occurs at doubling-plunging anticlines or domes. By radiometrically dating the titanite contained within the actinolite orbs, we showed that the age of 70.7 Ma fits well within the magmatic history of the Boulder Batholith, and the mineralization in the Butte District. The deposits to the south of Clementine (Quartz Hill, Cannivan Gulch, and Hecla) formed within a batholith that is isotopically distinct and clearly more crustally derived. What the Clementine system did share with the other deposits was the frontal thrust plane of the Sevier Fold and Thrust Belt. Regardless of the mantle or crustal source region, the magmas in both the Boulder and Pioneer Batholiths appear to have intruded up the same regional thrust fault ramps. Laccolith bodies at depth seem to be where most of the chemical fractionation occurs that is required for the high levels of metal enrichment to form the ore deposits.

field, perhaps about 30 bars (outside the purple area in fig. 5). It is fairly clear that fluid migration through the thick, highly reactive calcium carbonate-rich rock formations at depth in the axial plane of the anticline (fig. 3), where the Madison Limestone has a stratigraphic thickness of about 500 m, played an important role as a chemical buffer capable of supplying CO<sub>2</sub> gas. During orb growth, the fugacity of CO<sub>2</sub> was at least 23.5 bar to stabilize chalcopyrite. However, the CO<sub>2</sub> fugacity apparently rose even higher to a value above 30 bars, which caused the titanite–ilmenite line to move upwards and outside the biotite (annite) stability field. The white bleached color is due to local biotite destruction within the ring annulus. The hydrothermal fluid was either in equilibrium or slightly out of equilibrium with biotite, which is an essential alteration assemblage in early porphyry copper deposit genesis.

### Discussion

On a district scale, the axially symmetric position of the distal orbicular actinolite-titanite-calcite alteration with respect to the vein gossans, breccias, and felsic plutons is highly suggestive that all these features are genetically related. In cross section, the orbicular alteration appears to dip away from the center of the zoning pattern, implying that it is both distal and uppermost and was emplaced

## Conclusions

The intent of this work on orbicular alteration is to revise the distal and upper reaches of the geo-spatial patterns of porphyry copper paradigm and provide new field methods that help support the transition to deep porphyry copper exploration. Orb mapping can assist in targeting large deep porphyry copper deposits during early exploration through properly interpreting the orbicular zonation surrounding the typical alteration halo around these large intrusive systems as the exterior of the system's fracture pattern, providing a bullseye to focus follow-up exploration.

Orb alteration makes this subtle physical boundary feature macroscopically visible and contributes a powerful new mapping tool in lithologies where orbs are likely to form, such as in sedimentary and other wall rocks with connected pore space, allowing intergranular diffusion rather than in non-porous rocks with interlocking grains. The utility of orb cupolas as a targeting tool in deep exploration stems from several observations. First, it has been demonstrated that actinolite-titanite-calcite orbs can be mapped successfully even in completely timbered terrain and related geo-spatially to more proximal zone vein gossan systems, breccia bodies, and plutons as the distal and superjacent hydrothermal alteration feature. Second, the orbicular zones mark the position of a key hydrodynamic boundary that is largely invisible otherwise, which is the peripheral edge of the mineralized fracture permeability network at the time of coupled wall rock alteration and mineralization because disseminated chalcopyrite occurs near the orbs. Third, it has been demonstrated here that accurate radiometric dating of titanite (sphene) occurring within the actinolite-calcite-filled orbs is possible. Moreover, radiometric SHRIMP U/Pb dating works effectively even when high levels of common Pb occur within the hydrothermal titanite as long as the Terra-Wasserburg (1972) method is used, since it requires no assumptions about common lead compositions to generate a reliable radiometric age date. Fourth, if during geological mapping early on in exploration of a new region, orbs are found and the titanite ages ascertained, the resultant radiometric age can be a decisive factor in readily establishing the age of likely copper mineralization and compared with other age dates on plutons and regional plutonic episodes of metallogenic interest. Fifth, Concordia-constrained 3-D isochrons in fact yield both accurate ages and accurate common lead plane intercepts of  $^{206}\text{Pb}/^{204}\text{Pb}$  and  $^{207}\text{Pb}/^{204}\text{Pb}$  ratios. These common lead ratios have utility in comparing data on a new deposit with known common Pb ratios in productive mineral belts (Zartman, 1974) that will be described in a future publication. Sixth, since it has now been shown at the Clementine prospect that springs today occur near the orb bands, it is inferred that the gross permeability of the hornfels-altered rocks inside the orb cupola is lower than those outside the cupola in unaltered formations, forcing groundwater upwards into springs. Hence, the spatial association of springs with orb bands provide another exploration tool of using mapped springs from U.S. Geological Survey topographic maps to: (1) help find and map orbicular alteration and associated disseminated sulfide mineralization in new districts, and (2) infer on a potential district scale the position, size, and orientation of a new prospective region of interest once the orb pattern has been mapped.

More broadly, the fundamental challenge in advancing the paradigm used in deep porphyry copper deposit exploration is assembling a practical, cost-effective, new strategy based on definitive pathfinder mineral-isotopic indicators that significantly enlarges the target size, and provides regional results that can be classified so that only the largest deposits stand out in relation to the subordinate deposits during early stage, pre-drilling exploration. Hence, the essence of the approach described here is that for deep deposit exploration to prove more effective than it has in the past decade, PCD pathfinder mineral-isotopic indicators may offer a more effective strategy than the present search for traditional features of copper deposits exposed at their mid-sections, including leached cappings above supergene enrichment blankets, rather than the upper, low sulfide content, reaches of deep deposits amenable to deep underground mining with a far smaller environmental footprint.

It is suggested here that for deep PCD mineral exploration to once again become successful, a transformation in how applied science is judged in joint venture decisions is required as a "more of the same" approach has not worked. First, exploring through the tops of prospective new deep porphyry copper deposits means confronting the realities of a largely unfamiliar geological domain above the current upper tops of the porphyry copper paradigms, based on mined ore deposits whose surface exposures intersected the surface within or somewhat above ore grade levels, not 500 to 1,000 m above ore grade level as in deep deposits. Hence, special care



should be taken in evaluating deep prospect geology. A small shallow district with strong epithermal indications and a multitude of conventional data such as soil sample arrays and Cu assays might appear more prospective than a new superjacent zone defined by a large radiometrically dated orb ring surrounding a vein system and possible parental pluton but with fewer assay data. Risk aversion prompted by confirmation bias could motivate selecting the former as a superior target, especially if 3-D virtual reality viewing of prospect data density is deemed to be a decisive factor. In contrast, a radiometric titanite age that makes geological sense with respect to regional metallogenic magmatic and hydrothermal events, the size of the orb ring, and common Pb ratios may offer a more discerning glimpse of what could occur at depth than a myriad of assay data alone. Similarly, given the need to advance understanding of the superjacent zone in terms of new features, work on prospects needs to include support for geological mapping, polished thin section petrography, and petrology. New features observed may appear odd at first, but only when such observations are respected and mapped, and not merely discounted and deemed outside the realm of the PCD model, will new useful features be documented and put into widespread use. It is hoped that this work will help spur organizations to allocate personnel and resources to undertake advanced scientific mapping to find and describe new features of the deep PCD superjacent zone. Finally, for fieldwork to be effective, ergonomics must be considered with vehicles used to advantage supporting geologists with drop off and pick up shuttles to save time and energy.

### Acknowledgments

Doug Fuerstenau reviewed an early version of this manuscript, helping to improve its clarity significantly. Colleen Elliott and Stanley Korzeb also provided reviews. For the first author, this study is a coalescence of methods learned over a lifetime and inspired early on by a few special teachers. As an undergraduate at U.C. Berkeley (1965–1969), Brimhall is grateful for the exceptional opportunity of having learned the use of the petrographic microscope from two masters of optical mineralogy who were visiting professors: K. Naha of the Indian Institute of Technology Kharagpur, who urged us to: “learn rock-forming and accessory minerals like your friends—by sight,” and Stewart Agrell of Cambridge University, whose igneous petrology course included descriptions of orbicular rocks of igneous origin, which allowed Brimhall to understand how distinct, in contrast, are the hydrothermal processes that formed the actinolite-calcite-titanite orbs at Clementine. Two sabbatical leaves also afforded special opportunities to explore basic U/Pb isotopic principles implemented here. At Cal Tech (1985–1986), Brimhall absorbed U/Pb isotopic material from Clair Patterson and Geri Wasserburg, and at the Australian National University in Canberra (1992–1993), he learned SHRIMP analysis from Bill Compston, Ian Williams, and Trevor Ireland (Brimhall and others, 1994). In recent years his knowledge of indicator mineralogy in diamond exploration benefited from close associations with Ray Morley and Hugo Dummett (formerly of BHP San Francisco Global Exploration). Mary Jane Brimhall has served as the principal field safety coordinator, monitoring the locations of all personnel using SPOT satellite uplinkers during all the fieldwork involved in our geological mapping spanning 7 years. Ed Rogers has been a steadfast field companion in challenging terrains for a decade. Jay Ague was instrumental in locating an up-to-date thermodynamic code to calculate phase equilibria. Abel Vanegas provided technical support in digital mapping and community outreach education. Ray Morley, Dan Kunz, and Doug Fuerstenau are thanked for their ongoing enthusiastic commentary and support. Chris Gammons and Colleen Elliott of Montana Tech and the Montana Bureau of Mines and Geology continue to provide insightful scientific dialogue and access to laboratory equipment. Jim Freestone has conducted all forest restoration activities to the satisfaction of the USFS and Montana DEQ for Clementine Exploration. Jim and John Lundborg have also been a major help in shuttling field crews and vehicles, making mapping and sampling possible in steep forested terrain. Tim Teague provided the SEM and EDAX. Erik Torgeson (U.S. Forest Service) is thanked for field site visits of USFS staff so that we can maintain good working relations with the U.S. Forest Service.

## References

- Arth, J., Zen, E-An, Sellers, G., and Hammarstrom, J., 1986, High initial Sr isotopic ratios and evidence for magma mixing in the Pioneer Batholith of southwest Montana: *Journal of Geology*, v. 94, p. 419–430.
- Atkinson, W., and Einaudi, M.T., 1978, Skarn formation and mineralization in the contact aureole at Carr Fork, Bingham, Utah: *Economic Geology*, v. 75, p. 1326–1365.
- Brimhall, G.H., 1980, Deep hypogene oxidation of porphyry copper potassium-silicate protores: A theoretical evaluation of the copper remobilization hypothesis: *Economic Geology*, v. 75, p. 384–409.
- Brimhall, G.H., Compston, W., Williams, I.S., Reinfrank, R.F., and Lewis, C.J., 1994, Darwinian zircons as provenance tracers of dust-size exotic components in laterites: Mass balance and SHRIMP ion microprobe results, in *Soil micromorphology: Studies in management and genesis*, Ringrose-Voase, A.J., and Humphreys, G.S., eds.: Amsterdam, Elsevier, p. 65–82.
- Brimhall, G.H., and Marsh, B.D., 2017, Nature of the mineralization and alteration at the Clementine porphyry copper prospect in the northern Pioneer Mountains of southwest Montana: *Montana Bureau of Mines and Geology Open-File Report 699*, p. 55–58.
- Brimhall, G., 2018, Orbicular alteration at the Clementine porphyry copper prospect of southwest Montana: Defining the edges of advective flow in the porphyry copper paradigm: *Montana Bureau of Mines and Geology Special Publication 120*, p. 71–83.
- Doe, B., Tilling, R., Hedge, C., and Klepper, 1968, Lead and strontium isotope studies of the Boulder Batholith, southwestern Montana: *Economic Geology*, v. 63, p. 884–906.
- Foster, D., Mueller, P., Mogk, D., Wooden, J., and Vogl, J., 2006, Proterozoic evolution of the western margin of the Wyoming craton: Implications for the tectonic and magmatic evolution of the northern Rocky Mountains: *Canadian Journal of Earth Science*, v. 43, p. 1601–1619.
- Froude, D., Ireland, T., Kinny, P., Williams, I., Compston, W., Williams, I., and Myers, J., 1983, Ion microprobe identification of 4,100–4,200 Myr-old terrestrial zircons, *Nature*, v. 304 p. 616–618.
- Gustafson, L., and Hunt, J.P., 1975, The porphyry copper deposit at El Salvador, Chile: *Economic Geology*, v. 70, p. 857–912.
- Hildenbrand, T.G., Berger, B.R., Jachens, R.C., and Ludington, S.D., 2000, Regional crustal structures and their relationship to the distribution of ore deposits in the Western United States, based on magnetic and gravity: *Economic Geology*, v. 95, p. 1583–1603.
- Holland, R., 1959, Stability relations among the oxides, sulfides, sulfates and carbonates of ore and gangue metals, [Part] 1 of Some applications of thermochemical data to problems of ore deposits: *Economic Geology*, v. 54, p. 184–233.
- Holland, R., 1965, Some applications of thermochemical data to problems of ore deposits; [Part] 2, Mineral assemblages and the composition of ore forming fluids: *Economic Geology*, v. 60, p. 1101–1166.
- Holland, T., and Powell, R., 2011, An improved and extended internally consistent thermodynamic dataset for phases of petrological interest, involving a new equation of state for solids: *Journal of Metamorphic Petrology* v. 29, no. 3, p. 333–303.
- Houston, R., and Dilles, J., 2013, Structural geologic evolution of the Butte district, Montana: *Economic Geology*, v. 108, p. 1397–1424.
- John, D.A., Ayuso, R.A., Barton, M.D., Blakely, R.J., Bodnar, R.J., Dilles, J.H., Gray, F., Graybeal, F.T., Mars, J.C., McPhee, D.K., Seal, R.R., Taylor, R.D., and Vikre, P.G., 2010, Porphyry copper deposit model, Chap. B of *Mineral deposit models for resource assessment: U.S. Geological Survey Scientific Investigations Report 2010–5070–B*, 169 p.

- Johnson, J.W., Oelkers, E.H., and Helgeson, H.C. (1992) SUPCRT92—A software package for calculating the standard molal thermodynamic properties of minerals, gases, aqueous species, and reactions from 1-bar to 5000-bar and 0°C to 1000°C: *Computer and Geosciences*, v. 18, p. 899–947.
- Kalakay, T., John, B.E., and Lageson, D.R., 2001, Fault-controlled pluton emplacement in the Sevier fold-and-thrust belt of southwest Montana, USA: *Journal of Structural Geology*, v. 23, p. 1151–1165.
- Karlstrom, K.E., Whitmeyer, S.J., Dueker, K., Williams, M.L., Bowring, S.A., Levander, A., Humphreys, E.D., and Keller, G.R., the CD-ROM Working Group, 2004, Synthesis of results from the CD-ROM experiment: 4-D image of the lithosphere beneath the Rocky Mountains and implications for understanding the evolution of continental lithosphere, in Karlstrom, K.E., and Keller, G.R., eds., *The Rocky Mountain region: An evolving lithosphere—Tectonics, geochemistry, and geophysics: Geophysical Monograph Series*, 154, p. 421–480.
- Lowell, J.D., and Guilbert, J., 1970, Lateral and vertical alteration-mineralization zoning in porphyry ore deposits: *Economic Geology*, v. 65, p. 373–408.
- Meyer, C., and Hemley, 1967, Wall rock alteration, in *Geochemistry of hydrothermal ore deposits*, Barnes, H.L., ed.: New York, Holt, Rinehart and Winston, p. 166–235.
- Mueller, P., Heatherington, A., Kelly, D., Wooden, J., and Mogk, D., 2002, Paleoproterozoic crust within the Great Falls tectonic zone: Implications for the assembly of southern Laurentia: *Geology*, v. 30, p. 127–130.
- Pettke, T., Oberli, F., and Heinrich, C., 2010, The magma and metal source of giant porphyry-type ore deposits, based on lead isotope microanalysis of individual fluid inclusion: *Earth and Planetary Science Letters* 296 (2010) 267–277.
- Schaffer, R., 2018, Crisis in discovery; Improving the business paradigm for mineral exploration: *Mining Engineering*, May Issue, p. 26–27.
- Schmidt, H., Worthington, J., and Thomassen, R., 1979, K-Ar dates for mineralization in the White-Cloud-Cannivan Gulch porphyry molybdenum belt of Idaho and Montana: Discussion: *Economic Geology*, v. 74, p. 699.
- Schodde, R., 2013, Long term outlook for the global exploration industry: Geological Society of South Africa, Geo Forum Conference, Gloom or Boom?: Johannesburg, 2–5 July 2013, Oral Presentation.
- Sillitoe, R.H., 2010, Porphyry copper systems: *Economic Geology*, v. 105, p. 3–41.
- Sillitoe, R.H., Tolman, J., and van Kerkvoort, G., 2013, Geology of the Caspiche porphyry gold–copper deposit, Maricunga belt, northern Chile: *Economic Geology*, v. 108, p. 585–604.
- Sillitoe, R.H., Burgoa, C., and Hopper, D.R., 2016, Porphyry copper discovery beneath the Valeriano lithocap, Chile: *SEG Newsletter*, no. 106, July 2016, p. 1, 15–20.
- Snee, L., Sutter, J., and Zen, E-an, 1983, Ages of emplacement and cooling history of the Pioneer Batholith, southwest Montana: *Geological Society of America Abstract*, v. 15, no. 5, p. 412.
- Steiger, R. H., and Jäger, E., 1977, Subcommittee on geochronology: Convention on the use of decay constants in geo- and cosmochronology: *Earth and Planetary Science Letters*, v. 36, no. 3, p. 359–362.
- Tera, F., and Wasserburg, G.J., 1972, U-Th-Pb systematics in three Apollo 14 basalts and the problem of initial Pb in lunar rocks: *Earth and Planetary Science Letters*, v. 14, p. 281–304.
- Tilling, R., 1973, The Boulder Batholith, Montana: Product of two contemporaneous but chemically and isotopically distinct magma series: *Society of Economic Geologists, Butte Field Meeting Guidebook U.S.: Butte, Montana*.
- Williams, I., 1997, U-Th-Pb geochronology by ion microprobe, in *Society of Economic Geologists, Reviews in Economic Geology*, v. 7, p. 1–36.
- Wood, D., 2016, We must change exploration thinking in order to discover future orebodies: *SEG Newsletter*, no. 105, p. 16–18.



- Wood, D., and Hedenquist, J., 2019, Mineral exploration: Discovering and defining ore deposits: SEG Newsletter, no. 116, p. 1, 11–22.
- Zartman, R., 1974, Lead isotopic provinces in the cordillera of the western United States and their geologic significance: *Economic Geology*, v. 69, p. 792–805.
- Zen, E-An, 1988, Bedrock geology of the Vipond Park quadrangle: U.S. Geological Survey, Bulletin 1625.
- Zen, E-An, 1996a, Generation of magmas of the Pioneer Batholith and geologically-constrained thermal model: U.S. Geological Survey Open File Report 96-98.
- Zen, E-An, 1996b, Plutons in the eastern part of the Pioneer Batholith: Field relations and petrographic descriptions: U.S. Geological Survey Open File Report 96-97.
- Zinter, G., Snee, L., and Sutter, J., 1983, Geology, petrology, and age of emplacement of the Big Hole Canyon intrusion near Dewey, southwest Montana: *Geological Society of America Abstract*, v. 15, no. 5, p. 412.
- Zimmer, K., Zhang, Y.L., Lu, P., Chen, Y.Y., Zhang, G.R., Dalkilic, M. and Zhu, C., 2016, SUPCRTBL: A revised and extended thermodynamic dataset and software package of SUPCRT92: *Computer and Geosciences*, v. 90, p. 97–111.



Fluorite from Phosphate, MT. Courtesy of Michael J. Gobla.

# Ore Mineralogy and Stable Isotope Studies of the Hog Heaven Mining District, Montana

Ian Kallio,<sup>1</sup> Chris Gammons,<sup>1</sup> and Simon R. Poulson<sup>2</sup>

<sup>1</sup>*Department of Geological Engineering, Montana Tech, Butte, Montana*

<sup>2</sup>*Department of Geological Sciences & Engineering, University of Nevada-Reno*

## Introduction and Mining History

The Hog Heaven mining district in northwestern Montana is unique in that it is a high-sulfidation epithermal system containing high Ag-Pb-Zn relative to Au-Cu ore, with a very high Ag to Au ratio (2,330:1). The deposit is hosted within the Oligocene Hog Heaven Volcanic Field, which lies unconformably on the Precambrian Belt Supergroup. One idea to explain the metal ratios is that the Hog Heaven hydrothermal system may have scavenged Ag and base metals from deeper, preexisting stratabound Ag-Pb-Zn-Cu deposits hosted in the Belt Supergroup. This paper presents new data for the mineralogy and stable isotope compositions of ore and gangue minerals, which helps to constrain the hydrothermal mineralizing styles and stages, metal-bearing fluid sources, and the temperatures of ore formation at Hog Heaven.

The largest producer in the Hog Heaven district was the Flathead Mine, operated and/or leased by the Anaconda Copper Company between 1912 and 1975. Much of the early production focused on high-grade Ag-Pb ore shoots that had a semi-massive, “cellular” texture. Between 1975 and 2017, exploration drilling was conducted by CoCa Mines and Pan American Silver in an attempt to define a large, low-grade Ag resource (CoCa Mines, 1983). In 2017, Brixton Metals acquired the property and are continuing exploration efforts. The Hog Heaven district historically produced 192,776 kg of silver, 15 million kg of lead, 272,155 kg of copper, and 85 kg of gold (Rostad and Jonson, 1997).

## Mining District Geology

Previous descriptions of the geology and mineralization at Hog Heaven were given by Shenon (1935), Cossaboom (1981), Zehner (1987), Jepson (1993), and Lange and others (1994). The Hog Heaven precious metal system is underlain by Belt rocks that have a known affinity for stratabound Ag-Pb-Zn-Cu deposits (fig. 1). Mineral deposits are hosted within the Cenozoic Hog Heaven Volcanic Field (HHVF), a 30 to 36 Ma suite that consists predominantly of dacite flow-dome complexes and pyroclastic rocks (Lange and others, 1994). The HHVF erupted through and deposited on the Revett Formation of the Precambrian Belt Supergroup metasediments during Cenozoic regional extension.

Although several different ore deposit settings coexist in the HHVF, the main ore body is hosted in a diatreme that formed during the latest stages of dome emplacement. Lange and others (1994) characterized the other deposit types present at Hog Heaven as either replacement stratabound deposits along favorable contacts, open-space filling within lithic tuffs, or stockwork and vein deposits, all of which show a genetic relationship to dacite dome emplacement.

## Methods

Fieldwork included 1:12,000 geologic mapping in conjunction with 1:24,000 mapping (ongoing EDMAP and STATEMAP funded projects led by K. Scarberry and E. Coppage in the region) of the Oligocene volcanics, associated mineralization and alteration, and the surrounding Precambrian metasedimentary rocks of the Belt Supergroup (Revett Formation). Over 30 samples of sulfides and sulfates were collected from archived drill core for stable isotope, fluid inclusion, and petrography studies. Additional samples were collected from outcrops and dumps at the historic Flathead Mine. Furthermore, numerous hand samples and polished sections collected from the Hog Heaven district were available through the Anaconda Research Collection archived at Montana Tech, as well as archived specimens within the Montana Tech Department of Geological Engineering.

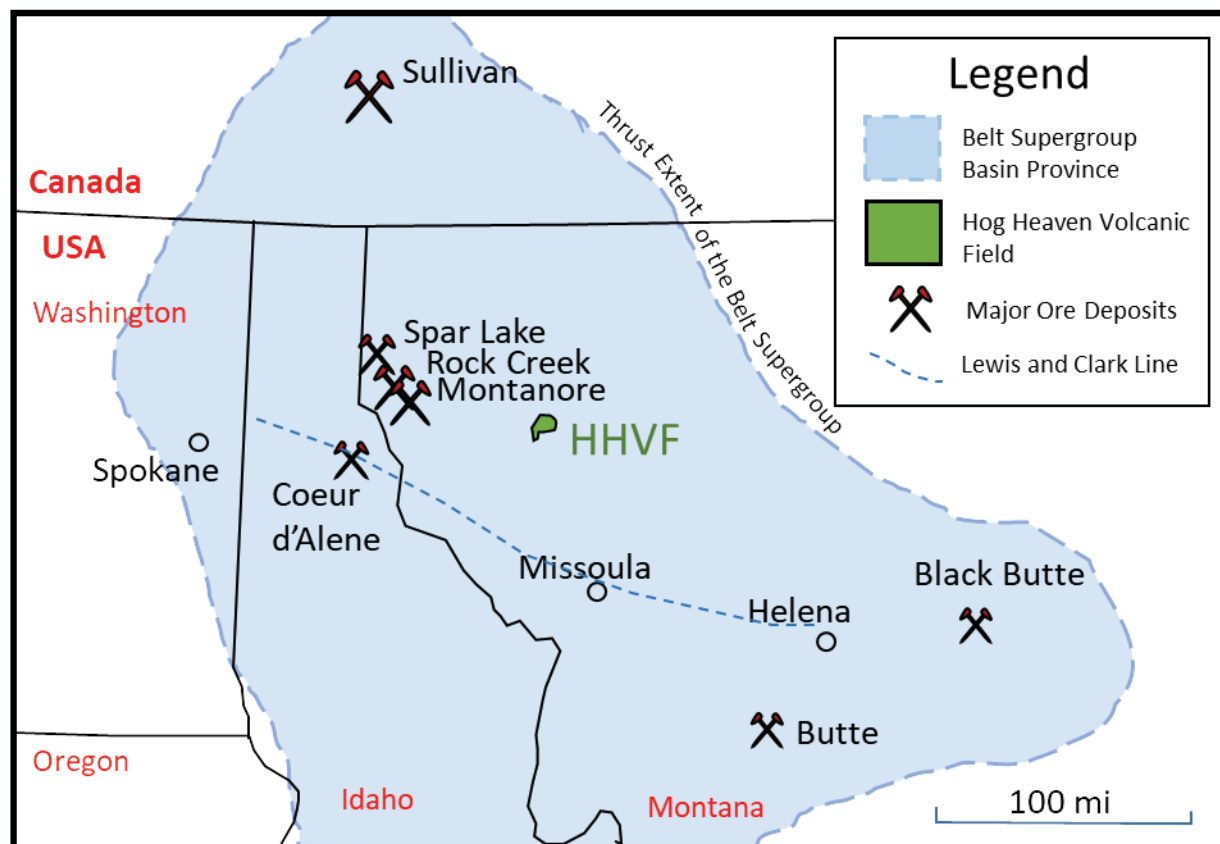


Figure 1. Generalized map showing the location of the Hog Heaven Volcanic Field (HHVF) and extent of the Belt Basin province (after Lydon, 2007; Vuke and others, 2007).

Ore samples were selected from preliminary reconnaissance work performed using a Niton portable X-ray fluorescence instrument, and studied by reflected and transmitted light microscopy and SEM-EDX at the Montana Tech campus.  $\delta^{34}\text{S}$  analyses of sulfides (pyrite, galena, and sphalerite),  $\delta^{34}\text{S}$  and  $\delta^{18}\text{O}$  analyses of barite, and  $\delta^{34}\text{S}$ , sulfate- $\delta^{18}\text{O}$ , and  $\delta\text{D}$  analyses of alunite were performed at the University of Nevada-Reno using a Eurovector elemental analyzer interfaced to a Micromass Isoprime stable isotope ratio mass spectrometer. For the alunite samples, the analytical method used provides the  $\delta^{18}\text{O}$  value of the sulfate ( $\text{SO}_4$ ) component only, and excludes the hydroxyl (OH) component. Preparation of mineral separates (e.g., alunite and pyrite) for isotopic analysis followed the method of Wasserman and others (1992).  $\delta^{34}\text{S}$  analyses were performed after the methods of Giesemann and others (1994) and Grassineau and others (2001),  $\delta^{18}\text{O}$  analyses were performed after the method of Kornexl and others (1999), and  $\delta\text{D}$  analyses were performed after the method of Hilker and others (1999).

## Results

### *Hydrothermal Alteration*

Outcrops and drill core samples from Hog Heaven show alteration patterns characteristic of volcanic-hosted, high-sulfidation epithermal deposits (Arribas, 1995). The most intensely altered rocks are a spongy mass of microcrystalline silica with vugs up to 3 to 5 cm in diameter outlining the former presence of sanidine phenocrysts that completely dissolved (figs. 2B,2D). The vuggy quartz transitions laterally into quartz-alunite alteration where sanidine has been replaced by fine-grained, pink alunite (fig. 2A), and/or argillic alteration that is marked by an abundance of white kaolinite clay (figs. 2C,2D). Marginal parts of the deposit are weakly altered to illite-montmorillonite. These alteration types, typical of high-sulfidation epithermal deposits, have previously been documented at Hog Heaven by Cossaboom (1981), Jepson (1993), and Lange and others (1994).





Figure 2. Advanced argillic alteration. (A) Pink, euhedral alunite. (B) Vuggy silica with sanidine feldspars completely dissolved. (C) Kaolinite (white) after feldspars. (D) Kaolinite, vuggy silica and Fe oxides.

### *Ore and Gangue Mineralogy*

The Flathead Mine and adjacent properties in the Hog Heaven district have an extensive and detailed mineral paragenesis. Textures observed in hand sample and under the microscope helped to identify three mineralizing stages, consisting of Stage 1 enargite-pyrite-alunite, Stage 2 Ag-Pb-Sb-Bi sulfosalts, and Stage 3 sphalerite-galena-barite. Pyrite and marcasite are prevalent throughout the deposit and in each stage of mineralization.

Stage 1 mineralization formed intergrown pyrite-enargite-alunite-aluminophosphate sulfate (APS) minerals (fig. 3A). The pyrite and marcasite frequently have elevated Cu, As, and Pb concentrations (0.5–6 wt% based on SEM-EDX), while enargite contains varying concentrations of Ag and Sb (0.2–1 wt%). Under SEM observation, it is common for each alunite blade to contain a small, euhedral grain of APS in the center. The most common APS minerals found at Hog Heaven are svanbergite ( $\text{SrAl}_3(\text{PO}_4)(\text{SO}_4)(\text{OH})_6$ ) and woodhouseite ( $\text{CaAl}_3(\text{PO}_4)(\text{SO}_4)(\text{OH})_6$ ). APS minerals are also found associated with kaolinite and quartz in argillically altered rock.

Stage 1 mineralization was followed by a complex Stage 2 mineralization consisting of entwined Pb-Sb-Bi-Ag sulfosalts (figs. 3E,3F). Phases identified so far in this study include aramayoite ( $\text{Ag}_3\text{Sb}_2(\text{Bi},\text{Sb})\text{S}_6$ ), jordanite ( $\text{Pb}_{14}(\text{As},\text{Sb})_6\text{S}_{23}$ ), matildite ( $\text{AgBiS}_2$ ), gratonite ( $\text{Pb}_9\text{As}_4\text{S}_{15}$ ), Ag-rich tetrahedrite, and members of the lillianite



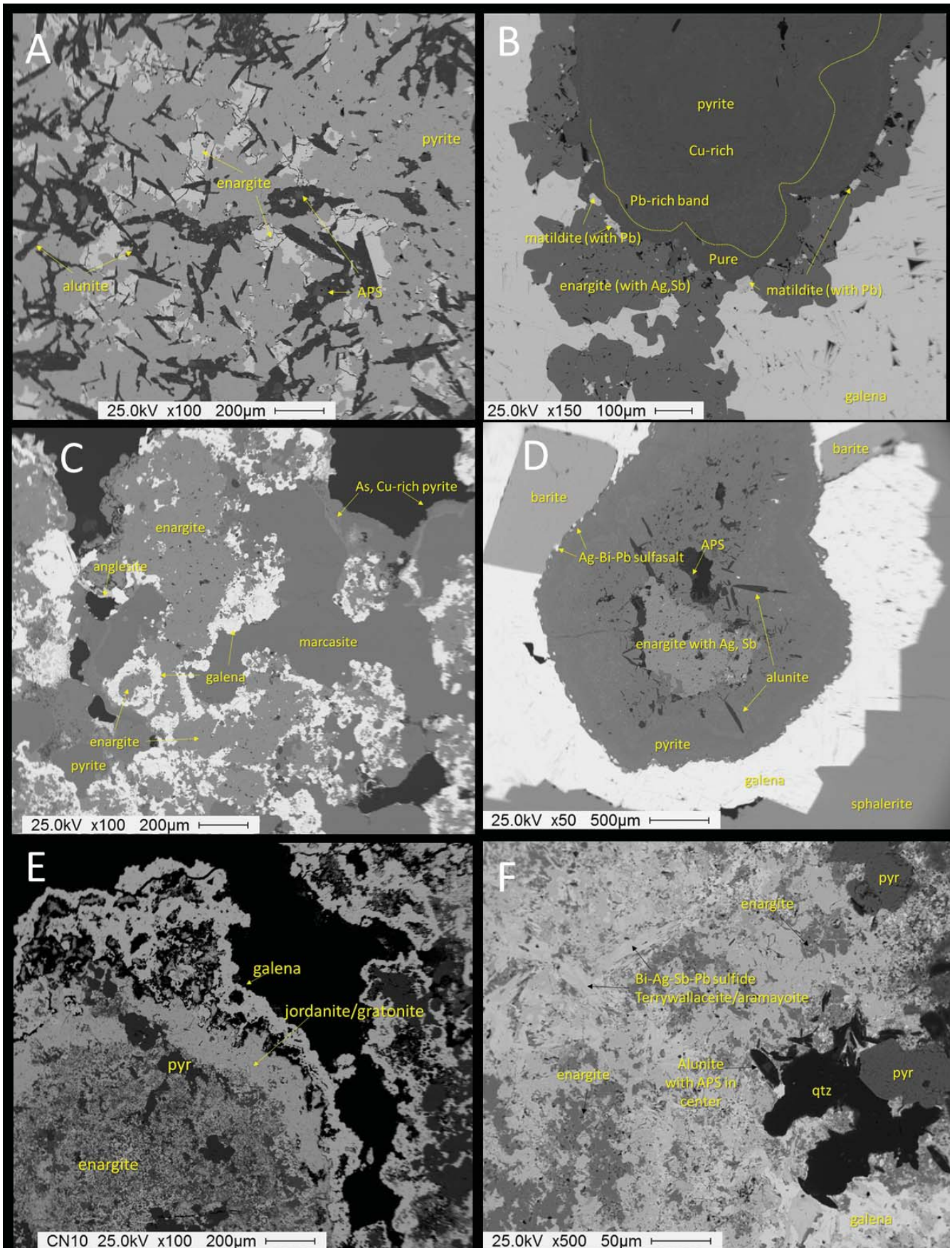


Figure 3. SEM-BSE image of mineralization at Hog Heaven. (A) Stage 1 mineralization of pyrite-enargite-alunite-APS. (B) Zoned pyrite (Cu/Pb-rich to pure) and enargite (Stage 1) lined with the Pb-matildite form of Stage 2. (C) All three stages with anglesite-Cu/As-rich pyrite form of Stage 2. (D) All three stages with small speckles of Ag-Bi-Pb sulfosalt form of Stage 2. (E and F) Complex retrograde intergrowths of all three stages. Mineral abbreviations are pyrite (pyr) and quartz (qtz).

group, including terrywallaceite ( $\text{AgPb}(\text{Sb,Bi})_3\text{S}_6$ ). Pyrite rich in As and Cu appears to have formed towards the end of this mineralizing stage with anglesite ( $\text{PbSO}_4$ ; fig. 3C). Due to the oxidized conditions of high-sulfidation deposits, and the occurrence of anglesite as discrete grains next to fresh galena, the anglesite is interpreted as possibly hypogene.

Open space deposition of coarse-grained galena, sphalerite, and barite was the final Stage 3 mineralizing event (figs. 3B–3E). Galena is found as large euhedral crystals and as reaction rims on Stage 1 and 2 minerals. Most of the sphalerite is pale brown to red brown and translucent, and is closely associated (often intergrown) with galena or filling vugs as euhedral crystals. Most of the sphalerite grains examined by SEM-EDS were Fe-poor ( $< 0.1$  wt% Fe), although one sample had a much higher Fe concentration (up to 8 wt% Fe). The barite is milky white to transparent, euhedral, and fills vugs left from advanced argillic alteration. The barite has abundant fluid inclusions.

### *Stable Isotopes*

All stable isotope results are reported in table 1. Sulfide minerals at Hog Heaven have a  $\delta^{34}\text{S}$  range of 0.4 to 5.8‰ (fig. 4). A progression from isotopically lighter to heavier  $\delta^{34}\text{S}$  values is observed for galena to sphalerite to pyrite, respectively. Sulfate  $\delta^{34}\text{S}$  values are isotopically heavy, ranging from 19.6 to 37.1‰, with barite being isotopically heaviest (fig. 4).

Samples containing two or more coexisting S-bearing minerals were used for S-isotope geothermometry calculations. This type of analysis assumes that the minerals in the sample formed at the same time at isotopic

Table 1. Stable isotope data.

| Sample       | Mineral    | $\delta^{34}\text{S}_{\text{VCDT}}(\text{‰})$ | $\delta^{18}\text{O}_{\text{VSMOW}}(\text{‰})$ | $\delta\text{D}_{\text{VSMOW}}(\text{‰})$ |
|--------------|------------|---|--|---|
| IK-HH-33B    | Galena     | 0.4   |  |   |
| IK-HH-6B     | Galena     | 0.8   |  |   |
| IK-HH-33A    | Sphalerite | 2.4   |  |   |
| IKHH-7       | Sphalerite | 2.7   |  |   |
| IK-HH-33C    | Pyrite     | 2.9   |  |   |
| IK-HH-34     | Pyrite     | 3.6   |  |   |
| IK-HH-36B    | Sphalerite | 3.7   |  |   |
| IK-HH-6C     | Sphalerite | 3.8   |  |   |
| IKHH-7       | Pyrite     | 3.9   |  |   |
| IK-HH-28A    | Pyrite     | 4.3   |  |   |
| IKHH-19      | Galena     | 4.6   |  |   |
| IK-HH-35     | Pyrite     | 4.9   |  |   |
| HH-AMC-1951  | Pyrite     | 5.3   |  |   |
| IKHH-19      | Pyrite     | 5.8   |  |   |
| IK-HH-28A    | Alunite    | 19.6  | -3.9   |   |
| IK-HH-28B    | Alunite    | 23.0  | 1.6  |   |
| AMC-1951     | Alunite    | 28.3  | 6.1  | -39                                       |
| CG-HH-7      | Alunite    | 28.3  | 6.8  | -40                                       |
| CG-HH-21     | Alunite    | 30.1  | 10.0   | -37                                       |
| HH-alunite-1 | Alunite    | 32.0  | 9.4  | -40                                       |
| IK-HH-6A     | Barite     | 34.5  | 9.0  |   |
| IK-HH-36A    | Barite     | 34.9  | 8.5  |   |
| HH-barite-1  | Barite     | 35.5  | 10.2   |   |
| HH-barite-2  | Barite     | 36.3  | 9.8  |   |
| HH-barite-3  | Barite     | 37.1  | 8.9  |   |



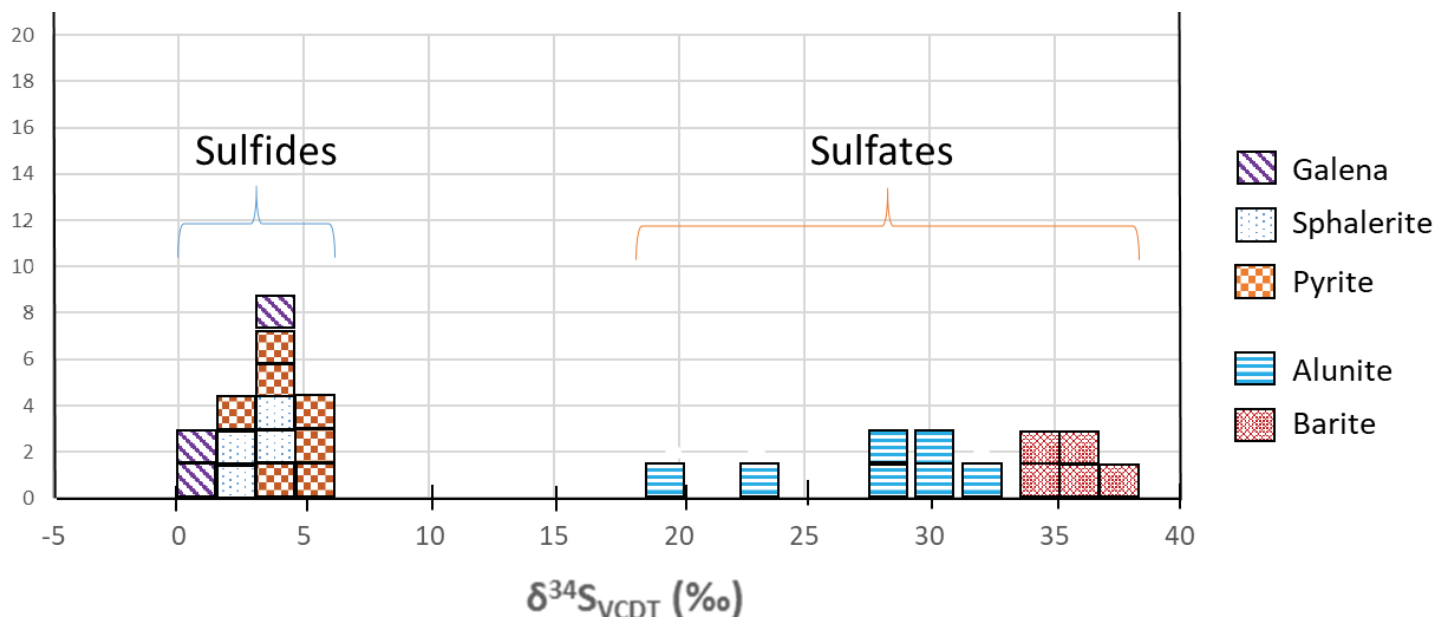


Figure 4. S-isotope results for sulfide and sulfate minerals from Hog Heaven.

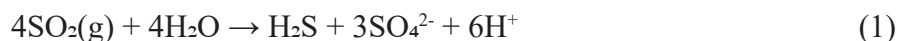
equilibrium, and were not isotopically reset by later events. Fractionation factors used to calculate temperatures were taken from the “Alpha Delta” website (Beaudoin and Therrien, 2004, 2009). The temperatures obtained (table 2) were 226°C for a pyrite–sphalerite pair, 249 and 304°C for two galena–sphalerite pairs, and 261 and 459°C for two pyrite–alunite pairs. With the exception of the 459°C value (which may be due to late alteration), these results are in good agreement with measured temperatures of homogenization for fluid inclusions in barite from Hog Heaven (I. Kallio, unpub. data), and are typical for epithermal deposits.

Table 2. Geothermometry results calculated from S-isotope data from sphalerite (sph), pyrite (pyr), galena (gal), and alunite (al) pairs.

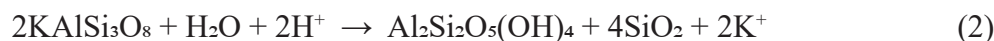
| Sample      | Mineral | Temperature (°C) | Depth (ft) |
|-------------|---------|------------------|------------|
| IK-HH-7     | sph-pyr | 226              | 337        |
| IK-HH-6     | gal-sph | 249              | 724        |
| IK-HH-33    | gal-sph | 304              | 890        |
| HH-AMC-1951 | pyr-al  | 261              | AMC        |
| IK-HH-28    | pyr-al  | 459              | 340        |

## Discussion

Consistent with previous work, this study has found mineral assemblages and temperatures similar to other high-sulfidation epithermal deposits. The deep, advanced argillic alteration is due to the disproportionation of magmatic-hydrothermal  $\text{SO}_2$  as it cools and mixes with meteoric waters at around 350°C (Arribas, 1995). The disproportionation of  $\text{SO}_2$  can be expressed by equation 1:



At Hog Heaven, the  $\text{H}_2\text{S}$  formed by this reaction precipitated as sulfide minerals; the sulfate formed APS, alunite, and barite; and the protons attacked the host rock to form advanced argillic and argillic alteration. An example reaction showing the breakdown of K-feldspar to kaolinite can be written as follows:



The excess silica released from reaction (2) formed gray, microcrystalline quartz veins.

Stage 1 pyrite–enargite–alunite mineralization at Hog Heaven closely resembles early stage mineralization in high-sulfidation (HS) epithermal deposits worldwide (Simmons and others, 2005). However, whereas HS

deposits are usually mined for Au with byproduct Ag-Cu, the mines in the Hog Heaven district were mainly mined for Ag and Pb. Worldwide, the HS epithermal deposit that most closely resembles Hog Heaven is the Julcani district, Peru. Like Hog Heaven, the ores at Julcani are rich in Ag-Sb-Bi-Pb sulfosalts with a high Ag/Au ratio (Deen and others, 1994; Sack and Goodell, 2002); the volcanic rocks that host the mineralization at Julcani and Hog Heaven are of similar composition and age (Miocene-Oligocene), and are deposited on an older, thick sequence of metasediments.

Figure 5 illustrates the  $\delta^{34}\text{S}$  and  $\delta^{18}\text{O}$  compositions of sulfate in alunites and barites from Hog Heaven. The orange boxes correspond to typical ranges for the isotopic composition of magmatic-hydrothermal alunites from Rye and others (1992), and assume a starting hydrothermal fluid with  $\delta^{18}\text{O} \approx +6$  and  $\delta^{34}\text{S} \approx 0\text{‰}$ . The lower the temperature of formation, the greater the isotopic separation between alunite and the parent fluid. The data for Hog Heaven alunites (green boxes in fig. 5) show a similar pattern, but require a starting hydrothermal fluid that is enriched in  $\delta^{34}\text{S}$  and depleted in  $\delta^{18}\text{O}$  relative to the fluid of Rye and others (1992). Barite (blue symbols in fig. 5) has the heaviest  $\delta^{34}\text{S}$  values at Hog Heaven, and may have formed at the lowest temperature (greatest isotopic separation from parent hydrothermal fluid).

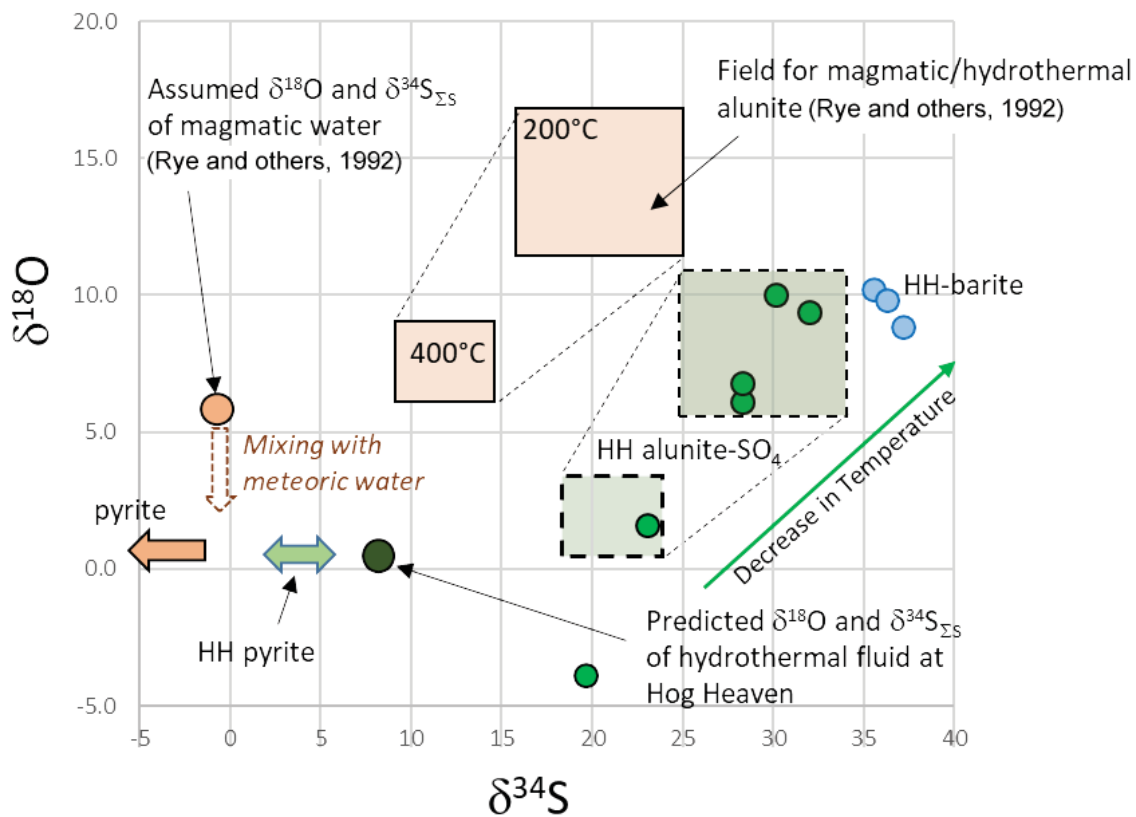


Figure 5. Hog Heaven  $\delta^{34}\text{S}$  and  $\delta^{18}\text{O}$  plot with magmatic alunite field from Rye and others (1992).

The sulfides and sulfates at Hog Heaven are enriched in  $\delta^{34}\text{S}$  and plot outside the range of “typical” hydrothermal alunite and pyrite as suggested by Rye and others (1992; fig. 5). By applying the same isotope fractionation factors for alunite-water that Rye and others used to construct the orange boxes in figure 5, but in reverse, we estimate that the  $\delta^{34}\text{S}$  value for bulk sulfur in the Hog Heaven hydrothermal fluid was close to +8‰, and the  $\delta^{18}\text{O}$  of the fluid was close to 0‰. A reasonable explanation for the  $\delta^{34}\text{S}$  enrichment is assimilation of sulfur from the Belt Supergroup. Field and others (2005) summarized Belt Supergroup  $\delta^{34}\text{S}$  analyses from the work of Lyons and others (2000), Chandler and Grégoire (2000), and Strauss and Schieber (1990), which show a wide range, with barite  $\delta^{34}\text{S} = 13.6$  to  $32.3\text{‰}$ , and pyrite as heavy as  $36.7\text{‰}$ . The Spar Lake Cu-Ag deposit, hosted in the Revett Formation and located 105 km northwest of Hog Heaven, has a similar range in  $\delta^{34}\text{S}$  for Cu-Fe sulfides of 2 to  $23\text{‰}$  (Hayes and others, 1989).

Field and others (2005) suggested that magmatic assimilation of isotopically heavy Belt sulfur could have been responsible for the heavier than normal  $\delta^{34}\text{S}$  of the parent hydrothermal fluid responsible for the Butte ore body, which they estimated to be +11%. In addition to assimilation of S, porphyry magmas could have assimilated metals from the Precambrian deposits, helping to explain the richness of the Butte ore body as well as its polymetallic nature (e.g., high Ag, Pb, Zn in addition to Cu-Mo). These same ideas could apply to Hog Heaven. Remobilization of metals and sulfur out of a deep, preexisting Sullivan-type SEDEX deposit beneath Hog Heaven could explain the unique style of HS epithermal mineralization that occurred more than a billion years later when the HHVF was emplaced (fig. 6).

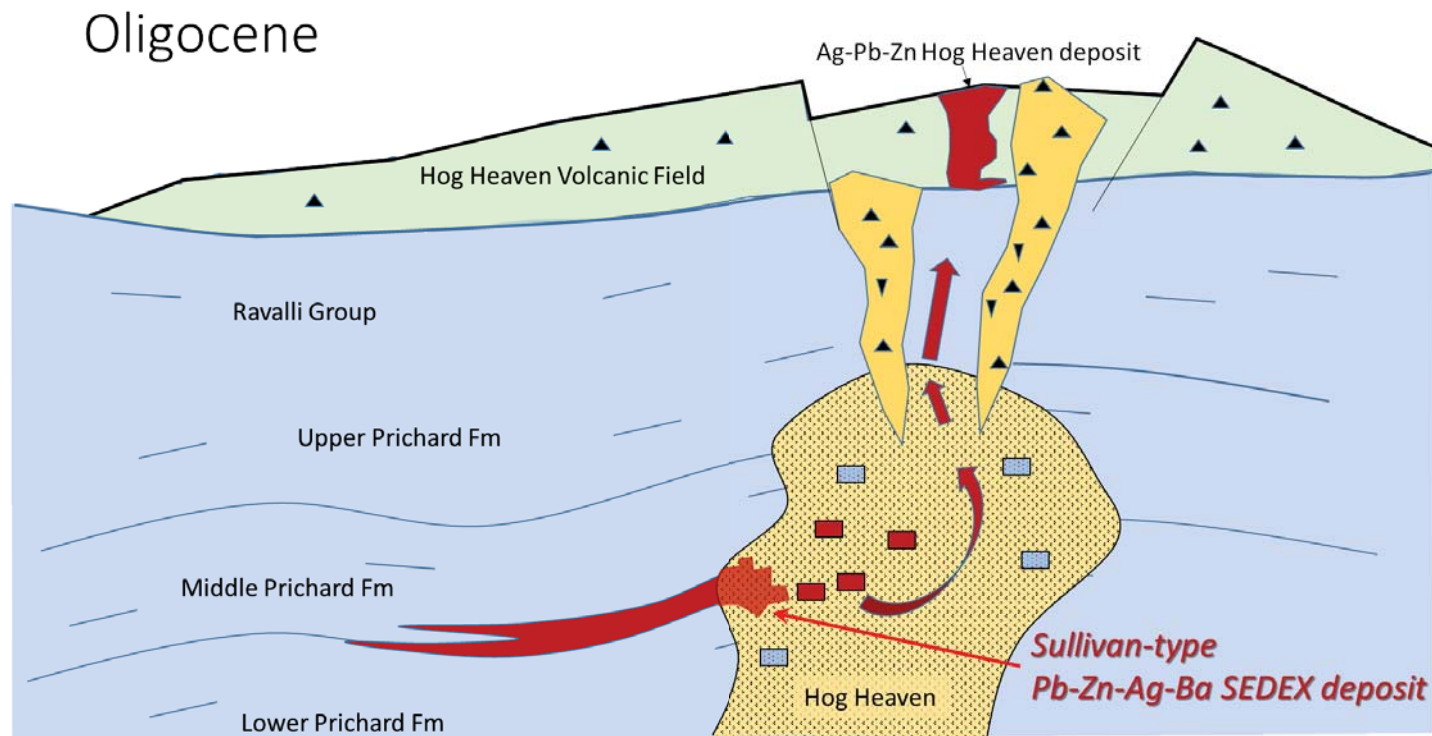


Figure 6. Schematic diagram showing the possible existence of SEDEX-style Ag-Pb-Zn-Ba mineralization in the lower Belt section that may have been remobilized by the Oligocene magmatic-hydrothermal event to form the Ag-Pb-Zn-Ba epithermal mineralization at Hog Heaven.

Most HS epithermal deposits show a clear genetic link to underlying porphyry-style mineralization (Simmons and others, 2005). To date, exploration drilling at Hog Heaven has focused on delineating a shallow, bulk-mineable target within the altered volcanic rocks. Testing the idea of a buried porphyry at Hog Heaven would likely require drilling of much deeper holes, possibly combined with geophysics.

### Acknowledgments

We would like to thank Brixton Metals for support and access to property throughout this whole study. We also thank Gary Wyss (SEM-EDS) for analytical work. MBMG geologist Kaleb Scarberry and Montana Tech graduate student Ethan Coppage helped tremendously with this project (EDMAP and STATEMAP). The field season was made possible by the EDMAP program from USGS. Additional funding came from the Montana Geological Society, the American Federation of Mineralogical Societies, and the Montana Tech Stan and Joyce Lesar Foundation.

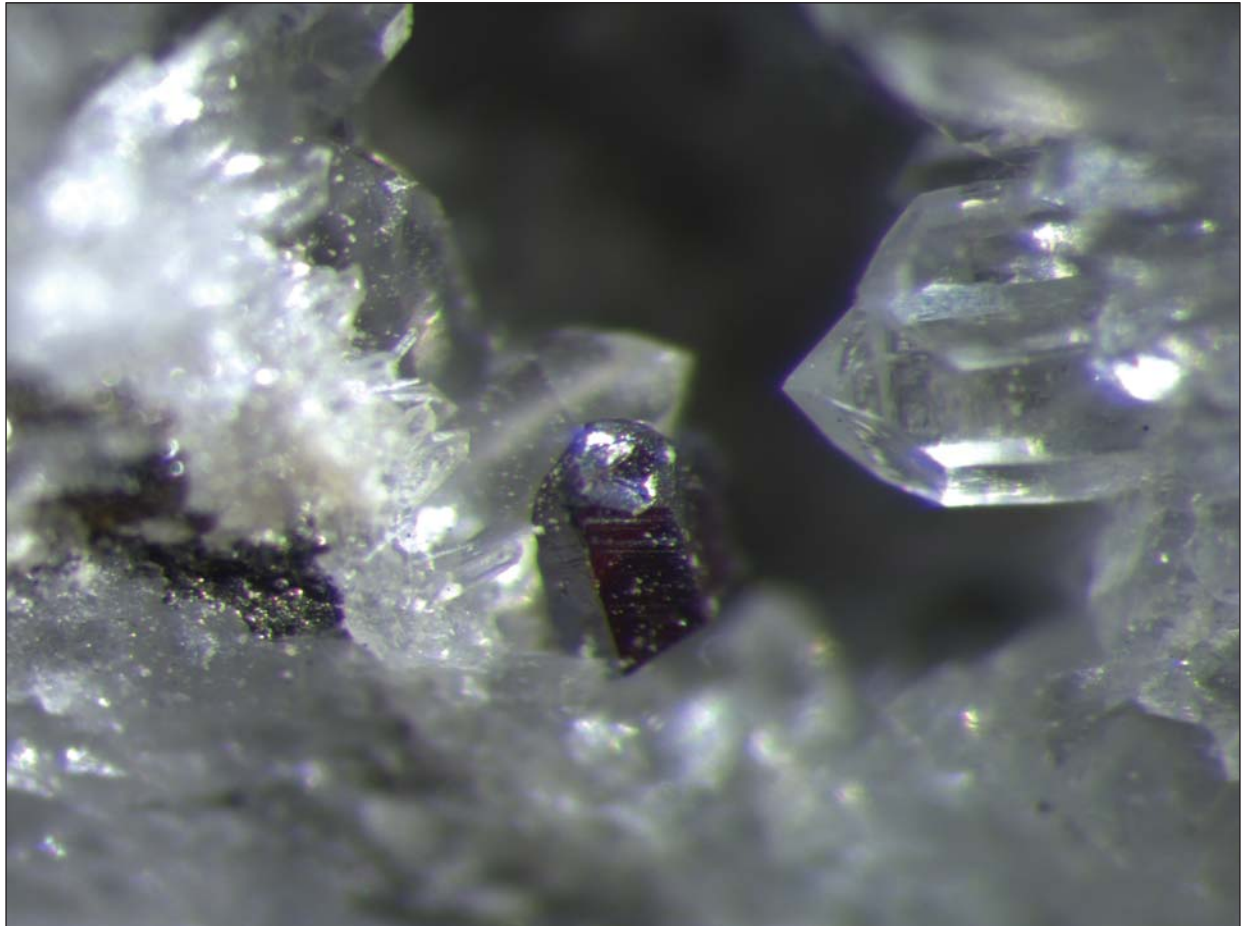
### References

- Arribas Jr., A., 1995, Characteristics of high-sulfidation epithermal deposits, and their relation to magmatic fluid: Mineralogical Association of Canada Short Course, v. 23, p. 419–454.
- Beaudoin, G., and Therrien, P., 2004, The web stable isotope fractionation calculator, in Handbook of stable isotope analytical techniques, Volume I, De Groot, P.A., ed.: Amsterdam, Elsevier, p. 1045–1047.



- Beaudoin, G., and Therrien, P., 2009, The updated web stable isotope fractionation calculator, in Handbook of stable isotope analytical techniques, Volume II, De Groot, P.A., ed.: Amsterdam, Elsevier, p. 1120–1122.
- Chandler, F.W., and Grégoire, D.C., 2000, Sulphur, strontium and boron isotopes from replaced sulphate evaporite nodules in the Altyn Formation, lower Belt Supergroup, Montana: Clues to the sedimentary environment of the Sullivan deposit: Geological Association of Canada, Mineral Deposits Division, Special Publication, v. 1, p. 251–258.
- CoCa Mines Inc., 1983, Hog Heaven project—Geology of the main mine and Ole Hill: CoCa Mines, Inc. Company Reports.
- Cossaboom, C.C., 1981, Alteration petrology and mineralization of the Flathead Mine Hog Heaven Mining District, Montana: M.S. Thesis, University of Montana, Missoula, MT.
- Deen, J.A., Rye, R.O., Munoz, J.L., and Drexler, J.W., 1994, The magmatic hydrothermal system at Julcani, Peru: Evidence from fluid inclusions and hydrogen and oxygen isotopes: *Economic Geology*, v. 89, p. 1924–1938.
- Field, C.W., Zhang, L., Dilles, J.H., Rye, R.O., and Reed, M.H., 2005, Sulfur and oxygen isotopic record in sulfate and sulfide minerals of early, deep, pre-Main Stage porphyry Cu–Mo and late Main Stage base-metal mineral deposits, Butte district, Montana: *Chemical Geology*, v. 215, p. 61–93.
- Giesemann, A., Jager, H.J., Norman, A.L., Krouse, H.P. and Brand, W.A., 1994, On-line sulfur-isotope determination using an elemental analyzer coupled to a mass spectrometer: *Analytical Chemistry*, v. 66, p. 2816–2819.
- Grassineau, N.V., Matthey, D.P., and Lowry, D., 2001, Sulfur isotope analysis of sulfide and sulfate minerals by continuous flow-isotope ratio mass spectrometry: *Analytical Chemistry*, v. 73, p. 220–225.
- Hayes, T.S., Rye, R.O., Whelan, J.F., and Landis, G.P., 1989, Geology and sulphur-isotope geothermometry of the Spar Lake stratabound Cu–Ag deposit in the Belt Supergroup, Montana, in Boyle, R.W., Brown, A.C., Jefferson, C.W., Jowett, E.C., and Kirkhom, R.V., eds., *Sediment-hosted stratiform copper deposits*: Geological Association of Canada, Special Paper 36, p. 315–338.
- Hilkert, A.W., Douthitt, C.B., Schlüter, H.J., and Brand, W.A., 1999, Isotope ratio monitoring gas chromatography/mass spectrometry of D/H by high temperature conversion isotope ratio mass spectrometry: *Rapid Communications in Mass Spectrometry*, v. 13, p. 1226–1230.
- Jepson, W.E., 1993, Lateral and vertical zonation of clay minerals and associated alteration products at the Hog Heaven Mine and Ole Hill deposit, Hog Heaven Mining District, Flathead County, Montana: Missoula, University of Montana, M.S. thesis.
- Kornexl, B.E., Gehre, M., Höffling, R., and Werner, R.A., 1999, On-line  $\delta^{18}\text{O}$  measurement of organic and inorganic substances: *Rapid Communications in Mass Spectrometry*, v. 13, p. 1685–1693.
- Lange, I., Zehner, R., and Hahn, A., 1994, Geology, geochemistry, and ore deposits of the Oligocene Hog Heaven volcanic field, northwestern Montana: *Economic Geology*, v. 89, p. 1939–1963.
- Lyons, T.W., Luepke, J.J., Schreiber, M.E., and Zieg, G.A., 2000, Sulfur geochemical constraints on Mesoproterozoic restricted marine deposition: lower Belt Supergroup, northwestern United States: *Geochimica et Cosmochimica Acta*, v. 64, p. 427–437.
- Lydon, J.W., 2007, Geology and metallogeny of the Belt–Purcell Basin: Geological Association of Canada, Mineral Deposits Division, p. 581–607.
- Rostad, O.H., and Jonson, D.C., 1997, Geology, geochemistry, and ore deposits of the Oligocene Hog Heaven volcanic field, northwestern Montana: *Discussion: Economic Geology*, v. 92, p. 749–750.
- Rye, R.O., Bethke, P.M., and Wasserman, M.D., 1992, The stable isotope geochemistry of acid sulfate alteration: *Economic Geology*, v. 87, p. 225–262.

- Sack, R.O., and Goodell, P.C., 2002, Retrograde reactions involving galena and Ag-sulphosalts in a zoned ore deposit, Julcani, Peru: *Mineralogical Magazine*, v. 66, p. 1043–1062.
- Shanon, P.J., 1935, Genesis of the ore at the Flathead Mine, northwestern Montana: *Economic Geology*, v. 30, p. 585–603.
- Simmons, S.F., White, N.C., and John, D.A., 2005, Geological characteristics of epithermal precious and base metal deposits: *Economic Geology 100th Anniversary Volume*, p. 485–522.
- Strauss, H., and Schieber, J., 1990, A sulfur isotope study of pyrite genesis: The Mid-Proterozoic Newland Formation, Belt Supergroup, Montana: *Geochimica et Cosmochimica Acta*, v. 54, p. 197–204.
- Vuke, S., Porter, K., Lonn, J., and Lopez, D., 2007, Geologic map of Montana: Montana Bureau of Mines and Geology Geologic Map 62.
- Wasserman, M.D., Rye, R.O., Bethke, P.M., and Arribas Jr, A., 1992, Methods for separation and total stable isotope analysis of alunite: U.S. Geological Survey Open-File Report, 92-9, 20 p.
- Zehner, R.E., 1987, Petrology, structure, and tectonic setting of the Hog Heaven volcanics, and their relationship to mineralization: Missoula, University of Montana, M.S. thesis.



Pyrrargyrite. Mystery Mine, MT. Courtesy of Stanley L. Korzeb.

# The Processing and Recycling of Garnet Tailings for Application in Concrete

Avimanyu Das,<sup>1</sup> Brandon Hill,<sup>1</sup> Peter Rossiter,<sup>2</sup> Gary Wyss,<sup>3</sup> Courtney Young,<sup>1</sup> and Matt Egloff<sup>4</sup>

<sup>1</sup>*Metallurgical and Materials Engineering, Montana Tech, Butte, Montana*

<sup>2</sup>*GMA Garnet, Alder, Montana*

<sup>3</sup>*Center for Advanced Mineral & Metallurgical Processing, Montana Tech, Butte, Montana*

<sup>4</sup>*Civil Engineering, Montana Tech, Butte, Montana*

## Abstract

Processing and recycling of tailings from a garnet processing plant were investigated with a goal to recover the garnet lost during their operations. The tailings contained around 15% garnet with a wide size distribution. To reduce processing costs, an investigation was restricted to two different size classes either with or without comminution. A combination of magnetic and gravity separation with Crossflow separator and shaking table in the absence of comminution failed to recover enough garnet from the tailings to warrant recycling. However, partial comminution with a roll crusher provided improved results in terms of garnet recovery and the simplicity of the processing scheme. After sizing, the +1.18 mm material was crushed and then homogenized with the -1.18 mm fraction. The mixture was processed using only tabling and magnetic separation. A garnet-rich concentrate was obtained at 15% mass yield with nearly 80% garnet content. Because this was significant garnet recovery, recycling of the tailings is likely to help plant economics significantly in addition to reducing the tailings volume. Results of that investigation are reported elsewhere. The resulting tailings were then reprocessed to remove as much mica as possible using similar gravity and magnetic separations. The tailings both before and after mica removal were used as a fine aggregate or sand to make concrete. In this paper, the performance of using the tailings in this capacity are reported.

## Introduction

Garnet is a silicate mineral. It is known in ancient times for its gemstone application, mainly the red variety. However, in modern times, it is best known for its industrial applications. These include abrasives for sand blasting and cutting (Curry, 2019) and fine aggregate for concrete and asphalt. Garnet sand is very abrasive. Fine aggregate suitable for concrete ranges in size from  $\frac{3}{8}$  in (9.5 mm) to #100 sieve (150  $\mu\text{m}$ ; ASTM, 2018).

Garnet actually refers to a group of minerals (Callaghan and Curry, 2016). The generic chemical formula for this group is  $A_3B_2(\text{SiO}_4)_3$ , with an isometric crystal structure where A represents  $\text{Ca}^{2+}$ ,  $\text{Mg}^{2+}$ ,  $\text{Fe}^{2+}$ , and/or  $\text{Mn}^{2+}$  and B represents  $\text{Al}^{3+}$ ,  $\text{Fe}^{3+}$ , and/or  $\text{Cr}^{3+}$ . Most of the time, garnet is found to be associated with gangue minerals such as quartz, mica, feldspar, and hornblende. Oxides and aluminosilicates such as pyroxene, magnetite, ilmenite, rutile, and even sulfides such as pyrite are also found to be associated with garnet as gangue minerals (Espadas and others, 2000).

Industrial processing of garnet relies heavily on gravity and magnetic separations. For the abrasive application, the larger garnet size is preferred because, after the initial application, they can be recycled. The size distribution affects properties such as air entrainment in concrete and compaction in asphalt.

Association of hornblende with garnet makes the separation more challenging for mineral processing personnel, especially when there is increasing Ca or Mg substitution into the garnet, which causes the specific gravity to decrease. Significant loss of garnet into tailings particularly occurs when recovery in the coarse size range is primarily targeted and the additional cost of comminution is avoided. Therefore, a study was done to recover the garnet from the tailings of an operating plant with and without comminution. Results without comminution required elaborate processing steps and yielded low recovery that did not justify the application. In contrast, partial comminution of the tailings led to a simple processing strategy that yielded a garnet concentrate at 15% mass yield with nearly 80% garnet content. Results of this study are reported in Das and others (2020).



A simultaneous study was undertaken to use the resulting tailings as a fine aggregate or sand additive in concrete. To do this, the tailings from garnet removal were reprocessed to remove as much mica as possible, because it was believed that the mica might act as shear planes and weaken the concrete. Experiments were therefore conducted on the tailings following garnet removal as well as the tailings following garnet and mica removal.

### Material Characterization

About 100 kg of sample was collected from the tailings stream at the operating plant and transported to the lab, where it was spread on a tarpaulin for air drying, homogenized by coning and quartering, and then split by fractional shoveling into 48 stock samples, each weighing approximately 2 kg. One of the stock samples was arbitrarily selected and subjected to different types of characterization (Das and others, 2020).

The materials were also used to make concrete. Batches of 208.4 lb were prepared using a small concrete mixer. A process was used to remove the mica. Three different fine aggregates were used: a purchased Sacrete brand sand was used as a baseline for comparison to unprocessed garnet sand and processed garnet sand (with significant mica removed). The properties and responses of the three batches were found to be nearly identical in these standard ACI concrete acceptance tests.

The concrete recipe used is shown in table 1. Slump, density, and air entrainment were measured (table 2). Standard 4-in-diameter by 8-in-tall cylinders were cast and cured. The results of the strength measurements on the concrete samples as they cured for 90 days are shown in table 3.

Table 1. Concrete recipe.

| Constituent                      | Parts by Weight | Weight (lbs) |
|----------------------------------|-----------------|--------------|
| Portland Cement Type I/II        | 1               | 31.3         |
| Fine Aggregate (Sand)            | 2               | 62.7         |
| Coarse Aggregate (3/4 in gravel) | 3               | 94.0         |
| Water                            | 0.65            | 20.4         |

Table 2. Curing temperature, slump, air entrainment, and density.

| Test                                     | Sacrete Brand Sand | Garnet Sand Unprocessed | Garnet Sand Processed |
|--|--------------------|-------------------------|-----------------------|
| Temperature (°F)                         | 60–80              | 60–80                   | 60–80                 |
| Slump (inches)                           | 6.5                | 7.0                     | 6.5                   |
| Density, as mixed (lbs/ft <sup>3</sup> ) | 149.4              | 151.2                   | 153.4                 |
| Air entrainment (%)                      | 0.5                | 0.6                     | 0.5                   |

### Results And Discussions

In accordance with applicable ACI standards, concrete cylinders were cast, cured, and tested for strength at failure in compression over a period of 90 days. Results shown in table 3 were plotted as strength (psi) as a function of time (day), as shown in figure 1.

The purchased Sacrete brand sand made concrete with the greatest strength at just over 6100 psi, which is well above failure range of 2000–4000 psi for typical applications as shown in table 4 (VWorks Mobile Mix Concrete, 2019; International Code Council, 2019). The unprocessed garnet sand made concrete that failed at 4950 psi, which is 81% of the strength of the concrete made with Sacrete sand. When significant mica was removed, the concrete made with processed garnet sand gave a strength of 5750 psi, which was approximately 94% of the strength of the Sacrete sand. Clearly, as anticipated, the presence of mica in the sand weakens the concrete. However, because the quality of the concrete is still well above the 2000–4000 psi range, it can still be used for most applications. This recipe that was used not only provided a very workable, low air-entrained, high-strength concrete, it also has been shown to give significant and repeatable variation in performance when small adjustments to its composition are made. Montana Tech has significant archival data on this.

Table 3. Strength measurements of concrete made with tailings as a function of curing time for 90 days.

| Days | Sacrete Brand Sand (psi) | Garnet Sand Unprocessed (psi) | Garnet Sand Processed (psi) |
|------|--------------------------|-------------------------------|-----------------------------|
| 1    | 1551                     | 1045                          | 1688                        |
| 3    | 2511                     | 2046                          | 2827                        |
| 7    | 3518                     | 2662                          |                             |
| 8    |                          |                               | 3469                        |
| 14   | 4246                     | 3353                          | 4081                        |
| 21   | 4735                     | 3767                          | 4617                        |
| 28   | 5273                     | 4166                          | 4710                        |
| 35   | 5378                     | 4290                          |                             |
| 42   | 5444                     | 4478                          |                             |
| 49   | 5853                     |                               |                             |
| 56   |                          | 4864                          |                             |
| 63   | 5935                     | 4920                          |                             |
| 70   | 5919                     | 4979                          |                             |
| 77   | 6013                     | 4938                          |                             |
| 90   | 6109                     | 4956                          | 5761                        |

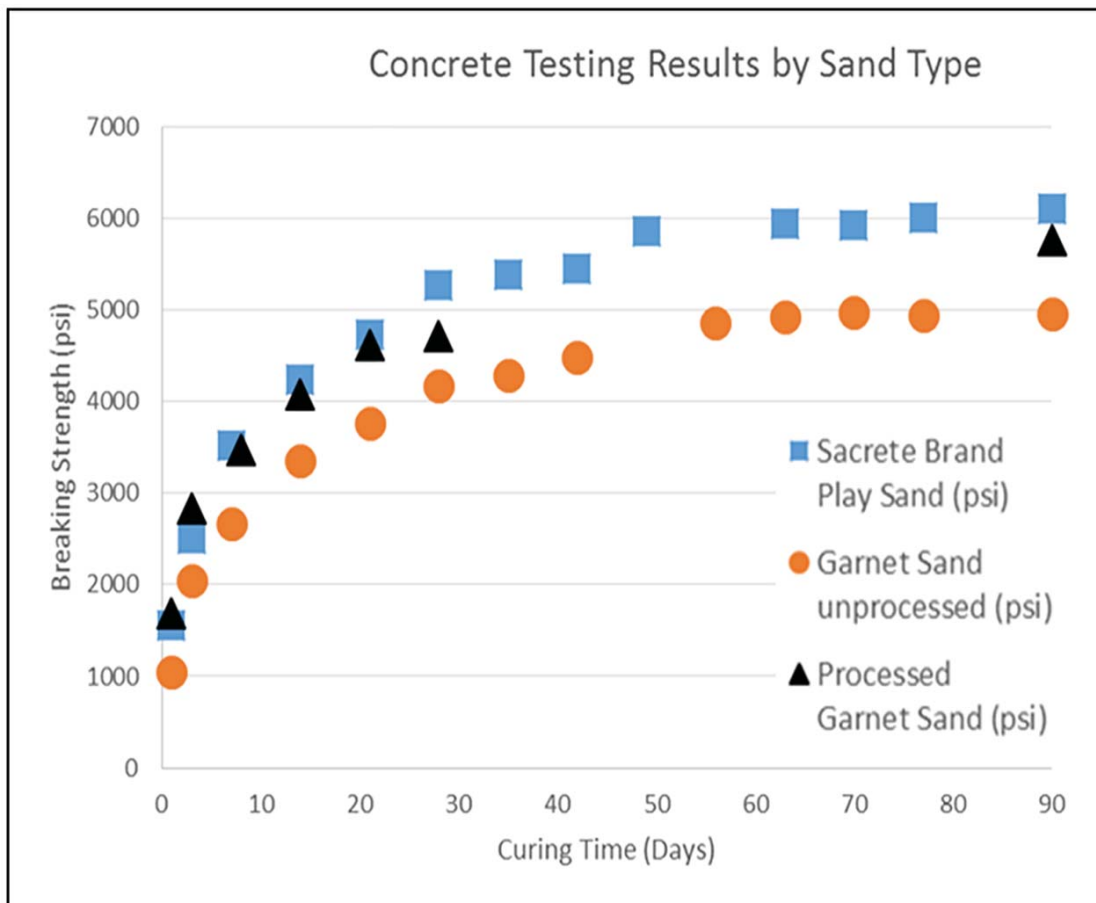


Figure 1. Concrete strength testing with curing time.

Table 4. Concrete Applications and Minimum Strengths  
(VWorks, 2019; International Code Council, 2019)

| Application                       | Strength (psi) |
|-----------------------------------|----------------|
| Fence posts, post holes           | 2500           |
| Residential sidewalks, patios     | 3000           |
| Steps, shed/trash slabs           | 3000           |
| Footings, foundations             | 3500           |
| Commercial sidewalks, curbs       | 3500           |
| Driveways, garage floors          | 3500           |
| Floor slabs, hot tub pads         | 3500           |
| Shops, warehouses, RV slabs       | 4000           |
| Roads, heavy traffic pavement     | 4000           |
| Suspended slabs, beams, walls     | 5000           |
| Dams, parking garages             | 6000+          |
| High-rise buildings, bridge decks | 10000+         |

### Conclusions

For most construction applications, a concrete with greater air entrainment, comparable slump and workability, and strength at failure in the 2000–4000 psi range is typically used. Because the tailings from an existing garnet operation essentially meet the size requirements of a sand, their use as a fine aggregate in concrete was investigated. However, the tailings contain significant amounts of mica that could cause the concrete to fail, so experiments were conducted on tailings in the absence and presence of mica. Results showed that, following garnet removal, adequate concrete can be made with a strength of 4950 psi, but the concrete is significantly stronger at 5750 psi with the mica removed. Thus mica removal is advisable but not a necessity for making the concrete as examined in this investigation.

### Acknowledgments

The financial assistance from Garnet USA to conduct the research and permission to publish the paper is greatly appreciated.

### References

- ASTM, 2018, Standard specification for concrete aggregates, ASTM International, West Conshohocken, PA, <https://www.astm.org/Standards/C33> [Accessed January 2020].
- Callaghan, R.M., and Curry, K.C., 2016, Garnet, industrial (advanced release), 2016 Minerals Yearbook, p. 28.1–28.4.
- Curry, K.C., 2019, Garnet (industrial), mineral commodity summaries: U.S. Geological Survey, 64-65, <https://prd-wret.s3-us-west-2.amazonaws.com/assets/palladium/production/s3fs-public/atoms/files/mcs-2019-garne.pdf> [Accessed January 2020].
- Das, A., Hill, B., Rossiter, P., Wyss, G., and Young, C., 2020, Characterization and processing of plant tailings for the recovery of fine garnet—A case study, Separation Science and Technology, submitted for publication.
- International Code Council, 2019, The strength of concrete, <https://shop.iccsafe.org/media/wysiwyg/material/9090S15-Sample.pdf> [Accessed January 2020].
- Munoz-Espadas, M., Lunar, R., and Martinez-Frias, J., 2000, The garnet placer deposit from SE Spain: Industrial recovery and geochemical features, Episodes, v. 23, no. 4, p. 266–269.
- VWorks Mobile Mix Concrete, 2019, Mix designs, <http://www.vworksmobileconcrete.com/Mix-Designs.htm?m=98&s=698> [Accessed January 2020]



## Merging Historical Data with Google Earth and ArcGIS

Anthony Roth

*Montana Bureau of Mines and Geology, Butte, Montana*

This project started as an idea in 2012 when the Mining Archives Department was asked to scan a collection donated to the Montana Historical Society by the Antonioli family. I was trying to figure out a fast and efficient way to geo-reference the center of mining claims or maps associated with each mining claim. The maps I use to reference locations come from survey and claim maps that have been donated to us by various people. Before we upload the map onto our website, each map is turned into a PNG file and overlaid on Google Earth for claim boundary identification. A placemark is set in the center of the claim location and a polygon drawn around the claim outline to track which claims were finished. Rather than deleting referenced locations, I started saving these files into a database that I have been compiling for 7 years.

Using the previously mentioned method, I have compiled a database that shows claim overlays throughout Montana, which includes interactive KML files for the Philipsburg, Butte, and New World mining districts (fig. 1). There are also KML files showing sample locations for the Richard Berg Collection as well as the Marion K. Jones collection, which shows structural and stratigraphic cross sections of the eastern part of Montana.

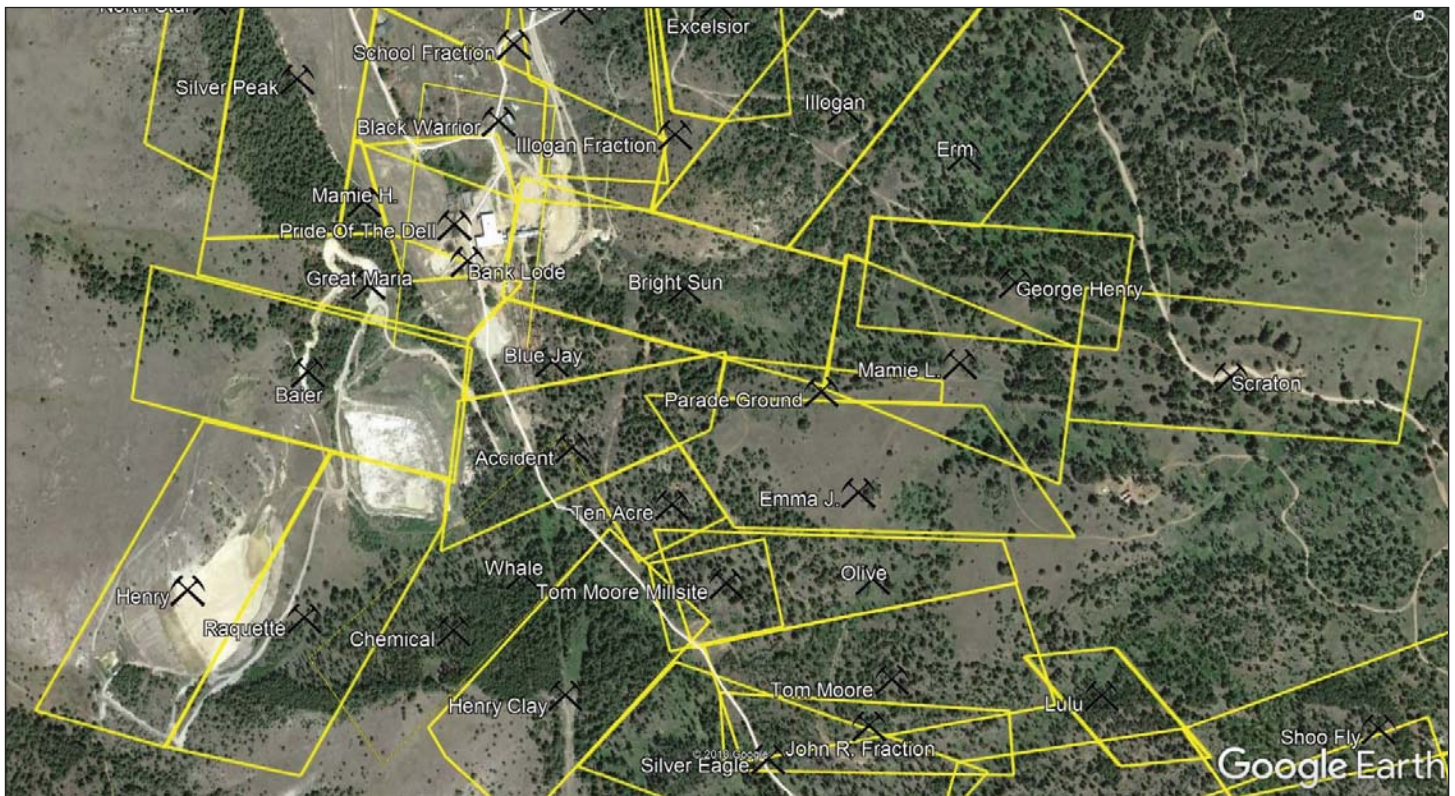


Figure 1. Mining claims overlay in Philipsburg mining district.

In April 2017, Tom Malloy learned about the database I had been compiling and brought me a file that showed 198 verified hazard locations and subsidence areas throughout the county of Butte–Silver Bow. By July 2019, using the method described, 1,286 hazard locations had been geo-referenced and 508 mining claims verified.

This information is critically useful in Butte, because every year, during the spring thaw, sinkholes from Butte’s underground mining years usually show up when the runoff water begins to saturate the ground. In July 2018, a subsidence occurred just days after an addition had been removed from a residence due to it pulling away from the original foundation (fig. 2). County officials then started asking what mine





Figure 2. Sinkhole related to the Carrie Shaft (Courtesy of The Montana Standard; 2018).

information we had in the area. We had information on file about a mine claim in the vicinity of the collapse and had referenced the hazards for the mine claim almost a year prior to the subsidence. After using a high-pressure water jetter, county employees found that the subsidence opened into the top of an underground stope approximately 70 ft below the surface. After confirming the shaft, we later found out that the shaft location on the survey map was approximately 12 ft from where I had previously geo-referenced the shaft almost a year prior.

Due to the end of underground mining in 1982, the underground pumps were shut off and billions of board feet of mine timbers and lumber were submerged, along with physical evidence of geology and mining engineering strategies practiced over the years. It would be a tremendous loss of information, if not for a salvage effort aided by technology.

Thanks to a Priority 2 grant sponsored by the National Geological and Geophysical Data Preservation Program, we are currently scanning a small portion of the Butte Stope Books from The New Butte Mining Company, which are in danger of theft or damage due to their storage location (fig. 3). These books are unique to Butte's mining heritage as they hold valuable mining and geologic data from the early 1880s to 1982, when mining was suspended on the Butte Hill. This information, if lost, could neither be replaced nor reduplicated. The 43 books we are currently scanning have not been seen by the public for over 30 years, if ever, and could be very helpful in finding areas of subsidence in uptown Butte.

The pages have 7-ft intervals, meaning that each page represents a 7-ft drop in elevation and cover 8,800 ft<sup>2</sup> on the Butte Hill from the mine collar on the surface to the bottom of a mine. Elevations are usually noted on every page.

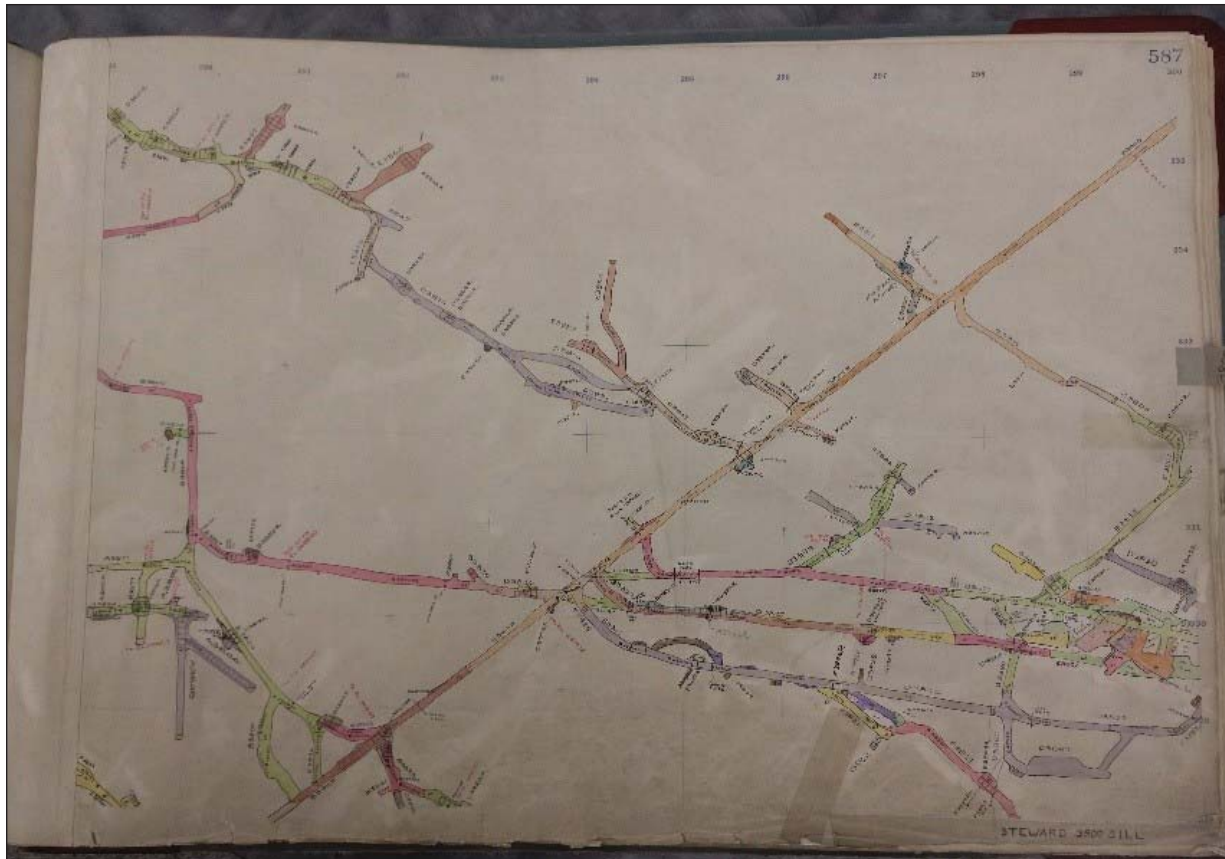


Figure 3. Portion of Steward Mine 3800 sill from a stope book.

Each color corresponds to the year the area was mined. The pages of the stope books also show survey locations, manways, chutes, bulkheads, fire doors, and ventilation doors. There are a total of 357 books in the collection (5 are unaccounted for). The rest of the collection is split into two parts, which are retained by the Butte–Silver Bow Public Archives and Montana Resources.

At the end of underground mining in 1982, the pumps in the mines were shut off and the underground workings were allowed to flood. The Emma Mine is one of several mines that once operated in the center of uptown Butte's business district. Currently, the water level in the Emma shaft is 214 feet below the surface (fig. 4). The Mountain Consolidated (Mt Con) shaft that resides almost 1 mi directly north of the Emma is the deepest mine in Butte, at a little over a mile deep. According to GIS determination, there are currently over 42 vertical miles of shafts and over 10,000 mi of underground workings in Butte. All of the underground mine workings in Butte below the Emma 300-19 level are underwater. The Emma 300 sill currently sits 114 ft below the water level. The only way to learn about the workings are through the Stope Books. This project should help preserve vital mining historical information for the future.

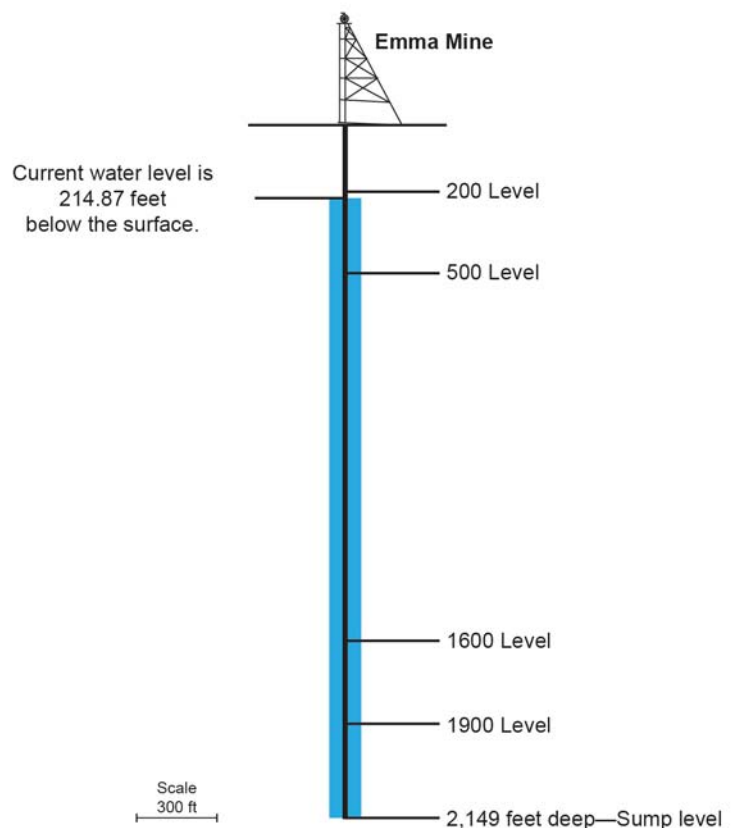


Figure 4. Water level in the Emma Mine as of July 2019.





Amethyst scepter from the Little Gem Mine, MT. Courtesy of Michael J. Goble.

# The Montana–Idaho Alkalic Belt: An Exploration Target for Critical Metals and Industrial Minerals

Christopher H. Gammons

*Department of Geological Engineering, Montana Tech, Butte, Montana*

The purpose of this paper is to draw attention to a NNW–SSE-trending belt of rare metal mineral occurrences and alkalic igneous complexes along the Montana–Idaho border (fig. 1). This belt is herein referred to as the Montana–Idaho Alkalic Belt (MIAB), after Lelek (1979) and Schissel (1981). Early workers noted a NW-trending belt of Th-REE-Ti-Nb deposits in extreme southwestern Montana and adjacent Idaho that includes carbonatite dikes in the Sheep Creek (MT) and Mineral Hill (ID) districts as well as Th-REE veins rich in Fe-oxides at Diamond Creek (ID), Lemhi Pass (ID–MT), and the northern Tendoy Mountains (MT). At a larger scale, this trend is part of a belt of rare metal deposits and associated alkalic igneous bodies that stretches from Salmon, ID, northward along the Montana–Idaho border into British Columbia, and further north into the Yukon Territories. The mineral deposits in question are rich in actinides (U, Th), fluorite, rare earth elements (Y, REE), and other large ion lithophile elements (e.g., Nb, Ti, Sc, Ba).

The discussion that follows is brief. Readers are referred to table 1 for a list of some of the mineral deposits of interest with references for more details. In addition, a number of papers, not reviewed here, describe carbonatites and other rare metal occurrences in the British Columbia Alkaline Province. For examples, see Millonig and others (2012), Simandl and others (2013), Trofanenko and others (2016), BCGS (2016), and Green and others (2017).

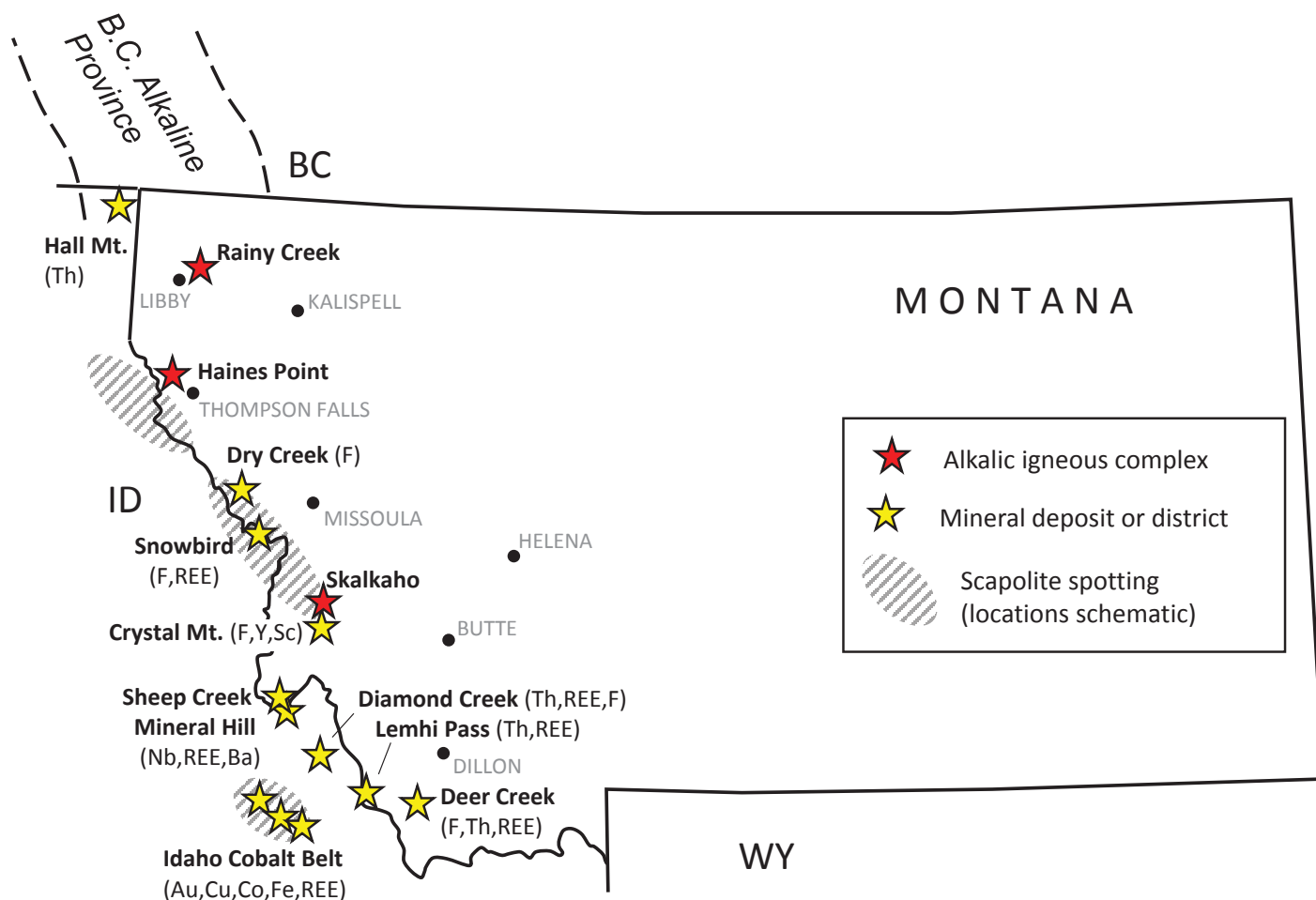


Figure 1. Selected mineral deposits and alkalic igneous rocks of the Montana-Idaho Alkalic Belt.

Table 1. Some mineral deposits of interest in the Montana–Idaho Alkalic Belt, with references.

| Locality                      | Deposit Type   | Primary References  |
|-------------------------------|--|---|
| Idaho Cobalt Belt, ID         | Exhalative Cu-Co-Au-Fe-REE with hydrothermal overprints    | Nash and Connor, 1993; Lund and others, 2011; Slack, 2006, 2012                                     |
| Deer Creek, North Tendoys, MT | Fluorite-Fe-REE-Th veins                                   | Trites and Tooker, 1953; Anderson, 1981   |
| Lemhi Pass, MT-ID             | Thorium-REE-Fe-Cu veins                                    | Anderson, 1961; Sharp and Cavender, 1962; Staatz and others, 1972; Gillerman and others, 2002, 2003 |
| Diamond Creek, ID             | Th-REE-fluorite veins                                      | Gillerman, 2011; Allison and others, 2019   |
| Mineral Hill District, ID     | Ti-Nb-REE-rich carbonatite dikes and veins                 | Kaiser, 1956; Anderson, 1960; Spence, 1984  |
| Sheep Creek Area, MT          | REE-Nb-Ba-rich carbonatite dikes and veins                 | Crowley, 1960; Heinrich and Levinson, 1961; Gammons, 2020   |
| Crystal Mountain, MT          | Fluorite masses, high Sc, Y                                | Taber, 1952; Foord and others, 1993; Grondin, 2019  |
| Skalkaho, MT                  | Alkalic igneous complex, vermiculite, fenite               | Lelek, 1979   |
| Snowbird, MT                  | Fluorite-REE in pegmatitic quartz-carbonate veins          | Metz and others, 1985; Ekambaram and others, 1986; Samson and others, 2004                          |
| Dry Creek District, MT        | Fluorite in pegmatitic quartz-carbonate veins and breccias | Sanford, 1972; Ekambaram and others, 1986; Rosenberg and Larson, 2000                               |
| Haines Point, MT              | Alkalic igneous complex, fenite                            | Schissel, 1981, 1983  |
| Rainy Creek, MT               | Alkalic igneous complex, vermiculite, fenite, fluorite     | Larsen and Pardee, 1929; Pardee and Larsen, 1929; Bassett, 1959; Boettcher, 1967; Montana, 2006     |
| Hall Mountain, ID             | Th-rich veins  | Staatz, 1972; Staatz and others, 1974   |

To be classified as an alkalic belt, alkalic intrusions and/or volcanic rocks must be present. Three alkalic intrusive complexes are documented in the MIAB: Skalkaho, Haines Point, and Rainy Creek. Each of these includes bimodal felsic (syenite) + ultramafic (pyroxenite) intrusions, as well as localized alkali metasomatism (i.e., “fenite”) of surrounding Belt country rock. Low-temperature alteration of pyroxenite at Rainy Creek produced the large Libby vermiculite mine, now defunct after a number of asbestos-related lawsuits. A significant deposit of vermiculite is also present at the Skalkaho complex. The type of alkaline magmatism exhibited in the MIAB is similar to that often associated with carbonatite (i.e., magmatic carbonate). Carbonatites are globally important as a source of rare earth elements and other critical metals (e.g., Nb, Ta, Ti, Sc), as well as fluorite. Small carbonatite bodies are said to exist in the Sapphire Mountains near Skalkaho Pass (La Tour, 1974), and a scattering of carbonate “vein-dikes” rich in REE, Ti, Nb, and Ba are found in the Sheep Creek district of southern Ravalli County, MT, and the adjacent Mineral Hill district of Lemhi County, ID. These deposits were discovered and described in the 1960s and 1970s, but very little work has been done since. A companion paper (Gammons, 2020) focuses on the mineralogy of the REE-rich vein deposits along Sheep Creek. The most abundant REE minerals are monazite, ancyllite, and allanite, and vein textures are strongly suggestive of a carbonatite origin.

Another interesting class of deposits that may be present in the MIAB are iron-oxide-copper-gold (IOCG) deposits (Hitzman and others, 1992; Williams and others, 2005). IOCG deposits are vein and/or breccia deposits that contain large concentrations of hypogene iron oxides (magnetite or hematite) along with copper (as chalcopyrite or bornite) and gold. Beyond this, IOCG deposits are difficult to classify. Some, such as the giant Olympic Dam deposit in South Australia, are enriched in U, Th, REE, and fluorite. Others have abundant apatite. Recent workers have suggested that the Th-REE deposits of Lemhi Pass and the Fe-Cu-Au-REE-U deposits of



the Idaho Cobalt Belt could be IOCG deposits (see Gillerman and others, 2000, and Slack, 2012, respectively). Veins and masses of specular hematite and magnetite are scattered throughout the MIAB, sometimes with associated gold and copper, as at the Copper Queen mine and Wonder lodes near Lemhi Pass (Sharp and Cavender, 1962). Robin McCulloch (oral commun., 2017) suggested a link between iron oxide lodes and the location of gold placers in Mineral and Missoula Counties, MT. Just north of the Montana border, at Iron Mountain, B.C., potential IOCG deposits are being explored (Galicki and others, 2012). Worldwide, IOCG deposits are often flanked by country rocks that experienced strong Na-metasomatism during the passage of large quantities of hot, highly saline fluids. Regional Na metasomatism is widespread within certain regions of the MIAB in the form of albite and scapolite spotting of Proterozoic metasediments, and is especially well developed in the Wallace and Yellowjacket Formations (Hietanen, 1967; La Tour, 1974; Nash and Connor, 1993; Lonn and Berg, 1996; Lewis, 1998).

Historic mining of fluorite in the MIAB has taken place at the Crystal Mountain, Snowbird, and Dry Creek localities (fig. 1). Recent fluid inclusion work at Montana Tech (Grondin, 2019; C. Gammons, 2020) shows that these fluorite deposits formed at considerable depth (>8 km) from fluids that were extremely saline and very hot (400–500°C). These findings agree with the fluid inclusion study of Samson and others (2004) of the Snowbird deposit. Snowbird is well known to mineral collectors as a locality to collect parisite, a REE-fluoro-carbonate mineral. Some workers have suggested that Snowbird is an unusual, carbonate-rich pegmatite, which helps to explain the presence of euhedral quartz crystals exceeding 1 m in diameter. The fluorite-carbonate veins at Wilson Gulch in the Dry Creek district also display pegmatitic textures. Fluorite at Crystal Mountain is rich in Y (Grondin, 2019), and the deposit is one of the few locations worldwide to contain thortveitite, a Sc-silicate (Foord and others, 1993). Based on their massive, mono-mineral nature and lack of hydrothermal alteration with surrounding country rock, Grondin (2019) suggested that the Crystal Mountain fluorite deposits were the product of immiscibility between coexisting granite and fluorite melts (Yang and van Hinsberg, 2019).

Other mineral deposit types of potential interest in the MIAB include hydrothermal barite, gem beryl, and porphyry Mo-W-Cu deposits. As reviewed by Berg (1988), all potentially mineable reserves of barite in Montana are in the western part of the State. The majority of these deposits are steeply dipping veins of pure barite, barite-quartz, or barite-quartz-carbonate cutting Belt metasedimentary units. A cluster of such deposits exists along the trace of the Lewis and Clark deformation zone. Because barite veins are sometimes associated with carbonatite intrusions, it is possible that some of the barite occurrences tabulated in Berg (1988) could be related to alkaline magmatism. That said, most of the deposits are probably not intrusion-related, and may simply represent mobilization of sedimentary-exhalative barite out of the Belt Supergroup by hydrothermal fluids. Stable isotopes of S and O could conceivably be used to differentiate sources and/or mechanisms of barite mineralization in western Montana (Berg, 1988).

Numerous occurrences of gem emerald and aquamarine beryl have been found in the “Western Canada Beryl Belt” that merges with the MIAB at its southern end (Groat and others, 2005). Although hardly a “belt”, it is notable that green or aquamarine beryl has been reported from at least three locations in western Montana (King, 1966; Pattee and others, 1968), and Be is concentrated in the Idaho Cobalt Belt (Slack, 2012).

The BC Alkaline Province contains a number of porphyry and/or skarn Mo-W-Cu deposits (BCGS, 2016). In the MIAB, Mo-W mineralization occurs at Liver Peak, less than 10 km northeast of Thompson Falls, and at the Spring Creek deposit, at the northwest edge of the Mineral Hill district of Lemhi County, ID (Worthington, 2007). A number of W-skarns and porphyry-style Mo occurrences exist further east in Montana, with distinct clusters of deposits in the Flint Creek–Philipsburg area and in the Pioneer Mountains (Worthington, 2007). Still further east is the world-class porphyry Cu-Mo deposit of Butte, the Bald Mountain Mo deposit near Marysville, and the Big Ben Mo deposit in the Little Belt Mountains. Also, large porphyry Cu deposits of Tertiary age have been drilled at Heddleston (near Lincoln, MT) and the New World district (near Cooke City, MT). The “Idaho Porphyry Belt,” which includes the Thompson Creek moly mine, lies south and west of the Idaho Cobalt Belt (Worthington, 2007). Considering the wide distribution of porphyry- and skarn-related Mo-W-Cu deposits in Montana and Idaho, it is hard to say that there is an anomalous concentration of these deposits along the MIAB trend.

### Age of Alkaline Magmatism and Associated Mineralization

Few studies have been conducted on the age of the deposits of interest in this paper. The Rainy Creek, Haines Point, and Skalkaho complexes are thought to be late Cretaceous in age. Metz and others (1985) reported a tentative U-Th-Pb age for paraisite at Snowbird of 71–72 Ma, and Jaffe and others (1959) published common-lead ages of 90 to 99 Ma for monazite from veins in the Sheep Creek district. Thus, most of the available dates, as well as the prevailing opinion in the literature, reflect a Cretaceous, or “Laramide” age for the deposits in question. However, more recent studies of carbonatite-related mineralization in British Columbia (Millonig and others, 2012, 2013) show that certain minerals, including monazite, may have experienced U-Th-Pb resetting during Cretaceous metamorphism. Much older ages for some of the B.C. carbonatites have been obtained, with clusters at 800–700 Ma (corresponding to the breakup of Rodinia), 500 Ma (corresponding to a period of continental rifting and extension in western North America), and 360–340 Ma (corresponding to another period of extension associated with postulated slab rollback; Millonig and others, 2012). This raises the possibility that the U-Pb dates of 90 to 99 Ma reported by Jaffe and others (1959) from Sheep Creek monazites could be reset ages. Jercinovic and others (2002) reported two age groupings of 800–1100 Ma and 200–400 Ma for monazites from the Lemhi Pass district, Idaho–Montana. Interestingly, both of these age groupings overlap with dates of carbonatite mineralization in southeastern British Columbia. As reviewed by Slack (2012), mineralization in the Idaho Cobalt Belt is believed to have begun in the mid- to late-Proterozoic, with later overprinting in the Cretaceous.

Whether or not the mineral deposits of the MIAB share a common age and plate tectonic setting remains to be determined. In the meanwhile, there is a lot of terrain in western Montana, most of it covered with dense forest. It seems plausible, if not probable, that important deposits of REE, rare metals, and industrial minerals exist in the region. Finding them will not be a simple task.

### References

- Allison, G.K., Appold, M.S., Gillerman, V.S., and Lamadrid, H.M., 2019, Fluid inclusion evidence for the temperature and composition of ore fluids in the Lemhi Pass and Diamond Creek REE-Th districts, Idaho-Montana: Geological Society of America, 2019 Annual Meeting, Phoenix, AZ, Abstract 256-11.
- Anderson, A.L., 1960, Genetic aspects of the monazite and columbium-bearing rutile deposits in northern Lemhi County, Idaho: *Economic Geology*, v. 55, p. 1179–1201.
- Anderson, A.L., 1961, Thorium mineralization in the Lemhi Pass area, Lemhi County, Idaho: *Economic Geology*, v. 56, p. 177–197.
- Anderson, J.M., 1981, The origin of rare earth, thorium, and uranium mineralization in the northern Tendoy Mountains, Beaverhead County, Montana: Bellingham, Western Washington University, M.S. thesis, 101 p.
- Bassett, W. A., 1959, The origin of the vermiculite deposit at Libby, Montana: *American Mineralogist* v. 44, p. 282–299.
- BCGS, 2016, Rare metal deposits in British Columbia: British Columbia Geological Survey, Information Circular 2016-4, 2-p poster.
- Berg, R.B., 1988, Barite in Montana: Montana Bureau of Mines and Geology Memoir 61, 100 p.
- Boettcher, A. L., 1967, The Rainy Creek alkaline-ultramafic igneous complex near Libby, Montana. I: Ultramafic rocks and fenite: *Journal of Geology*, v. 75, p. 526–553.
- Crowley, F.A., 1960, Columbium-rare-earth deposits, southern Ravalli County, Montana: Montana Bureau of Mines and Geology, Bulletin 18, 47 p.
- Ekambaram V., Brookins D, Rosenberg P.E., and Emanuel K.M., 1986, Rare-earth element geochemistry of fluorite-carbonate deposits in western Montana, USA: *Chemical Geology*, v. 54, p. 319–331.
- Foord, E.E., Birmingham, S. D., Demartin, F., Pilati, T., Gramaccioli, C.M., and Lichte, F. E., 1993, Thortveitite and associated Sc-bearing minerals from Ravalli County, Montana: *Canadian Mineralogist*, v. 31, p. 337–346.

- Galicki, M., Marshall, D., Staples, R., Thorkelson, D., Downie, C., Gallagher, C., Enkin, R., and Davis, W., 2012, Iron oxide  $\pm$  Cu  $\pm$  Au deposits in the Iron Range, Purcell Basin, southeastern British Columbia: *Economic Geology*, v. 107, p. 1293–1301.
- Gammons, C. H., 2020, Mineralogical investigation of the Sheep Creek Nb-REE carbonatite veins, southern Ravalli County, Montana: *Proc. 2019 Montana Mining and Minerals Symposium*, in press.
- Gillerman, V. S., 2011, Rare earth elements and other critical metals in Idaho: Idaho Geological Survey, *GeoNote* 44, 4 p.
- Gillerman, V. S., Otto, B. R., and Griggs, F., 2000, Lemhi Pass thorium district: A variant of Proterozoic iron oxide (Cu-REE) deposits?: *Geological Society of America, Abstracts with Programs* v. 32, p. 83.
- Gillerman, V. S., Jercinovic, M. J., and Stein, H. J., 2002, U-Pb and Re-Os geochronology suggests a multistage Precambrian-Mesozoic history for thorium and copper mineralization, Lemhi Pass, Idaho: *Geological Society of America, Abstracts with Programs*, v. 34(6), p. 337.
- Gillerman, V.S., Lund, K., and Evans, K.V., 2003, Stratigraphy, structure, and mineral deposits of the Lemhi Pass area, central Beaverhead Mountains, eastern Idaho: *Northwest Geology*, v. 32, p. 134–146.
- Green, C., Simandl, G. J., Paradis, S., Katay, F., Hoshino, M., Kon, Y., Kodama, S., and Graf, C., 2017, Geological setting of the Rock Canyon Creek REE-fluorite deposit, British Columbia, Canada: *British Columbia Geological Survey, Paper* 2017-1.
- Groat, L.A., Hart, C.J.R., Lewis, L.L., and Neufeld H.L.D., 2005, Emerald and aquamarine mineralization in Canada: *Geoscience Canada*, v. 32(2), p. 65–76.
- Grondin, F., 2019, Mineralogy and fluid inclusion study of the Crystal Mountain fluorite mine, Ravalli County, Montana: M.S. thesis, Montana Tech, Butte, MT.
- Heinrich, E.W., and Levinson, A.A., 1961, Carbonatic niobium-rare earth deposits, Ravalli County, Montana: *American Mineralogist*, v. 46, p. 1424–1447.
- Hietanen, A., 1967, Scapolite in the Belt Series in the St. Joe-Clearwater Region, Idaho: *Geological Society of America Special Paper* 86, 56 p.
- Hitzman, M.W., Oreskes, N., and Einaudi, M.T., 1992, Geological characteristics and tectonic setting of Proterozoic iron oxide (Cu-U-Au-REE) deposits: *Precambrian Research*, v. 58, p. 241–287.
- Jaffe, H.W., Gottfried, D., Waring, C.L., and Worthing, H.W., 1959, Lead-alpha age determinations of accessory minerals of igneous rocks (1952–1957): *U.S. Geological Survey, Bulletin* 1097-B, p. 65–148.
- Jercinovic, M.J., Gillerman, V.S., and Stein, H.J., 2002, Application of microprobe geochronology to hydrothermal monazite and thorite, Lemhi Pass district, Idaho: *Geological Society of America, Abstracts with Programs*, v. 34(6), p. 172.
- Kaiser, E.P., 1956, Preliminary report on the geology and deposits of monazite, thorite, and niobium-bearing rutile of the Mineral Hill district, Lemhi County, Idaho: *U.S. Geological Survey Open-File Report* 390, 41 p.
- King, R.H., 1966, Beryl in a Montana tactite body: *American Mineralogist*, v. 51, p. 502–503.
- Larsen, E.S., and Pardee, J.T., 1929, The stock of alkaline rocks near Libby, Montana: *The Journal of Geology*, v. 37(2), p. 97–112.
- La Tour, T.E., 1974, Examination of metamorphism and scapolite in the Skalkaho region, southern Sapphire Range, Montana: M.S. thesis, University of Montana, Missoula, MT, 95 p.
- Lelek, J.J., 1979, The Skalkaho pyroxenite–syenite complex east of Hamilton Montana and the role of magma immiscibility in its formation: M.S. thesis, University of Montana, Missoula, MT.
- Lewis, R.S., 1998, Preliminary geologic map of the Montana part of the Missoula West 30' x 60' quadrangle: *Montana Bureau of Mines and Geology Open-File Report* 373.



- Lonn, J.D., and Berg, R., 1996, Geologic map of the Hamilton 30' x 60' quadrangle, western Montana: Montana Bureau of Mines and Geology Open-File Report 340.
- Lund, K., Tysdal, R.G., Evans, K.V., Kunk, M.J., and Pillers, R.M., 2011, Structural controls and evolution of gold-, silver-, and REE-bearing copper-cobalt ore deposits, Blackbird district, east-central Idaho: *Epigenetic origins: Economic Geology*, v. 106, p. 585–618.
- Metz, M.C., Brookins, D.G., Rosenberg, P.E., and Zartman, R.E., 1985, Geology and geochemistry of the Snowbird deposit, Mineral County, Montana: *Economic Geology*, v. 80, p. 394–409.
- Millonig, L.J., Gerdes, A., and Groat, L.A., 2012, U-Th-Pb geochronology of meta-carbonatites and meta-alkaline rocks in the southern Canadian Cordillera: A geodynamic perspective: *Lithos*, v. 152, p. 202–217.
- Millonig, L.J., Gerdes, A., and Groat, L.A., 2013, The effect of amphibolite facies metamorphism on the U-Th-Pb geochronology of accessory minerals from meta-carbonatites and associated meta-alkaline rocks: *Chemical Geology*, v. 353, p. 199–209.
- Montana, A., 2006, The Rainy Creek alkaline ultramafic igneous complex near Libby, Montana: *Northwest Geology*, v. 35, p. 11–16.
- Nash, J.T., and Connor, J.J., 1993, Iron and chlorine as guides to stratiform Cu-Co-Au deposits, Idaho cobalt belt, USA: *Mineralium Deposita*, v. 28, p. 99–106.
- Pardee, J.T., and Larsen, E.S., 1929, Deposits of vermiculite and other minerals in the Rainy Creek district, near Libby, Montana: U.S. Geological Survey Bulletin 805, 14 p.
- Pattee, E.C., Van Noy, R.M., and Weldin, R.D., 1968, Beryllium resources of Idaho, Washington, Montana, and Oregon: U.S. Department of the Interior, Bureau of Mines Report of Investigations 7148, 183 p.
- Rosenberg, P.E., and Larson, P.B., 2000, Isotope geochemistry of ankerite-bearing veins associated with the Coeur d'Alene mining district, Idaho: *Economic Geology*, v. 95, p. 1689–1699.
- Samson, I.M., Wood, S.A., and Finucane, K., 2004, Fluid inclusion characteristics and genesis of the fluorite-parisite mineralization in the Snowbird deposit, Montana: *Economic Geology*, v. 99, p. 1727–1744.
- Sanford, S.R., 1972, The geology and geochemistry of the Spar and related deposits, Mineral County, Montana: M.S. thesis, Washington State University, Pullman, WA, 95 p.
- Schissel, D., 1981, Fenitization in the Heather Ann complex, Thompson Falls, Montana: M.S. thesis, University of Montana, Missoula, MT, 77 p.
- Schissel, D., 1983, Fenitization in the Haines Point alkalic complex, Thompson Falls, Montana: *Northwest Geology*, v. 12, p. 1–12.
- Sharp, W.N., and Cavender, W.S., 1962, Geology and thorium-bearing deposits of the Lemhi Pass area, Lemhi County, Idaho, and Beaverhead County, Montana: U.S. Geological Survey, Bulletin 1126, 16 p.
- Simandl, G.J., Reid, H.M., and Ferri, F., 2013, Geological setting of the Lonnie niobium deposit, British Columbia, Canada: *British Columbia Geological Survey Paper 2013-1*, p. 127–138.
- Slack, J.F., 2006, High REE and Y concentrations in Co-Cu-Au ores of the Blackbird district, Idaho: *Economic Geology*, v. 101, p. 275–280.
- Slack, J.F., 2012, Strata-bound Fe-Co-Cu-Au-Bi-Y-REE deposits of the Idaho cobalt belt: Multistage hydrothermal mineralization in a magmatic-related iron oxide copper-gold system: *Economic Geology*, v. 107, p. 1089–1113.
- Spence, J.G., 1984, Geology of the Mineral Hill interlayered amphibolite-augen gneiss complex, Lemhi County, Idaho: M.S. Thesis, University of Idaho, Moscow, ID, 239 p.
- Staatz, M.H., 1972, Thorium-rich veins of Hall Mountain in northernmost Idaho: *Economic Geology*, v. 67, p. 240–248.

- Staatz, M.H., Shaw, V.E., and Wahlberg, J.S., 1974, Distribution and occurrence of rare earths in the thorium veins on Hall Mountain, Idaho: *Journal of Research U.S. Geological Survey*, v. 2, p. 677–683.
- Staatz, M.H., Shaw, V.E., and Wahlberg, J.S., 1972, Occurrence and distribution of rare earths in the Lemhi Pass thorium veins, Idaho and Montana: *Economic Geology*, v. 67, p. 72–82.
- Taber, J.W., 1952, Crystal Mountain fluorite deposits, Ravalli County, Montana: U.S. Bureau Mines Report of Investigations, 4916(8).
- Trites, A.F., and Tooker, E.W., 1953, Uranium and thorium deposits of east-central Idaho and southwestern Montana: U.S. Geological Survey Bulletin 988-H, p. 157–209.
- Trofanenko, J., Williams-Jones, A.E., Simandl, G.J., and Migdisov, A.A., 2016, The nature and origin of the REE mineralization in the Wicheeda carbonatite, British Columbia, Canada: *Economic Geology*, v. 111, p. 199–223.
- Williams, P.J., Barton, M.D., Johnson, D.A., Fontboté, L., de Haller, A., Mark, G., Oliver, N.H.S, and Marschik, R., 2005, Iron oxide copper-gold deposits: Geology, space-time distribution, and possible modes of origin: *Economic Geology 100th Anniversary Volume*, p. 371–405.
- Worthington, J.E., 2007, Porphyry and other molybdenum deposits of Idaho and Montana: Idaho Geological Survey Technical Report 07-3, 22 p.
- Yang, L. and van Hinsberg, V.J., 2019, Liquid immiscibility in the CaF<sub>2</sub>-granite system and trace element partitioning between the immiscible liquids: *Chemical Geology*, v. 511, p. 28–41.

## **Nature and Implications of Breccias at the Lamprophyre-Hosted Sapphire Deposit, Yogo**

Tracey Cotterell and John Ridley

*Department of Geosciences, Colorado State University, Fort Collins, Colorado*

Sapphires in the lamprophyre dike at Yogo are some of the finest in the world, and their origin has not been fully constrained. Sporadic breccias associated with the dike that appear to be spatially related to sapphires have been noted, but not evaluated, and may play a role in the generation of sapphires. The objectives of the project are (1) to determine the origin and mode of formation of different types of breccias and their clasts in the Yogo dike and (2) to test the relationships between sapphires and breccia types and different phases of the dike rock. Field observations, sample collecting, and preliminary geochemical data suggest that there are two types of breccias in the area. The first is a paleokarst breccia in the host Madison Limestone that ranges from yellow to orange and is clast supported with very little matrix. The matrix is composed of a mixture of clays and iron oxides, while the clasts are a combination of coarse sand to boulder-sized, yellow to gray limestone with minor coarse sand to pebble-sized red siltstone, probably derived from the overlying Kibbey Formation. Paleokarst breccias in the area are found as limestone spires, irregular shaped bodies up to 200 ft tall and 50 ft wide, and semi- to unconsolidated sediment cones. The second breccia type has been interpreted as paleokarst as well, but differs in that it is deep orange to red in color, semi-consolidated to unconsolidated, and is generally matrix supported, with clast sizes ranging from coarse sand to boulder. These breccias have irregular shaped “blobs” of dike rock incorporated into them and have a higher concentration of red siltstones and shales. The incorporation of magma into the poorly consolidated paleokarst breccias may be evidence of magmatic brecciation or the result of magma intruding into the breccia. No textural or mineralogical evidence has been found to suggest hydrothermal brecciation occurred. The main body of the lamprophyre has abundant lower crustal xenoliths, which exhibit alteration rims, and very few xenoliths of the Madison Limestone have been incorporated into the dike. Two phases of the dike have been identified, one coarser grained and more susceptible to weathering and the other finer grained with no obvious weathering pattern.



# Late Cretaceous to Early Eocene Lamprophyric Textural and Pyroxene Mineral Chemistry Variation from Calc-Alkaline Subduction-Related Magmatism and the Central Montana Alkalic Province

Jacob A. McCane and John Ridley

*Department of Geosciences, Colorado State University, Fort Collins, Colorado*

Late Cretaceous and early Eocene lamprophyric rocks were sampled and analyzed to determine textural and pyroxene mineral chemistry variations from calc-alkaline subduction-related magmatism and the Central Montana Alkalic Province (CMAP) of Montana. Porphyritic pyroxene macrocrysts display resorption during growth and a spongy texture within the core and rims, and exhibit complex zonations. Biotite and phlogopite, within the groundmass and as large macrocrysts, display differing zonations, and are often bent or strained. Cretaceous samples analyzed originate from the Bull Mountain Range, just north of the Golden Sunlight Au-Ag-telluride deposit, and CMAP samples originate from the Highwood Mountains, the Crazy Mountains, and the Yogo sapphire lamprophyre dyke. Understanding the petrogenesis of these bizarre, potassium-rich rocks could aid in field exploration of future economic deposits. There are three competing proposals and petrogenetic models tested in this study. The mantle metasomatism model after the work of Rock (1984) proposed that lamprophyres originate from low degrees of partial melting of volatile rich metasomatized mantle. The hybridization model by Prostka (1973) interprets lamprophyres to be the product of hybridization between syenitic and gabbroic magmas. The third model after Cogne (1962) surmises an origin from the mixing of mafic and felsic components through selective diffusional exchange. Petrographic textural features and analysis coupled with a mineral chemistry study with emphasis on pyroxenes aims to find which model is best suited for lamprophyric rocks from the CMAP. Spongy texture within pyroxenes is interpreted as evidence for disequilibrium of pyroxene within an evolving magma. The analytical traverses of pyroxenes in this region display normal, reverse, and inverse zoning. Patchy zoning and concentric zoning are common within the same crystal; thus a complex history of magma mixing, mingling, and hybridization is captured within pyroxene textural and zonal compositional changes.

## References

- Cogne, J., 1962, The sizunite (cap Sizun, Finistère) and the problem of the origin of lamprophyres: *Bulletin of the Geological Society of France*, v. 7, p. 141–156.
- Protska, H.J., 1973, Hybrid origin of the Absarokite-Shoshonite-Banakite series, Absaroka Volcanic Field, Wyoming: *Geological Society of American Bulletin*, v. 84, p. 697–702.
- Rock, N.M.S., 1984, Nature and origin of calc-alkaline lamprophyres: Minettes, vogesites, kersantites and spessartites: *Royal Society of Edinburgh, Earth Sciences, Transactions*, v. 74, p. 193–227.



The Basin Montana Tunnel Company was incorporated in 1927 by William H. Hax, New York City, and Carl J. Trauerman of Butte. The company had the Gray (Grey Eagle) and Comet patented claims and more than 100 additional patented and unpatented claims, about 21,000 acres, on the west side of High Ore Gulch in the Cataract District, extending about 3 miles south of the Comet Mill to the Great Northern Railroad station at Fuller, Montana, and about 6 miles northeast of Basin, Montana. The claim contained silver, gold, lead, and zinc ore. The company had the only custom milling plant in Montana outside of Anaconda, and the company was the largest producer of base metals in Montana outside of Butte. The company employed 100 men. The mine was considered played out by 1941, and the company was inactive by 1949. Courtesy of MBMG's Mining Archives.